NASA CR—135236

ADVANCED SUPERSONIC PROPULSION SYSTEM TECHNOLOGY STUDY

PHASES III AND IV—FINAL REPORT

by

Roy D. Allan and Warren Joy

GENERAL ELECTRIC COMPANY

(NASA-CR-135236)   ADVANCED SUPERSONIC   N78-13058
PROPULSION STUDY, PHASES 3 AND 4 (General
Electric Co.)   297 p HC A13/MF A01   CSCL 21E

                                                          Unclas
                                                    33/07   55136

Prepared For

National Aeronautics and Space Administration

1. Report No. NASA CR-135236	2. Government Accession No.	3. Recipient's Catalog No.
4. Title and Subtitle Advanced Supersonic Propulsion Study, Phases III and IV - Final Report		5. Report Date November 30, 1977
		6. Performing Organization Code
7. Author(s) R.D. Allan and W. Joy		8. Performing Organization Report No. R77AEG635
		10. Work Unit No.
9. Performing Organization Name and Address General Electric Company Aircraft Engine Group Cincinnati, Ohio 45215		
		11. Contract or Grant No. NAS3-19544 (Modification 4)
		13. Type of Report and Period Covered Contractor Report
12. Sponsoring Agency Name and Address National Aeronautics and Space Administration Washington, D.C. 20546		
		14. Sponsoring Agency Code

15. Supplementary Notes

Project Manager, Edward A. Willis, Wind Tunnel and Flight Division
NASA-Lewis Research Center, Cleveland, Ohio 44135

16. Abstract

The continuation of the General Electric Advanced Supersonic Propulsion Study to evaluate various advanced propulsion concepts for supersonic cruise aircraft has resulted in the identification of the Double-Bypass Variable Cycle Engine as the most promising concept. This engine design utilizes special variable geometry components and an annular exhaust nozzle to provide high take-off thrust and low jet noise. The engine also provides good performance at both supersonic cruise and subsonic cruise. Emission characteristics are excellent. The advanced technology Double-Bypass Variable Cycle Engine offers an improvement in aircraft range performance relative to earlier supersonic jet engine designs and yet at a lower level of engine noise. Research and technology pr   re required in certain design areas for this engine concept to realize its potential benefits. This report summarizes the work conducted under Phases III and IV of the Advanced Supersonic Propulsion Study including refined parametric analysis of selected variable cycle engines, screening of additional unconventional concepts, and engine preliminary design studies. In addition, required critical technology programs are summarized.

17. Key Words (Suggested by Author(s)) Supersonic Transport Advanced Supersonic Technology Supersonic Cruise Airplane Research Variable Cycle Engines Annular Acoustic Plug Nozzles Double Bypass	18. Distribution Statement Unclassified - Unlimited		
19. Security Classif. (of this report) Unclassified	20. Security Classif. (of this page) Unclassified	21. No. of Pages	22. Price*

*For sale by the National Technical Information Service, Springfield, Virginia 22151

TABLE OF CONTENTS

TABLE OF CONTENTS (Concluded)

LIST OF ILLUSTRATIONS

v

LIST OF ILLUSTRATIONS (Continued)

LIST OF ILLUSTRATIONS   (Continued)

LIST OF ILLUSTRATIONS   (Continued)

LIST OF ILLUSTRATIONS   (Continued)

LIST OF ILLUSTRATIONS (Continued)

LIST OF ILLUSTRATIONS   (Concluded)

LIST OF TABLES

LIST OF TABLES (Concluded)

1.0 SUMMARY

The National Aeronautics and Space Administration (NASA) is engaged in a study of the application of advanced technology to long-range, supersonic, commercial transport aircraft under the Supersonic Cruise Aircraft Research (SCAR) program. As part of this program, the General Electric Company has been conducting advanced supersonic propulsion studies with the overall objective of identifying the most promising advanced engine concepts and related technology programs necessary to provide a sound basis for design and possible future development of an advanced supersonic propulsion system. Phases I and II of this effort were conducted under NASA Contract NAS3-16950 and were reported in NASA CR-143634 and NASA CR-134913, respectively. GE Phase III effort, conducted under NASA Contract NAS3-19544 and including airframe integration studies, is the subject of this report.

Phase I studies included the design and analysis of several conventional supersonic engines and several supersonic engines having variable cycle features. Phase II was a follow-on study in which specific variable cycle features or arrangements (both dual-cycle and double-bypass) were incorporated in a mixed-flow turbofan cycle. The engines were modified to incorporate annular nozzles so as to take advantage of their simplicity and light weight and their inherent acoustic suppression characteristics. Phase II studies identified a double-bypass variable cycle engine having high-flowed fan and annular nozzle as the most attractive of those studied, considering range performance and noise.

Results of Phase II studies also indicated that further refinements in engine cycle and nozzle design and further nacelle integration studies would be required.

The overall objective of Phase III was to provide parametric and refined preliminary design studies and to identify critical technology requirements for attractive engine designs which would result. Emphasis was placed on unique engine components, such as an annular nozzle, a main combustor having low emissions, and a high-flowed fan. In addition, definitions of the most promising engines were provided to NASA SCAR airframe contractors in the form of data packs for their airplane system assessments. The engine concepts were evaluated in terms of aircraft range performance and environmental characteristics (i.e., noise and emissions).

In Phase III the double-bypass variable cycle engine was identified as the most promising concept. The improved double-bypass variable cycle engine incorporates advanced technology features, including:

- Mechanical design improvements

- Annular acoustic nozzle

- Reduced levels of turbine cooling air

- Special variable geometry components

- Improved fan and compressor aerodynamics

- Lightweight components

- Improved aerodynamic flowpaths

- High-flowed fans

- Low emissions combustor

- Advanced electronic controls

The engine also provides good performance at both supersonic cruise and subsonic cruise and the emission characteristics are acceptable. The advanced technology double-bypass variable cycle engine offers an improvement in aircraft range performance relative to earlier supersonic jet engine designs and with a lower level of engine noise.

Cooperative studies with aircraft systems contractors have identified a cycle which best matched their aircraft with the following representation parameters:

- Fan high-flowed 10%

PR_F	3.7
PR_{OA}	15 to 17
BPR	2.5 to 0.35
$T41_{Max.}$	$1538°$ C ($2800°$ F)
$T41_{Supercruise}$	$1482°$ C ($2700°$ F)

Studies show that range improvements from 555 to 926 km (300 to 500 nmi) resulted.

Studies of low emission combustors have identified a double-annular combustor which provides significant emission reductions and meets the 1984 EPA proposed airport standard.

Studies indicate that final emission standards may have a major impact on the AST aircraft and its propulsion system.

The Lockheed-California Company was subcontracted to evaluate inlet concepts for a typical variable cycle engine. There were additional sub-contracts with the three major SCAR airframe companies (McDonnell Douglas, Lockheed-California, and Boeing) for the purpose of conducting nacelle integration studies.

2

Data packs were provided for selected engines and consisted of engine definitions in terms of performance, noise, and installation characteristics. From the results of these airframe studies it is concluded that:

- Satisfactory inlets can be designed to match flow and other performance characteristics of General Electric variable cycle engines.

- Acceptable nacelle designs can be achieved for General Electric GE21/J11 double-bypass variable cycle engines with only minor engine configuration changes which result in a minimum impact on aircraft drag.

- Engine size selection is greatly affected by jet nozzle acoustic characteristics, take-off requirements, and aircraft size.

- General Electric GE21/J11 engines with annular nozzles are estimated to meet FAR 36 noise requirements without the need for a mechanical suppressor.

Data packs of militarized versions of selected engines were prepared and provided to NASA-Lewis for overall mission studies.

Studies of three additional unconventional engine concepts were conducted. The concepts studied included a modified version of a VCE for an airplane utilizing flap-blowing, a supersonic inflow fan engine, and use of power management techniques during take-off and climb-out.

Technology requirements for the VCE include:

Combustors having low emissions

Annular nozzle

High-flow fans

Special variable geometry components

Acoustics

Electronic controls

Inlet/engine/nacelle integration

The multi-year NASA AST/SCAR Test-Bed Program, in which GE is a participant, will provide for some of the required technology development areas.

3

2.0 INTRODUCTION

As part of the NASA Supersonic Cruise Airplane Research (SCAR) program, The General Electric Company has been conducting advanced supersonic propulsion studies under NAS3-16950 (Phases I and II) and NAS3-19544 (Phase III). The overall objective of this study program was to identify the technology necessary to provide the basis for design and possible future development of an advanced supersonic propulsion system.

2.1 BACKGROUND

Phase I studies involved the design and analysis of several conventional supersonic engines and several supersonic engines having variable cycle features. Engine dimensions, weight, and performance characteristics were estimated from preliminary design activity. Each engine was "sized" for, and "flown" in, a hypothetical supersonic transport aircraft on a specified supersonic transport mission. Engine types studied included some with mechanical suppressors and some without mechanical suppressors.

Phase I study results indicated that the low bypass ratio, mixed flow, augmented turbofan cycle gave the best range performance. In addition, it was determined that a jet noise suppressor would be required if an acceptable AST aircraft was the desired goal.

Phase I studies also indicated that the modulating airflow 3-rotor engine design had some desirable features. A new engine was devised which was basically a mixed-flow turbofan but combined with the desirable features of the 3-rotor engine.

The Phase I study illustrated that noise constraints had a definite impact on the selection of engine types and cycle parameters. It was also shown that an advanced supersonic transport would benefit from the application of advanced engine technology.

Phase II was a follow-on study in which specific variable cycle features or arrangements were evaluated using a mixed-flow turbofan cycle as a basis. Both dual-cycle and double-bypass types were analyzed. Phase II also sought to identify what new or advanced technology would have to be developed to assure success of, or otherwise exploit the potential advantages of, the variable cycle engine (VCE). In these studies noise goals were between FAR 36 and FAR 36 minus 5 dB.

During the Phase II studies the acoustic benefits of the annular nozzle became better understood. As a consequence, the VCE's were modified to incorporate annular nozzles in order to take advantage of their simplicity, light weight, and inherent acoustic suppression characteristics. Additional information on the forward-flight effects on the acoustic characteristics of mechanical suppressors was obtained in this time period and was factored

4

into the analysis. Engine designs were identified, some with mechanical suppressors and some with annular nozzles having no mechanical suppressors.

Phase II studies identified a double-bypass variable cycle engine having a high-flowed fan and an annular nozzle as the most promising concept of those studied, considering range performance and noise. The advantages of this particular engine were:

- Better subsonic sfc

- Thrust modulation features

- Reduced spillage drag

- Better match between takeoff thrust and noise

Results of the Phase II studies also indicated that further refinements in engine cycle, nozzle design, and nacelle integration would be required, and these areas were included in Phase III work.

2.2 DESCRIPTION OF PHASE III STUDY TASKS

The overall objective of Phase III was to continue parametric refinement and preliminary design studies of the most promising variable cycle engine concepts and to identify critical technology requirements for these engines. These concepts were evaluated on an overall basis by GE in terms of range and environment characteristics (noise and emissions). In addition, definition of the most promising engines were provided to NASA SCAR airframe contractors in the form of data-packs for their airplane system assessments.

The following tasks were conducted to meet these program objectives:

Task A - Engine Studies

This task included the refinement of the double-bypass VCE concept including use of an annular nozzle for noise benefits. In addition, a low-bypass, mixed-flow engine was studied.

Task B - Airframe Related Studies

A subcontract was established with the Lockheed-California Co. to evaluate inlet integration for a typical variable cycle engine. Additional subcontracts were let to the three major SCAR airframe companies, McDonnell Douglas Corp. (Douglas Aircraft Company), Lockheed-California Co., and the Boeing Commercial Airplane Company for the purpose of conducting nacelle integration studies.

5

Data-packs were provided for selected engines which consisted of engine definition in terms of performance, noise, and installation characteristics.

Task C - Special Studies

Studies of three additional engine concepts were conducted. The concepts included a modified version of a VCE for a blown-flap airplane, a supersonic inflow fan engine, and the use of power management techniques during take-off and climb-out.

Task D - Preliminary Design

The preliminary design studies initiated in Phase II were continued under this task. Emphasis was placed on unique engine components, such as the annular acoustic nozzle and the main combustor having low emissions.

Task E - Military Applications

Data-packs of militarized versions of selected engines were prepared and provided to NASA-Lewis for overall mission studies.

Task F - Technology Recommendations

Based on the results of the Phase III studies, the critical technology requirements were identified and recommendations were made.

6

3.0 LIST OF SYMBOLS AND NOMENCLATURE

Measurement values used in this report are stated in SI units followed by English units in parentheses. The study was conducted using customary English units for the principal measurements and calculations.

Symbol	Definition	SI Units	English Units
A_c	Inlet Capture Area	m^2	ft^2
ADEN	Augmented Deflecting Exhaust Nozzle	–	–
A_i	Inlet Capture Area	m^2	ft^2
ALT,alt	Altitude	m	ft
AST-2	Advanced Supersonic Transport	–	–
AST	Advanced Supersonic Technology	–	–
ATEGG	Advanced Turbine Engine Gas Generator	–	–
ATL	Advanced Technology Laboratories, Inc.	–	–
atm	Atmosphere	–	–
Aux	Auxiliary	–	–
Avg	Average	–	–
A_8	Exhaust Nozzle Throat Area	m^2	ft^2
A_9	Exhaust Nozzle Exit Area	m^2	ft^2
A_o/A_c A_o/A_L A_c/A_o	Inlet Mass Flow or Area Ratio	–	–
BFL	Balanced Field Length	m	ft
BPR	Bypass Pressure Ratio	–	–
Btu	British Thermal Unit	J	ft-lbf

SYMBOLS AND NOMENCLATURE (Continued)

Symbol	Definition	SI Units	English Units
°C	Degree Celsius	–	–
C_D	Drag Coefficient	–	–
Cfg	Nozzle Thrust Coefficient	–	–
c.g.	Center of Gravity	–	–
CIAP	Climatic Impact Assessment Program	–	–
C_L	Lift Coefficient	–	–
$C_{L_{TO}}$	Lift Coefficient at Takeoff	–	–
cm	Centimeter(s)	–	–
CO	Carbon Monoxide	–	–
$C_x H_y$	Unburned Hydrocarbons	–	–
D	Drag	N	lbf
DBTF	Duct-Burning Turbofan (Ph I, II)	–	–
dB	Decibel, Unit of Noise Pressure Level	–	–
DIST	Distance	km	nmi
DOT	Department of Transportation	–	–
D/A	Double-Annular	–	–
EAS	Equivalent Airspeed	m/sec	kn
ECCP	Experimental Clean Combustor Program	–	–
ECS	Environmental Control System(s)	–	–
EPA	Environmental Protection Agency	–	–
EPNL } EPNdB }	Unit of Noise Measurement	dB	dB
°F	Degree Fahrenheit	–	–

8

SYMBOLS & NOMENCLATURE (Continued)

Symbol	Definition	SI Units	English Units
FAA	Federal Aviation Agency	–	–
FAR	Federal Air Regulation	–	–
FAR 36	Federal Air Regulation Part 36 Noise Level	dB	dB
ft	Feet	–	–
Flt	Flight	–	–
F_n	Thrust	N	lbf
Fwd	Forward	–	–
g	Acceleration of Gravity	m/sec^2	ft/sec^2
GE	General Electric Company	–	–
h	Height of Inlet Duct	m	ft
HP	High Pressure	–	–
HPT	High Pressure Turbine	–	–
hr	Hour	–	–
IGV	Inlet Guide Vane	–	–
in.	Inch(es)	–	–
$in.^2$	Square Inches	–	–
ISA	Temperature of the International Standard Atmosphere	–	–
JENOTS	General Electric Jet Noise Test Facility	–	–
kg	Kilogram	–	–
kn	Knots	–	–
kW	Kilowatts	–	–

SYMBOLS AND NOMENCLATURES (Continued)

Symbol	Definition	SI Units	English Units
lb	pound(s)	--	--
LP	Low Pressure	--	--
LPT	Low Pressure Turbine	--	--
L_T	Length of Inlet Duct	m	ft
L/D	Lift-to-Drag Ratio	--	--
m	Meter(s)	--	--
M	Mach Number	--	--
McAir	McDonnell Aircraft Company	--	--
mi	mile(s)	--	--
min	Minute(s)	--	--
Min.	Minumum	--	--
M_L	Local Mach Number	--	--
M_o	Free-Stream Mach Number	--	--
M_r	Rolling Moment	N.m	ft-lb
MT	Mount	--	--
MTW	Maximum Taxi Weight	kg	lb
$m*/M_i$	Inlet Mass-Flow Ratio	--	--
N	Newtons	--	--
NASA	National Aeronautics and Space Administration	--	--
N_c	Corrected Engine rpm	1/min	1/min
nmi	Nautical Mile(s)	--	--
NO_x	Oxides of Nitrogen	--	--

10

SYMBOLS AND NOMENCLATURE (Continued)

Symbols	Definition	SI Units	English Units
OAT	Outside Air Temperature	$^\circ$ C	$^\circ$ F
OBJ	Objective	–	–
OEO	One-Engine-Out	–	–
OEW	Operating Weight Empty	kg	lb
OGV TE	Outlet Guide Vane Trailing Edge	–	–
P_A	Ambient Pressure	N/m^2	lb/ft^2
$P_{max.}$	Maximum Inlet Cowl Total Pressure	N/m^2	–
PNdB	PNL in dB Units	dB	dB
PNL	Noise Pressure Level	dB	dB
lb/sec	Pounds per Second	–	–
PR	Pressure Ratio	–	–
PR_F, PR_{FAN}	Fan Pressure Ratio	–	–
PR_{OA}	Overall Engine Pressure Ratio	–	–
lb/ft^2	Pounds per Square Foot	–	–
psi	Pounds per Square Inch	–	–
PTO	Power Takeoff	–	–
P_{T2}, P_2	Total Pressure at Fan Face	N/m^2	lb/ft^2
P_{To}, P_o	Total Pressure Free-Stream	N/m^2	lb/ft^2
$P_{2.5}$	Total Pressure at Inlet of Core	N/m^2	lb/ft^2
P3	Compressor Exit Total Pressure	N/m^2	lb/ft^2
$(P/P)_{FAN}$	Fan Pressure Ratio	–	–
(P_{T2}/P_o)	Inlet Ram Recovery (Ratio)	–	–

11

SYMBOLS AND NOMENCLATURE (Continued)

Symbols	Definition	SI Units	English Units
q	Free-Stream Dynamic Pressure	N/m^2	lb/ft^2
rad	Radian(s)	–	–
RF	Range Factor	km	nmi
R_i	Radius of Inner Wall of Annulus	m	ft
R_o	Radius of Outer Wall of Annulus	m	ft
rpm	Engine Rotating Speed	1/min	1/min
SAE SN	Society of Automotive Engineers Smoke Number	–	–
SCAR	Supersonic Cruise Airplane Research	–	–
SCAT	Supersonic Cruise Air Transport	–	–
sec	Second(s)	–	–
sfc	Specific Fuel Consumption	kg/hr/N	lb/hr/lbf
SF2	Specific Range Factor	km/kg	nmi/lb
SI	Internation System of Units	–	–
SL	Sea Level	–	–
SLS	Sea Level Static	–	–
Spec	Specification, Specified	–	–
SR	Specific Range	km/kg	nmi/lb
SST	Supersonic Transport	–	–
Stat mi	Statute Mile(s)	–	–
Std	Standard	–	–
T	Thrust	N	lbf
T_{am}	Ambient Air Temperature	° C	° F

12

SYMBOLS AND NOMENCLATURE (Continued)

Symbols	Definition	SI Units	English Units
Temp	Temperature	–	–
TND LE	Turbine Nozzle Diaphragm Leading Edge	–	–
TO	Takeoff	–	–
TOFL	Takeoff Field Length	–	–
TOGW	Takeoff Gross Weight	kg	lb
TSEN	Two-Stage Ejector Nozzle	–	–
T_t	Total Temperature	$^\circ$ C	$^\circ$ F
T_o	Ambient Temperature	$^\circ$ C	$^\circ$ F
T_3	Compressor Exit Temperature	$^\circ$ C	$^\circ$ F
T_{41}	Turbine Rotor Inlet Temperature	$^\circ$ C	$^\circ$ F
T_8	Tailpipe Augmentor Temperature	$^\circ$ C	$^\circ$ F
T/W	Aircraft Thrust-to-Weight Ratio	–	–
V	Velocity	m/sec	ft/sec
VABJ	Variable Area Bypass Injector	–	–
V_{app}	Aircraft Approach Flight Velocity	m/sec	ft/sec
VCE	Variable Cycle Engine	–	–
V_j	Exhaust Jet Velocity	m/sec	ft/sec
$V_{j\ max.}$	Maximum Exhaust Jet Velocity	m/sec	ft/sec
W	Installed Weight	kg	lb
w	Inlet Internal Width	cm, m	in., ft
w_a	Engine Airflow	kg/sec	lb/sec
WAT_2	Total Fan Airflow	kg/sec	lb/sec

SYMBOLS AND NOMENCLATURE (Concluded)

Symbols	Definition	SI Units	English Units
W_{cool}	Cooling Airflow	kg/sec	lb/sec
W_E	Engine Weight	kg	lb
WL	Water Line	–	–
Wt	Weight	kg	lb
WUTO	Warmup and Takeoff	–	–
W1R,W2R	Total Fan Airflow	kg/sec	lb/sec
W/S	Aircraft Wing-Loading	kg/m^2	lb/ft^2
2-D	Two-Dimensional	–	–
α_1	Initial Wedge Angle	radian	degree
α_2	Final Wedge Angle	radian	degree
α_3	Shock Reflection Point Angle	radian	degree
α_4	Cowl Internal Angle	radian	degree
α_5	Inlet Duct Throat Angle	radian	degree
δ	Ratio of Total Pressure to Sea Level Ambient Pressure	–	–
Δ	Denotes a Difference, or an Addition	–	–
ΔT_{am}	Difference Between Ambient Temperature and ISA Temperature	° C	° F
$\delta_{1,2,3}$	Inlet Ramp Angle	radian	degree
η	Efficiency	–	–
θ	Ratio of Total Temperature at Fan Inlet to Ambient	–	–
ψ	Sideline Angle	radian	degree

14

4.0 RESULTS AND DISCUSSION

The following sections describe the task activity accomplished in the Advanced Supersonic Propulsion Studies, Phase III, under Contract NAS3-19544.

4.1 ENGINE STUDIES

The double-bypass Variable Cycle Engine (VCE) reported in Phase II was the GE21/J9 Study B1 with the physical characteristics as shown in Table 1. The J9B1 engine has a mechanical jet noise suppressor which provided 15-PNdB suppression at takeoff. Near the end of the Phase II study effort, significant amounts of suppression with annular exhaust systems had been identified through tests conducted at the GE noise testing facility, (JENOTS) under the Duct-Burning Turbofan (DBTF) Contract with NASA (NAS3-18008). Phase III studies of double-bypass Variable Cycle Engines utilized the inherent annular suppression of an annular nozzle with a center plug.

The Phase III double-bypass VCE studies included 10%, 20%, and 30% high-flowed fans, whereas the Phase II J9B1 engine had a 20% high-flowed fan.

The fan percent high flow is defined by taking the ratio of fan flow at takeoff (using the auxiliary inlet) to the fan flow with a nominal inlet flow at 100% speed, subtracting 1.0 and expressing the resulting decimal as a percentage quantity.

4.1.1 Variable Cycle Engine Description

The AST variable cycle engine (VCE) is basically a variable bypass ratio (0.25 to 0.60) dual rotor turbofan engine with a low temperature augmentor, designed for dry power supersonic cruise, using the afterburner for transonic climb and acceleration only. The cruise Mach number range of 2.2 to 2.4 allows selection of a high cycle pressure ratio. The higher turbine inlet temperatures and component efficiencies predicted for the 1980's allow use of a bypass cycle with improved subsonic and supersonic specific fuel consumption.

Figure 1 is a schematic of the double-bypass VCE concept. The basic difference between a VCE and a conventional turbofan engine is the separation of the fan into two blocks with an outer bypass duct between the fan blocks and the normal bypass duct after the second fan block, i.e., double bypass. The airflow size of the front block is larger than would be possible with a conventional turbofan using the same core size.

Oversizing the front block is accomplished by using the same core size but increasing the physical size (diameter) of the fan. High flowing is accomplished with higher spool speed and variable inlet guide vanes. The

Table 1. GE21/J9 Study B1 Double-Bypass Variable Cycle Engine.

Takeoff Thrust, N, (lb)	273,107 (61,400)
W_a, kg/sec, (lb/sec)	408-496 (900-1093)
Fan Pressure Ratio	4.0
Overall Pressure Ratio	22.5
Maximum Turbine Inlet Temperature, ° C, (° F)	1538 (2800)
Supersonic Cruise Turbine Inlet Temperature, ° C, (° F)	1482 (2700)
Mechanical Jet Noise Suppression, PNdB	15
Suppressor Design Point, m/sec, (ft/sec)	762 (2500
Takeoff Jet Velocity, m/sec, (ft/sec)	765 (2510)
FAR Part 36 Noise Level, EPNdB	-25
Engine Weight, kg, (lb)	9072 (20,000)
Maximum Diameter, cm, (inches)	214.4 (84.4)
Engine Length, cm , (inches)	815.1 (320.9)

Forward VABI

Rear VABI

Split Fan

Variable
Low Pressure
Turbine
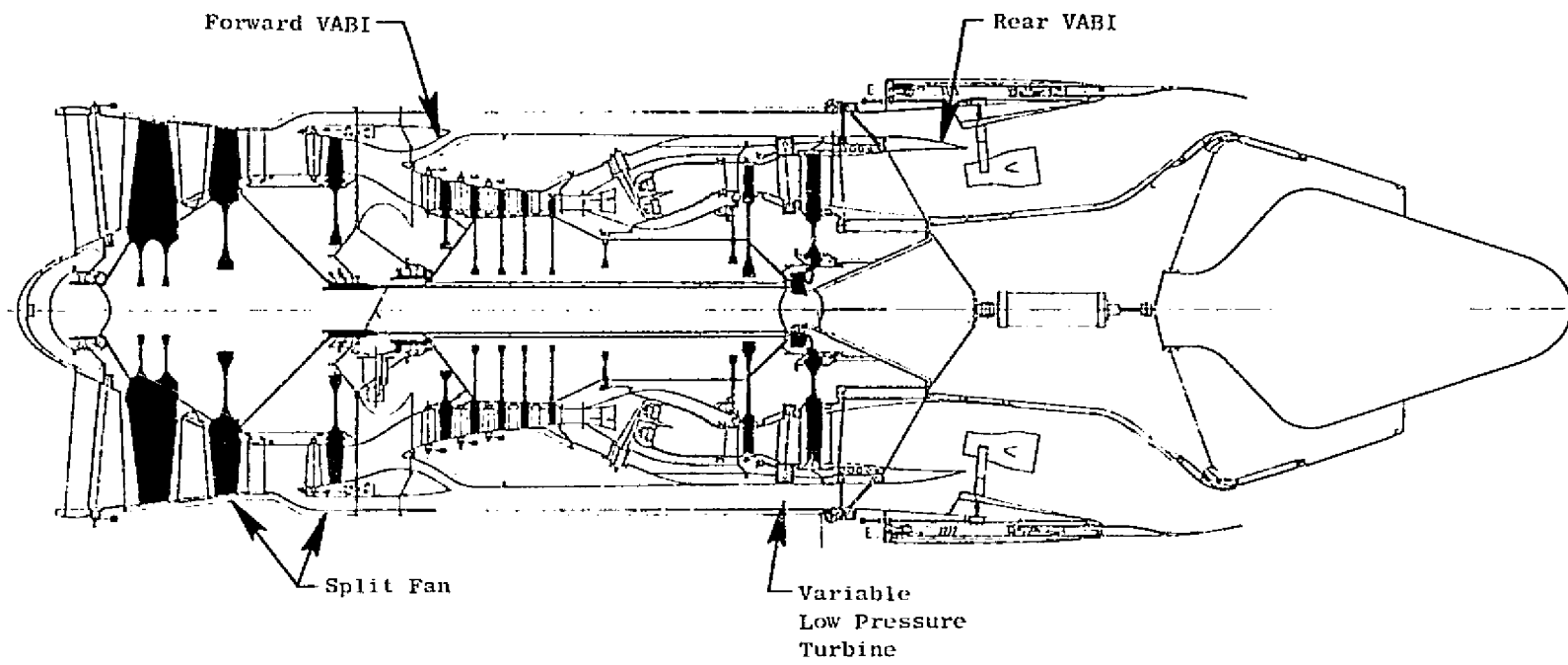
Figure 1.   Variable Cycle Engine.

percent high flow is the ratio of the airflow in the high-flow mode at take-off to the sea level static airflow at 100% fan corrected speed minus 1 expressed as a percentage quantity.

.For the low noise takeoff mode the front block of the fan is set at its high-flow flow configuration. The second fan block is operated to "tailor" the jet exhaust velocity and flow so as to produce the desired thrust/noise relationship for takeoff.

The VCE exploits the concept of coannular suppression by allowing adjustment of the velocities and flows of the inner and outer streams to meet takeoff thrust and noise requirements.

During subsonic cruise operation the front fan block is set to provide the best match between inlet spillage and internal performance. In this mode the second fan block is set to provide the proper cruise thrust. A high inlet airflow can be maintained down to the required subsonic cruise thrust requirement, which practically eliminates inlet spillage drag, and also reduces the afterbody drag.

In the climb/acceleration and supersonic cruise modes, the front block fan is set to satisfy the aircraft inlet flow supply, the rear block fan and high pressure compressor are set to pass all of the front block fan flow, and the engine opera' 's the same as a conventional low bypass ratio turbofan engine.

Another advantage of the split fan configuration is that, for high takeoff airflow sizing, only the front block fan and low pressure turbine are affected. Thus, a large weight saving is realized over the weight of a conventional turbofan engine sized for the same takeoff airflow and noise level.

Figure 1 illustrates the four variable cycle features that give the double-bypass VCE its flexibility when compared to mixed-flow turbofans.

- Split fan bypass duct between the higher flow front block and rear block with its variable stators

- Exhaust variable area bypass injector (rear VABI)

- Fan variable bypass injector (forward VABI)

- Variable area low pressure turbine

These four VCE features allow the independent control of the high and low pressure rotor speeds to provide higher airflow levels at subsonic, part-throttle conditions and at transonic/supersonic high thrust conditions than possible with mixed-flow turbofans, thus resulting in a variable bypass ratio engine.

18

The high-flow front fan block provides the high-takeoff and subsonic-transonic airflow capability of the VCE without having the weight penalty of oversizing the complete engine. The maximum dry-power airflow can be maintained down to the cruise thrust requirement, and this eliminates the spillage drag that is present when a mixed-flow turbofan is throttled back. As the VCE subsonic cruise thrust is obtained at constant inlet airflow, the variable stators on the rear fan block are modulated to reduce the flow into the HP compressor and the excess air is bypassed around the engine. The improvement in cycle performance due to the VCE's higher operating bypass ratio, and therefore higher propulsive efficiency, together with the reduced installation losses caused by the elimination of inlet spillage drag and reduced afterbody drag, reduces installed subsonic sfc by about 15% compared to a conventional mixed-flow turbofan.

With a correctly sized VCE fan that provides the required supersonic cruise airflow, the inlet supply curve can be met. This results in minimum spillage drag and also an increase in acceleration thrust from the higher engine airflow.

The exhaust variable area bypass injector (rear VABI) allows the independent variation of high and low rotor speeds by eliminating the normal mixed-flow turbofan dependence on matching static pressures of the primary and bypass streams in the tailpipe. The rear VABI varies the Mach number in the bypass stream to the correct value for the flow and total pressure to obtain the static pressure balance for mixing the flows. This same concept is also used in the front VABI and eliminates the need for separate full-length bypass ducts for the two bypass streams.

The variable area low pressure turbine stator helps accommodate the large swings in LP turbine power extraction caused by the higher flow front fan block. The variable LP turbine also increases the flexibility in HP and LP speed variations beyond that of the rear VABI alone.

4.1.2 Parametric Cycle Optimization

A double-bypass VCE parametric cycle study was conducted which included an evaluation of engine performance, dimensions, weight, and mission range. The engine configuration was:

- Split fan, double-bypass

- Fan front block 30% high-flowed

- Mid-nacelle exhaust nozzle for takeoff

- High radius ratio primary exhaust nozzle for annular suppression effect

- Low temperature-rise augmentor

The matrix of prime cycle parameters studied was:

- Fan pressure ratio   3.7 to 4.5

- Overall pressure ratio   14 to 20

- Bypass ratio   0.2 to 0.5

Engine cycle constraints imposed on the study were:

- Engine size, airflow 408-531 kg/sec (900-1170 lb/sec)

- Turbine rotor inlet temperature, T41 1538° C (2800° F) maximum; 1482° C (2700° F) at supersonic cruise

- Compressor discharge temperature, T3 621-649° C (1150-1200° F) maximum

- Tailpipe augmentor temperature, T8 1038° C (1900° F) maximum

- Climb/accel inlet/engine airflow matched

- Evaluation based on installed performance (inlet and afterbody drags included)

- Supersonic cruise design flight condition

  2.32 Mach No.
  16,319 m (53,540 ft) altitude
  Temperature, standard day +8° C (+14.4° F)

4.1.3 Engine Size Selection and Acoustics

Engine airflow size is dependent primarily on thrust requirements and power setting at several flight conditions, such as takeoff, accelerated climb, and supersonic cruise (objective is supersonic cruise without augmentation).

A further restriction is that certain noise levels must not be exceeded. Results of previous supersonic transport studies have indicated that takeoff is usually the critical condition for thrust sizing.

The takeoff thrust sizing condition has been analyzed using a time-sharing computer program which accepts information on aircraft aerodynamics and weight characteristics, engine thrust variation with flight velocity, and takeoff distance stated in terms of a balanced field length. It then solves the equations of motion for both takeoff distance with engine failed and for aborted takeoff distance with engine failed also. This permits the determination of required thrust for a given balance field length, or the field length capability for an engine of a given thrust size.

Once thrust requirements for takeoff are determined, a flight path for normal (i.e., all engines operating) takeoff and climb-out can be calculated using the same time-sharing computer program. An acoustic study is carried out to determine the critical operating condition of the three specified in Federal Aviation Regulation 36:

Sideline (takeoff)

Community (with cutback)

Approach

Past studies of supersonic transports and their powerplants have indicated that the sideline condition is generally critical from a noise standpoint and that the critical condition occurs at a power setting, air speed and altitude not far from the take-off condition (which is already critical for thrust requirements).

The take-off thrust requirements and the desired noise levels therefore combine to fix a jet velocity and finally an airflow size at the take-off power setting. This selection then results in an engine size and cycle match which provides the correct thrust to meet all flight requirements (including takeoff) and also has noise characteristics which satisfy the noise goals of the study. A necessary ingredient in this solution is the definition of a noise supression device to be used (if any) and a knowledge of its aerodynamic and acoustic performance characteristics when deployed and when stowed.

It should be noted that almost any noise goal can be met without a noise suppressor. The jet velocity will have to be low in order to meet a low-noise requirement or goal. If a suppressor is used the allowable jet velocity increases. If a suppressor is used, the engine airflow size shrinks due to the higher allowable jet velocity.

The ground rules for this study were specified by NASA and are briefly summarized here. The aircraft configuration and aerodynamic characteristics (both low-speed and high-speed) are those presented in the LTV Report, "Advanced Supersonic Technology Concept Study - Reference Characteristics," Dec. 21, 1973, (issued as NASA CR-132374). The balanced field length is taken as 3200 m (10,500 ft) for a takeoff on a hot day with OAT at ISA plus 15° C (27° F). Engine thrust characteristics are from General Electric AST engine studies. Noise level goals are to achieve a traded average noise corresponding to 103 dB to 108 dB EPNL. These levels are often denoted as FAR 36 minus 5 to FAR 36. Conversion of engine noise characteristics which vary according to aspect angle (i.e., the angle related to the exhaust vector direction) from PNL to EPNL are carried out using standard procedures developed by the General Electric Company.

The General Electric Acoustics group at the Evendale plant has created calculation procedures for estimating engine noise and has updated these procedures based on results of testing work and refined analysis of engine acoustic phenomena. These testing and analysis activities have included evaluation of:

- Engine component noise

- Fan noise

- Inlet noise suppression

- Jet noise

- Jet suppressors

- Coaxial nozzle configurations

Time-sharing computer programs were devised for use in Preliminary Design to permit engine noise predictions.

Program STNOIE - calculates noise per 4/7/75 assumptions
                - uses STNOI3, STNOI4 subroutines

Noise prediction assumptions and methods are constantly being updated as more test results become available, particularly relating to:

- relative velocity effects

- effects of jet shock noise

- coannular nozzle acoustics

- directivity of nozzle noise

Prediction methods have been discussed with NASA personnel and information has been transmitted in the Phase II Study Comprehensive Data Report.

The bulk of studies have been based on the use of an annular nozzle with assumed inherent noise suppressor characteristics. A few engines with chute-type or spoke-type mechanical suppressors were studied. Annular nozzle noise suppression characteristics are based in part on results of test carried out in connection with NASA Contract NAS3-197, , "Acoustic and Performance Investigation of Coannular Plug Nozzles."

One further factor relating to engine sizing is the fact that certain engine types (i.e., those with high-flow fans in which such a feature used only during low-speed aircraft operations) have two engine airflow size definitions:

- Nominal size (high-flow feature not in use)

- "High flow" size (high-flow feature being used)

The study procedure outlined above yields results somewhat different from results of airframe manufacturers. For example, engine size of airfram-

Wing Control Surfaces

Mod. W.T. Data	* Number	Area ft² Each
t_1	1 and 2	116
t_2	3 and 4	100
t_3	5 and 6	61
t_4	7 and 8	91
L_1	9 and 10	198
L_2	11 and 12	195
L_6	13 and 14	92
	15 and 16	40
	17 and 18	26
	19 and 20	18
	21 and 22	6
	23 and 24	8

* Odd Numbers - Left Wing
Even Numbers - Right Wing

Geometry			Wing	Horiz	Vert	Vert Fin on Wing
Area (Gross)	S	ft²	10996.365	600.000	109.000	233.275 EA
MAC (Gross)	$\bar{C}$	in.	1343.0684	254.964	194.124	310.560
Area (Ref)	S	ft²	9969.000			
MAC (Ref)	$\bar{C}$	in.	1154.8625			
Area (Exposed)	S	ft²		441.0		
Span	b	ft	137.7778	32.0	7.6	16.75
Aspect Ratio (Gross)			1.72627	1.707	0.527	0.495
Aspect Ratio (Ref)			1.90417			
Sweep Λ LE		deg	74.0;70.84; 60.00	60.64	68.20	73.42
Root Chord		in.	2196.935	367.200	278.400	458.400
Tip Chord		in.	211.6667	82.80	66.00	62.40
Root T/C		%	See Fig V-7	3.0	2.996	2.996
Tip T/C		%	See Fig V-7	3.0	2.996	2.996
Taper Ratio				0.257	0.237	0.136
Incidence		deg				
Dihedral		deg		-15.0		
Vol Coeff (Gross)	$\bar{V}$			0.070	0.011	0.026
Vol Coeff (Ref)	$\bar{V}$			0.090	0.012	0.029

1653.3334
420.0

278.002
1438.533
2128 (at 0.597 MAC Ref)
1727.248 (Ref Wing)
3° 12'
84.0
Static Ground Line
900.000
2198.000

Figure 2. NASA Reference Aircraft

Scale - meters
0   10   20

Scale - inches
0 100 200   400   600

0   10   20   30   40   50
Scale - feet
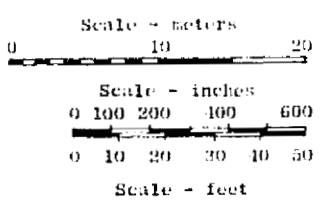
Note: All dimensions are in inches.

2.250°
BL600.000

1.500°
BL438.000

0.750°
BL264.000

384.00

$\overline{C}$ = 1154.8625 (Ref)

Ref MAC LE

278.002

1438.533

1/4 Wing Ref MAC

2128 (at 0.597 MAC Ref)

1727.248 (Ref Wing)

1735.880

1867.853

1012.383

See Chart (Typ)

1/4 MAC

Lower Surface

Lower Surface

Aircraft

1/4 MAC   Wing Ref Plane

6° 18' Ref

326.0

Nose Gear

Main Gear

Line

9° 30'

00.000

2198.000

3780.000
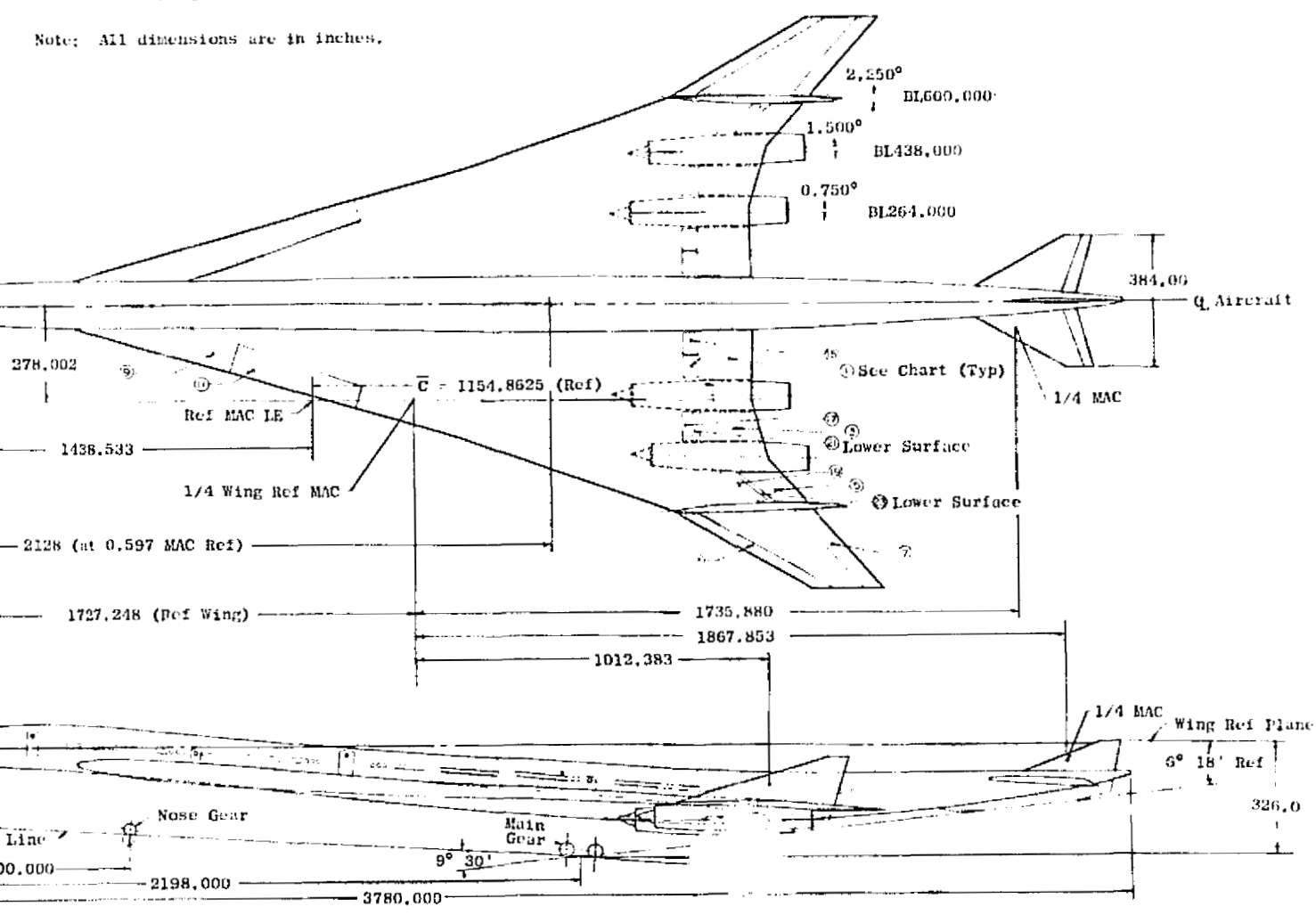
Reference Aircraft Configuration.

23

er's studies are generally smaller than those of GE study results. This
probably is due to differences in airframe aerodynamics, in operational
ground rules in the calculation of balanced field length, and in balanced
field length goals. The use of smaller engine size (in the case of the
airframers) produces a more shallow climb-out trajectory, with the result
that airframer airplanes find themselves at lower altitudes at the time power
cutback is made. Thus, community noise levels of airframer's aircraft tend
to be relatively higher. Traded FAR levels of airframers may be higher or
not, depending on the methods used in noise analysis. The point is that,
what appear to be rather subtle or small differences in assumptions and
ground rules can have major effects on the study results with regard to cycle
selection and engine size.

4.1.4 Mission Analysis Methods

The evaluation of engine cycles was made by "flying" each one in air-
craft and missions defined in NASA CR-132374. The basic aircraft character-
istics are shown on Figure 2. The aircraft drag polar was input into the
missions analysis program with drag variations for changing wing loading and
aircraft takeoff gross weight. Two mission profiles were used. The first
is an all-supersonic mission (See Figure 3) in which the aircraft climbs to
supersonic cruise after takeoff, cruises, and descends to the landing. The
second mission has a 1111 km (600 nmi) subsonic leg which is flown at the
start of the mission.

Each engine was installed using a calculation procedure to size an
inlet and determine the inlet and afterbody drag. The effects of varying the
nacelle size or shape were not calculated since in most cases the performance
difference is minimal.

Parametric engine designs were run through the mission to determine the
best combination of engine cycle parameters such as overall pressure ratio,
bypass ratio, fan pressure ratio and turbine temperature. With the best
engine cycle, the method of engine operation was evaluated to determine
potential payoff. The basic problem was one of matching the supersonic
cruise thrust at a dry power setting and providing a low enough exhaust
velocity at sea level takeoff to meet the FAR 36 noise level required. A
series of engines having high-flowed fans were run to determine the mission
range with up to 30% high-flow. The result is that the noise sets the SLS
airflow and the supersonic cruise sets the amount of fan high-flowing. An
engine cycle having greater thrust for supersonic cruise by overspeed (or
efficiency increases or drag decreases) has a smaller basic engine size and
greater missions range. High-flowing the fan increases airflow and increases
thrust at takeoff, leading to smaller airflow size to meet the takeoff thrust
requirement. Overspeeding also decreases bypass ratio and leads to increased
thrust and lower supersonic sfc.

Results of a typical range calculation for two different AST missions
are presented in Figure 4. These results indicate that there is merit in

24
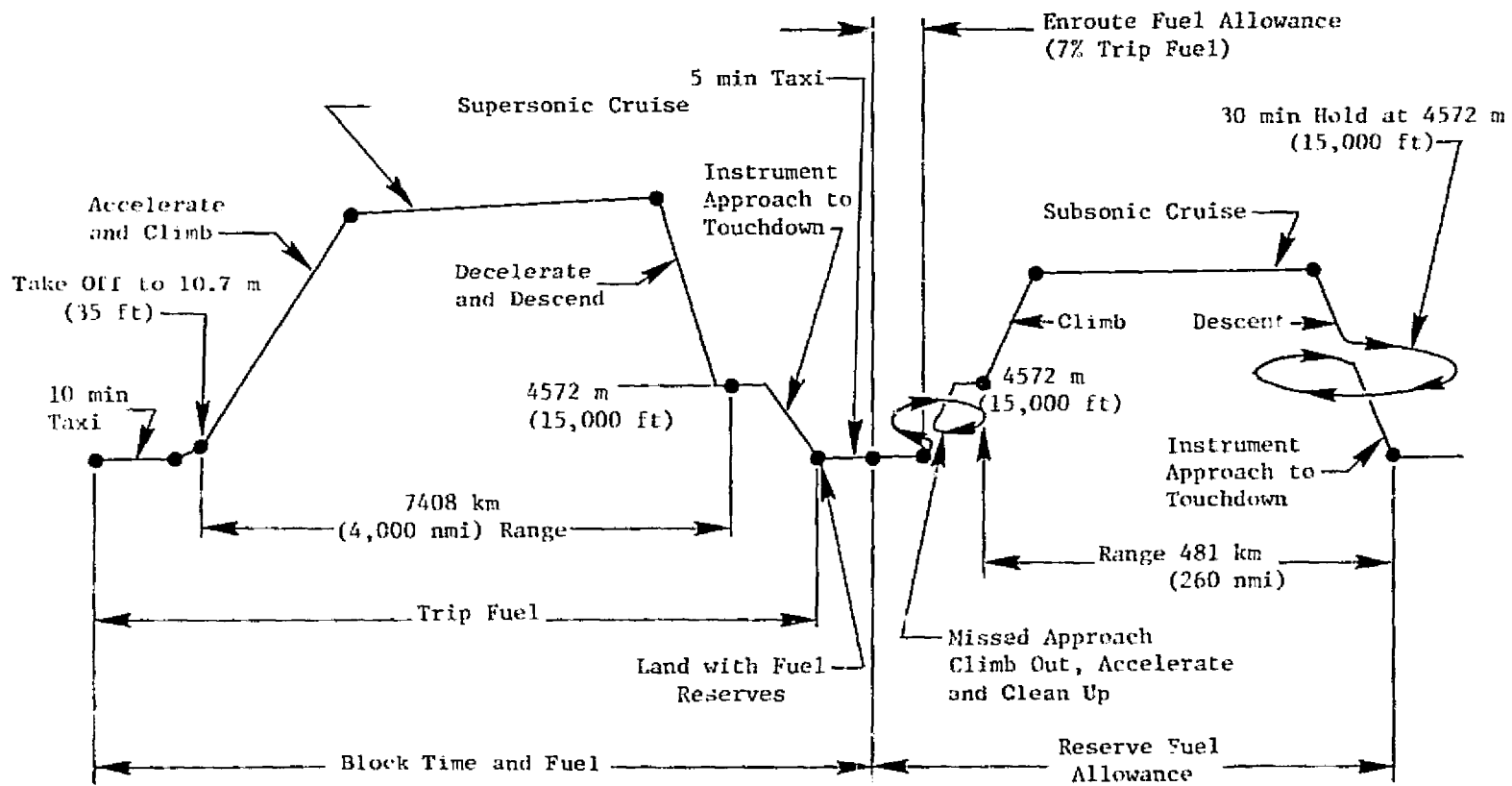
Figure 3. Mission Profile.
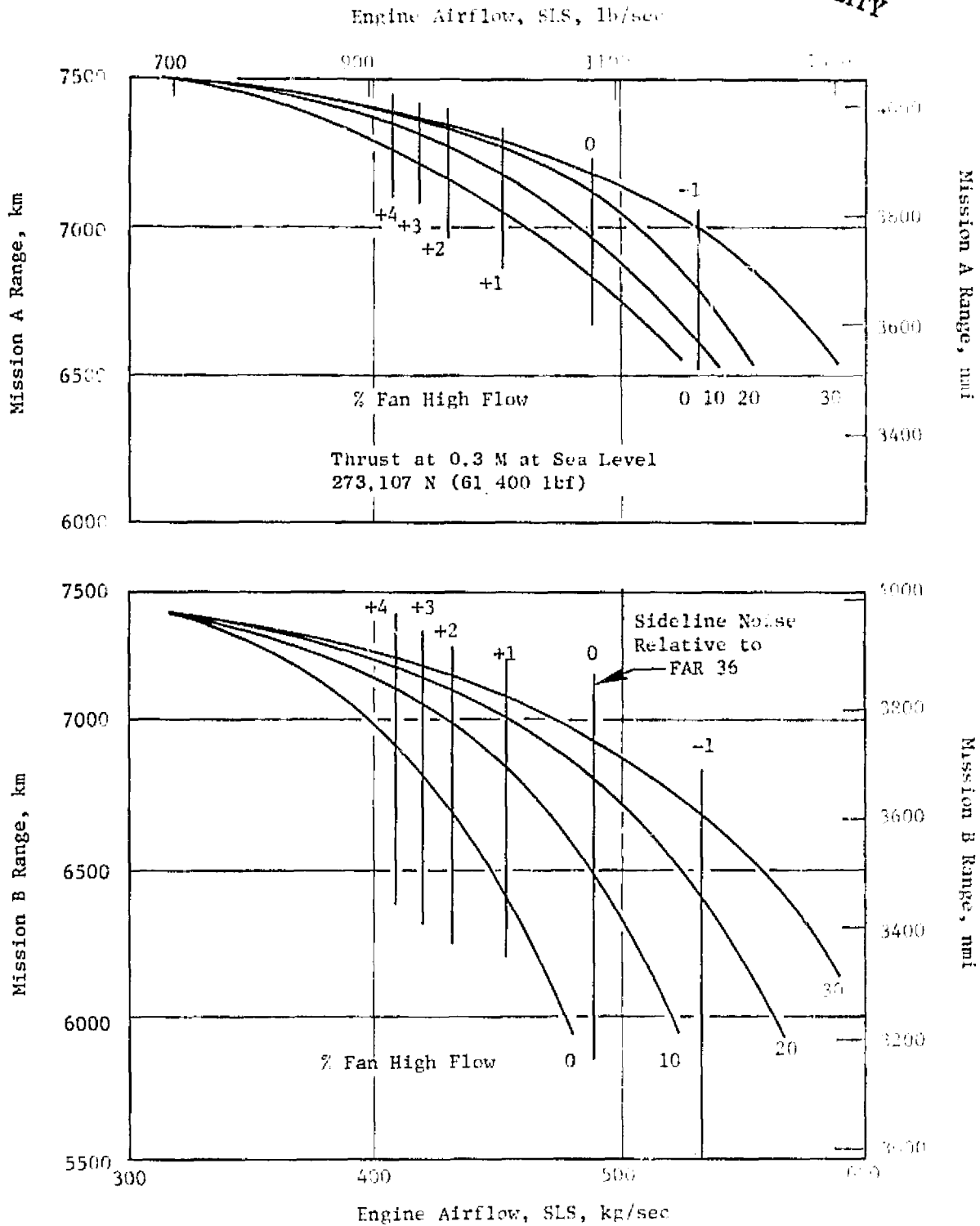
Figure 4. AST Mission Ranges - Effect of Fan High-Flowing.

using some amount of high-flowing (say 10% to 20%) in mission. However, a point of diminishing returns is reached as further high-flowing is used. The optimum amount of high-flowing will be sensitive to the engine total airflow size, which in turn is dependent somewhat on the noise level goal used in the study. The lower the noise goal (i.e., the quieter the engine is supposed to be), the larger the airflow size resulting, and the greater the payoff for using larger amounts of the high-flowing (see Figure 4).

4.1.5 Parametric Cycle Analysis

Figures 5 through 19 present results of a parametric analysis of a family of variable cycle engines having 30% high-flow fans. The 30% high-flow fan was selected based on results of studies conducted in Phase II (see NASA CR-134913 "Advanced Supersonic Propulsion System Technology Study - Phase II - Final Report").

The supersonic cruise installed maximum dry thrusts for the VCE matrix are shown for engine design BPR's of 0.35, 0.2, and 0.5 (Figures 5, 6, and 7). The thrust trend is to increase with the lower BPR, lower fan pressure ratio (relatively small effect), and lower overall pressure ratio. The engine selected from the matrix for further study is indicated by the dark circle in Figure 5.

The corresponding supersonic cruise installed sfc's (Figures 8, 9, and 10) exhibit an sfc trend which decreases with lower BPR, lower fan pressure ratio, and higher overall pressure ratio.

The subsonic cruise installed sfc's for a typical cruise thrust are shown for the same engine designs in Figures 11, 12, and 13. The sfc trend is to decrease with higher BPR, lower fan pressure ratio, and higher overall pressure ratio.

The relative engine weights are shown on Figures 14, 15, and 16. The engine weight trend is to decrease with higher BPR, higher fan pressure ratio, and higher overall pressure ratio.

The engine data, together with hold and climb/acceleration installed performance data, were incorporated in the mission analysis (described in Section 2.1.3). The mission relative ranges are shown for Mission B, which has a subsonic 1111 km (600 nmi) initial leg before supersonic cruise (Figures 17, 18, and 19). The configuration limit shown on Figure 17 is an engine LP turbine loading limit for a one-stage turbine. The range trend is best with BPR = 0.35 to 0.5, lower fan pressure ratio, and higher overall pressure ratio.

The performance characteristics of this VCE matrix (Figure 17 through 19) indicate that overall performance is achieved with values of BPR's in the 0.35 to 0.5 range for missions having some subsonic cruise. As missions vary toward an all-supersonic mission, the value of the best BPR will decrease and
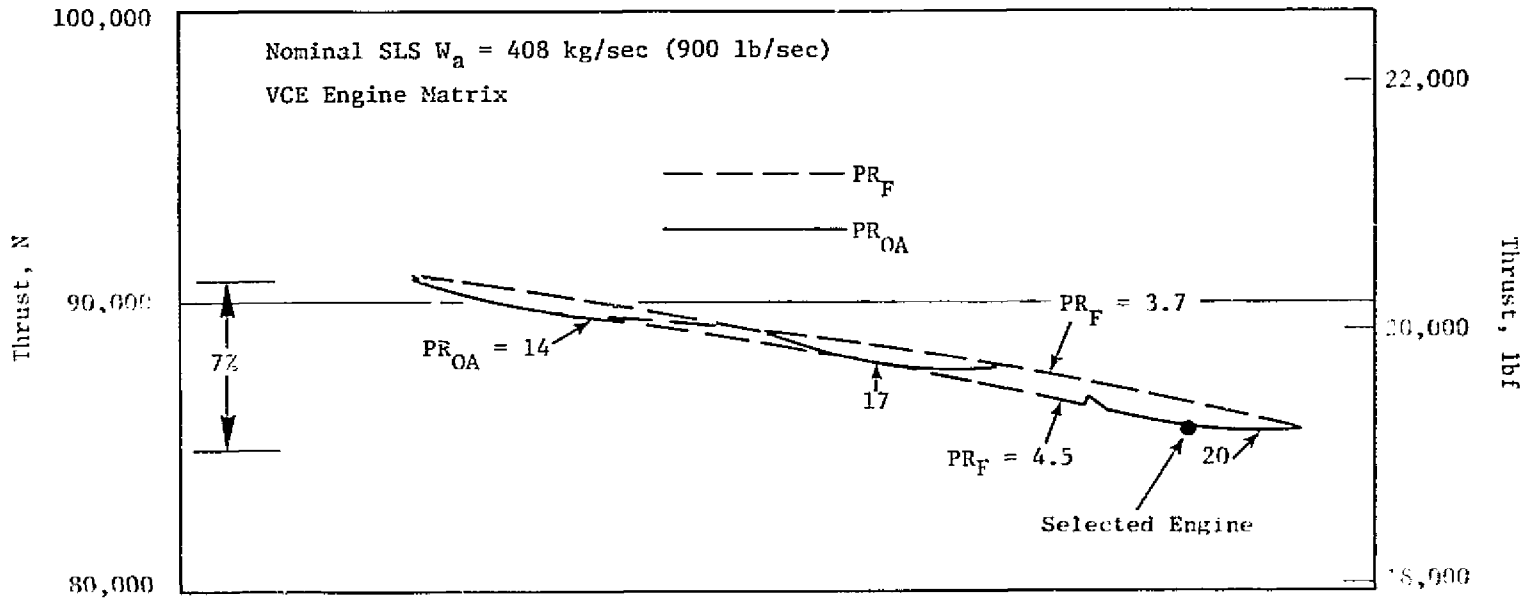
Figure 5. Dry Thrust Potential at Supersonic Cruise, BPR = 0.35.
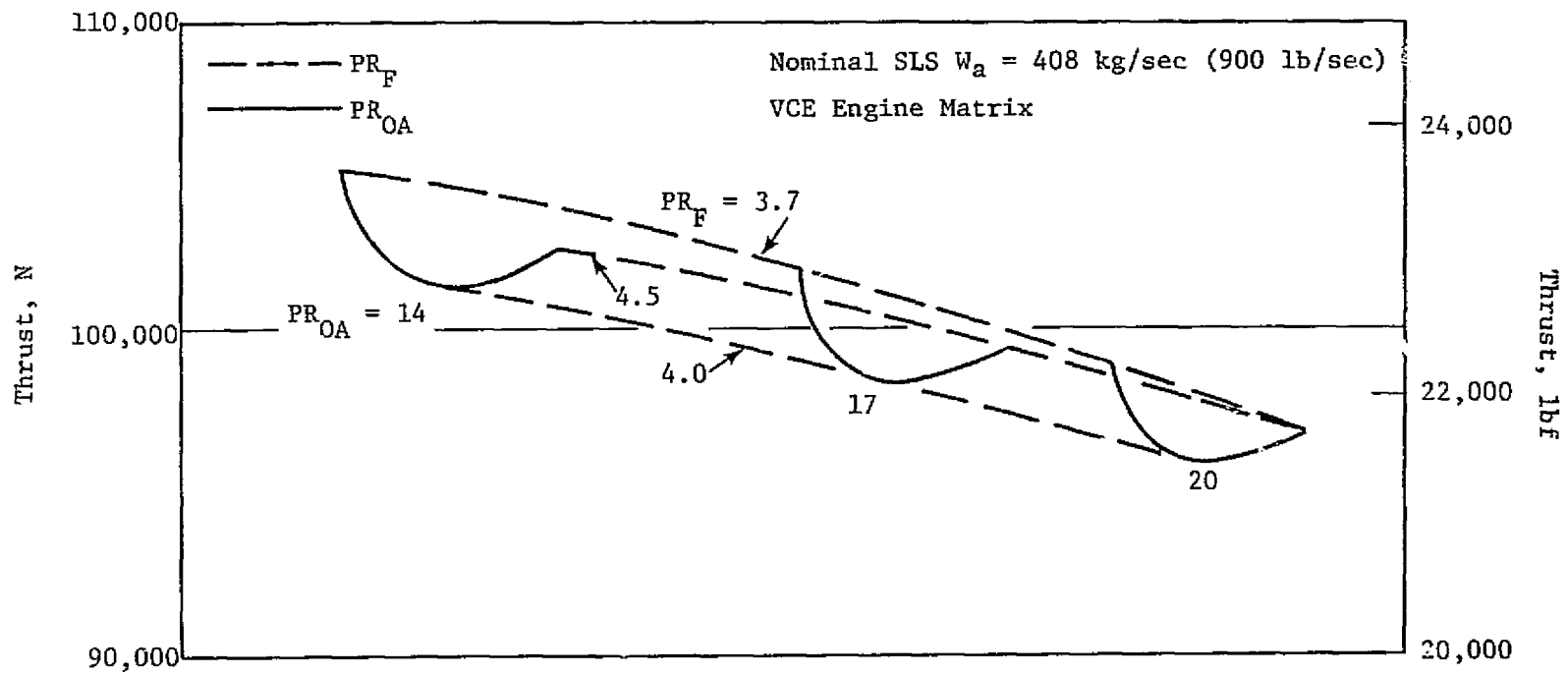
Figure 6. Dry Thrust Potential at Supersonic Cruise, BPR = 0.2.
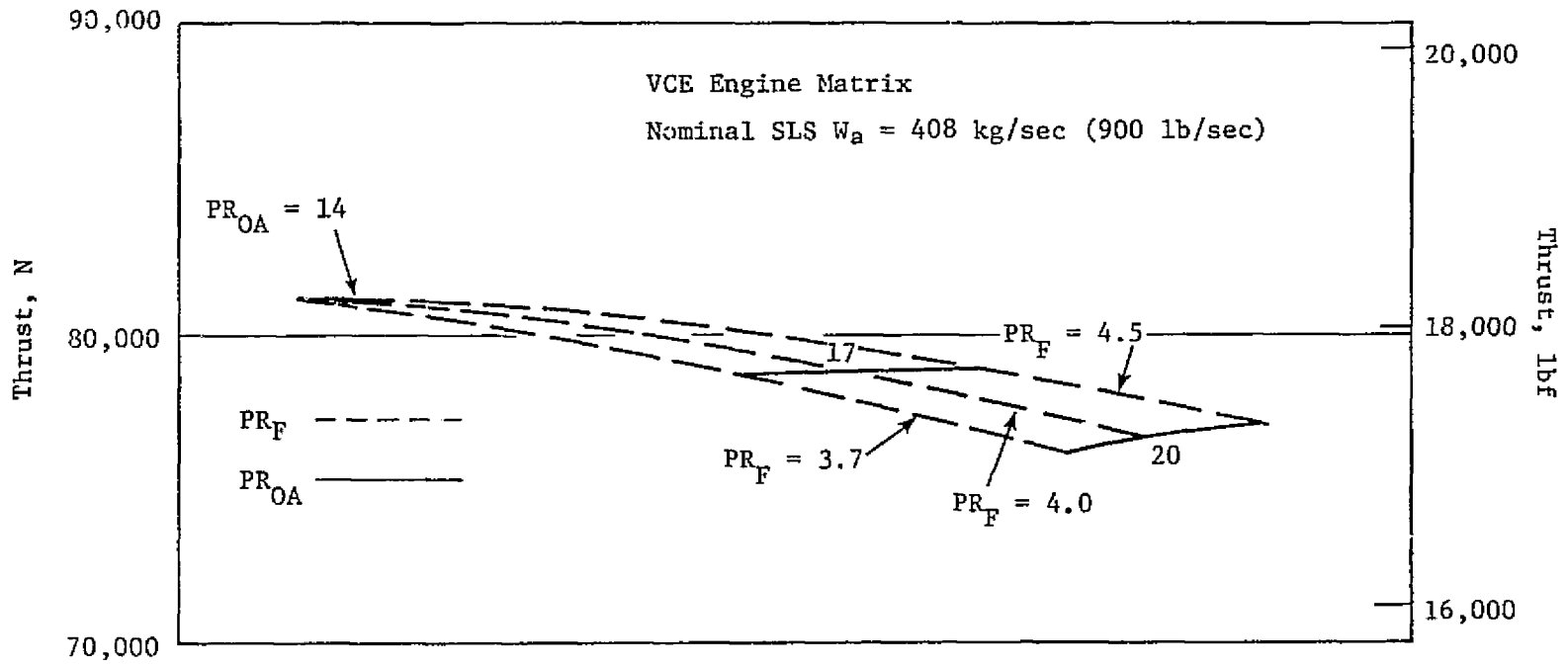
Figure 7. Dry Thrust Potential at Supersonic Cruise, BPR = 0.5.
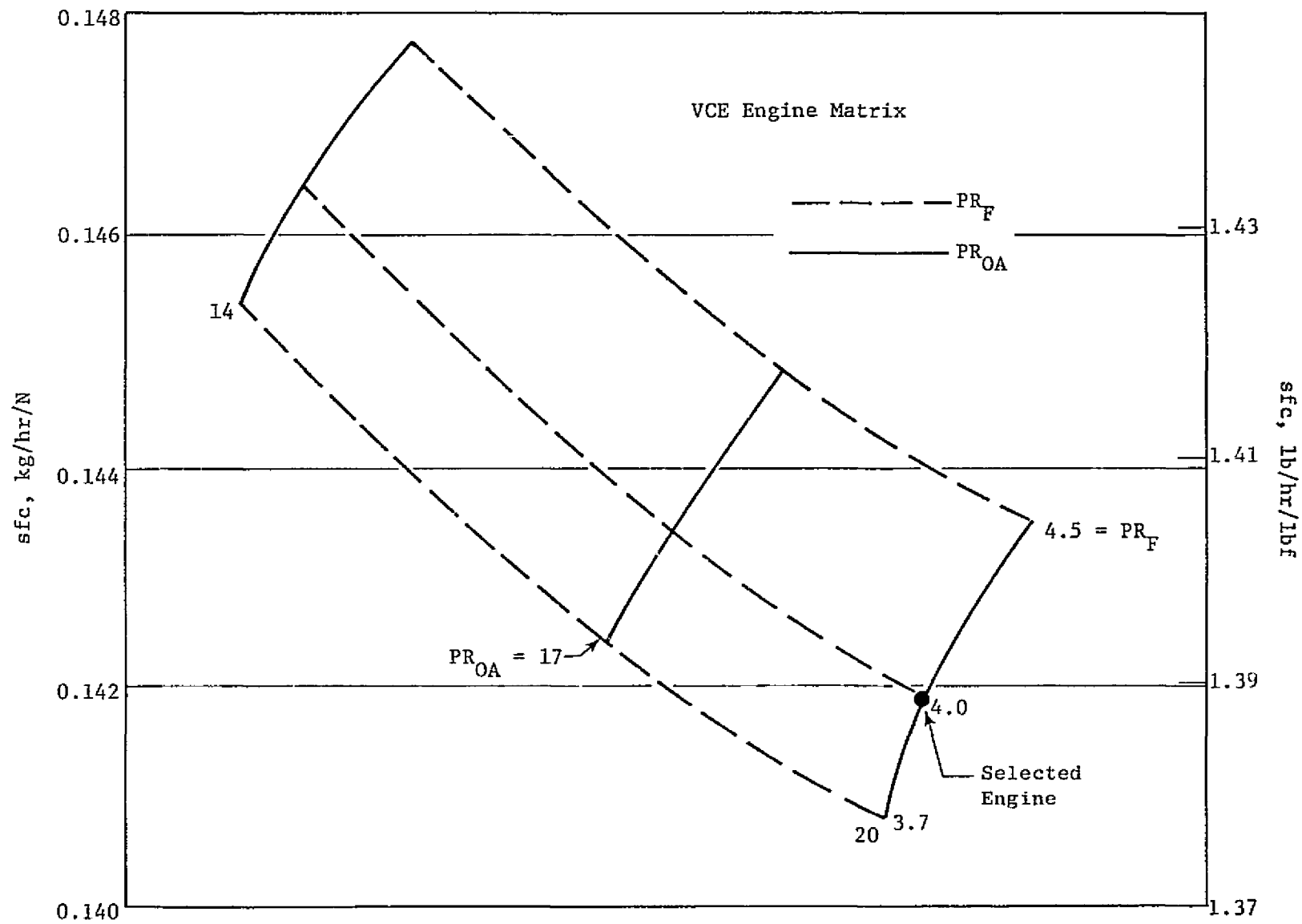
Figure 8. Supersonic Cruise SFC Comparison, BPR = 0.35.
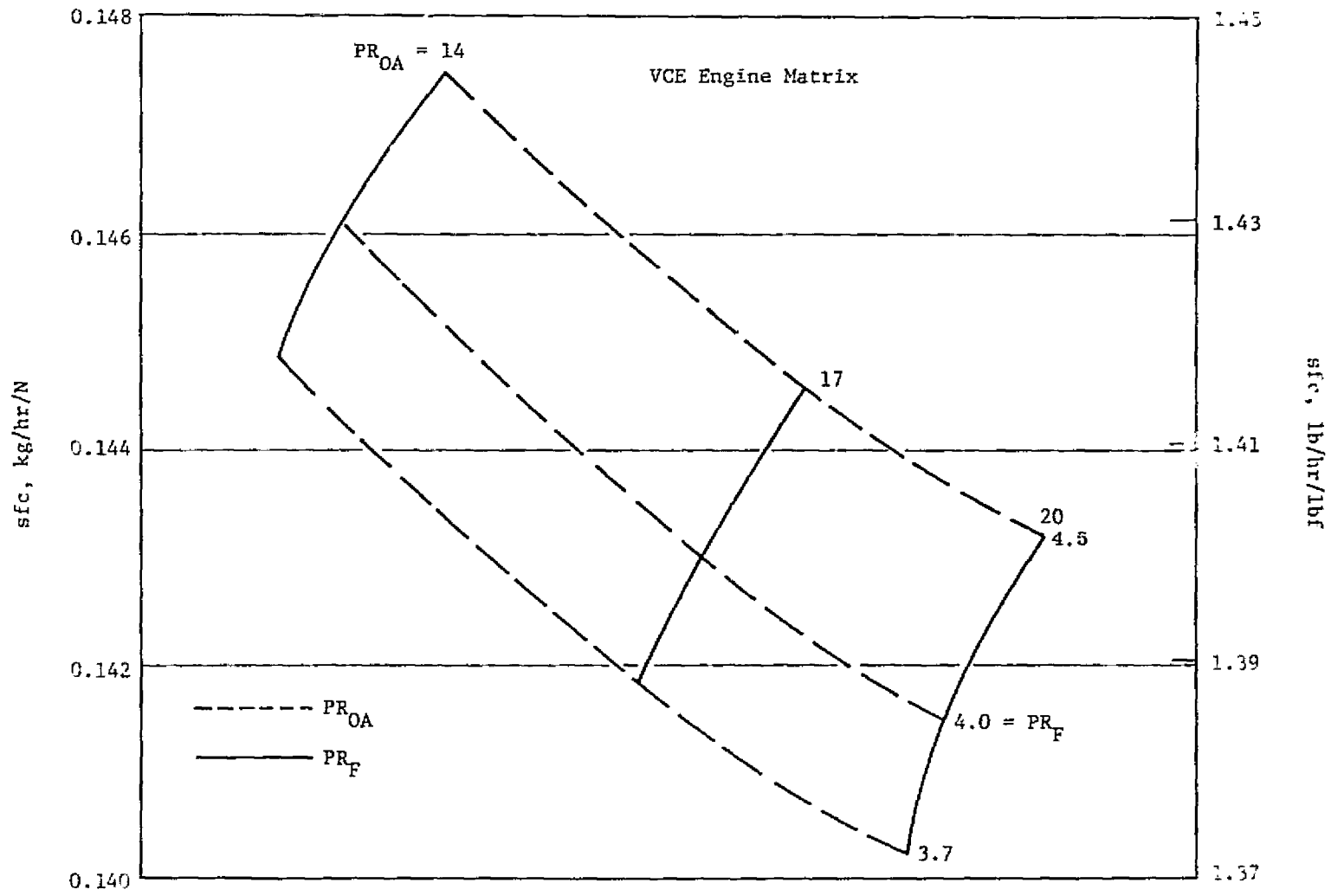
Figure 9. Supersonic Cruise SFC Comparisons, BPR = 0.2.
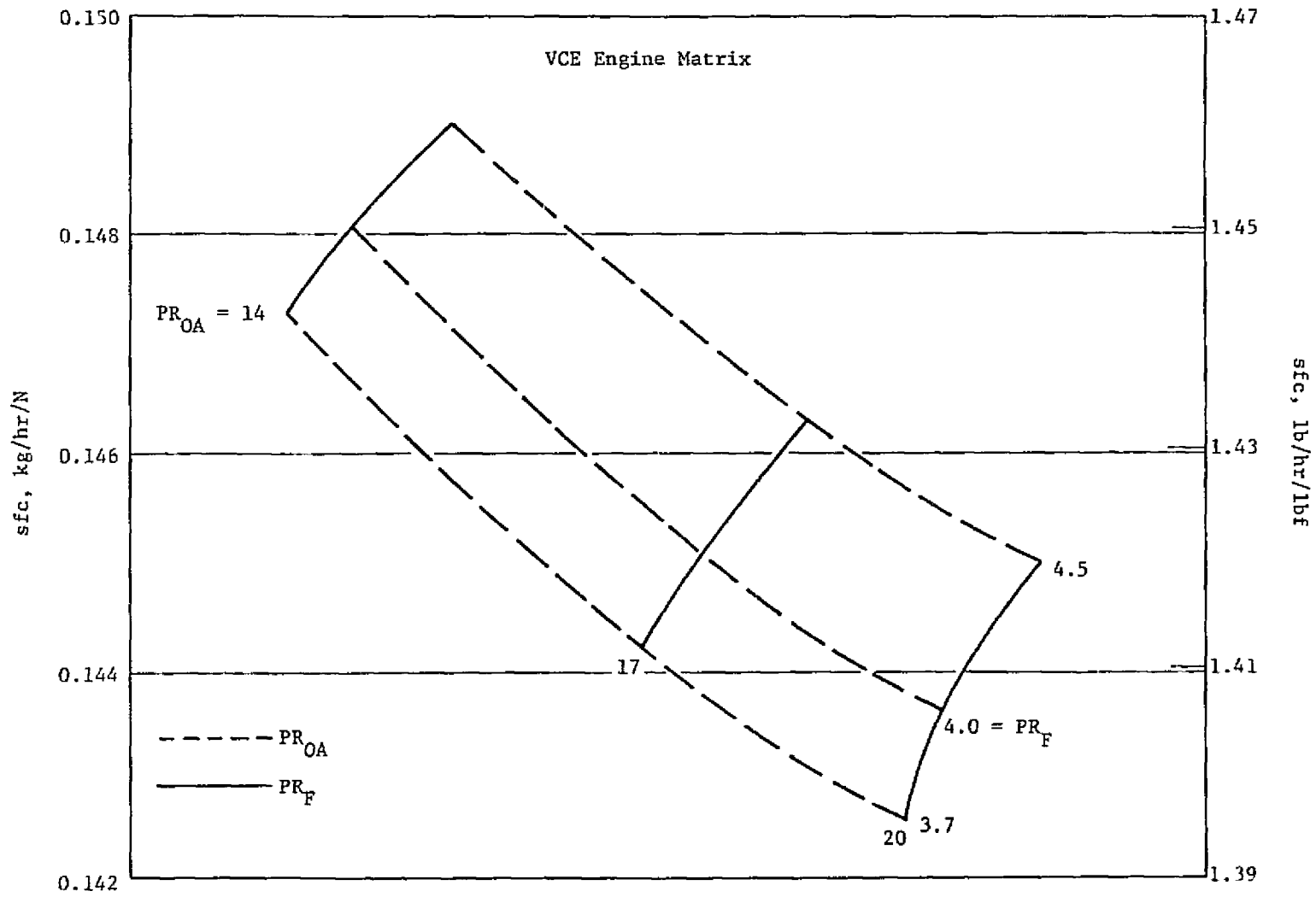
Figure 10. Supersonic Cruise SFC Comparisons, BPR = 0.5.
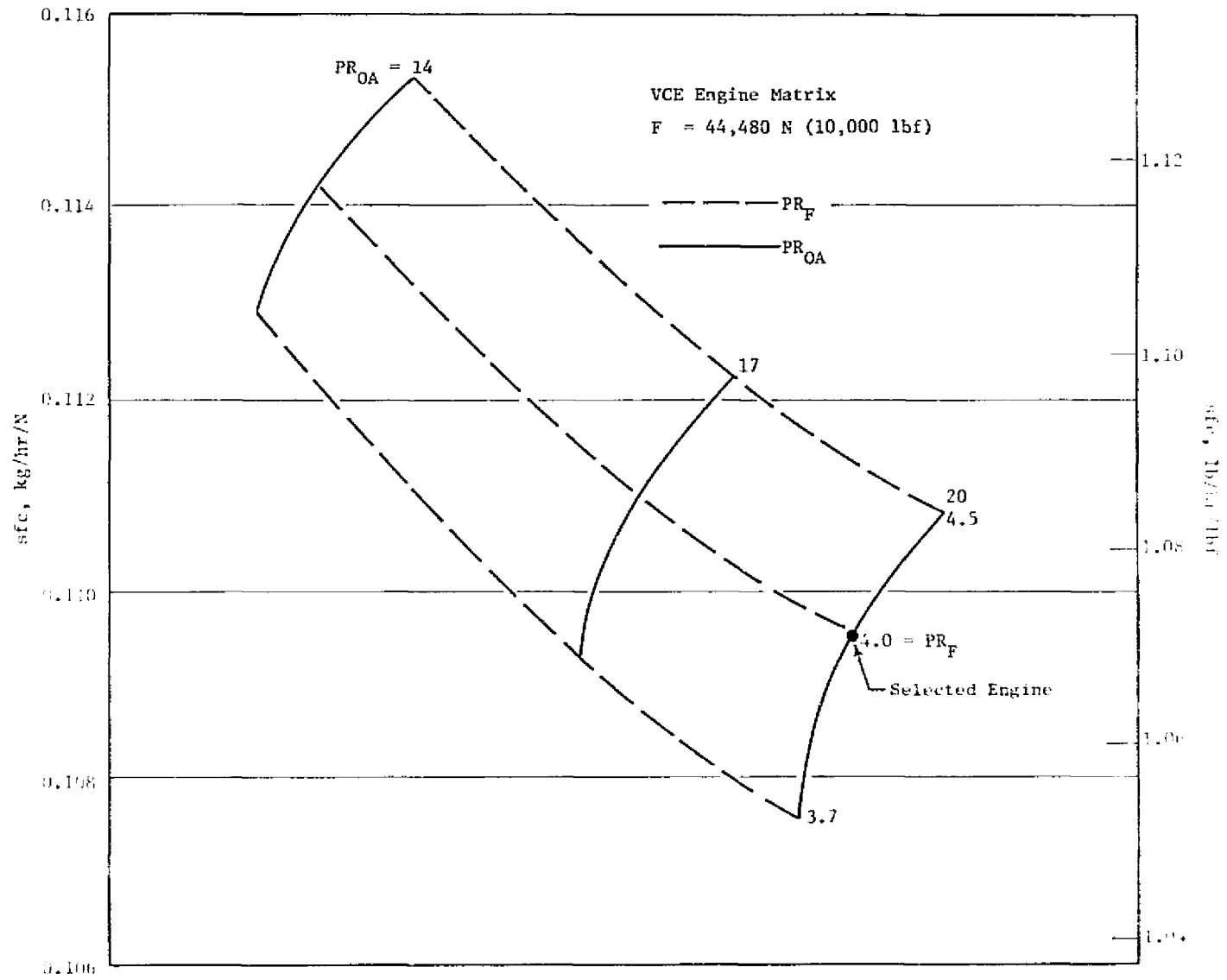
Figure 11.   Subsonic Cruise SFC Comparisons, BPF = 0.35.
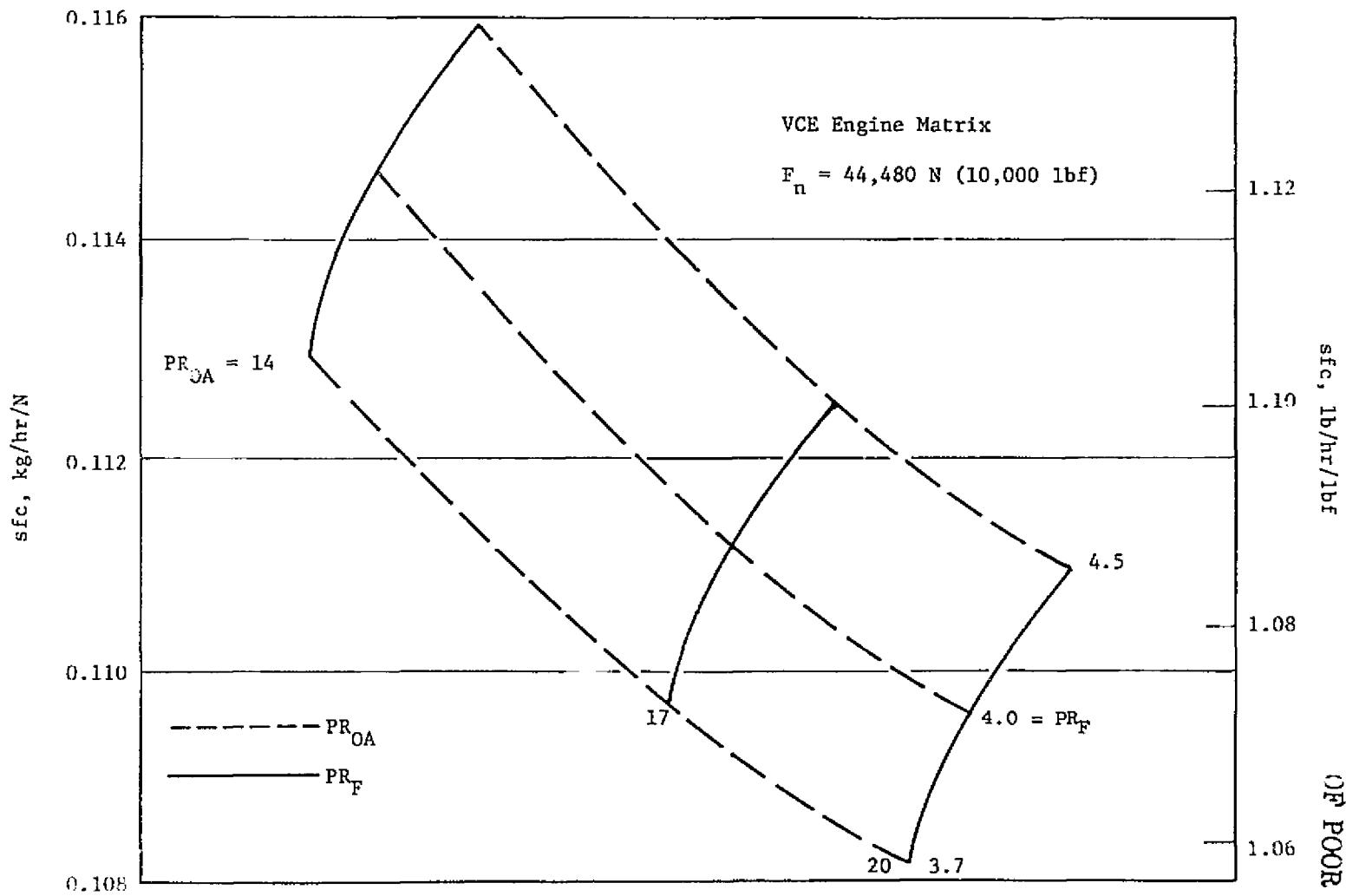
Figure 12. Subsonic Cruise SFC Comparisons, BPR = 0.2.
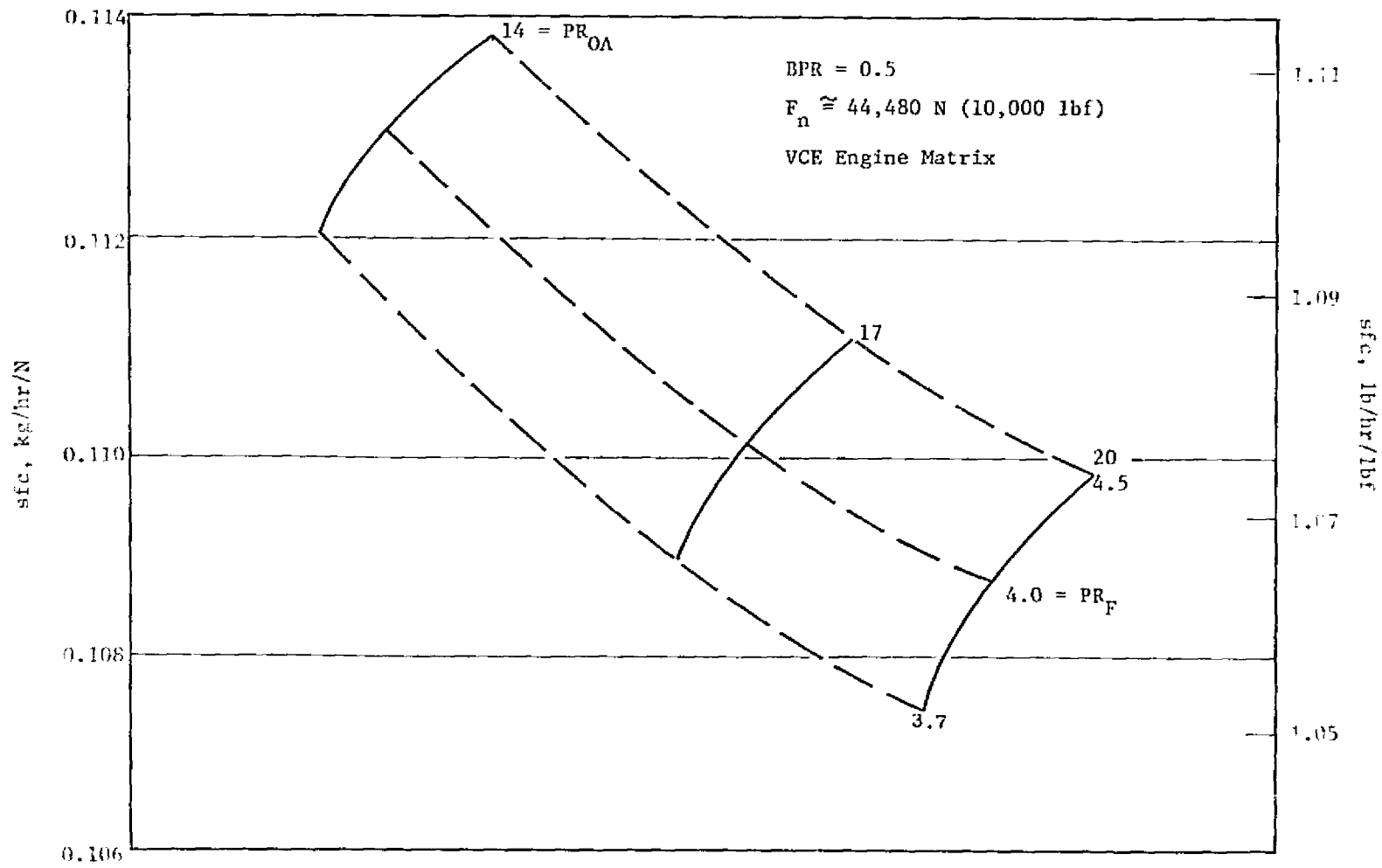
Figure 13. Subsonic Cruise SFC Comparisons, BPR = 0.5.
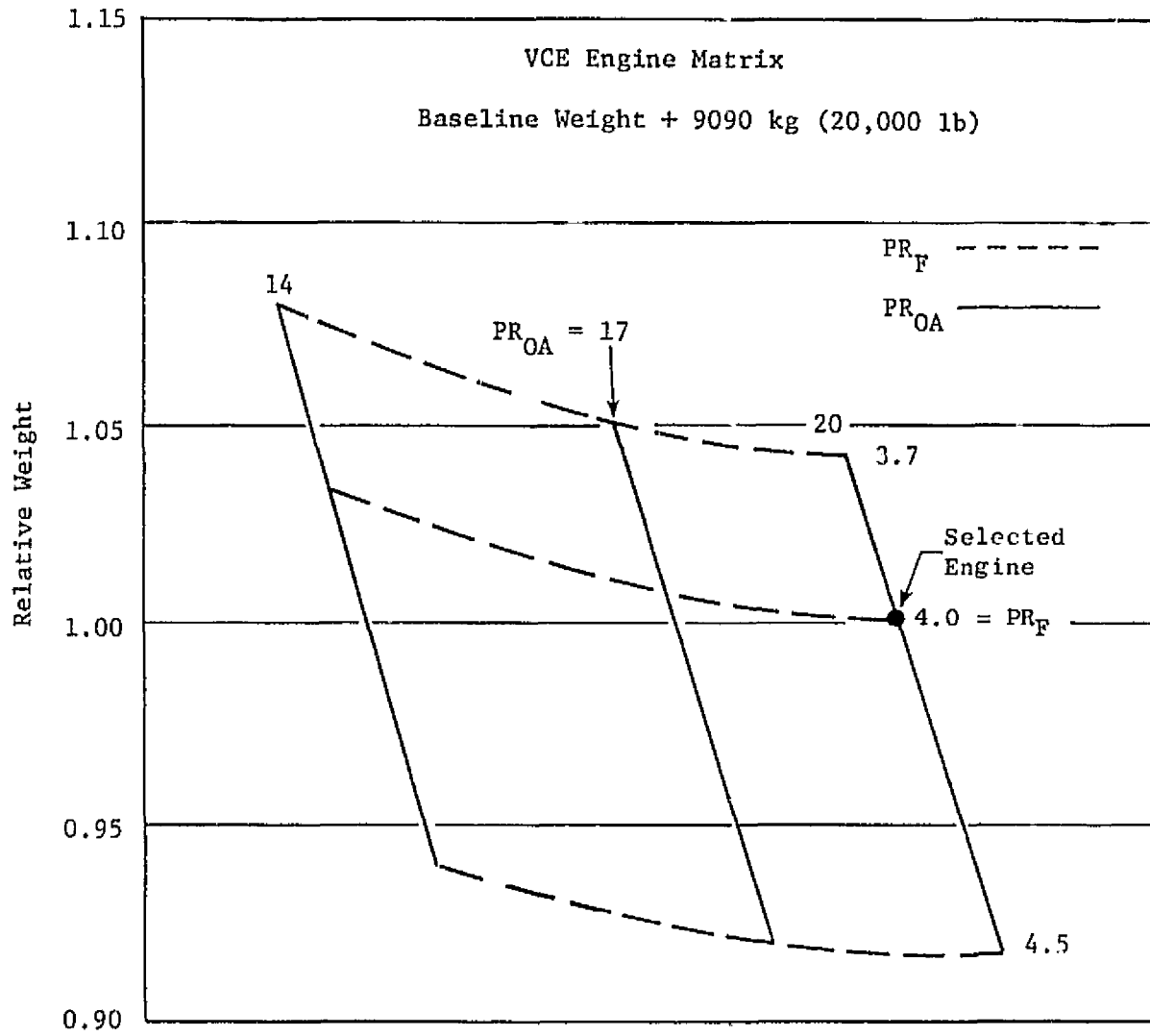
Figure 14. Relative Weight Comparisons, BPR = 0.35.
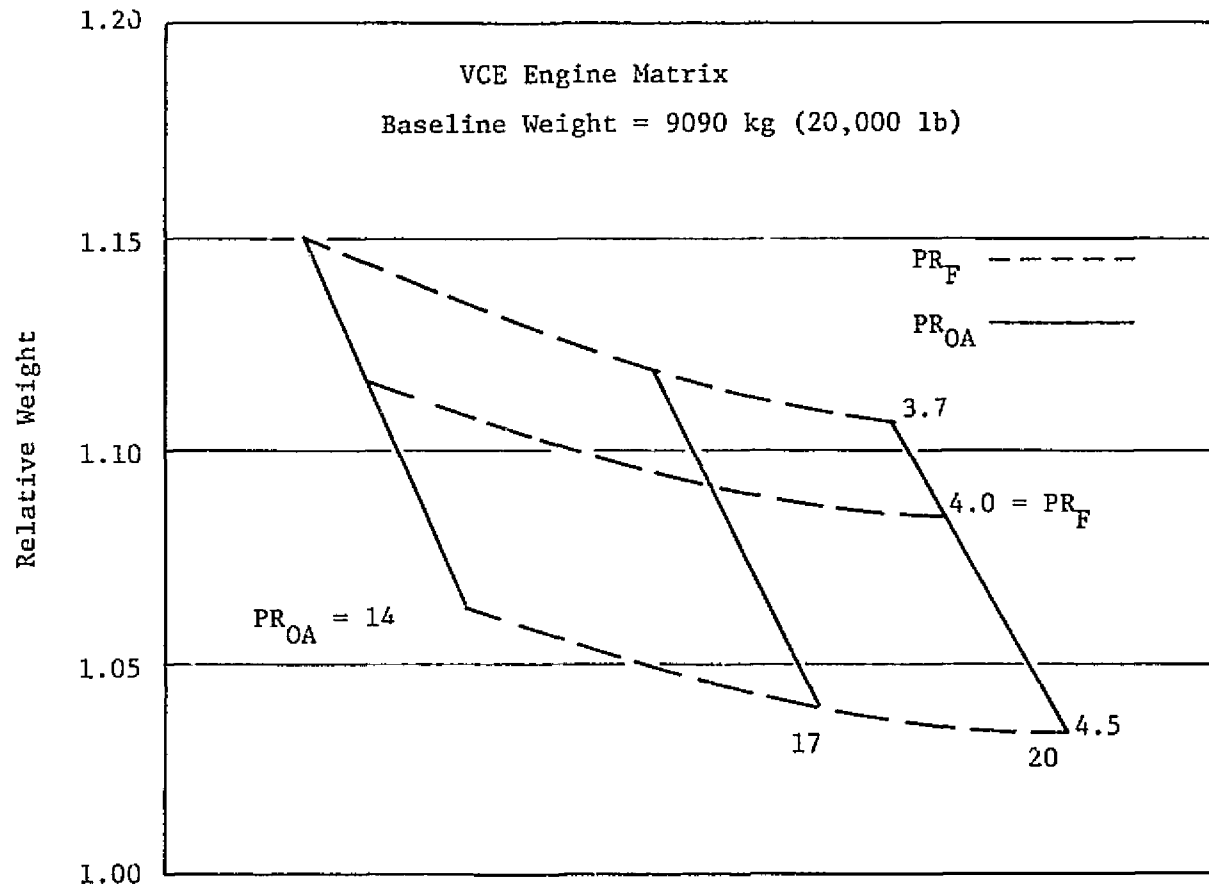
Figure 15. Relative Weight Comparisons, BPR = 0.2.
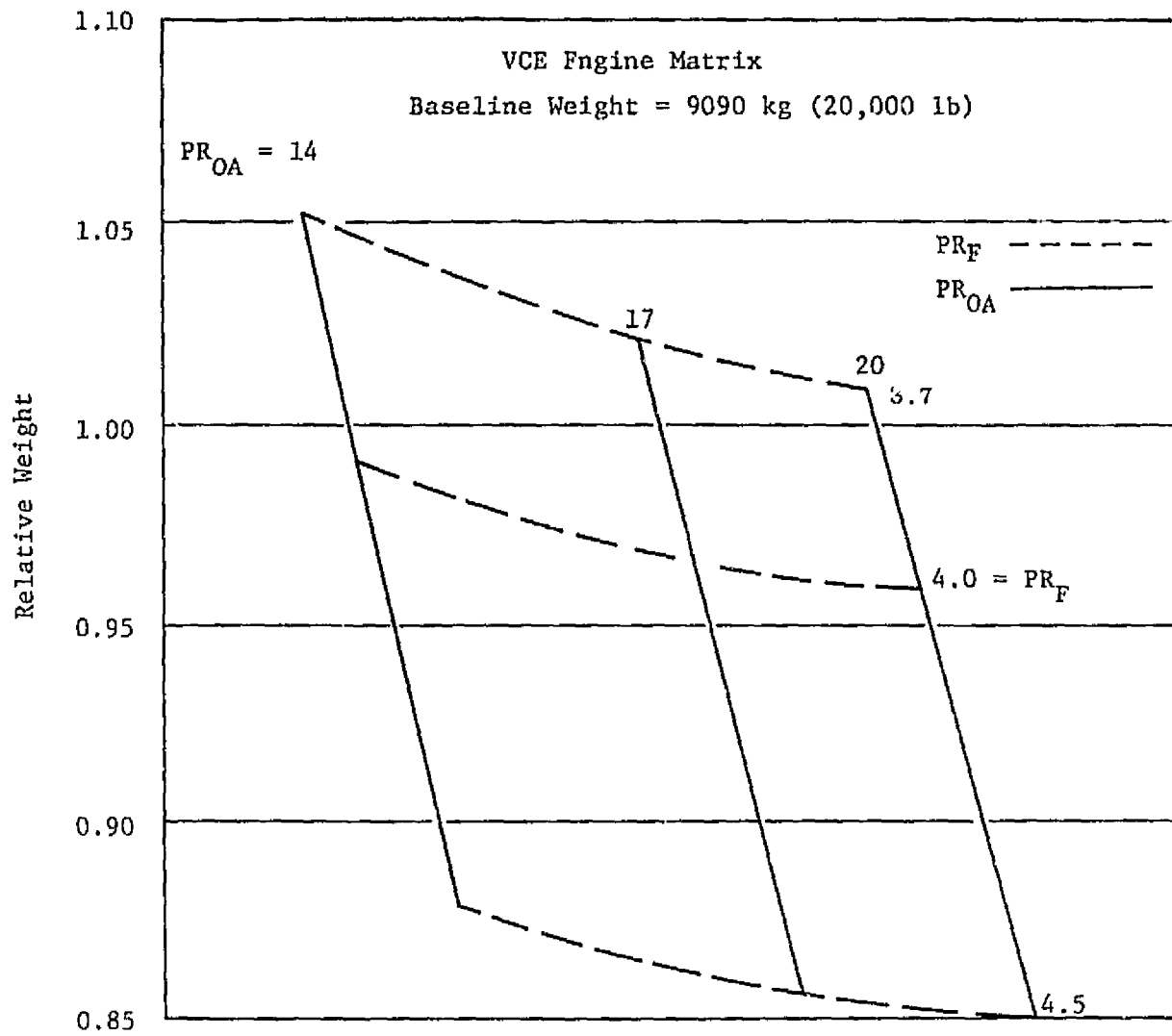
Figure 16. Relative Weight Comparisons, BPR = 0.5.
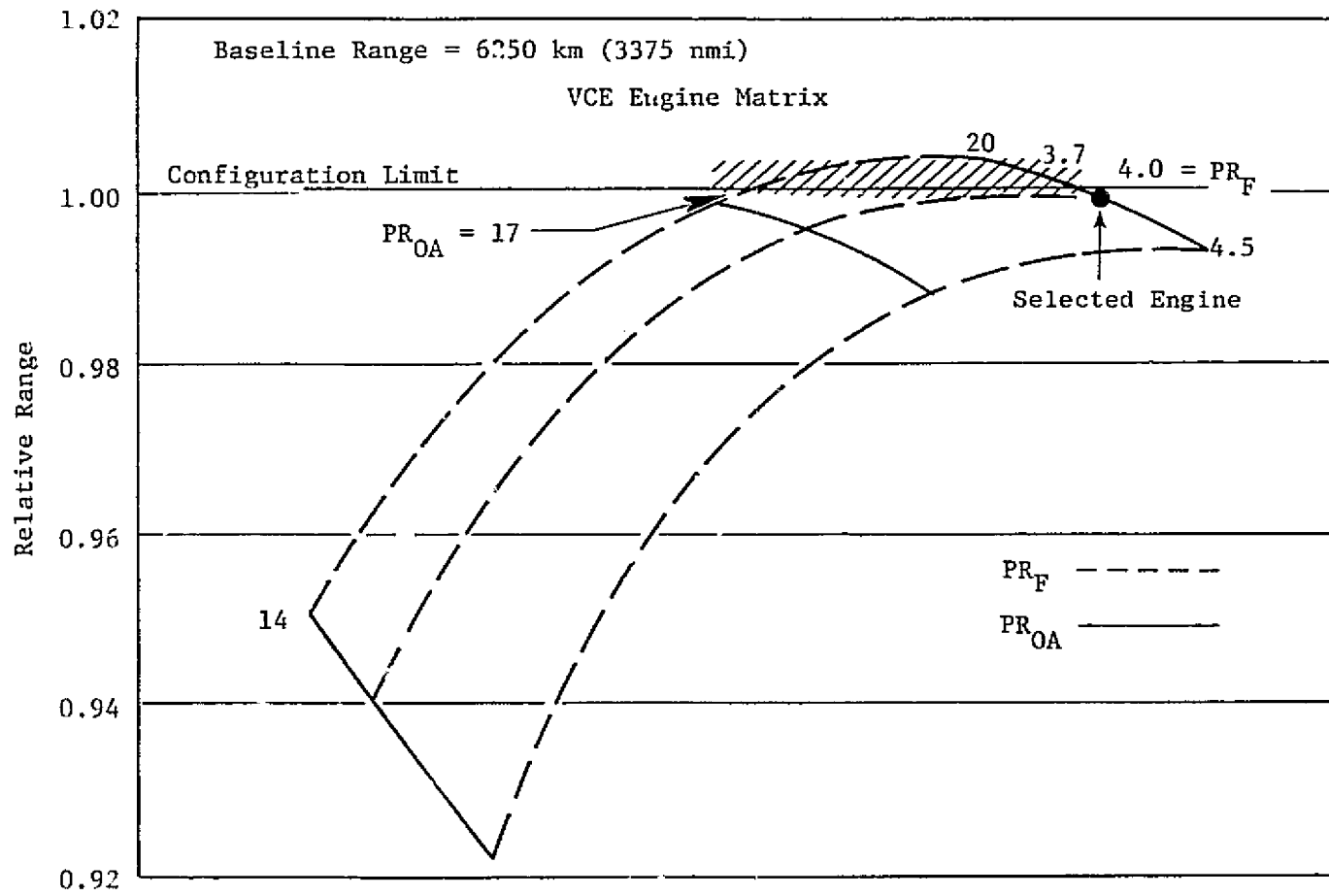
Figure 17.   Relative Range Potential, BPR = 0.35, 1111 km
(600 nmi) Initial Leg.
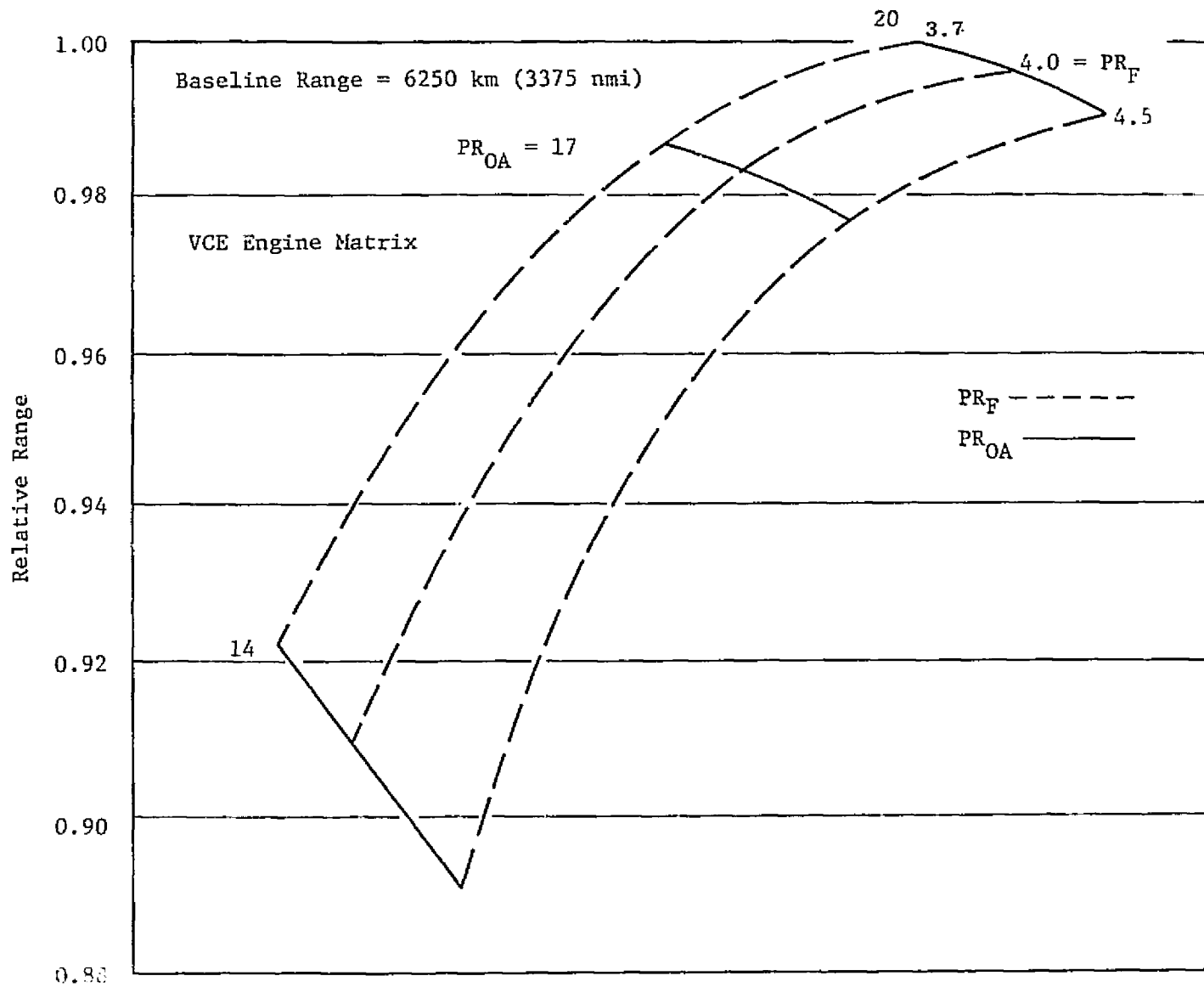
Figure 18.   Relative Range Potential, BPR = 0.2, 1111 km
(600 nmi) Initial Leg.
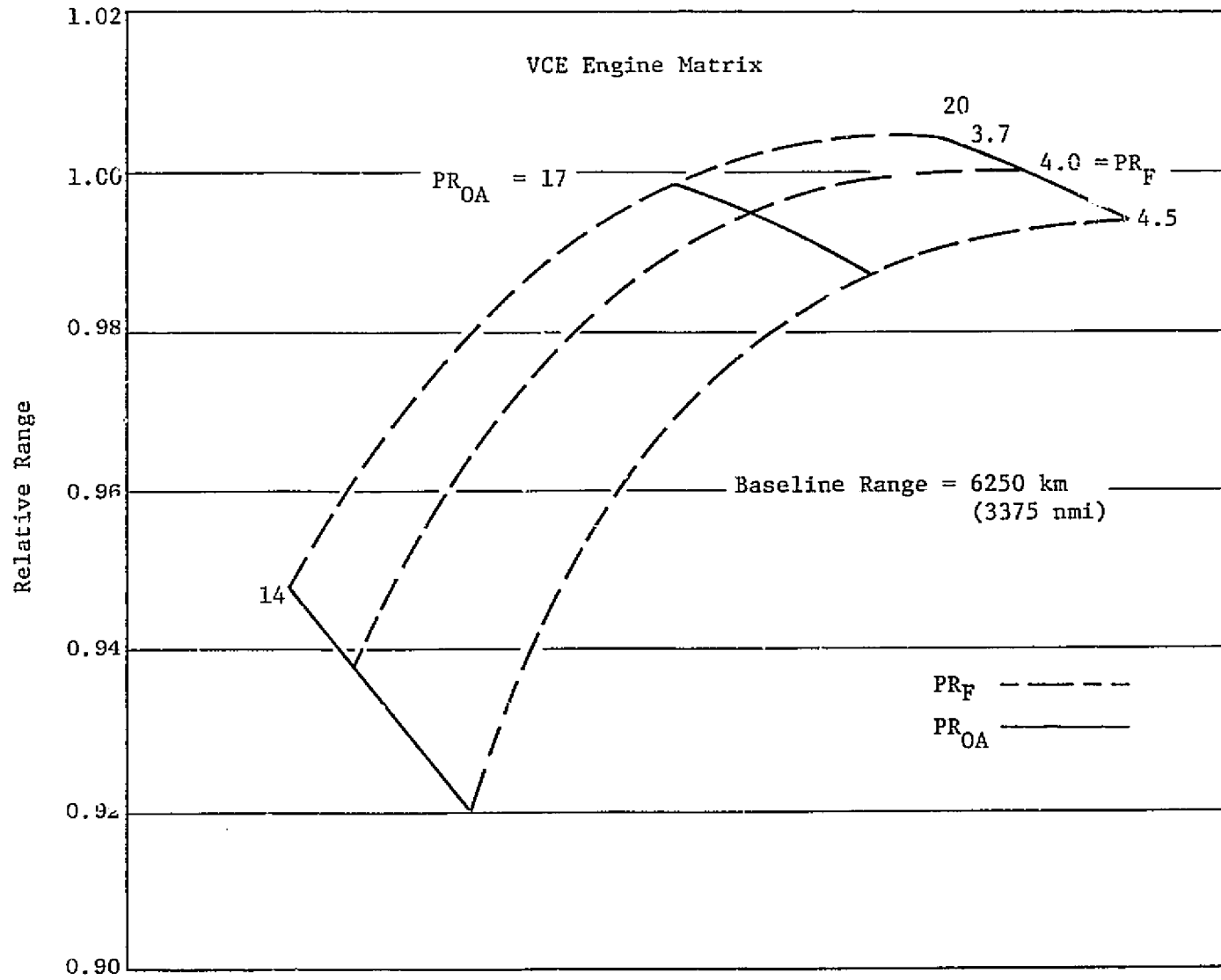
Figure 19. Relative Range Potential, BPR = 0.5, 1111 km (600 nmi) Initial Leg.

0.35 looks best for an all-supersonic mission. For this reason a BPR of 0.35 was selected for further analysis. The engine selected from the matrix which exhibited the best mission range is described on Table 2.

Additional double-bypass variable cycle engines with fan high-flow of 0%, 10%, and 20% were defined to complement the 30% high-flowed fan VCE selected from the previously described matrix study. The BPR of 0.35 and fan pressure ratio of 4.0 were maintained. However, the overall pressure ratio was reduced from 20 (30% high-flowed fan) to 17.5.

Installed engine performance and weights were input into the mission analysis program. The results are shown on Table 3. Mission range increases with increased fan high-flow at a specified FAR 36 noise level. As the required FAR 36 noise level is reduced, the range decreases. For a rotation, 0.3 M/SL, thrust of approximately 253,500 N (57,000 lb), the FAR 36 noise level is reduced approximately 1.5 dB for a VCE fan high-flow from 10% to 20% and approximately 1.0 dB from 20% to 30% (Table 4).

The influence of varying the amount of fan high-flow is illustrated in Figure 4 and is the result of an interplay between installed powerplant weight and cruise thrust sfc matching. As engine size becomes larger, the cruise mismatch becomes progressively worse and the penalty for a nonover-sized fan increases (or to put it another way, the advantages of an oversize fan are increased).

4.1.6 Double-Bypass Study Engine Definition for Airframe Companies and NASA

Detailed evaluation of aircraft company aircraft characteristics revealed that our previous variable cycle engines were not matched properly to the aircraft companies' aircraft. For example, in some cases less take-off thrust was required. In our aircraft studies, climb thrust was not con-sidered to be important and therefore we did not attempt to get maximum thrust during climb. Also, in our studies cruise thrust was not as important as with the aircraft companies. Evaluation of these differences indicated that a VCE with high-flowing of 10% or 20% would be satisfactory. Therefore, the VCE's with the 10% and 20% high-flowed fans were redefined to match each airframe company's airflow schedule and thrust requirements at the appro-priate supersonic cruise design Mach number.

A VCE with a 20% high-flowed fan was defined for NASA Studies at 2.62 design Mach number. Engine performance, dimensions, and weights were pro-vided to the airframe companies and to NASA in brochures and card packs (Table 5). The J11B9, J11B11, and J11B12 VCE's include changes in fan and compressor efficiencies and in turbine cooling flow relative to the prior VCE's to be consistent with configuration changes. These engines were also defined at a lower BPR of 0.25 (the other VCE's were 0.35) and a lower fan pressure ratio of 3.7 (the other VCE's were 4.0) to better match the Boeing and Lockheed inlet characteristics and thrust requirements. All VCE's incor-porate component design and materials of 1985 technology level, improved

Table 2. Selected VCE at 30% High-Flowed Fan.

- Engine Cycle

  Airflow, kg/sec, (lb/sec)   408-530, (900-1170)

  Fan Pressure Ratio   4.0

  Overall Pressure Ratio   20

  Bypass Ratio   0.35

  Max. Turbine Rotor Inlet   1538 (2800)
  Temperature, T_{41} ° C, (° F)

- Engine Design, 2.4 M

  2.32 M Max. Dry Uninstalled   93,408 (21,000)
  Thrust, N (lb)

  2.32 M Corrected Airflow   263 (580)
  kg/sec (lb/sec)

  0.3 M/SL/+27° F Thrust at   273,552 (61,500)
  FAR 0, N (lb)

Table 3. Mission Results of High-Flowed Fans.

Ground Rules – 1111 km (600 nmi) Initial Subsonic Leg
NASA M = 2.4 Aircraft TOGW
of 345,643 kg, (762,000 lb)

Effect on Range

	Fan High-Flow			
408 kg/sec (900 lb/sec) Total Takeoff Flow	0%	+10%	+20%	+30%
Noise ∿ FAR 36 + 4				
Range km, (nmi)	6907 (3730)	7111 (3840)	7185 (3880)	7204 (3890)
490 kg/sec (1080 lb/sec) Total Takeoff Flow				
Noise ∿ FAR 36				
Range km, (nmi)	5778 (3120)	6463 (3490)	6797 (3670)	6926 (3740)

Table 4. Fan High-flow Study.

(~Equivalent Thrust – Lower Noise)

At Rotation	% Fan High-Flow		
	10%	20%	30%
$W\sqrt{\theta/\delta}$ kg/sec (lb/sec)	449 (990)	490 (1080)	531 (1170)
$W_{jet\ hot}$ kg/sec (lb/sec)	366 (806)	313 (690)	289 (637)
$V_{jet\ hot}$ m/sec (ft/sec)	750 (2460)	738 (2420)	741 (2430)
$W_{jet\ cold}$ kg/sec (lb/sec)	88 (194)	184 (405)	245 (541)
$V_{jet\ cold}$ m/sec (ft/sec)	478 (1570)	466 (1530)	460 (1510)
$V_{j\ cold}/V_{j\ hot}$	0.64	0.63	0.62
$W_{j\ cold}/W_{j\ hot}$	0.24	0.59	0.85
Thrust N (lbf)	254,650 (57,250)	252,910 (56,860)	255,760 (57,500)
Relative FAR 36 Noise	+1.5 dB	Base	-1.0 dB
Range km (nmi)	6852 (3700)	6797 (3670)	6686 (3610)

Table 5. AST Engine Study Data.

Company	Engine	Description
Douglas		
	J11B2	VCE, 2.2 M, +20% Fan
	J11B6	VCE, 2.2 M, +10% Fan
	J11B10	VCE, 2.2 M, +10% Fan
Boeing		
	J11B3	VCE, 2.32 M, +20% Fan
	J11B5	VCE, 2.32 M, +10% Fan
	J11B9	VCE, 2.32 M, +10% Fan
Lockheed		
	J11B1	VCE, 2.55 M, +20% Fan, Inlet No. 1
	J11B4	VCE, 2.55 M, +20% Fan, Inlet No. 2
	J11B8	VCE, 2.55 M, +10% Fan, Inlet No. 2
	J11B1	VCE, 2.55 M, +20% Fan, Inlet No. 3
	J11B11	VCE, 2.55 M, +10% Fan, Inlet No. 2
	J11B12	VCE, 2.55 M, +10% Fan, Inlet No. 1
NASA	J11B7	VCE, 2.62 M, +20% Fan

Data was provided in Brochures and Card Packs during NASA Phase III
and Engine Airframe Integration Studies.

aerodynamic flowpaths, and advanced electronic controls. Current technology dual-cycle engines, J10B1 and J10B2, were provided to Boeing and Douglas for consideration as baseline engines in their studies.

The Douglas VCE's utilized fans of 20% and 10% highflow at a bypass ratio of 0.35 (Table 6). The Douglas axisymmetric inlet airflow was matched during climb/acceleration operation with the J11B2 and J11B6 engines (Figure 20). The J11B10 corrected airflow at 2.2 M is 17% higher than the J11B2 and J11B6 and consequently the inlet capture area is 17% larger. The J11B10 engine airflow is less than the inlet airflow supply at flight Mach numbers below 1.9 as a result of this supersonic sizing. The slight increase in inlet drag is not important or significant. At supersonic cruise, 2.2 M/18288 m (60000 ft)/ Standard Day, the J11B2 and J11B6 have essentially the same installed thrust and specific fuel consumption, (Figure 21). The J11B10 provides 15% additional dry thrust at 2.2 M at 4.6% less sfc. The Douglas airplane/mission performance improved 13% on range with the J11B10 engine relative to the J11B2 engine.

The engines studied by Boeing had fans of 10% and 20% highflow and bypass ratios of 0.35 and 0.25 as shown in Table 7. The J11B3, J11B5, and J11B9 engine airflows and Boeing inlet were matched over the range of climb/acceleration Mach numbers (Figure 22). At supersonic cruise, 2.32 M/16319 m (53540 ft) Standard Day +8° C (+14.4° F), the installed thrust and sfc of the J11B3 (20% high-flowed fan) and J11B5 (10% high-flowed fan) are approximately equal (Figure 23). The J11B9 provides 23% more thrust and 3.4% less sfc at the maximum dry power setting. The better supersonic cruise performance of the J11B9 is attributed primarily to the lower design BPR (0.25) and increased airflow, 231 kg/sec (510 lb/sec), which resulted in engine operation at 2.32 M at a BPR nearer to that of a turbojet. At 2.32 M, each of the engines operate to a compressor discharge temperature less that 649° C (1200° F) and at a turbine rotor inlet temperature of 1482° C (1700° F). The Boeing airplane/mission range improved approximately 852 km (460 nmi) with the J11B9 over the range with the J11B5.

The double-bypass VCE's studied by Lockheed were matched to 2-D over-wing and under-wing inlet characteristics. The J11B1 and J11B4 are the same engine operating to the two respective inlet characteristics. A similar relation exists between the J11B11 and J11B12 engines and inlets.

The J11B1 and J11B4 engines have a 20% high-flowed fan and design BPR of 0.35 (Table 8). The supersonic cruise, 2.55 M/18288 m (60000 ft)/Standard Day +8° C (+14.4° F), better performance of the J11B4 relative to the J11B1 is due to the higher inlet ram recovery of the under-wing inlet (Figure 24). The inlet/engine airflows were matched over the range of climb/acceleration Mach numbers (Figure 25). The over-wing inlet/engine performance provided approximately 20% more climb/acceleration thrust than the under-wing inlet (Figure 26). At subsonic cruise, 0.35 M/10668 m (35000 ft), use of the over-wing inlet resulted in a 2.2% lower installed sfc (Figure 27). At hold, 0.5 M/4572 m (15000 ft), use of both inlets resulted in the same installed performance (Figure 28).

48

Table 6. Engines Studied by McDonnell Douglas.

GE21 Engine	J11B2	J11B6	J11B10
Sea Level Static			
W1R, kg/sec (lb/sec)	317/381 (700/840)	317/349 (700/770)	317/349 (700/770)
Fan PR	4.0	4.0	3.7
Overall PR	17.3	17.3	17.4
BPR	0.35	0.35	0.35
2.2 M/18,290 m (60,000 ft)/Std Day			
W1R, kg/sec (lb/sec)	222 (490)	222 (490)	260 (573)
Relative Inst. Fn Dry	Base*	1.025	1.182
Relative Inst. sfc Dry	Base	1.00	0.954
0.3 M/SL/+10° C (18° F)			
W1R, kg/sec (lb/sec)	381 (840)	349 (770)	349 (770)
Inst. Fn Dry, N(lbf)	201,230 (45,240)	199,890 (44,940)	219,060 (49,250)

*Base Thrust = 57,895 N (13,016 lbf)
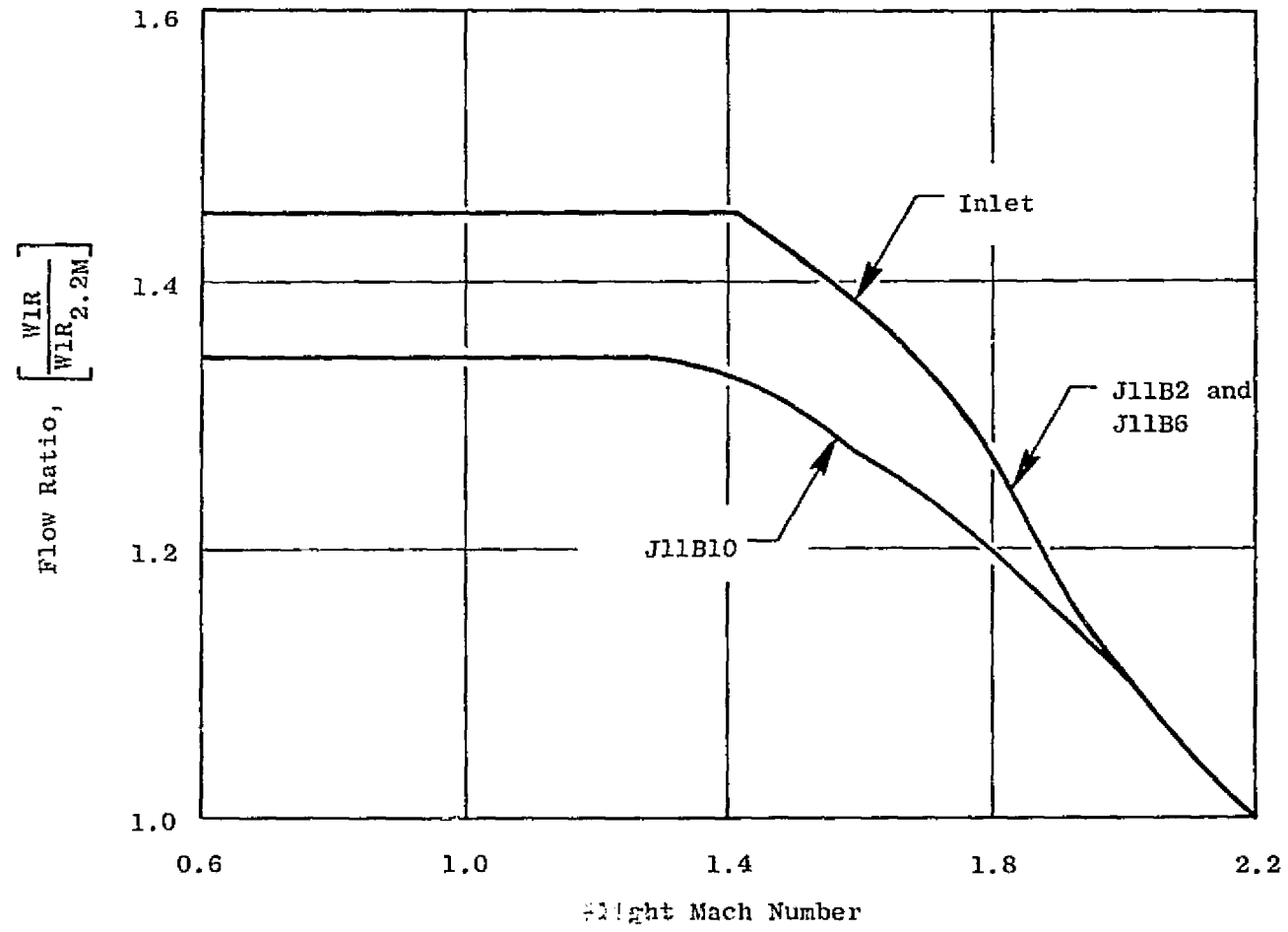
Figure 20. McDonnell Douglas Axisymmetric Inlet/Engine Airflow Match.
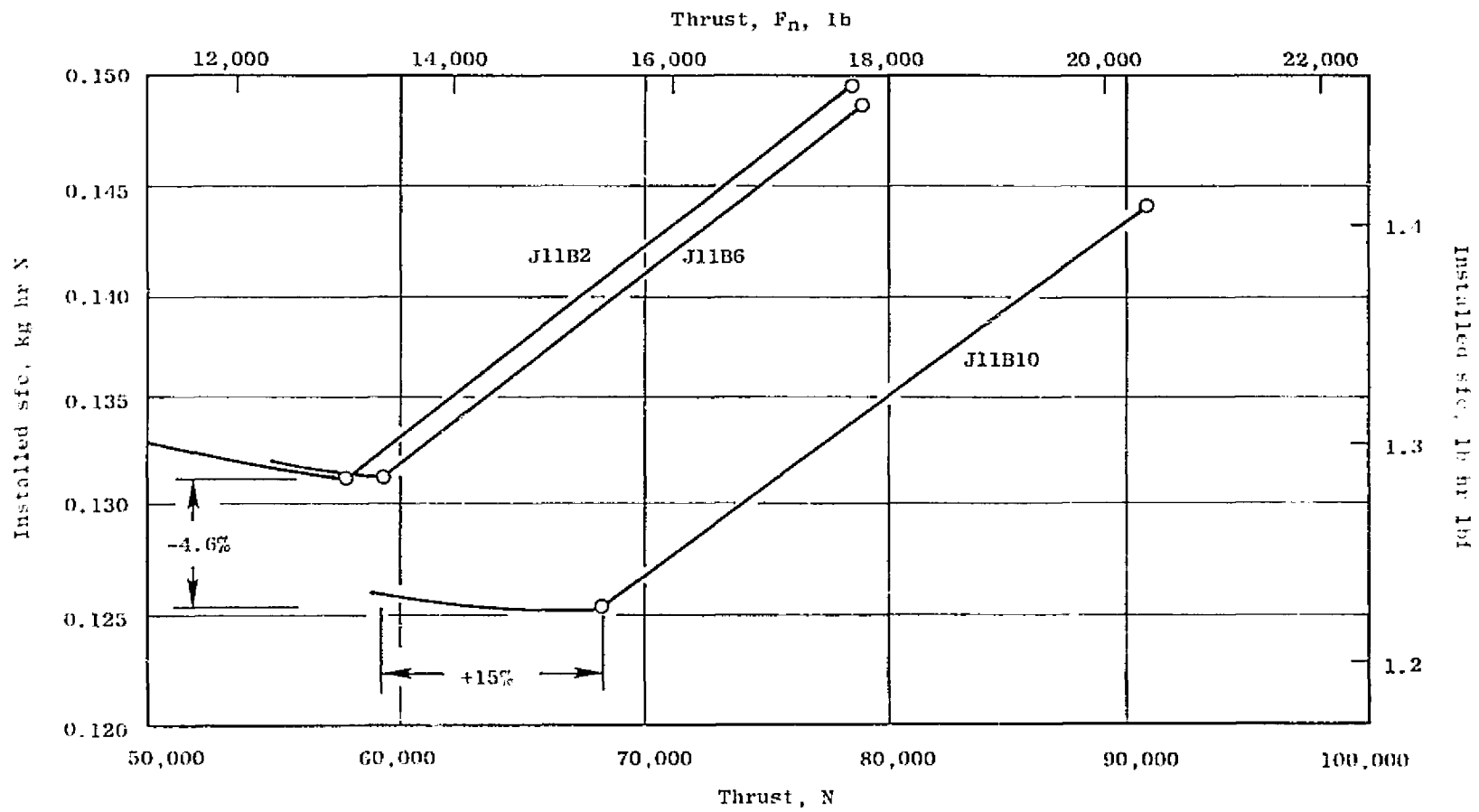
Figure 21. McDonnell Douglas Supersonic Cruise SFC.

Table 7. Engines Studied by Boeing.

GE21 Engine	J11B3	J11B5	J11B9
Sea Level Static			
W1R, kg/sec (lb/sec)	317/381 (700/770)	317/349 (700,840)	317/349 (700/770)
Fan PR	4.0	4.0	3.7
Overall PR	17.3	17.3	16.1
BPR	0.35	0.35	0.25
2.32 M/16,320 m (53,540 ft)/ +8° C (+14° F)			
W1R, kg/sec (lb/sec)	214 (472)	214 (472)	231 (510)
Relative Inst. Fn Dry	Base*	1.001	1.228
Relative Inst. sfc Dry	Base	0.997	0.963
0.3 M/SL/+15° C (+27° F)			
W1R, kg/sec (lb/sec)	381 (840)	349 (770)	349 (770)
Inst. Fn Dry N, (lbf)	196,960 (44,230)	198,070 (44,530)	212,930 (47,870)

*Base = 73,392 N (16,500 lbf)
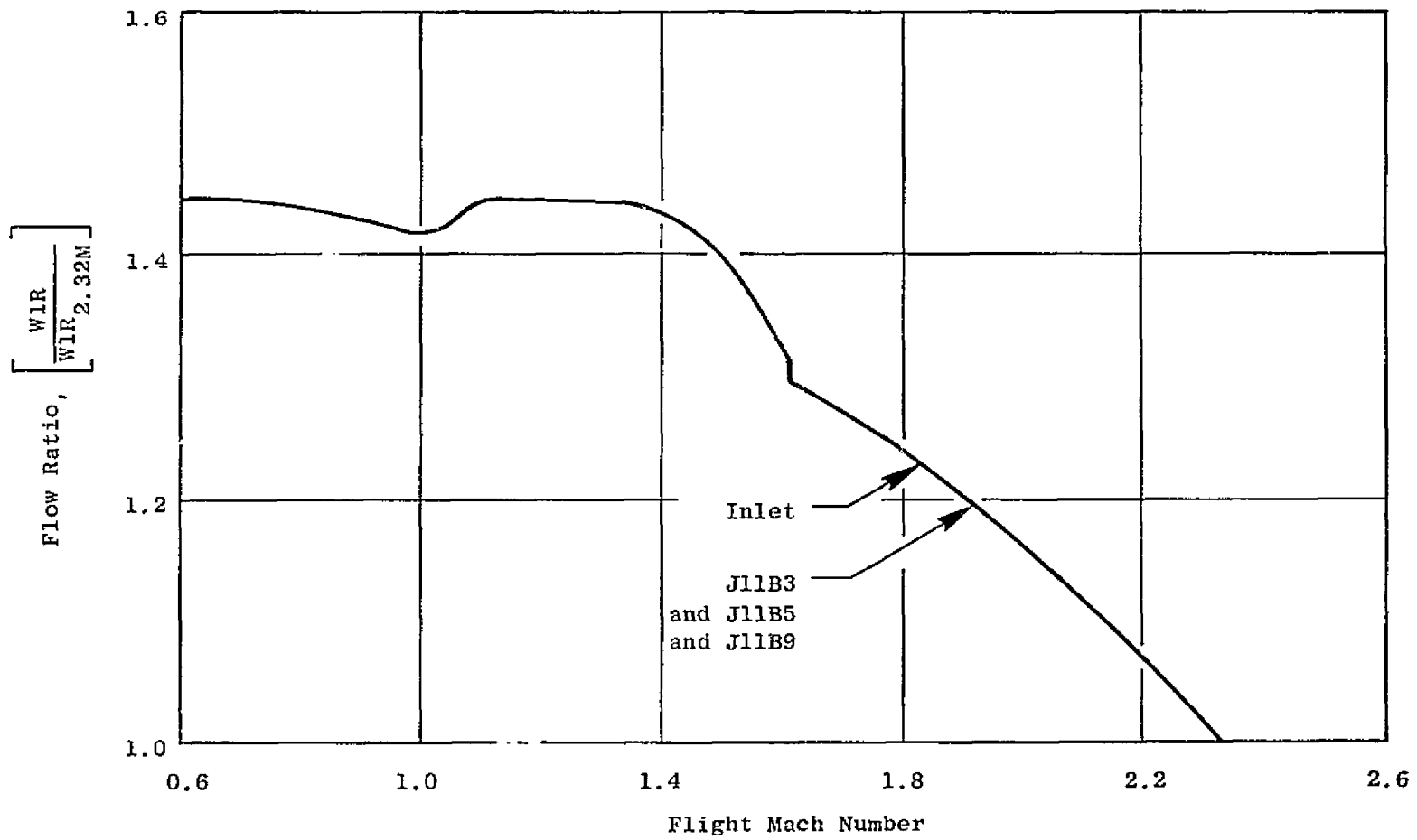
Figure 22. Boeing Axisymmetric Inlet/Engine Airflow Match.
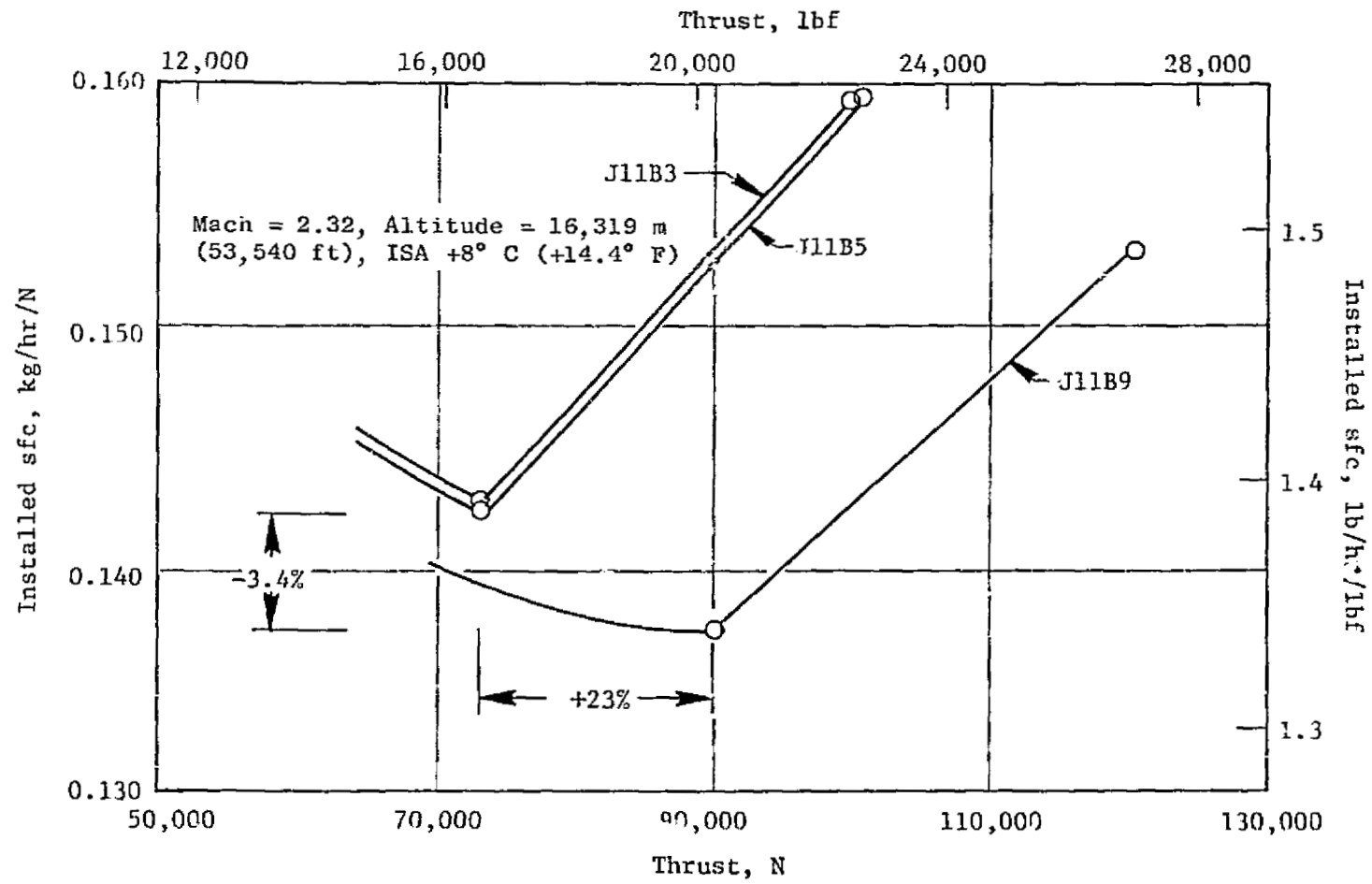
Figure 23. Boeing Supersonic Cruise SFC.

Table 8. Engines Studied by Lockheed.

Inlet	Overwing	Underwing
GE21 Engine	J11B1	J11B4
Sea Level Static		
W1R, kg/sec (lb/sec)	317/381 (700/840,	317/381 (700/840)
Fan PR	4.0	4.0
Overall PR	17.3	17.3
BPR	0.35	0.35
2.55 M/18,290 m (60,000 ft/)/+8° C (+14° F)		
W1R, kg/sec (lb/sec)	179 (395)	179 (395)
Relative Inst. Fn Dry	Base*	1.058
Relative Inst. sfc Dry	Base	0.9797
0.3 M/SL/+15° C (+27° F)		
W1R, kg/sec (lb/sec)	381 (840)	381 (840)
Inst. Fn Dry N (lbr)	201,630 (45,330)	201,630 (45,330)

*Base = 52,353 N (11,770 lbf)
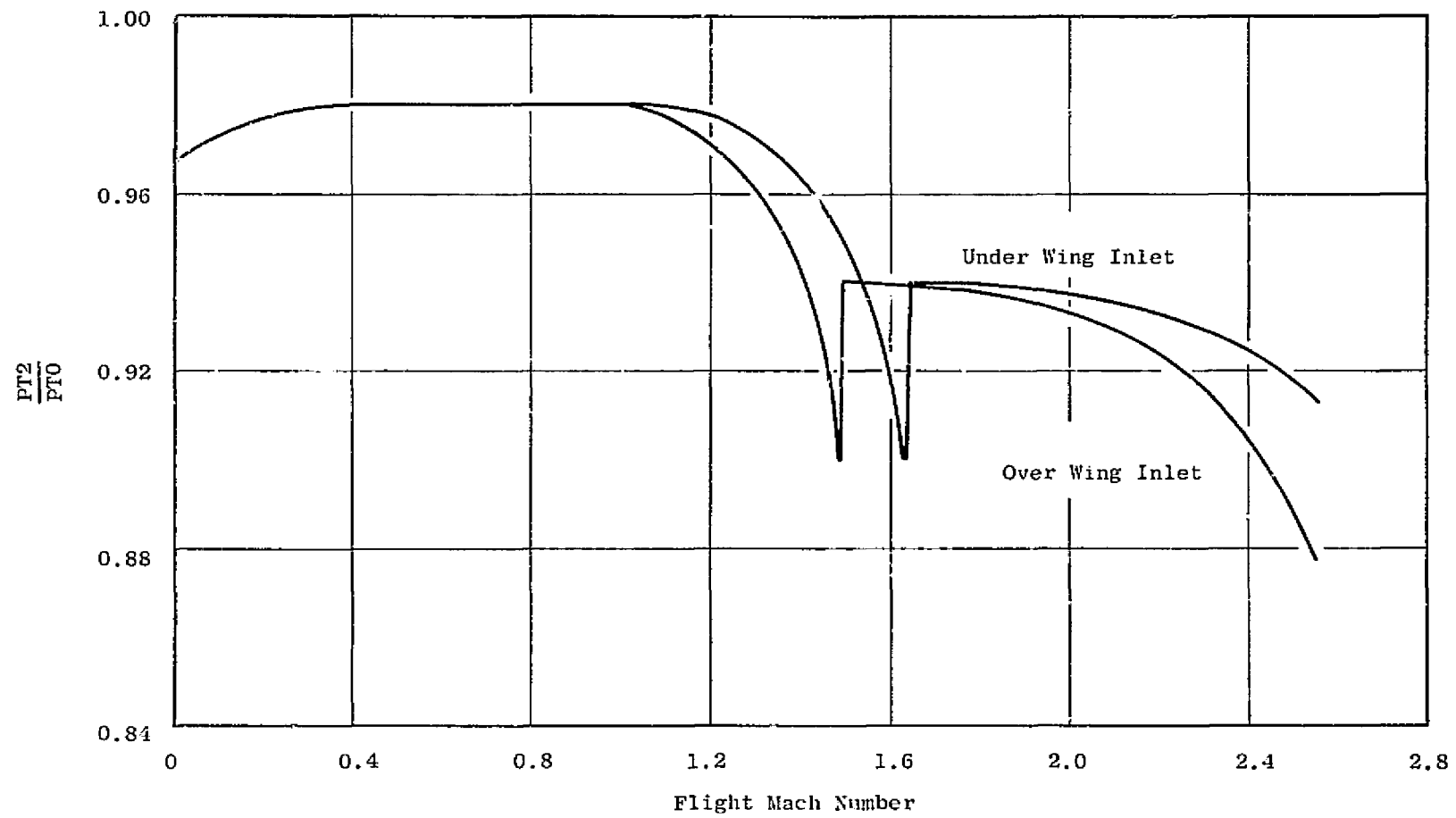
Figure 24. Lockheed Two-Dimensional Inlet Recovery.
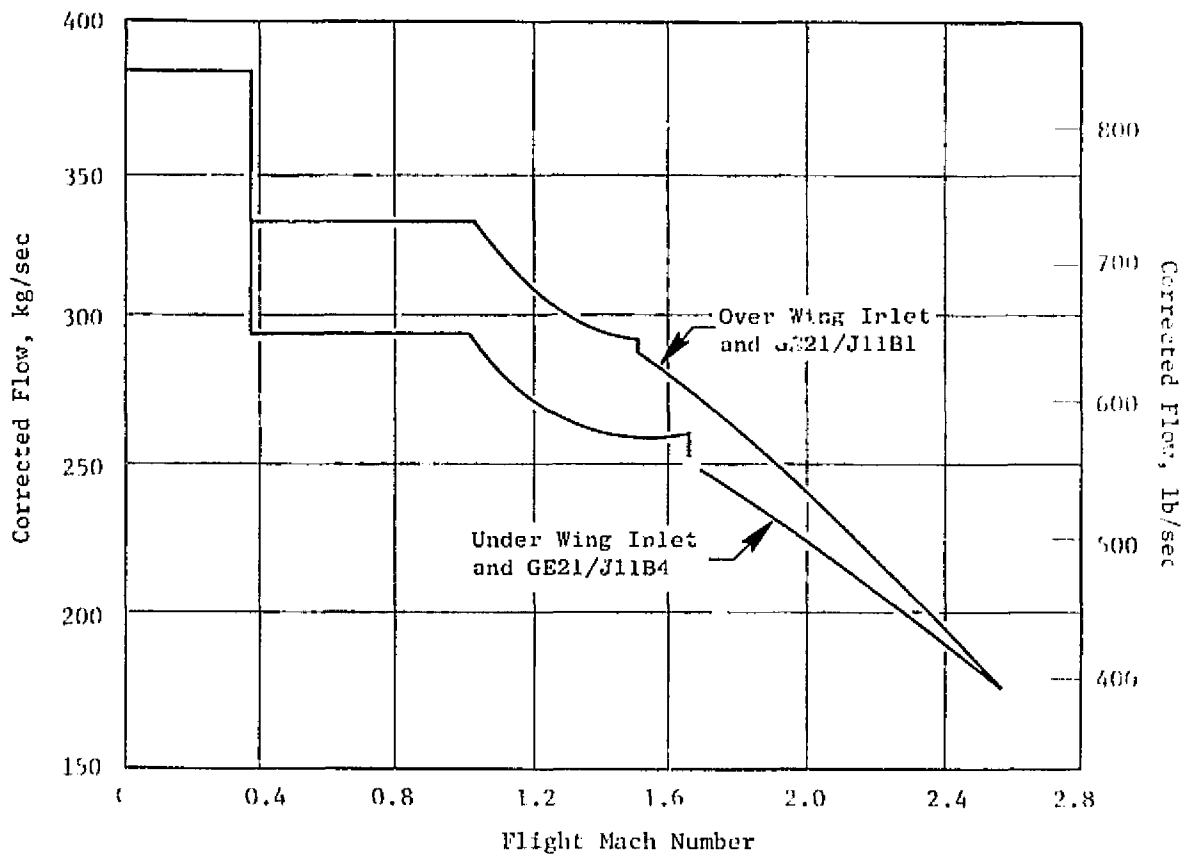
Figure 25. Lockheed Inlet/Engine Airflow Match.
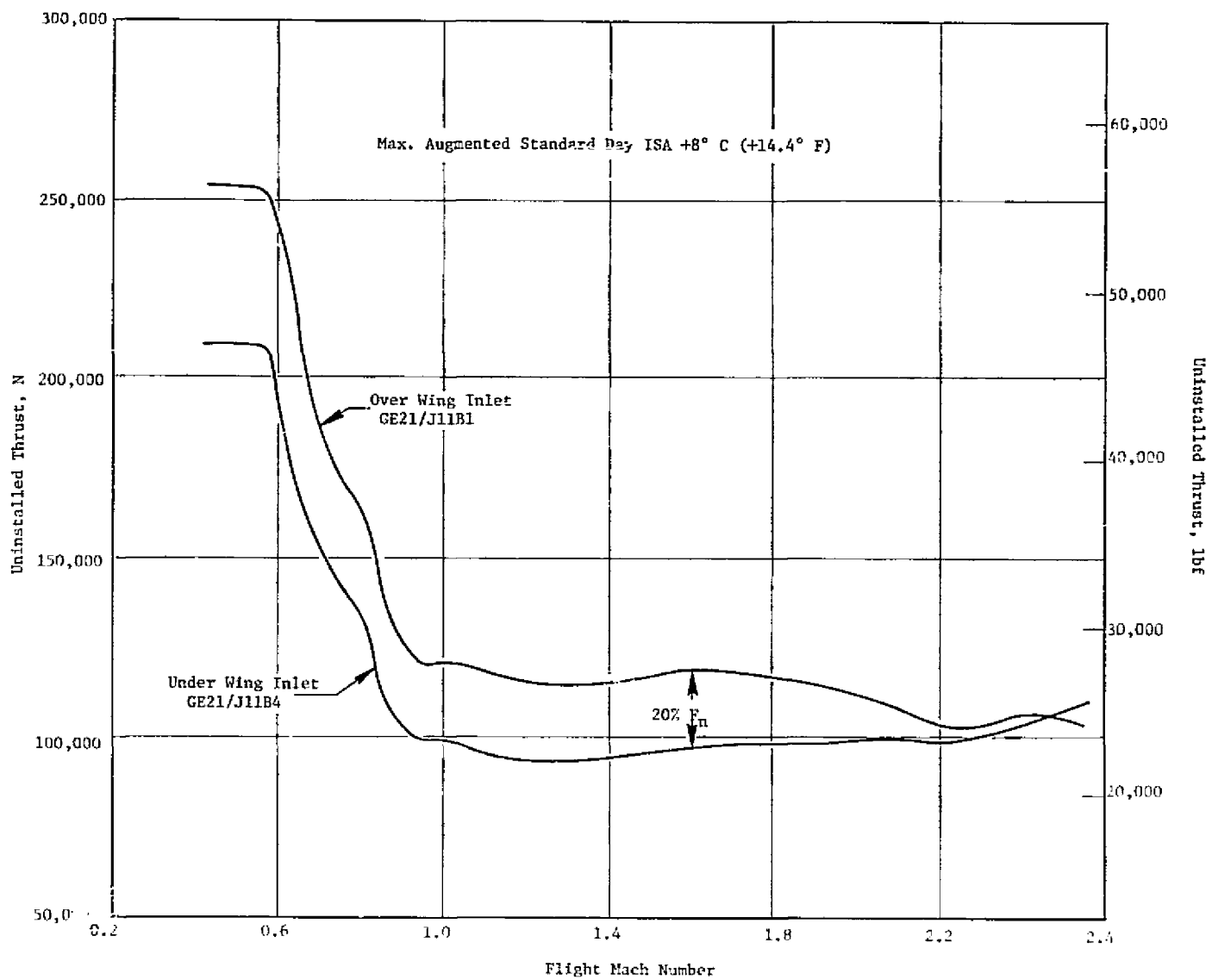
Figure 26. Lockheed Climb/Acceleration Thrust.
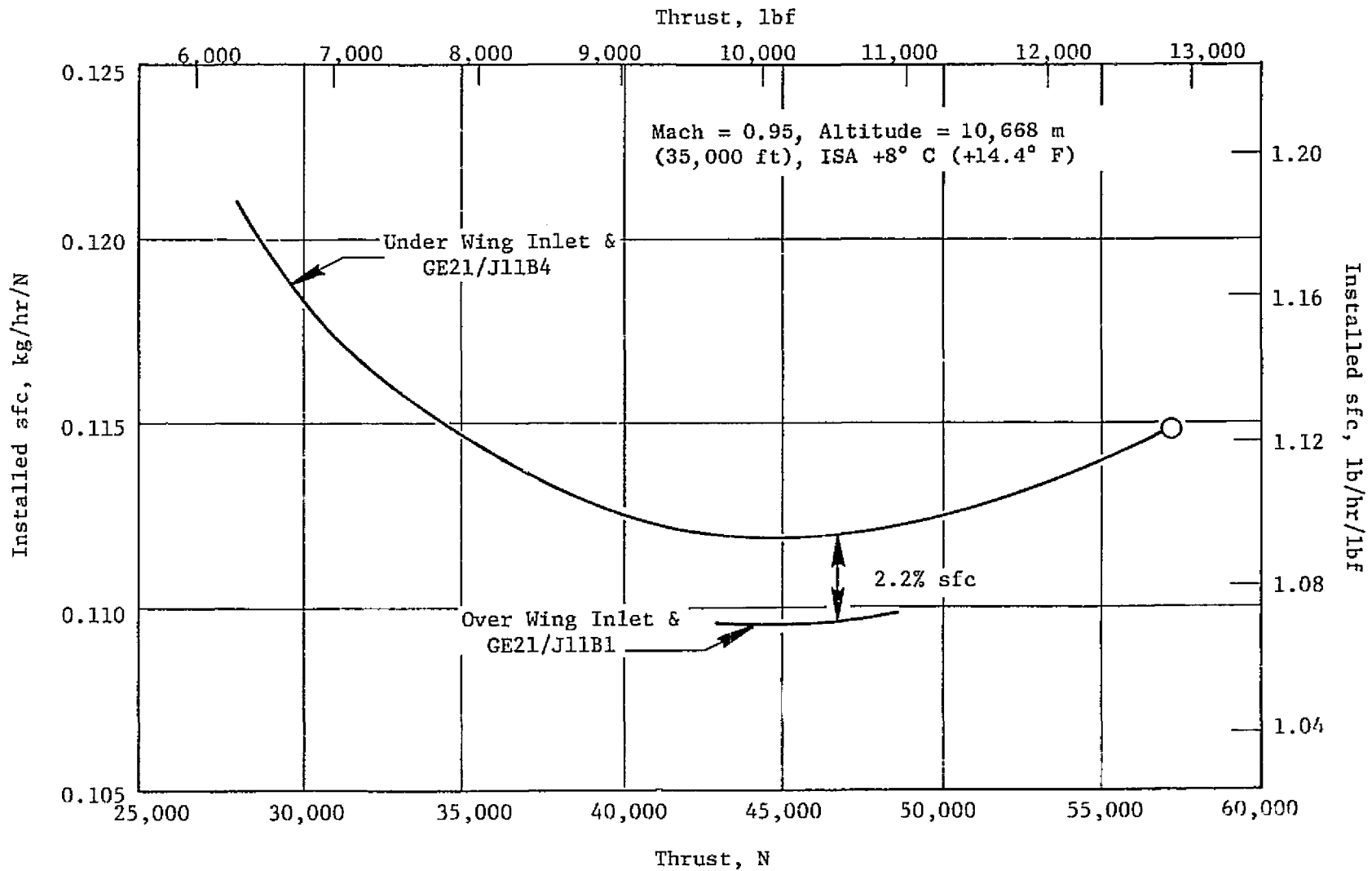
Figure 27.   Lockheed Subsonic Cruise SFC.
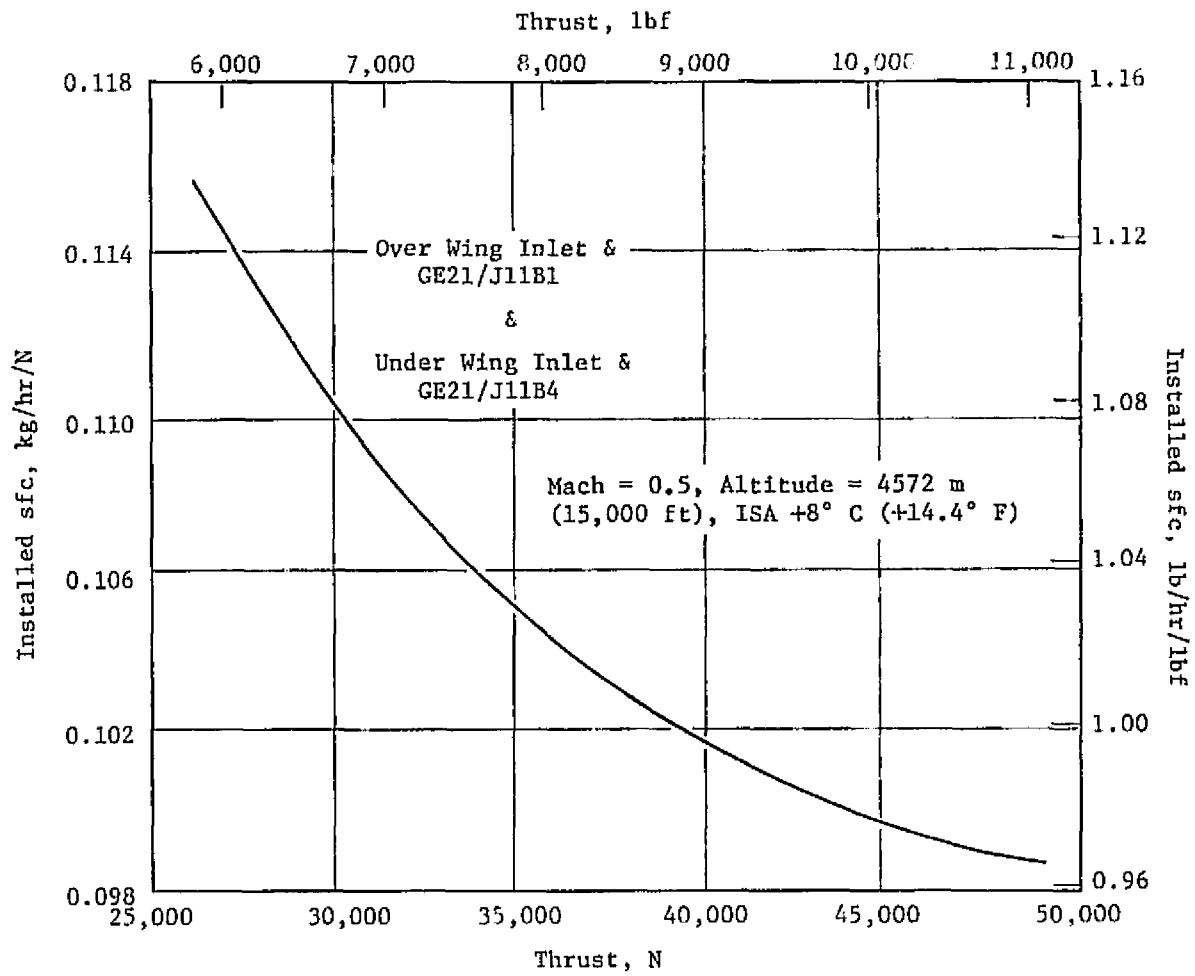
Figure 28. Lockheed Hold SFC.

The Engine cycle and performance for the under-wing inlet/engines J11B4, J11B8, and J11B11 are shown on Table 9. The J11B4 and J11B8 inlet/ engine airflows were matched during climb/acceleration operation (Figure 29). Lockheed later provided an inlet maximum airflow, and the J11P4 engine airflow was matched to it. The J11B11 engine airflow did not match the inlet maximum airflow, however, it could match the inlet supply airflow first provided by Lockheed. Relative to the airflow match, it is signifi- cant that the 2.55 M corrected airflow of the J11B11 engine 199.6 kg/sec (440 lb/sec) is 11.4% greater than the J11B8 engine 179 kg/sec (395 lb/sec). Thus, the larger inlet capture area has the capability of supplying more airflow than the engine demand at transonic Mach numbers.

At supersonic cruise, 2.55 M/18288 m (60000 ft)/Standard Day +8° C (+14.4° F), the installed performance of the J11B4 (20% high-flowed fan) and J11B8 (10% high-flowed fan) are approximately equal (Figure 30). The J11B11 provides 30% more thrust at 2.9% less sfc at the maximum dry power setting. The improved performance is primarily attributed to the lower design BPR (0.25) and increased supersonic cruise airflow 199.6 kg/sec (440 lb/sec).

The lower over-wing inlet ram recovery (0.878 versus 0.913) reduced the engine 2.55 M thrust by 5% (Figure 30). A range improvement of approxi- mately 926 km (500 nmi) was identified with the J11B11 engine relative to the J11B4 engine.

Engine brochures and card packs were provided to NASA for requested engines. The double-bypass VCE J11B7 was defined for study by NASA with a supersonic cruise design Mach number of 2.62. It has a 20% high-flowed fan and a design BPR of 0.35. The inlet characteristics provided by NASA were for the NASA "P" inlet with reference to NASA CR-1977 lated March, 1972.

The J11B7 engine characteristics are compared to the J11B3 and J11B5 engines which were also studied by NASA (Table 10). The J11B7 compressor discharge maximum temperature is 621° C (1150° F) and the supersonic cruise turbine rotor inlet temperature is 1482° C (2700° F). The J11B7 2.62 M thrust 49043 N (11026 lb) scaled down by the airflow ratio of 317/363 (700/800) is 42914 N (9648 lb), which is 2.7% more than the J11B3. No mission analysis was conducted with the J11B7 engine by General Electric. The GE in-house studies were confined to engines with M = 2.4 mission design points.

4.1.7 Low Bypass, Mixed-Flow Study Engine

An advanced technology (1985) conventional cycle engine was defined for a supersonic cruise design Mach number 2.32. It was a dual rotor engine, single-bypass configuration, with a fixed LP turbine nozzle diaphragm, and incorporated an annular exhaust system for low takeoff noise. The design BPR was 0.35 at a fan pressure ratio of 4.0, and overall pressure ratio of 17.5 (Table 11). The engine was matched to and operated to the Boeing inlet characteristics. Figure 31 presents a comparison of supersonic sfc charac- teristics of this engine as compared to three VCE's also matched to Boeing's inlet curve taken from Figure 23).

Table 9. Engines Studied by Lockheed.

Two-Dimensional Under-wing Inlet

GE21 Engine	J11B4	J11B8	J11B11
Sea Level Static			
W1R, kg/sec (lb/sec)	317/381 (700/840)	317/349 (700/770)	317/349 (700/770)
Fan PR	4.0	4.0	3.7
Overall PR	17.3	17.3	15.1
BPR	0.35	0.35	0.25
2.55 M/18,290 m (60,000 ft)/+8° C (+14° F) W1R, kg/sec (lb/sec)	179 (395)	179 (395)	(440)
Relative Inst. Fn Dry	Base*	1.0063	1.311
Relative Inst. sfc Dry	Base	0.9973	0.9692
0.3 M/SL/+15° C (+27° F) W1R, kg/sec (lb/sec)	381 (840)	349 (770)	349 (770)
Inst. Fn Dry, N (lbf)	201,630 (45,330)	198,660 (44,650)	220,221 (49,510)

*Base = 55,400 N (12,455 lbf)
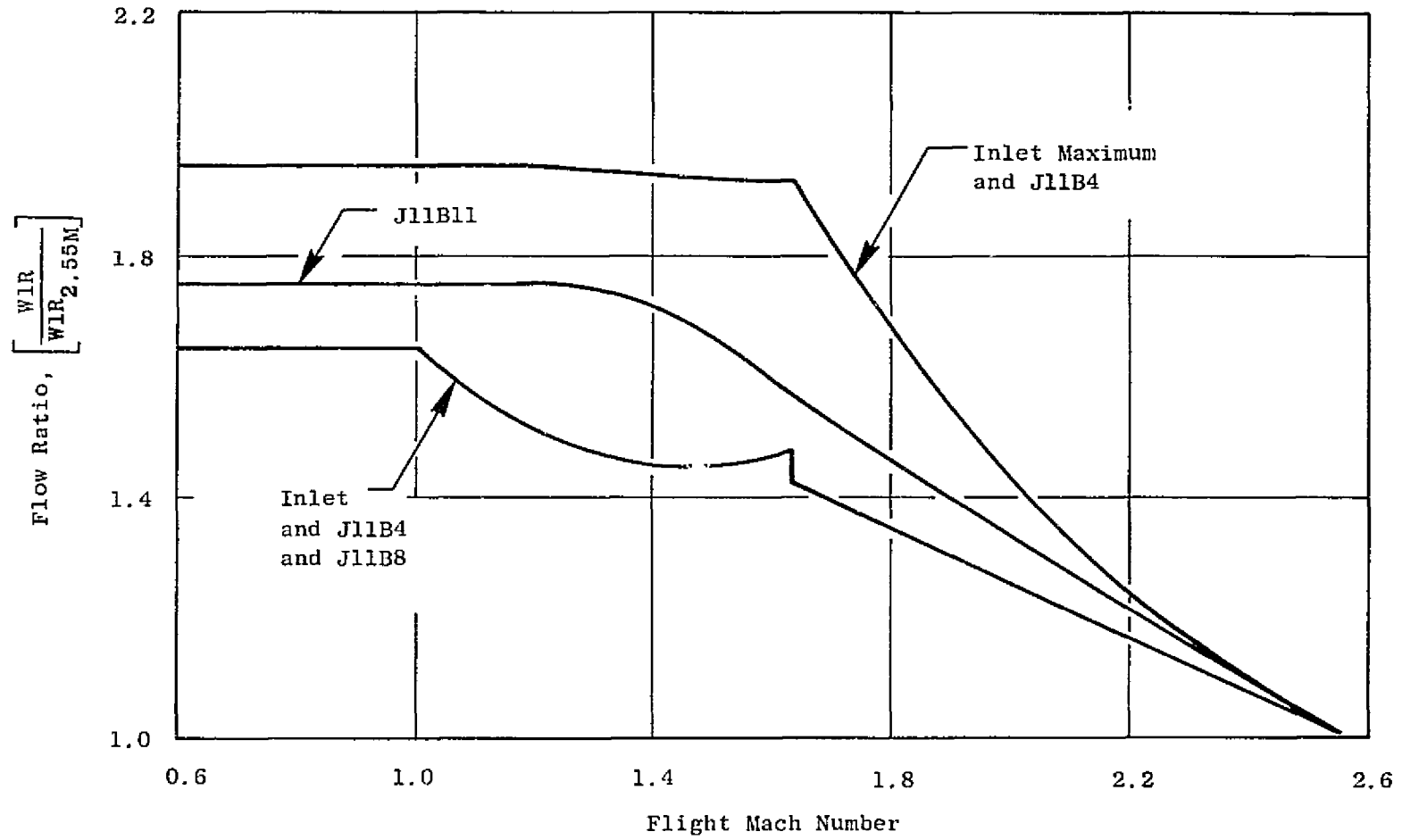
Figure 29. Lockheed Two-Dimensional Under Wing Inlet/Engine Airflow Match.
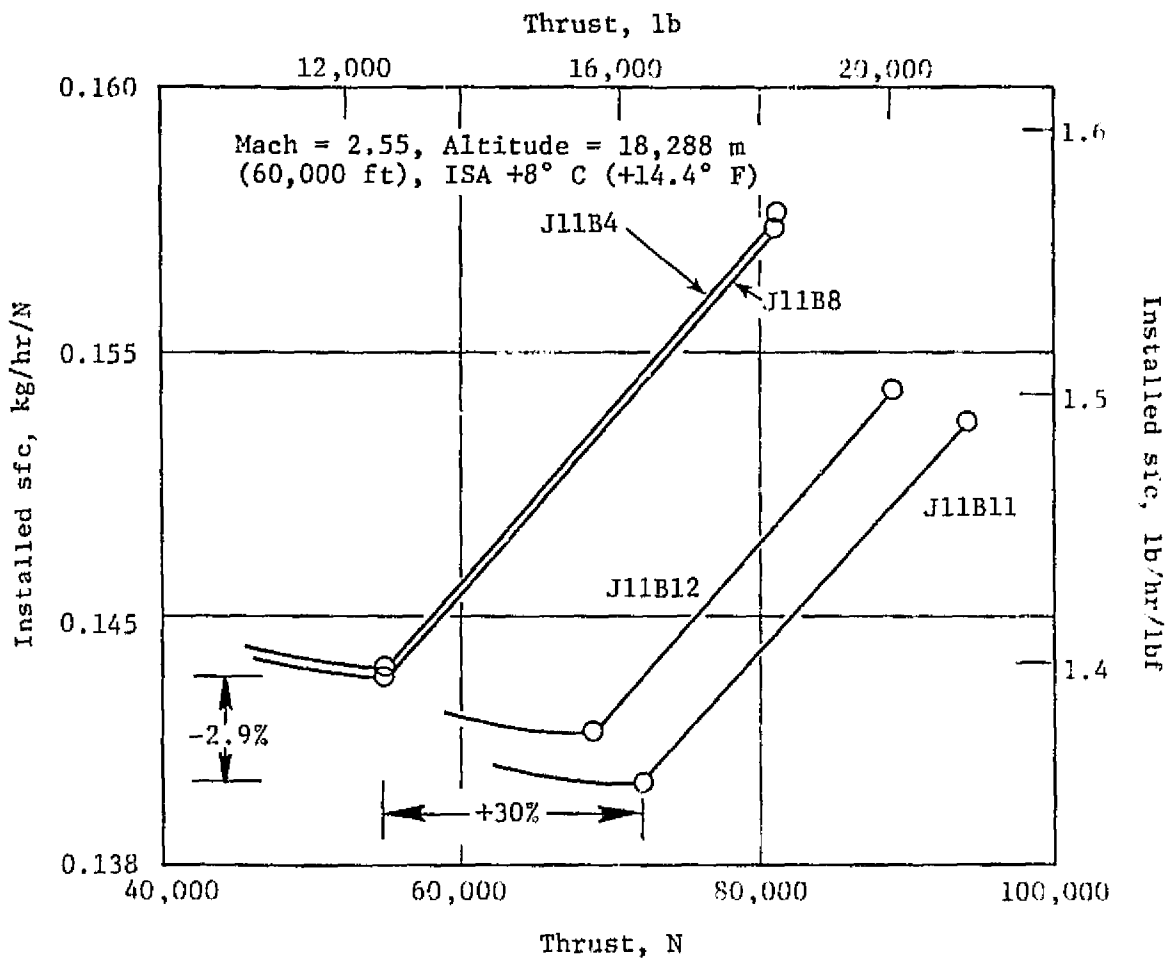
Figure 30. Lockheed Supersonic Cruise SFC.

Table 10. Engines Studied by NASA.

GE21 Engine	J11B3	J11B3	J11B7
Sea Level Static			
W1R, kg/sec (lb/sec)	317/381 (700/840)	317/349 (700/770)	363/435 (800/960)
Fan PR	4.0	4.0	4.0
Overal PR	17.3	17.3	17.3
BPR	0.35	0.35	0.35
19,812 m (65,000 ft)/+8° C(+14.4° F)			
Mach No.	2.32	2.32	2.62
Inlet η_r	0.932	0.932	0.907
W1R, kg/sec (lb/sec)	214 (472)	214 (472)	194 (427)
Relative Inst. Fn Dry	Base*	1.001	1.173
Relative Inst. sfc Dry	Base	0.9964	1.01
0.3 M/SL/+15° C (+27° F)			
W1R, kg/sec (lb/sec)	381 (840)	349 (770)	435 (960)
Inst. Fn Dry, N (lof)	196,960 (44,280)	198,070 (44,530)	229,470 (51,590)

*Base = 41,748 N (9,397 lbf)

Table 11. Baseline Turbofan.

- Updated to VCE Cycle Parameters

	New (Phase III)	Old (Phase II)
- PR_{OA}	17.5	22.0
- PR_F	4.0	4.0
- BPR	0.35	0.40
- $T_{41\ max.}$	1538° C(2800° F)	1538° C(2800° F)

- New Feature

  - Annular Acoustic Exhaust Nozzle

  Baseline is now Dual Cycle VCE
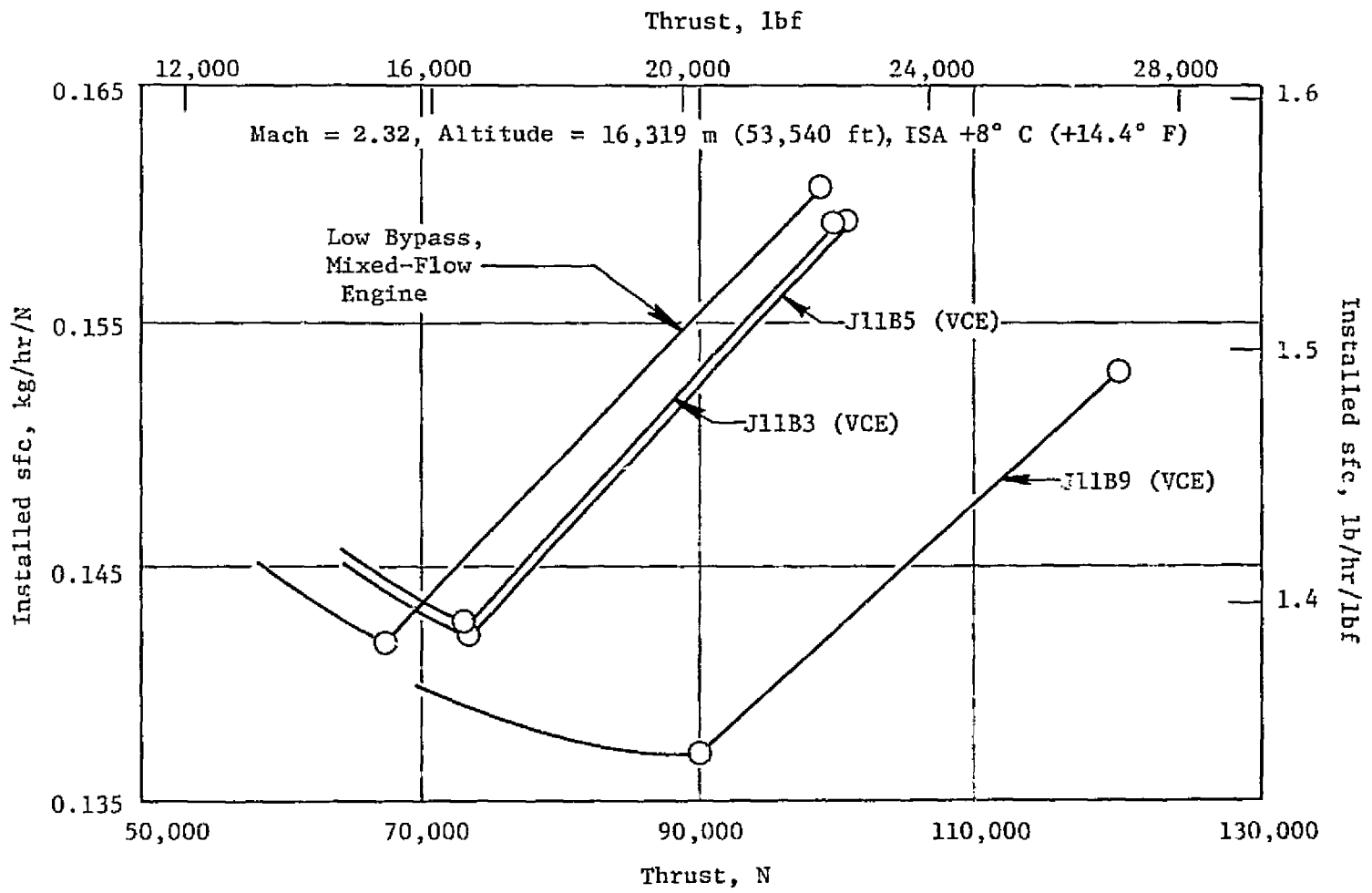
Figure 31. Supersonic Cruise SFC Comparison.

Brochures and card packs for this engine were not provided to airframe companies or NASA. Engine performance data and engine weight were incorporated in the AST-2 airplane/mission program and mission range was calculated. The engine airflow size of 485 kg/sec (1070 lb/sec) resulted in a noise of traded FAR 36 and an all-supersonic mission range of 6480 km (3500 nmi) (Table 12). This engine was an updated version of the Phase II baseline turbofan, used as a base cycle for the early variable cycle engines. Poor range performance is largely due to the high engine weight and large engine size. AST range performance is very sensitive to engine size (see Figure 4).

4.1.8 Engine Cycle Effects on Main Combustor Emissions

The Environmental Protection Agency (EPA) has proposed emission standards for newly certificated SST engines which would be effective January 1, 1984. These standards apply to operation around the airport and are shown in Table 13. The high-altitude emission of oxides of nitrogen (NO_x has also been a source of serious concern. The U.S. Department of Transportation (DOT) Climatic Impact Assessment Program (CIAP) has suggested (see Table 14) that the NO_x emission target for operation above 12 km ($\sim$39000 ft) altitude is approximately 3 kg/1000 kg (3 lb/1000 lb) of fuel. Other studies currently in progress are also investigating the NO_x emission problem (Table 15).

The airport emissions consist of unburned hydrocarbons (C_xH_y), carbon monoxide (CO) and oxides of nitrogen (NO_x). The C_xH_y and CO emissions are primarily caused by low combustion pressures and temperatures at low power conditions accompanied by low combustion efficiency (see Figure 32). Figure 33 shows the relationship between combustion efficiency and C_xH_y and CO emissions. High NO_x emissions, however, are caused by high combustor flame temperatures and long combustion zone gas dwell times (Figure 34). Low flame temperature and resulting low NO_x formation rates can be obtained with low fuel-air equivalence ratios (lean mixtures) as shown on Figure 35. Figure 35 also shows the importance of low combustor inlet temperature on the NO_x formation rate.

Because the combustor emissions around the airport and NO_x emissions at high-altitude cruise are affected by the engine cycle selection and the resulting high-pressure compressor discharge temperature and pressure (T_3, P_3), a study (covering a range of overall pressure ratios from about 14 to 20) was performed using the VCE engine matrix from Section 2.1.1. For each engine cycle, the EPA emissions indices and altitude NO_x emissions were calculated, and the effects of the different cycles on emissions levels were found. The baseline combustor used in the General Electric VCE engines is a double-annular design (Figure 36) based on the NASA Experimental Clean Combustor Program (ECCP). This work was done in connection with NASA Contracts NAS3-16830 and NAS3-18551 entitled "Experimental Clean Combustor Program." This combustor design provides excellent low power performance by providing fuel only to the outer annulus swirl cups at these conditions and,

68

Table 12. Baseline Turbofan Noise and Range.

AST-2 Airplane-TOGW 34,564 kg (762,000 lb)
Balanced Field Length 3,200 m (10,500 ft)
Optimized Subsonic and Transonic Climb/Acceleration

	Old Baseline	New Baseline
Airflow kg/sec (lb/sec)	485 (1,070)	485 (1,070)
Takeoff Thrust N (lbf)	273,110 (61,400)	273,110 (61,400)
Traded FAR 36 EPNL	-2.5	0
90 PNdB Takeoff footprint area ha (nmi^2)	6,170 (18)	5,140 (15)
Range		
All-Supersonic km (nmi)	6,430 (3,470)	6,480 (3,500)
600 nmi Initial Subsonic km (nmi)	5,870 (3,170)	5,960 (3,220)
All Subsonic km (nmi)	4,390 (2,370)	4,630 (2,500)

Table 13.   EPA Proposed Emissions Standards on Newly Certificated SST Engines.

For Operations Around Airports.

- Effective Date - January 1, 1984

- Standards:

  C_xH_y 2.0(1.0) kg/1000 N-hr/Cycle (1b/1000 lbf-hr/Cycle)

  CO 15.8(7.8) kg/1000 N-hr/Cycle (1b/1000 lbf-hr/Cycle)

  NO_x 10.1(5.0) kg/1000 N-hr/Cycle (1b/1000 lbf-hr/Cycle)

  Smoke (SAE SN) Same as for Class T_1/T_2 Engines

- Prescribed Cycle

	% Power	Minutes
Taxi-Idle	Ground Idle	19.0
Takeoff	100	1.2
Climb-Out	65	2.0
Descent	15	1.2
Approach	34	2.3
Taxi-Idle	Ground Idle	7.0

Table 14. U.S. DOT CIAP Findings Concerning No_x Emissions.

- NO_x Introduction into Stratosphere Above 11,890 m (39,000 ft) is of concern

- NO_x from 100 AST's Will Reduce Stratospheric Ozone in Northern Hemisphere by:

    ~1.7% - at Cruise Altitude of 19,510 m (64,000 ft)
    ~1.0% - at Cruise Altitude of 16,460 m (54,000 ft)

- Engines for AST and Future Subsonic Transport Applications Should Be Developed to Have Low Cruise NO_x Levels:

    - Suggested Target is $\frac{1}{6}$ of NO_x Levels of Current Operational Engines

    - Resulting Suggested Target for AST Engines is ~3kg/1000kg (3 lb/1000 lb) Fuel

Table 15. U.S. DOT/FAA High-Altitude Pollution Program.

- Objectives

    - Determine Needed Reductions, if Any, in Emissions Levels at High Altitude Cruise Operating Conditions

    - Define Appropriate Aircraft Engine Regulations, if Needed

- Key Milestones   End of

    - Initial Assessments   1976

    - Interim Assessments   1978

    - Structure Appropriate Regulations   1980

● Primarily Occur at Low Power

● Primarily Due to:

- Relatively Low T_3 & P_3
- Relatively Poor Fuel Atomization
- Low Combustion Zone F/A's
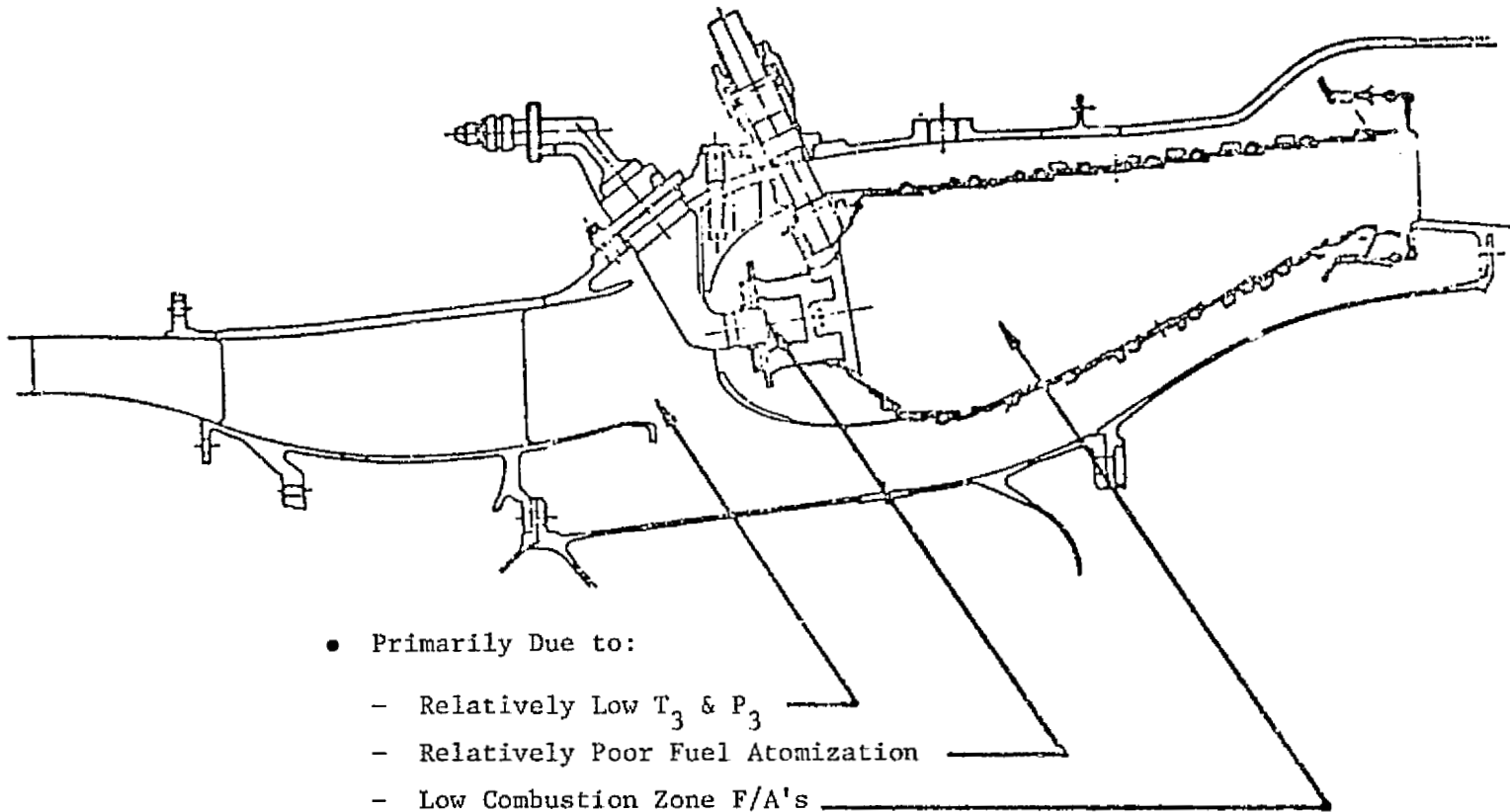
Figure 32. C_xH_y and CO Emissions.
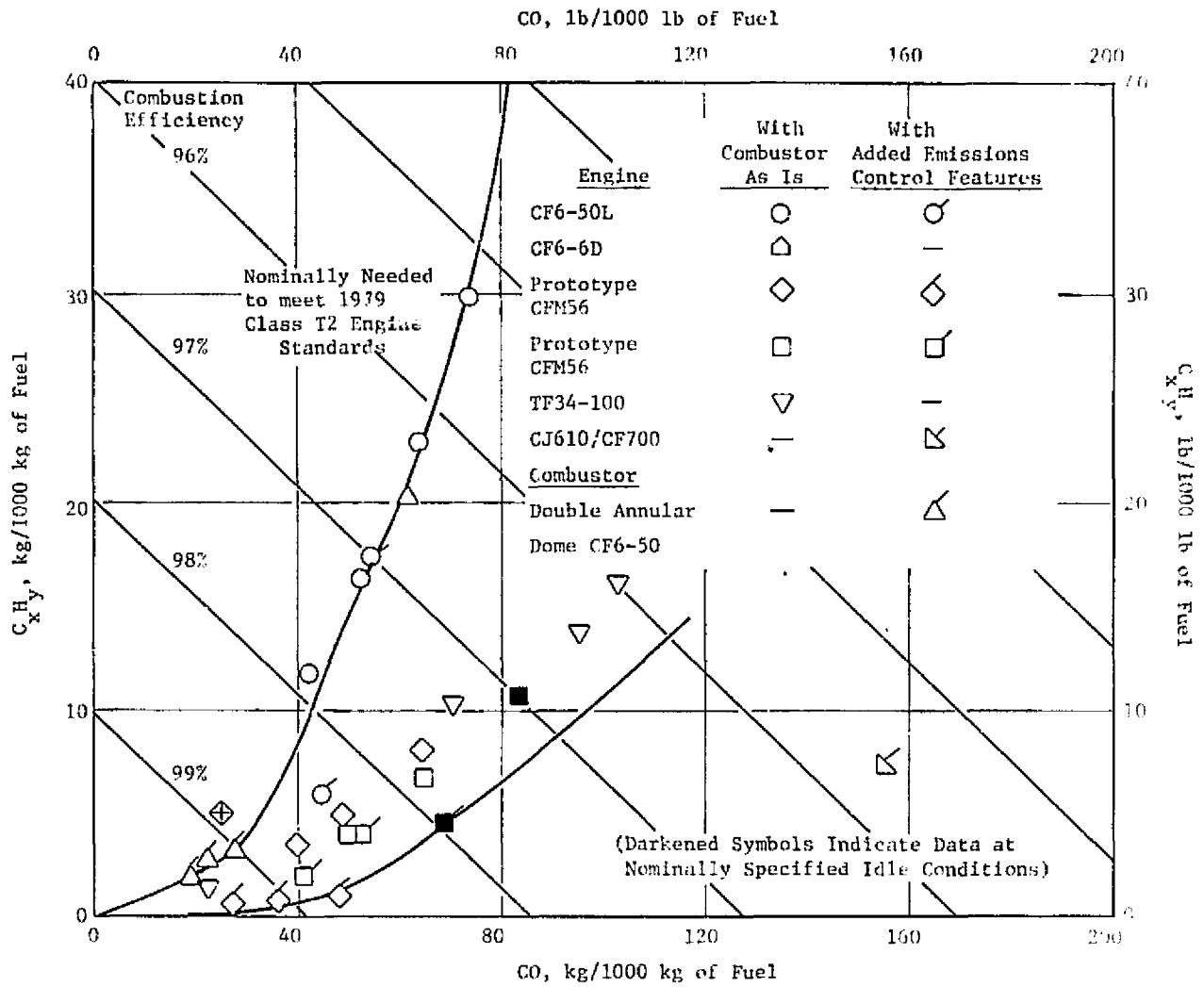
Figure 33. Combustion Efficiency and CO and C_xH_y Levels with Engines at Low Thrust.

● Primarily Occur at High Power

● Primarily Influenced by:

- Inlet T_3
- Flame Temperature in Combustion Zone
- Gas Dwell Time in Combustion Zone
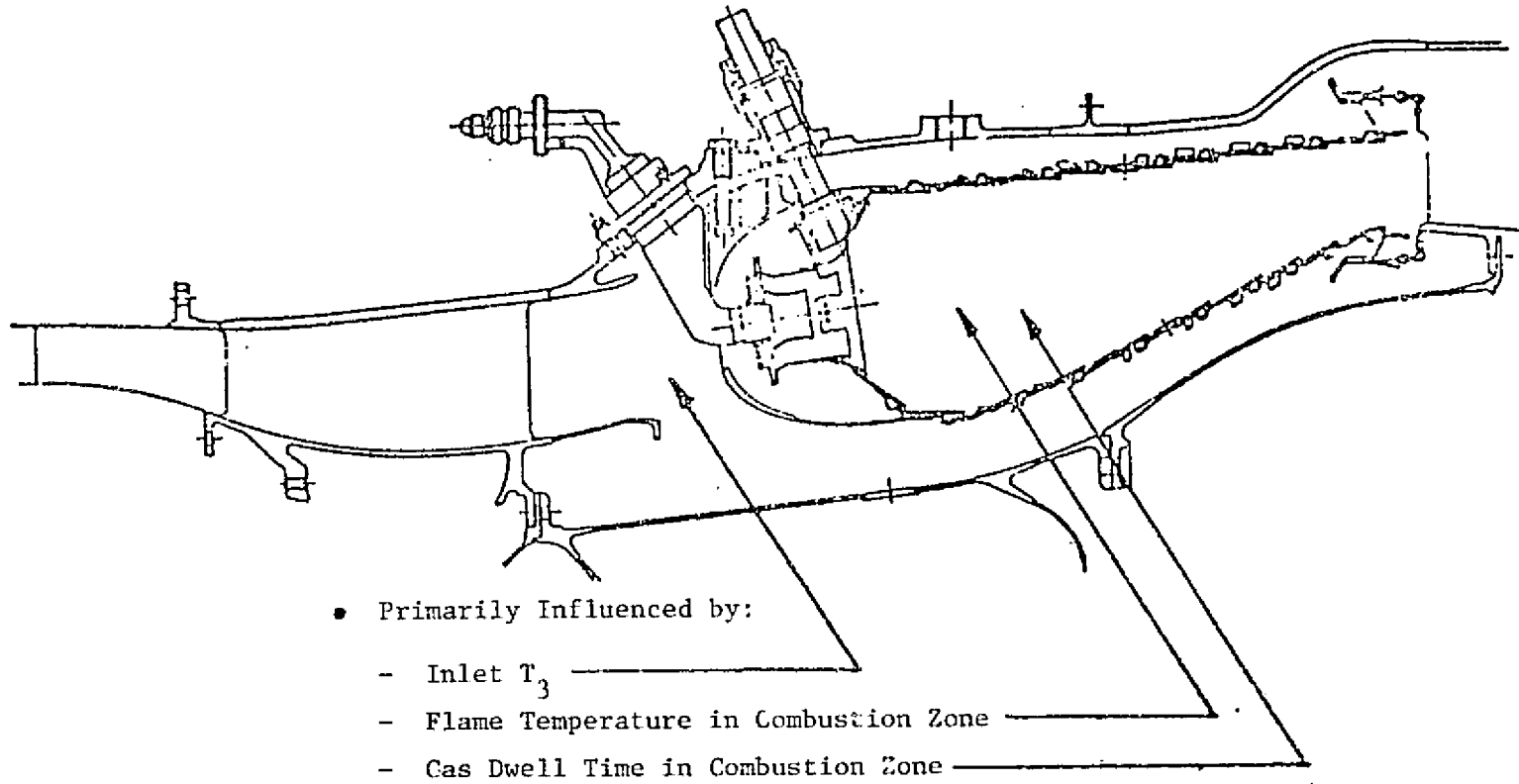
Figure 34. NO_x Emissions.
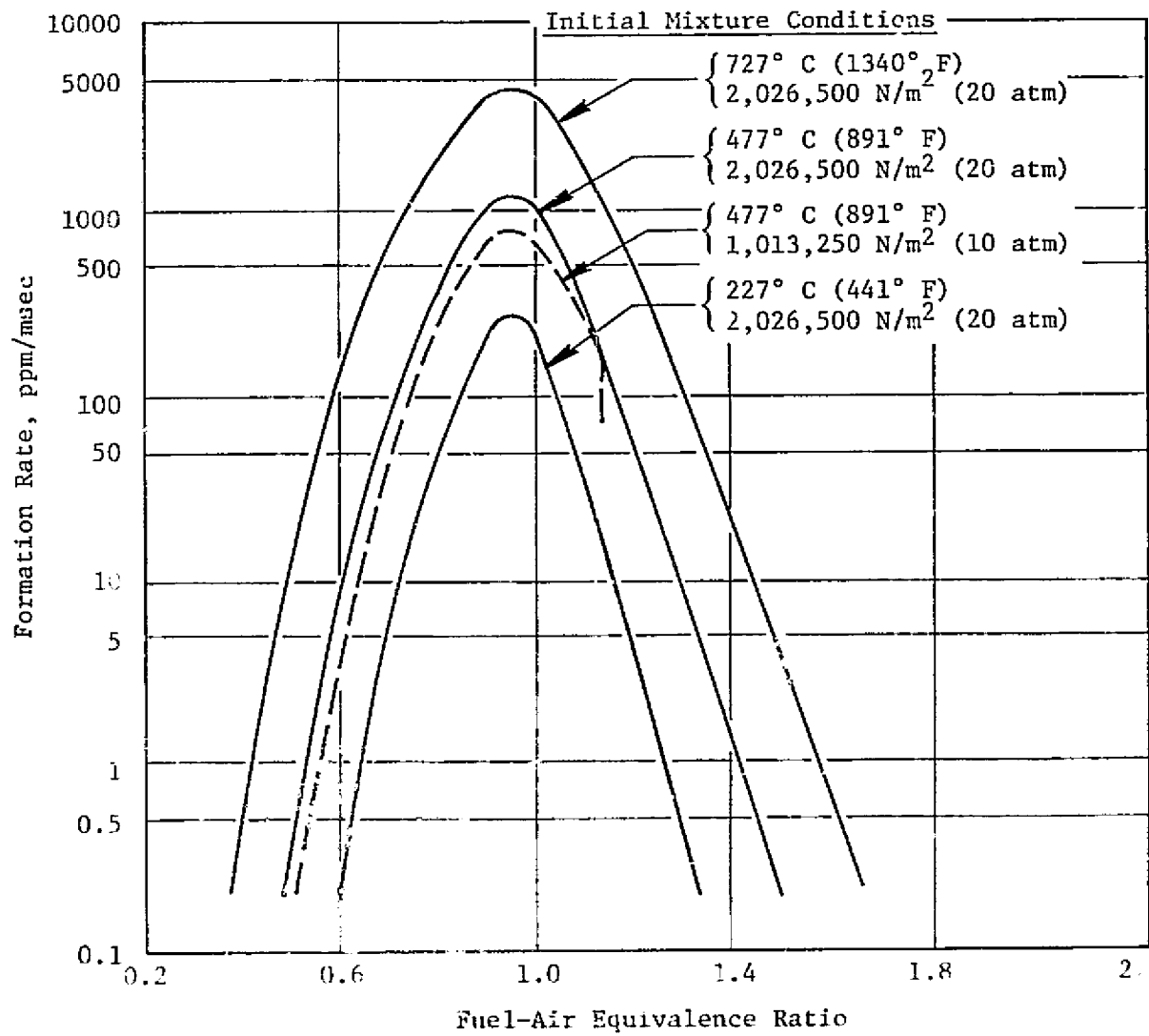
Figure 35. Nitric Oxide Formation Rate.
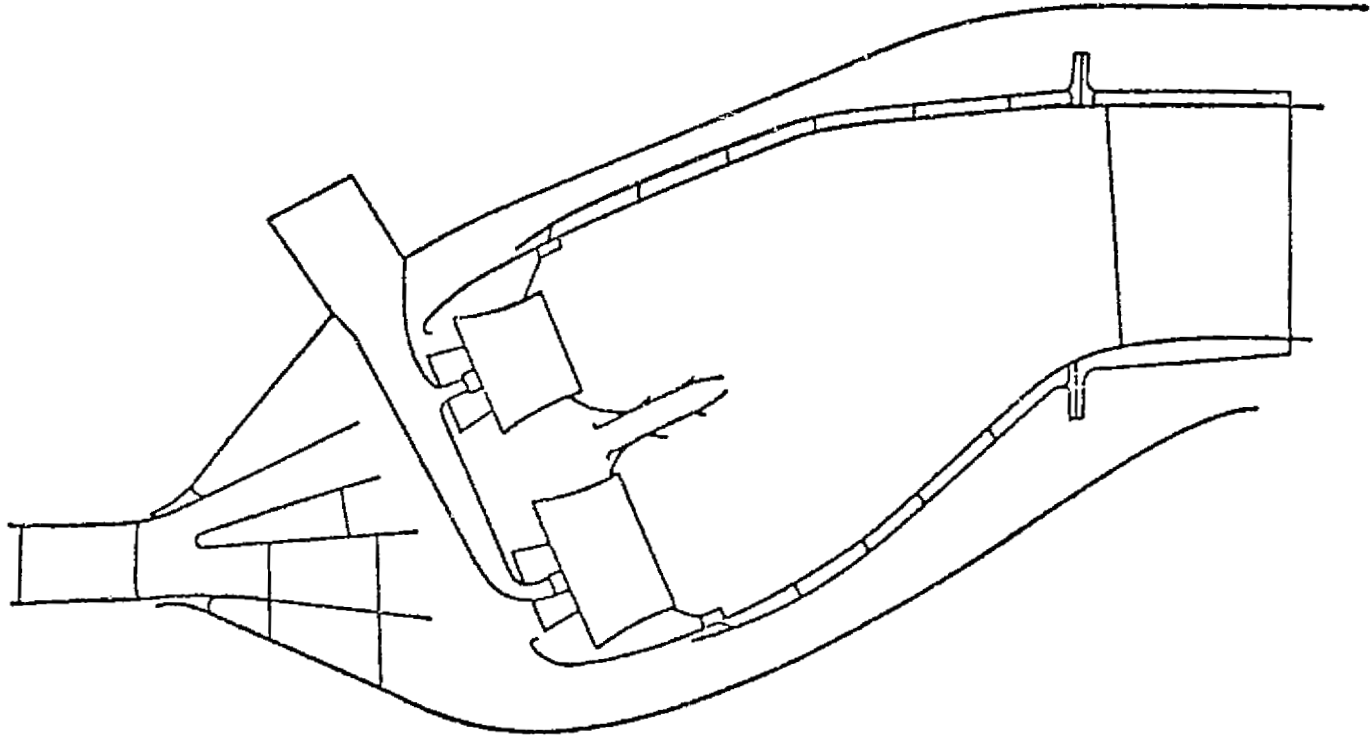
Figure 36. Double-Annular Combustor Design - AST GE21 VCE.

as power is increased, adding fuel to the inner annulus. At high power settings both inner and outer annulus swirl cups are used. A complete description of the operation of this combustor is covered in Section 4.4.2.1. A conventional, current single-annular combustor design was used as a base, so that improvements obtained with the low emissions combustors could be evaluated.

The NO_x CO and C_xH_y airport emissions for the complete VCE matrix are shown on Figures 37, 38, and 39. In all cases the double-annular (D/A) combustor has provided a large improvement in emissions levels over the conventional single-annular combustor. In the range of cycle pressure ratio that showed the best AST airplane range (17-20), the double-annular combustor emissions level estimates are actually lower than the EPA-proposed 1984 airport standards. These results indicate that a VCE cycle definition specifically tailored to meet airport emissions standards is not required.

The NO_x high-altitude emissions calculations are shown on Figure 40 and indicate that a combustor technology beyond that of the double-annular combustor will be required to meet the suggested CIAP target. The double-annular combustor gives a major improvement over the conventional combustor. However, a technology improvement beyond it is required. Again, it is apparent that use of very low combustor inlet temperatures has no large payoff. Even at temperatures of 538° C (1000° F) the NO_x emission levels would have to be reduced by 3 to 4 times to meet the suggested target level.

The double-annular low-emissions combustor is predicted to meet the EPA-proposed 1984 airport standards with no compromise to the engine cycle. The altitude NO_x suggested target cannot be met with this combustor design even with cycle changes. A new high-technology, low-emissions combustor will be required, therefore, to meet or exceed the CIAP suggested target for altitude cruise conditions.

The feasibility of an advanced low emission burner concept has been demonstrated by NASA under laboratory conditions. Figure 41 shows that NO_x altitude emissions may be reduced by utilizing premixing burners with low equivalence ratios. This will require thorough mixing of the fuel and air before combustion, to ensure that the fuel-air ratio is uniform. This will allow the lean mixtures and low flame temperatures required for low NO_x emissions. A concept of a premixing low emission combustor for the AST variable cycle engines is shown on Figure 42. In this combustor fuel is injected into a premixing section for high-power operation, and variable geometry is required to bypass air around the combustor for good low-power operation. A description of the operation of this combustor concept is given in Section 4.4.2.1.

Estimates of altitude cruise NO_x emissions for the premixing combustor in the VCE are shown on Figure 43. It is estimated that NO_x emissions close to the CIAP suggested target can be obtained at equivalence ratios of about 0.5. The effect of combustor inlet temperatures on NO_x emissions can also be seen on this figure. As combustor inlet temperatures increases, the equiva-
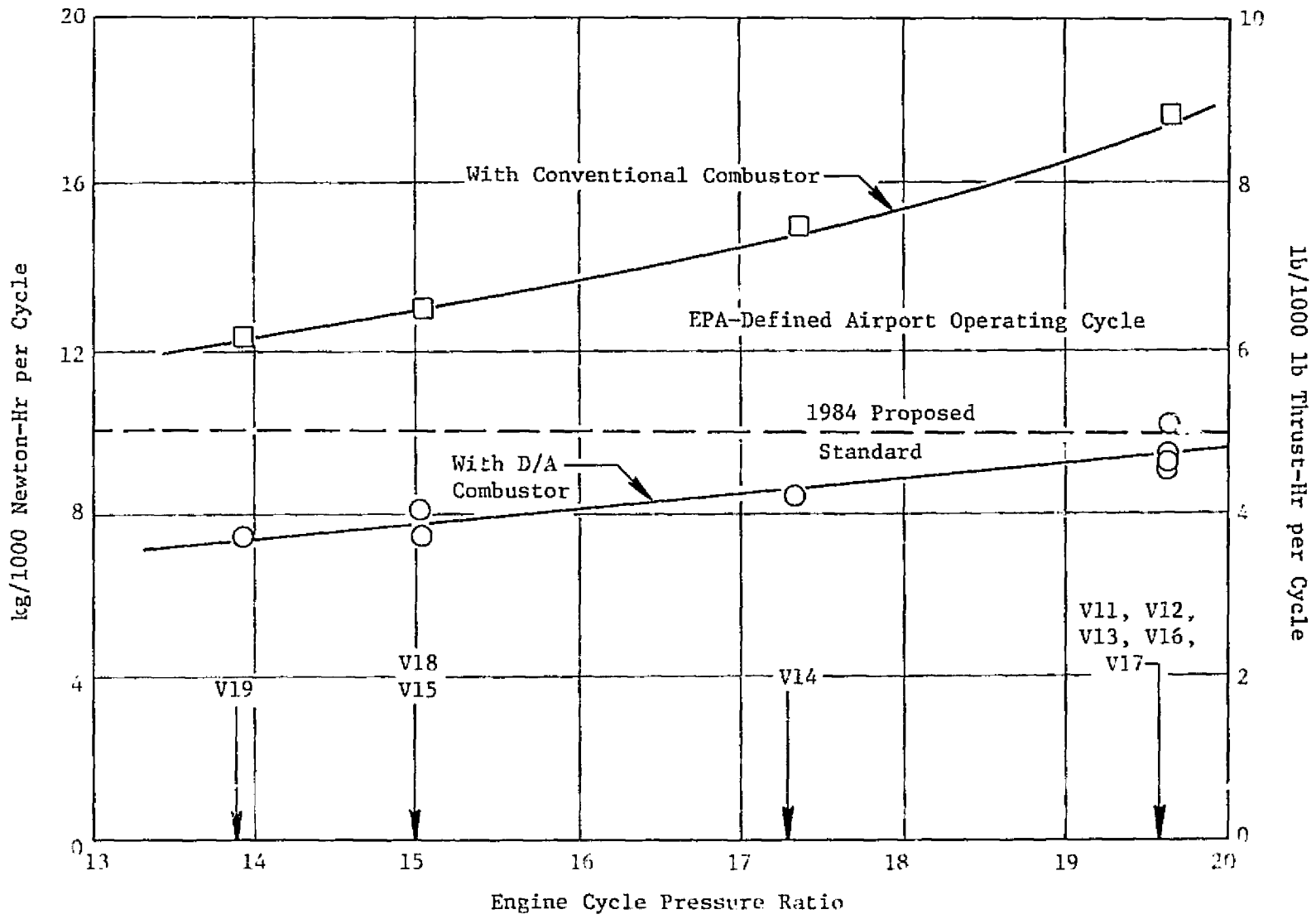
Figure 37. NO$_x$ Levels of AST VCE.
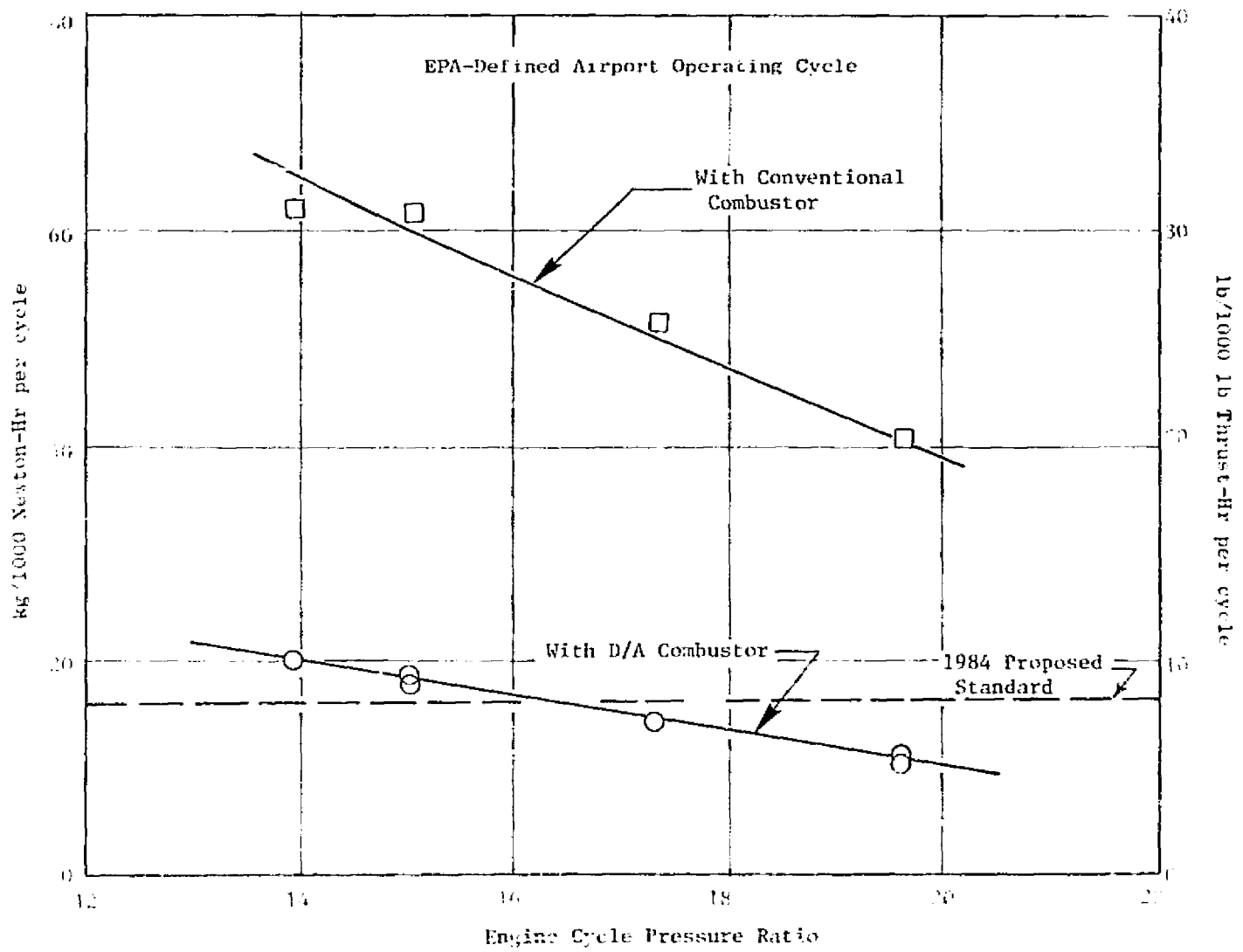
Figure 38.   CO Levels of AST VCE.
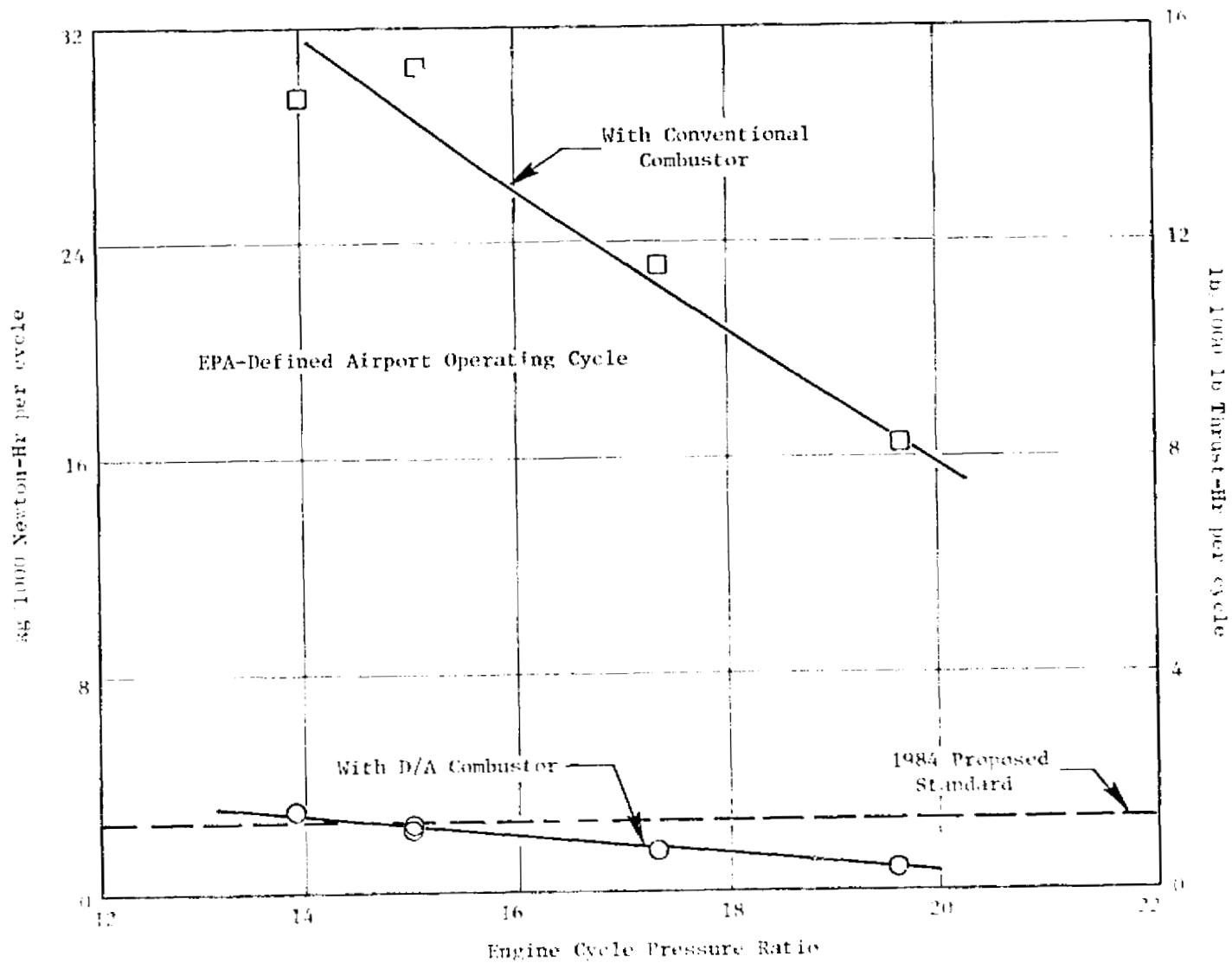
Figure 39. $C_x H_y$ Levels of AST VCE.
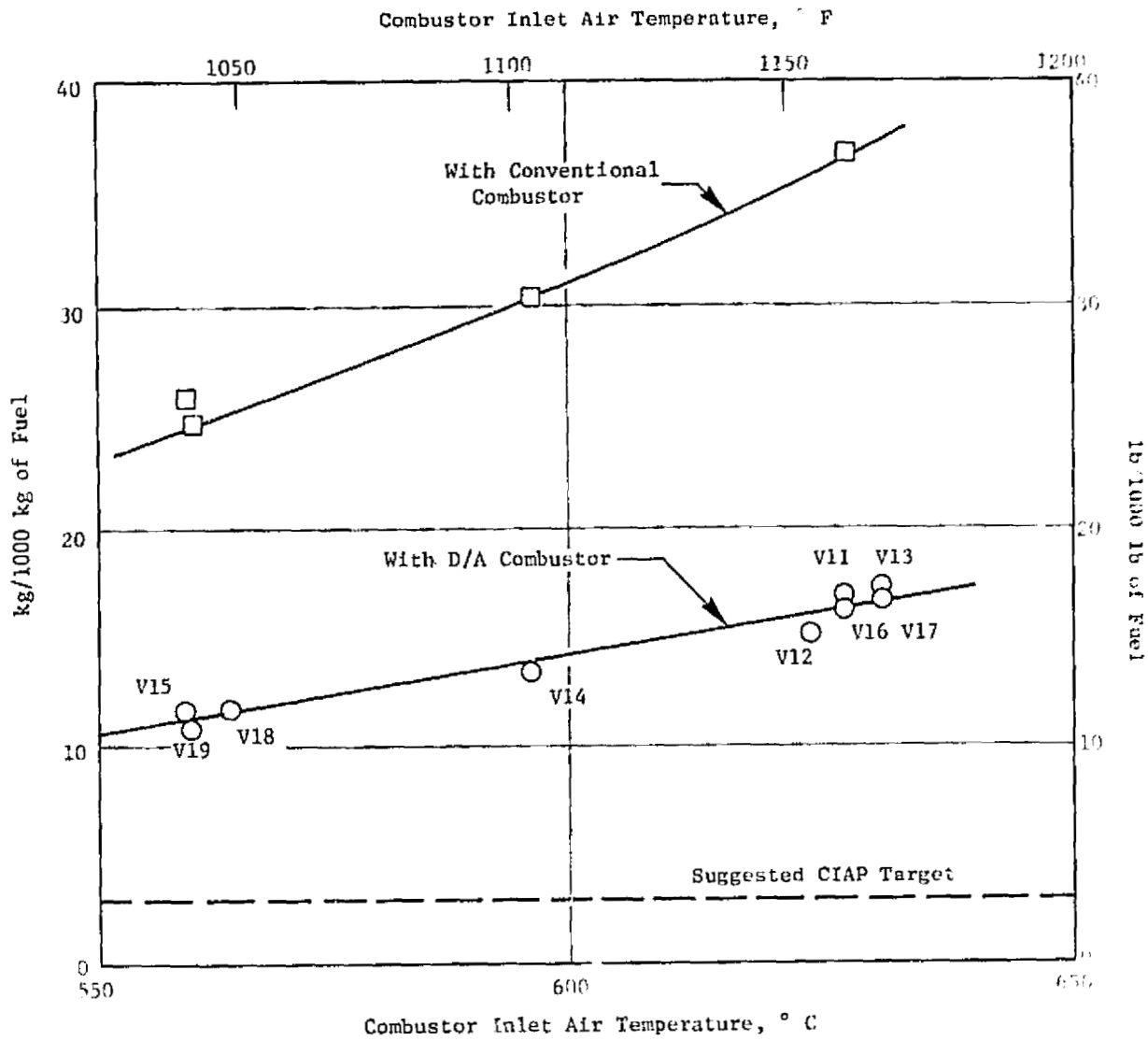
Figure 40. NO$_x$ Levels of AST VCE, Mach = 2.32.
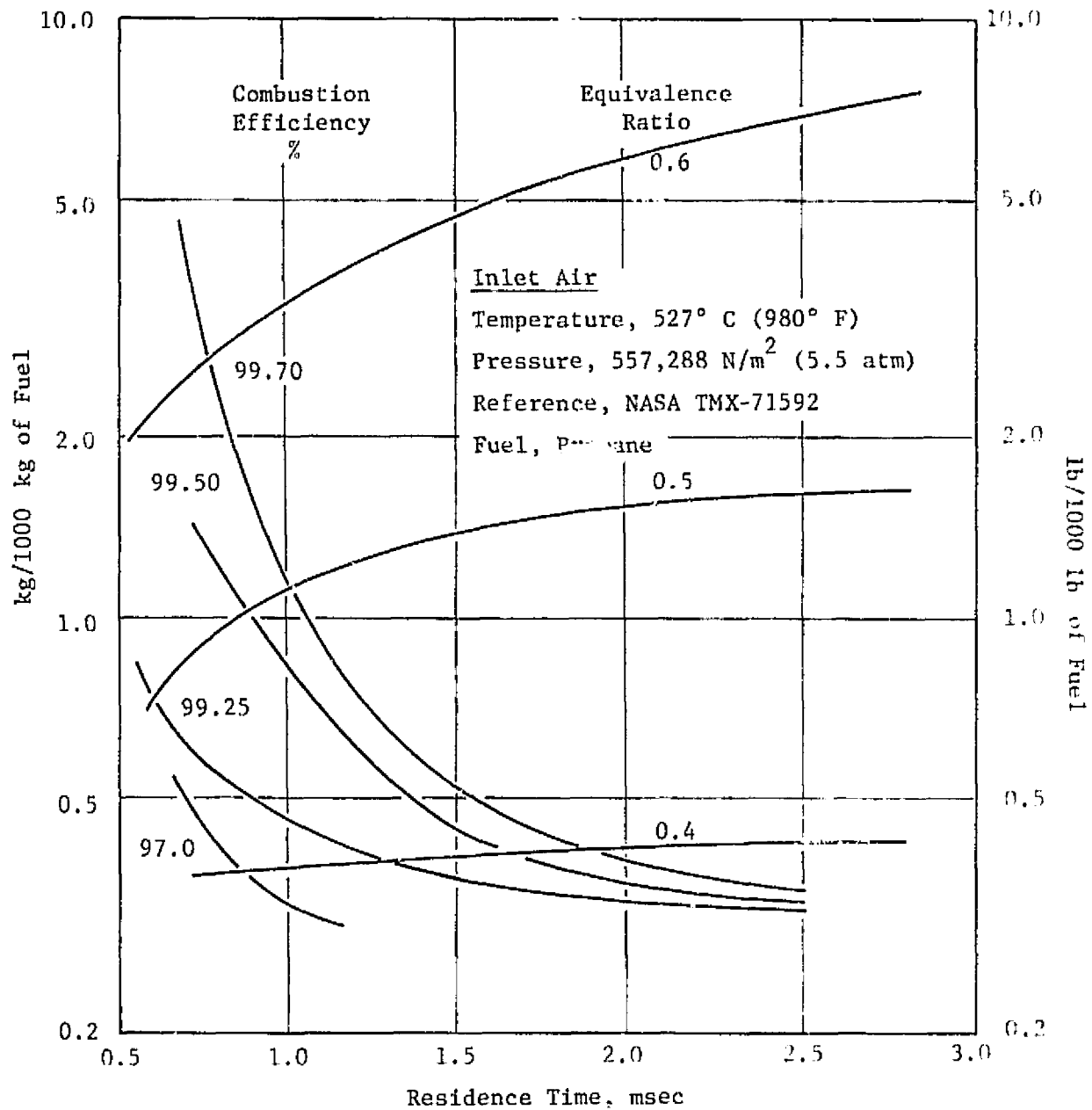
Figure 41. NO$_x$ Levels Obtainable with Lean Fuel-Air Mixtures.
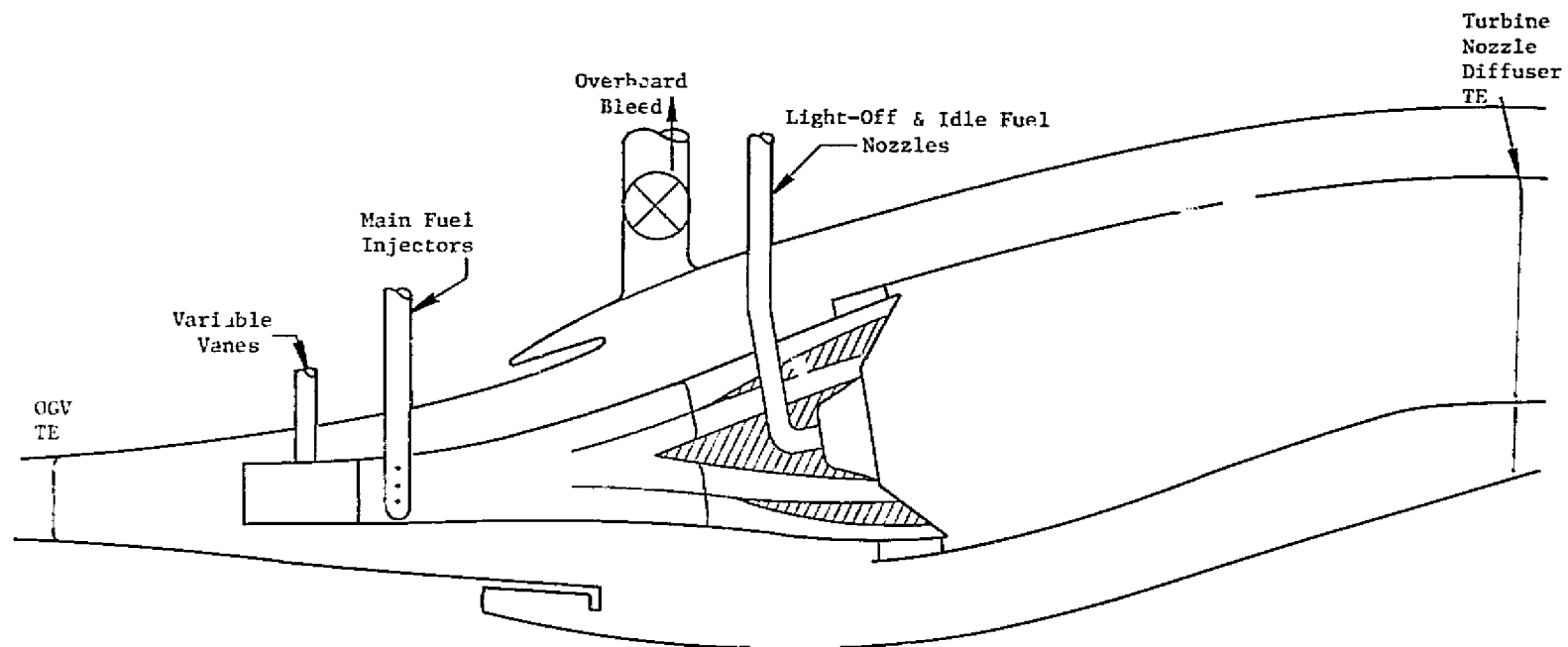
Figure 42. Premixing Combustor Design Concept - AST VCE.
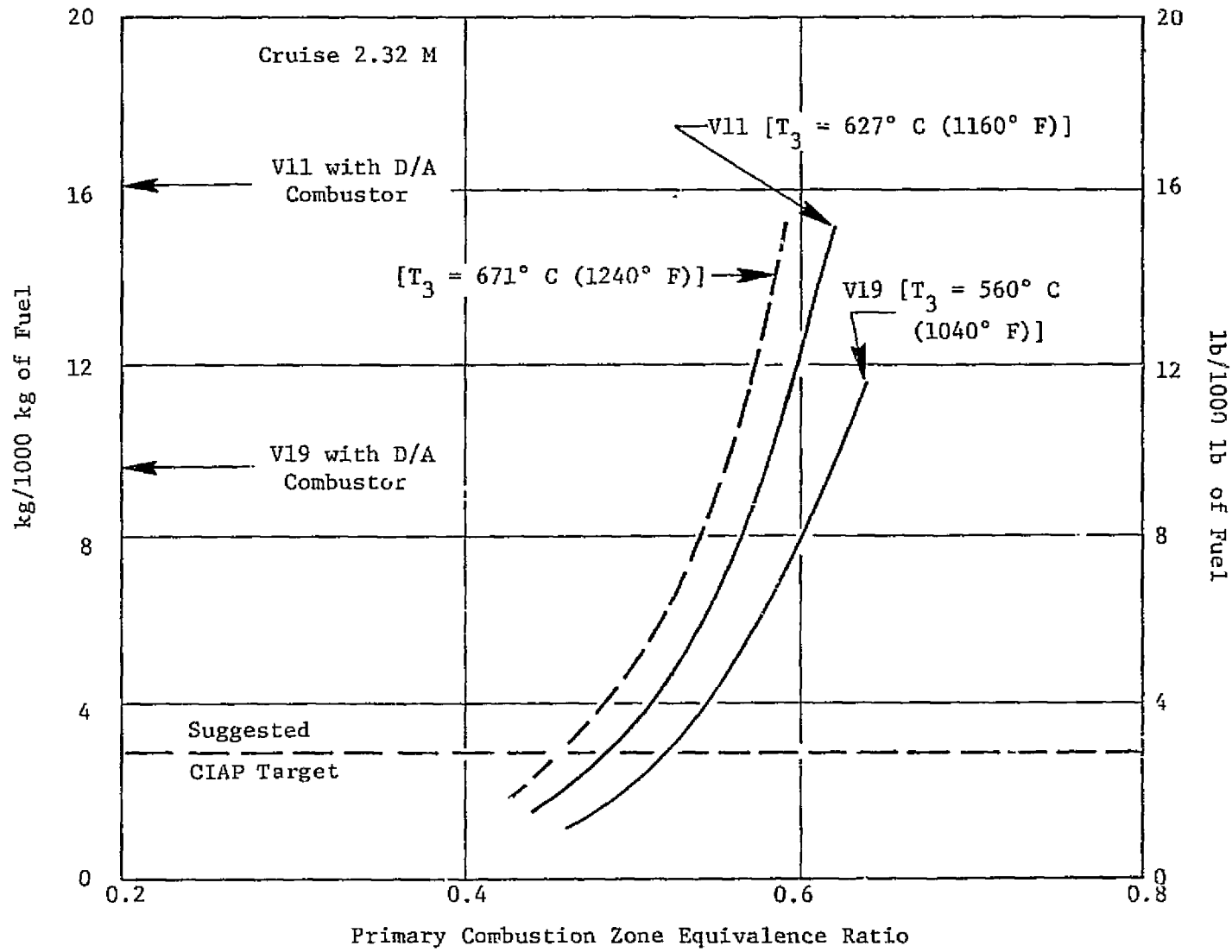
Figure 43. Estimated NO$_x$ Levels of AST VCE with Premixing Combustor.

lence ratios required for low NO_x emission must also decrease, increasing the possibility of combustion stability. The current VCE combustor inlet temperatures are kept below 627° C (1160° F), which should maintain equivalence ratios safely above the combustor stability limits.

The premixing combustor may provide a means for reducing main combustor high-altitude NO_x emissions. However, much research, development, and testing will be required to determine if it is a concept which can provide the necessary safety, reliability, and performance required for a commercial airplane.

The GE21/J11 Study B3 was selected as a representation variable cycle engine early in the Phase III study (before airframer studies had been completed). The estimated emissions levels for the Mach 2.4 cruise GE21/J11 Study B3 are shown on Table 16 for the double-annular combustor and Table 17 for the premixing combustor. The double-annular combustor is estimated to meet the EPA-proposed 1984 airport standards, but has higher than desired cruise NO_x emission levels. The premixing combustor provides lower cruise NO_x levels, but may cause problems in meeting the EPA CO required levels. Further research will be required to come up with a design which will show further reductions in altitude cruise NO_x levels.

Table 16. Double-Annular Combustor Estimated Emissions.

	GE21/ J11B3	1984 Standard T5 Engines	% Reduction Required
CO kg/1000 N Thrust-hr/Cycle	15.5(7.7)	15.7(7.8)	0
C_xH_y (1b/1000 1bf hr/Cycle)	1.6(0.8)	2.0(1.0)	0
NO_x	7.5(3.7)	10.1(5.0)	0

Estimated Cruise NO_x = 13.5 kg/1000 kg of Fuel (13.5 1b/1000 1b of Fuel)

Table 17. Premixing Combustor Estimated Emissions.

	GE21 J11B3	1984 Standard T5 Engines	% Reduction Required
CO kg/1000 N Thrust - hr/Cycle	17.8(8.8)	15.7(7.8)	12
C_xH_y (1b/1000 1bf - hr/Cycle)	1.2(0.6)	2.0(1.0)	0
NO_x	9.5(4.7)	10.1(5.0)	0

Estimated Cruise NO_x = 4.4 kg/1000 kg of Fuel (4.4 1b/1000 1b of Fuel)

4.2 MILITARY APPLICATIONS

4.2.1 Military Variable Cycle Engine Data

Data-packs for seven different double-bypass variable cycle engines were supplied to NASA for their use in studies of military aircraft. The engines utilize the same design concepts as those used in AST VCE designs and the component technology is similar. The engine thermodynamic cycles are somewhat different due to differences in military requirements.

The military engines have the following general characteristics:

Full afterburning capability

Flow size 68-130 kg/sec (150-300 lb/sec)

Single-flow nozzle (no noise suppression devices)

Both conventional cruise nozzles and vectored thrust nozzles
   (two types of latter, block-and-turn and ADEN)

Overall pressure ratio of 20 to 28

Fan pressure ratio of 3.5 to 4.5

Turbine rotor inlet temperature, T41, 1538°-1760° C (2900°-3200° F)

4.3 SPECIAL STUDIES

As part of this contract NASA requested that several special studies be carried out by the General Electric Company. These studies are listed below:

- Flap blowing at takeoff

- Power management for takeoff

- Variable bypass engine (supersonic inflow fan)

These studies are described and the results are presented in the following discussions.

4.3.1 Flap Blowing at Takeoff

A short study was undertaken in order to determine whether the use of flap blowing would significantly improve the performance of the baseline AST aircraft (AST-2) currently being used in General Electric's AST studies. The study examined the interaction between takeoff aerodynamics of flap-blowing systems, engine size, noise characteristics, and mission performance. Many simplifying assumptions were used - generally favoring the flap-blowing

system. A detailed presentation of this study, including methods and results, is given below.

4.3.1.1 Assumptions

The assumptions used in the analysis are listed with little or no discussion.

Airplane layout
- baseline AST-2 aircraft
- no changes in plan form or wing area

Aircraft TOGW
- 345,643 kg (762,000 lb)
- no change due to use of flap-blowing
- no weight penalty for flap-blowing system and equipment

Empty Weight
- only change is due to engine weight change
- engine weight is f (engine airflow size)
- $W_E \sim (airflow)^{1.2}$
- no weight penalty to airframe structure due to installation of flap-blowing system or due to existence of other special equipment required in connection with flap-blowing

Flap-Blowing
- used for takeoff only
- uses fan air 67.6 kg/sec (149 lb/sec) per engine

Takeoff BFL
- held fixed at 3200 m (10,500 ft)

Landing
- speed held fixed
- flap-blowing not used

Drag Characteristics Takeoff
- NASA statement regarding drag characteristics was used $\Delta C_L = 0.1$, $\Delta C_D = 0.019$
- two different interpretations are possible and were evaluated (see Figure 44)
- two sets of study results followed (called CASE I and CASE II)
- no drag penalty as engine size is increased
- no credit for bleed air lift and thrust. Assumed to be included in ΔC_L, ΔC_D assumptions (Case Ia is an exception)

88
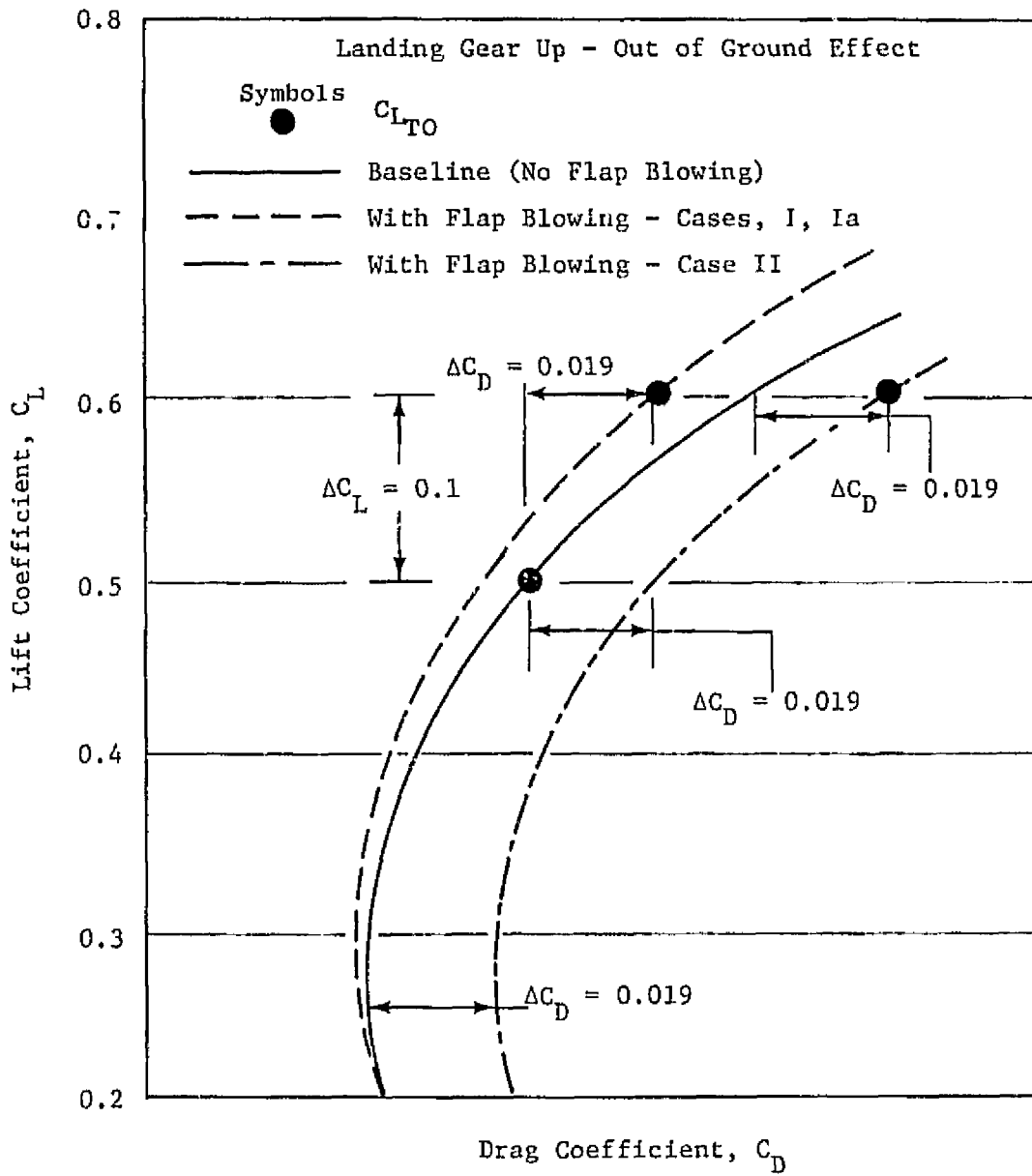
Figure 4. Assumed Takeoff Aerodynamics AST-2 Aircraft.

Noise   -   latest in-house GE noise calculations
Characteristics

                         -   no penalty for possible added noise of bleed air
                             impinging on, and scrubbing over, flap surfaces

                         -   bleed air noise assumed equal to that of normal fan
                             air exhausting through the fan nozzle

                         -   7.5 dB noise credit applied to jet noise due to
                             annular and radius ratio nozzle effects (at high
                             power setting only)

4.3.1.2 Analysis

The process used to analyze the problem and to calculate results is out-
lined here.

1. Baseline was established - AST-2 aircraft

                             -   4 GE21/variable cycle engines

                             -   408 kg/sec (900 lb/sec) nominal airflow
                                 size each

2. Assumptions were made (see previous discussion).

3. Two different drag polars were defined, each yielding $\Delta C_L = 0.1$ and
    $\Delta C_D = 0.019$ (see Figure 44). The curve labeled Case II is con-
    structed by adding $\Delta C_D = 0.019$ to all points on the original curve.
    This results in an equal displacement of the whole curve to the
    right. The curve labeled Case I is constructed by holding C_D
    at $C_L = 0.0$ unchanged and by decreasing the induced drag co-
    efficient so that the curve is, in effect, rotated to the left.
    The result is that the drag coefficient of Case I at $C_L = 0.6$
    is higher than the baseline drag coefficient at $C_L = 0.5$ by a
    $\Delta C_D = 0.019$. Thus, both curves meet the requirement that $\Delta C_D = 0.019$
    and $\Delta C_L = 0.1$ by different interpretations.

4. Takeoff C_L was assumed to increase by 0.1 when flap blowing was
    used.

5. Takeoff computer program was used to establish engine thrust re-
    quired to meet 3200 m (10,500 ft) Balanced Field Length for the two
    cases.

6. Takeoff computer program was used to establish the climb-out path
    with specified aerodynamics and engine size for two cases. Program
    also established noise cutback point and the thrust required for
    cutback operation.

7. Approach characteristics were left unchanged.

90

8. Acoustic calculations were carried out to establish engine noise characteristics for typical operating conditions.

9. Engine thrust losses (due to removing fan air for flap bleed) were calculated. Two different assumptions were used (Case I/II and Ia).

10. Required nominal engine airflow size was determined for the two cases.

11. Noise characteristics at actual operating conditions and for actual engine sizes were estimated by interpolation, extrapolation, and correction. Noise values for the three FAR 36 measuring conditions were estimated.

12. Takeoff noise "footprint" for 90 dB contour was estimated.

13. Range at constant payload was estimated using results of previous calculations.

4.3.1.3 Results (Including Discussion)

The results of the above analysis are presented in tabular form in Tables 18, 19, and 20.

Use of large amounts of fan air for flap blowing results in a substantial thrust loss in the main propulsion system. This requires an oversizing of engine nominal airflow so that sufficient bleed air and thrust can be supplied simultaneously.

Although the two different drag polars used in the analysis yield differing answers, the results at least agree, namely, that no improvements are made in either aircraft performance or in community noise levels.

The baseline case is the standard baseline AST-2 aircraft without flap blowing. It is retained throughout this study to permit comparisons to illustrate the changes introduced by flap blowing and in order to establish the payoff through flap blowing. Case II differs from Case I in the construction of the aircraft drag polar (see Figure 44).

In Case I thrust required for takeoff is low. However, when the appropr- thrust losses are accounted for, a slightly larger engine size is required Table 19). The climb-out performance is poor due to lower installed .st and the higher drag. As a result, the aircraft reaches 6.5 km (3.5 nmi) noise measuring point at an altitude significantly lower than that of the baseline case. Thus, results show a small range loss (versus baseline) with increased community noise level.

Table 18. Takeoff, Climb Out, and Landing Characteristics.

	Base Case		Case I/Ia		Case II	
Balanced Field Length m (ft)	3200	(10,500)	3200	(10,500)	3200	(10,500)
TOGW kg (lb)	345,640	(762,000)	345,640	(762,000)	345,640	(762,000)
Wing Area m^2 (ft^2)	926	(9,969)	926	(9,969)	926	(9,969)
Flap Blowing Used	No		Yes		Yes	
Takeoff Lift Coefficient, $C_{L_{TO}}$	0.773		0.873		0.873	
Drag Polar Representation	Base		Case I		Case II	
Takeoff Thrust Required N[*] (lbf)[**] [M = 0.3 SL, OAT = Std Day +15° C (+27° F)	273,110	(61,400)	249,470	(56,087)	278,670	(62,650)
Cutback Thrust Required N[*] (lbf)[**] (4% gradient, no acceleration)	153,200	(34,442)	151,510	(34,062)	198,590	(44,647)
Altitude Reached at 6.5 km (3.5 nmi) from Start of Ground Roll	570 m (1870 ft)		504 m (1653 ft)		438 m (1438 ft)	
Landing Thrust Required N[*] (lb)[*]	62,270	(14,000)	62,270	(14,000)	62,270	(14,000)
Altitude at 1.8 km (1.0 nmi) Point	113 m	(370 ft)	113 m	(370 ft)	113 m	(370 ft)

[*] per engine

[**] Flaps still in takeoff configuration, landing gear retracted

Table 19. Engine Thrust Losses at Takeoff Conditions.

[M = 0.3 at Sea Level, OAT = Std Day +15° C (+27° F)

	Baseline		Cases I/II		Case Ia	
Fan Bleed for Flaps	No		Yes		Yes	
Nominal Engine Size kg/sec (lb/sec)	408	(900)	408	(900)	408	(900)
Total Fan Flow kg/sec (lb/sec)	536	(1181)	536	(1181)	536	(1181)
Core Flow kg/sec (lb/sec)	352	(777)	352	(777)	352	(777)
Duct Flow – Bled Off kg/sec (lb/sec)	0	(0)	68	(149)	68	(149)
Duct Flow – Out Exhaust kg/sec (lb/sec)	183	(404)	116	(255)	116	(255)
Core Exhaust Velocity m/sec ft/sec	711*	(2332)*	711*	(2332)*	711*	(2332)*
Duct Exhaust Velocity m/sec ft/sec	498*	(1636)*	498*	(1636)*	498*	(1636)*
Net Thrust – Installed (After Bleed) N (lbf)	273,110	(61,400)	240,590	(54,090)	253,870	(57,075)
Required Nominal Airflow for Fn = 249,470 N (56,087 lbf)	–	–	425 kg/sec	(936 lb/sec)	396 kg/sec	(872 lb/sec)
Required Nominal Airflow for Fn = 278,670 N (62,650 lbf)	–	–	473 kg/sec	(1042 lb/sec)	–	–

*Fully expanded

Table 20. Noise Characteristics for Range Estimates.

Effects of Flap-Blowing Usage

	Baseline		Case I		Case Ia		Case II	
			with Flap Blowing					
TOGW kg (lb)	345,640	(762,000)	345,645	(762,000)	345,643	(762,000)	345,642	(762,000)
Balanced Field Length m (ft)	3200	(10,500)	3200	(10,500)	3200	(10,500)	3200	(10,500)
Engine Size Nominal Airflow kg/sec (lb/sec)	408	(900)	424	(836)	396	(872)	473	(1438)
Altitude at 6.5 km (3.5 nmi) Point m (ft)	570	(1870)	504	(1653)	504	(1653)	438	(1438)
Estimated Propulsion Noise - EPNdB								
Sideline	110.1		110.2		110.0		110.8	
Community	102.0		105.6		104.5		110.7	
Approach	104.4		104.2		104.5		104.0	
Traded (per FAR 36 Rules)	108.1		108.2		108.0		104.3	
Estimated Takeoff Noise Footprint (90 dB Contour) - ha (nmi²)	5490	(16)	10,290	(30)	11150	(32.5)	171	(50)
Relative Range, Fixed (Baseline) Payload km (nmi)	0	(0)	-55	(-30)	+55	(+30)	-30	(-1653)
Relative Range (Baseline is Base)	1.0		0.941		1.056		.953	

Case Ia is a variation of Case I in that some thrust recovery is assumed
for the flow exiting from the jet flap nozzles themselves. It is assumed
that half of the gross thrust is recovered and that it is applied at an angle
of 0.523 rad (30°) from the horizontal. Takeoff calculations were modified
to account for this change in forces. It was further assumed that the air-
craft aerodynamic characteristics were not changed.

In Case II, no credit for thrust recovery was assumed. Thrust required
for take off is high, and cutback thrust required is very high due to the un-
favorable shape of the drag polar. In addition, the climb-out performance is
poor. Thus, results show larger range loss, with large increase in community
noise.

The actual drag polar of an AST aircraft aerodynamic system optimized to
exploit flap-blowing use is not known. Until such a drag polar can be defined
in detail, it will not be possible to correctly and fairly assess the possible
advantages of flap blowing. It is of interest to note, however, that, if the
drag polar is similar to and falls between the two shapes identified in
Figure 44 (Case I and Case II), the study results would fall between those in
Case I and Case II, and conclusions would be similar to those reached in this
study.

No attempt was made to optimize the aircraft wing plan form wing size,
flap size, and flap setting to better suit flap blowing. Future studies
should include examination of wing plan forms having higher aspect ratio
values and suitable changes in flap geometry.

4.3.1.4 Conclusions

Several general – and necessarily tentative – conclusions have been
reached based on the study results:

1. For the assumptions made and methods used, AST range performance is
    not improved through the use of flap blowing.

2. For the assumptions made and methods used, when flap blowing is
    used, AST sideline and community noise levels are increased, yield-
    ing less acceptable levels of Traded Noise (versus FAR 36 goals).

It may be desirable to conduct additional evalutions in which a more
detailed evaluation is made and in which the aircraft configuration is
changed. It may also be desirable to consider use of core bleed air.

4.3.2 Takeoff Power Management

During the analysis of engine noise characteristics of climb out after
takeoff , it was discovered that engine noise varies with altitude in a pre-
dictable manner (see Figure 45). For each throttle setting (and correspond-
ing level of exhaust jet velocity) there is a different curve of engine noise
versus altitude (see Figure 46).
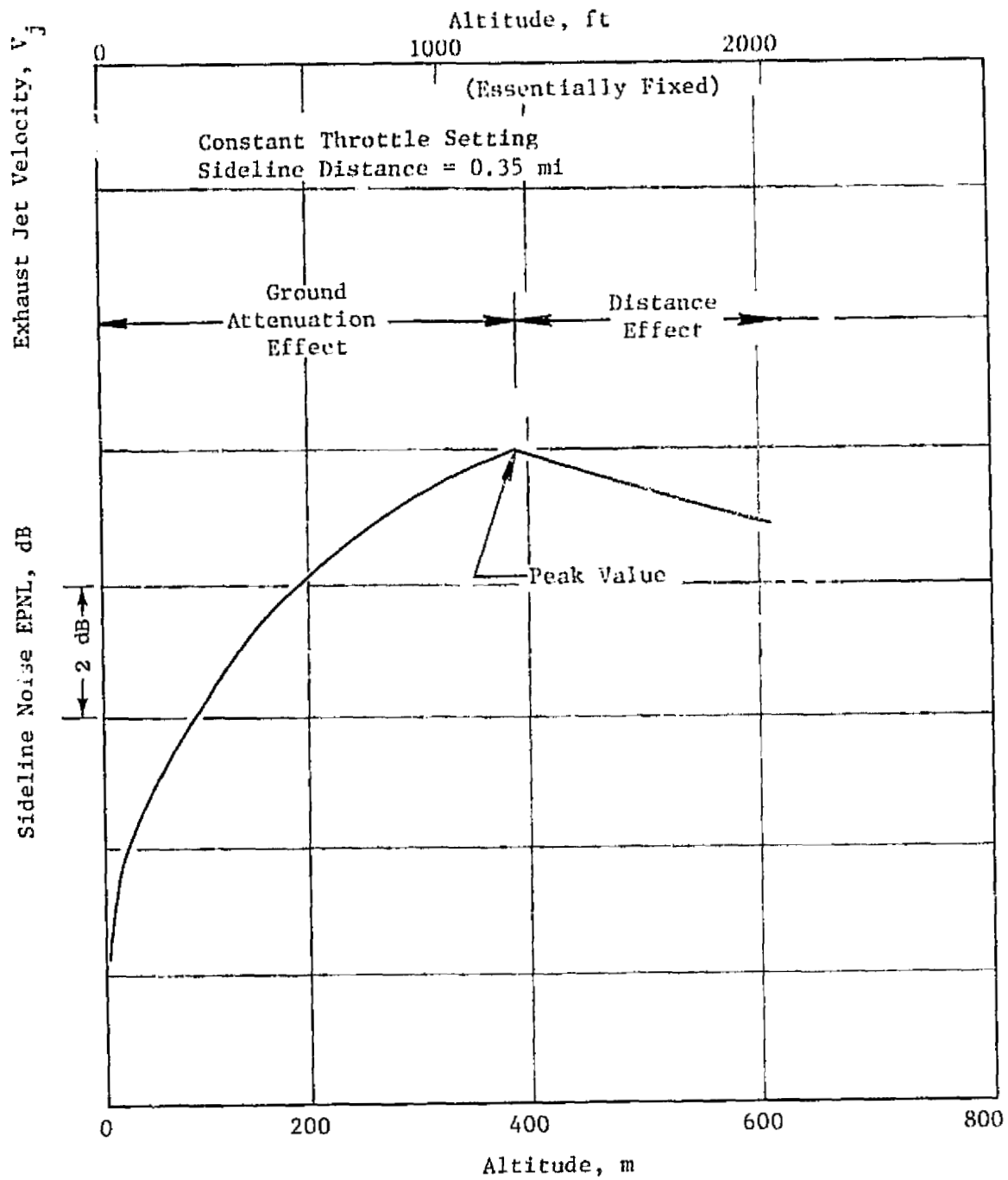
Figure 45. Sideline Noise During Climb-Out, AST-2 Aircraft.
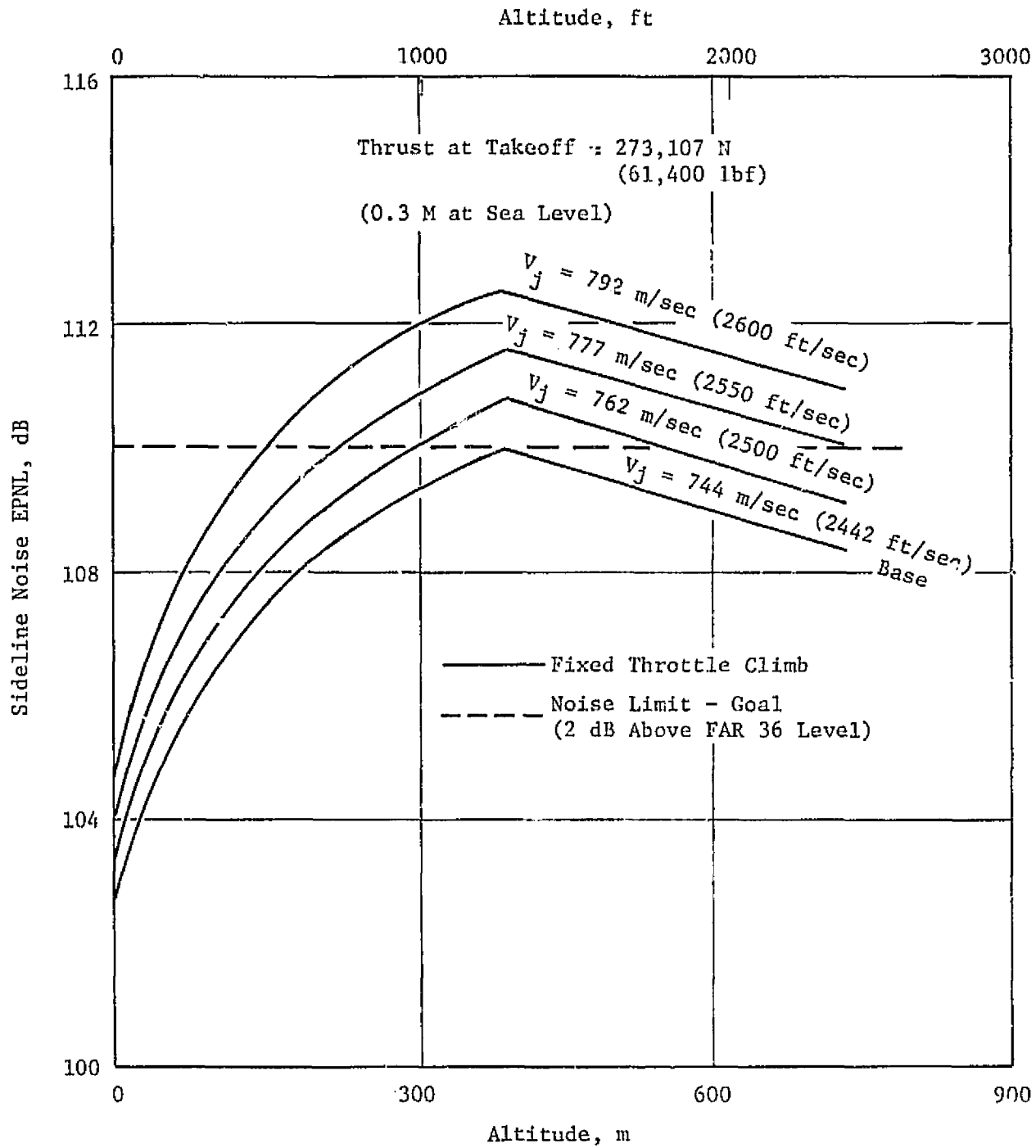
Figure 46. Sideline Noise Characteristics AST-2 Aircraft.

Because FAR 36 regulations specify that the peak noise level during climb out is to be used in the noise certification procedure, the engine cycle exhaust jet velocity is generally chosen so that the peak noise level falls within a goal or limit chosen by the designer (or the user). If the engine is operated at a constant throttle setting (with jet velocity approximately constant), the noise level is below the peak level at all points other than the peak level itself (see also Figure 45).

4.3.2.1 Analysis

It has been suggested that a better engine/airframe integration might be achieved if the exhaust jet velocity (V_j) were to be varied during the climbout in such a way so as to attain maximum thrust levels at all times and yet stay within a given sideline noise level. Figure 47 depicts a possible mode of operation to achieve this end. In this case, the exhaust jet velocity is increased initially to a maximum allowable level [say 777 m/sec (2250 ft/sec)] and held at that level during climbout only until the noise level limit goal is reached. At that point, jet velocity is reduced and varied so that the noise is held fixed and does not exceed the desired level. Eventually the jet velocity is increased back up to its maximum allowable level (see Figure 47).

A study was carried out in order to evaluate the advantages of the power management technique. Four different double-bypass variable cycle engine sizes were selected. Each had the same basic cycle but operated at a different value of maximum jet velocity at the sizing condition. All engines were sized to yield the same takeoff thrust of 273,107 N (61,400 lb) at 0.3 M sea level for an OAT of ISA +15° C (+27° F).

The specifying of thrust and jet velocity at take off fixes the engine airflow for each engine cycle selected. As the jet velocity is increased, required airflow size decreases (see Figure 48).

Each engine was operated in a manner similar to that depicted in Figure 47, such that each engine had the same peak sideline noise value of 110 dB (so that a traded noise level of 108 dB could be achieved). All engines start out the climb-out procedure at the same thrust level (due to having been sized for the take off thrust requirement). During the climbout, each engine is gradually throttled back at the appropriate altitude so as not to exceed 110 dB sideline noise. As a consequence, the thrust level is reduced during the throttled-back portion of the climbout (see Figure 49). For convenience the curves in Figure 49 represent a climbout without cutback.

This thrust reduction affects the aircraft climb gradient and causes the aircraft in each case to reach the 6.5 km (3.5 nmi) noise measuring point at a different altitude (Figure 50). Of course, the greater the amount of thrust reduction during power management, the lower the altitude reached at the 6.5 km (3.5 nmi) point. This variation in altitude affects the level of community noise at cutback, with those cases arriving at lowest altitudes being the noisiest to the observer on the ground.

98
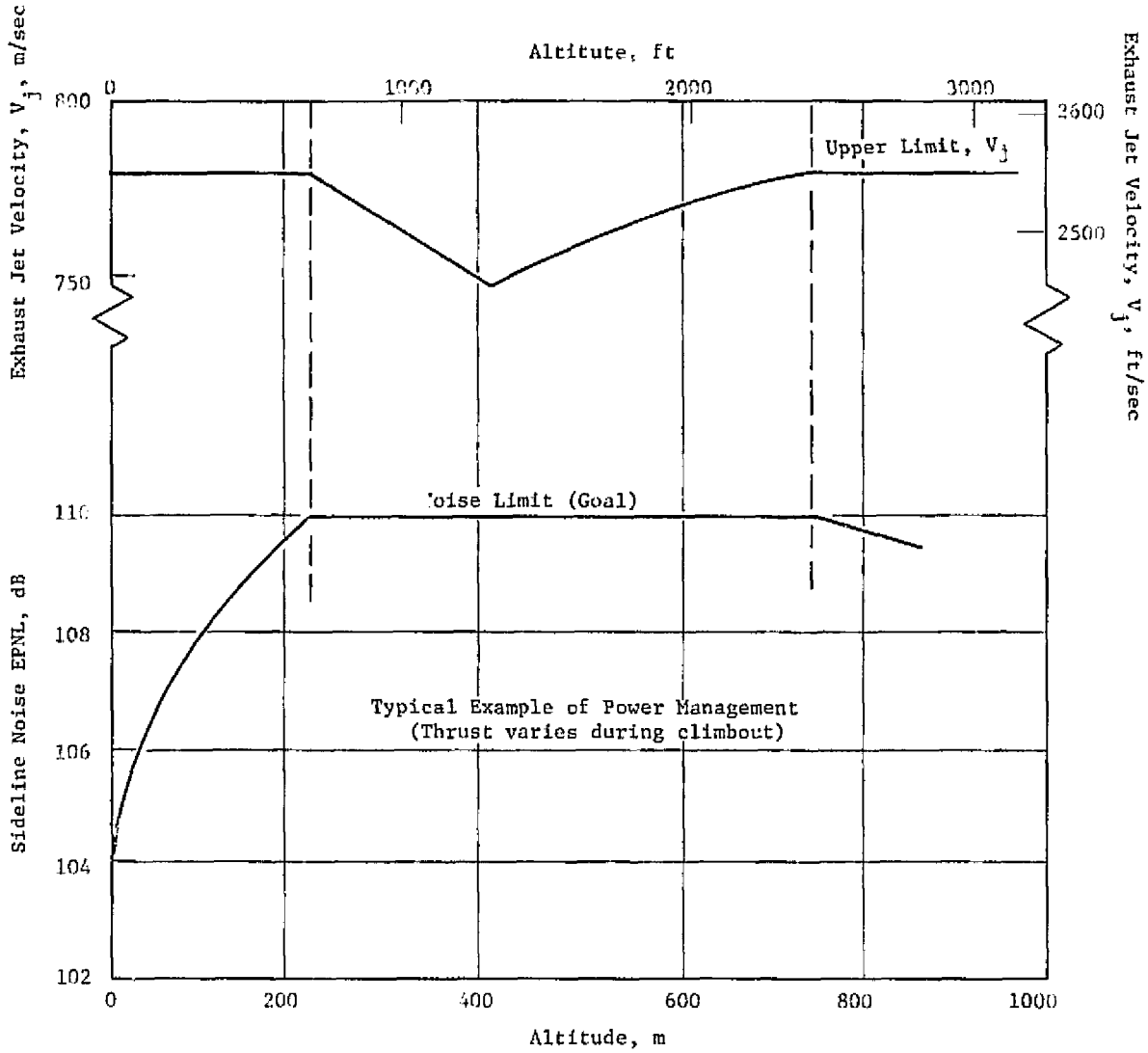
Figure 47. Exhaust Jet Velocity and Sideline Noise During Climb-Out.
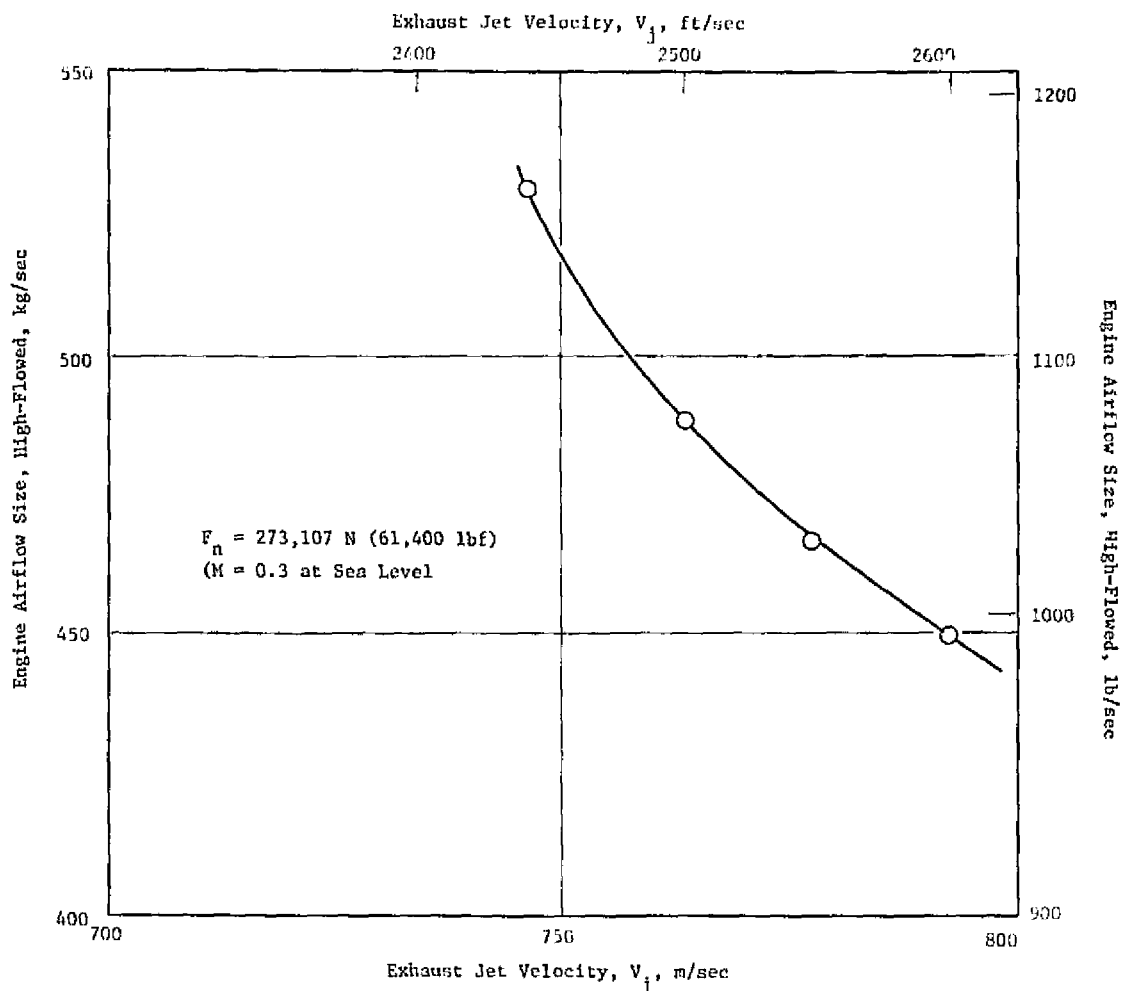
Figure 48. Engine Sizing for Take-Off.
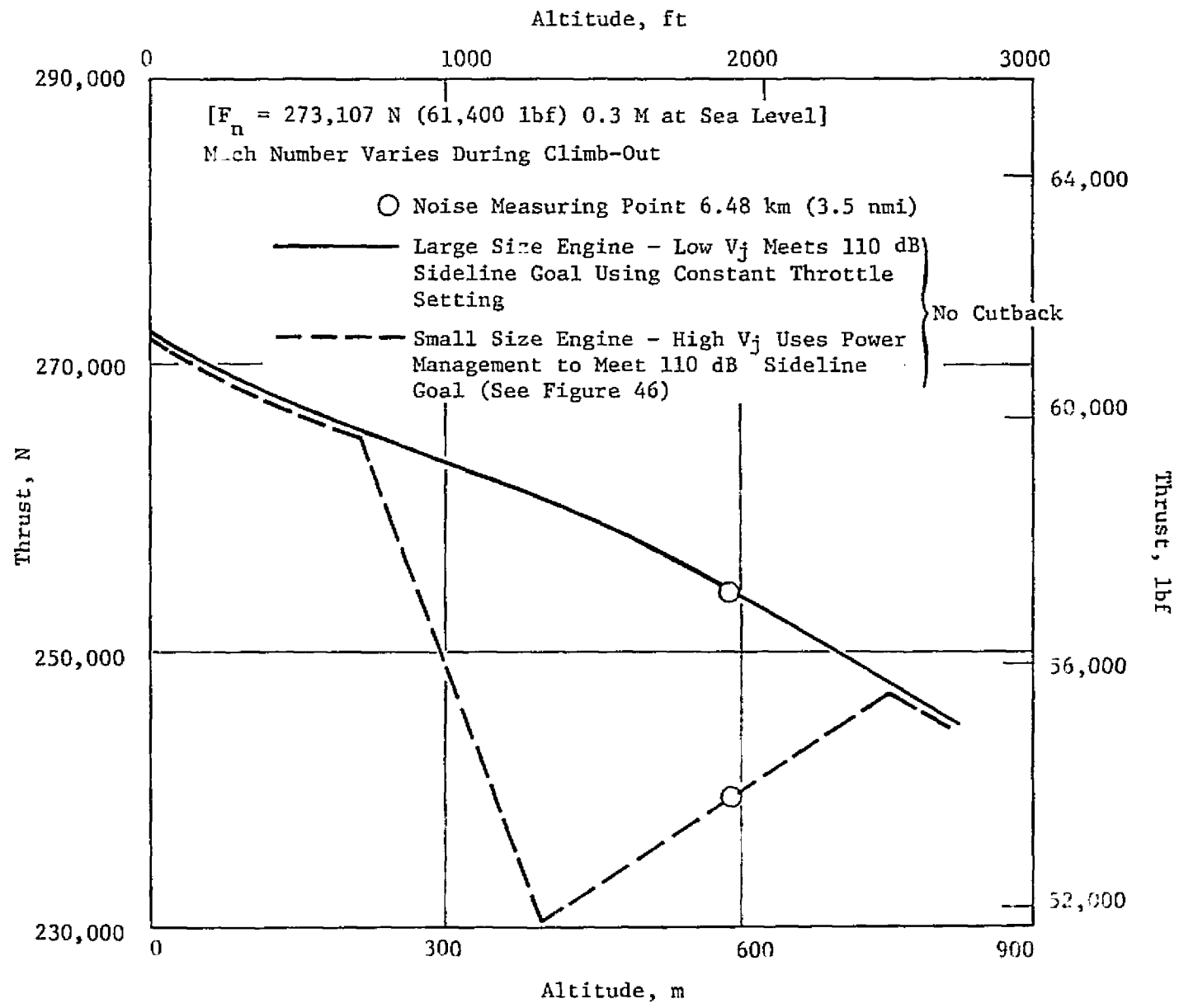
Figure 49. Thrust Variation During Climb-Out.
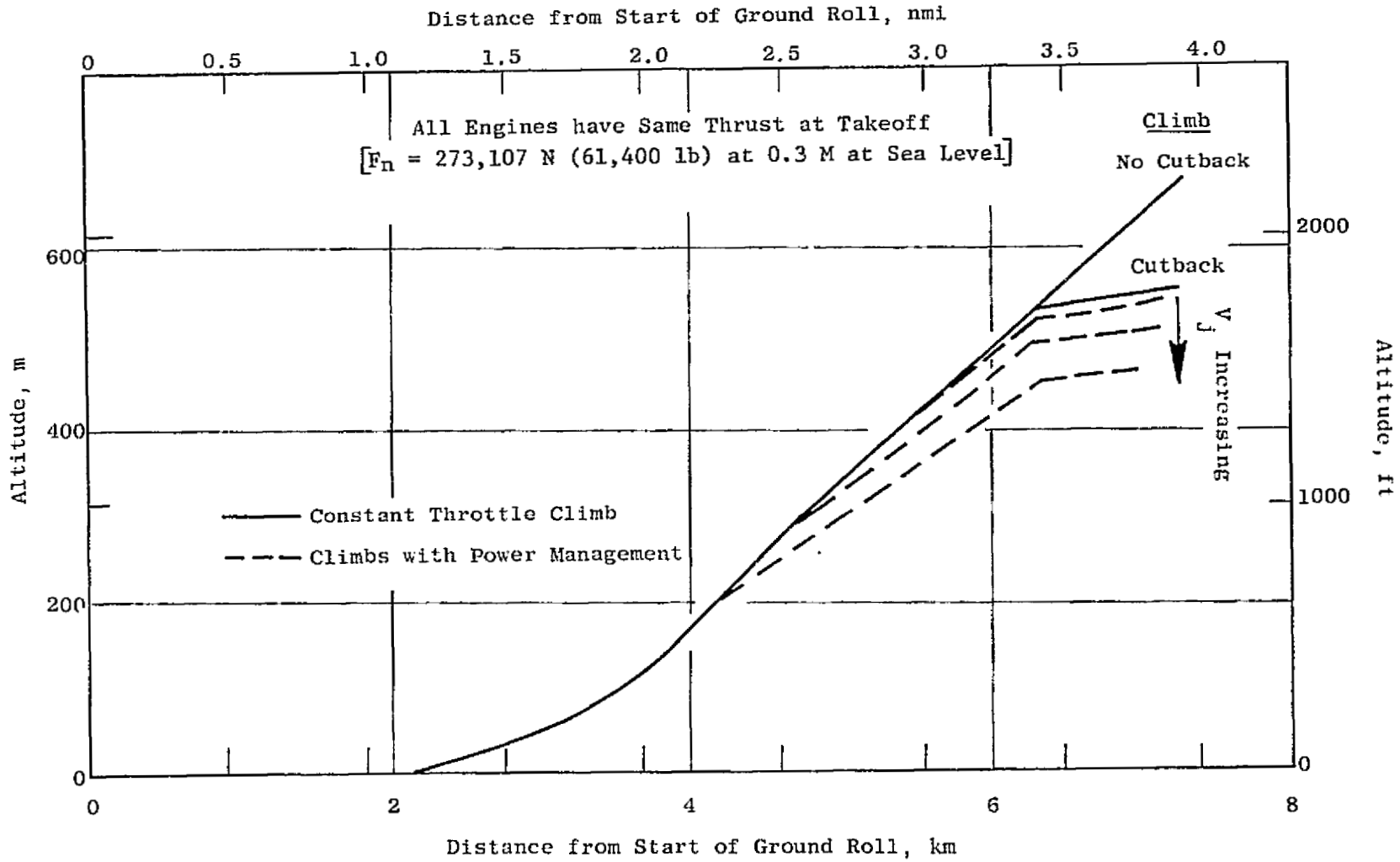
Figure 50. Climb Trajectories.

In addition, since each engine has a different airflow size, it must operate at a different power setting after cutback in order to generate the required cutback thrust level. The smaller engines are forced to operate at higher power settings. This variation in cutback power setting also affects the community noise level, with those engines having the highest power setting in cutback having the greatest noise to the observer on the ground.

4.3.2.2 Results

As engine size is reduced, engine weight is reduced and the aircraft range is improved (see Figure 51). Overall results of the study are tabulated in Table 21. Although estimates of noise contours (i.e., footprints) were not made, it is also obvious that footprint area will increase as community noise level increases due to two reasons:

- Higher community noise level

- High noise levels last longer in the initial portion of the climbout path.

4.3.2.3 Discussion

The technique described in Section 4.3.2.1 was designed primarily to improve aircraft range performance, while keeping noise levels within certain goal levels. This particular technique is not the only power management procedure possible. Others can be devised to achieve different ends or to concentrate on other AST performance or environmental parameter improvements, such as:

lower sideline noise

lower community noise

smaller takeoff footprint areas

lower emissions

Such other techniques may combine the scheduling of jet velocity together with the scheduling of flight velocity and aircraft variable geometry features in order to achieve the specific goal in mind. Each technique will have its own unique engine operating schedule tailored for this task and the schedule may differ from that used in the study described in this report.

4.3.2.4 Conclusions

It is concluded that although there is a range gain achievable through the use of the power management technique (described in Section 4.3.2.1) this range gain comes at the expense of increased community noise levels and increased noise footprint areas. Further evaluation in greater detail is required to determine if the range/noise trade-off would be an attractive one. In addition, further study is necessary to determine whether there are other schemes of engine control to better achieve the goals addressed in this brief study.
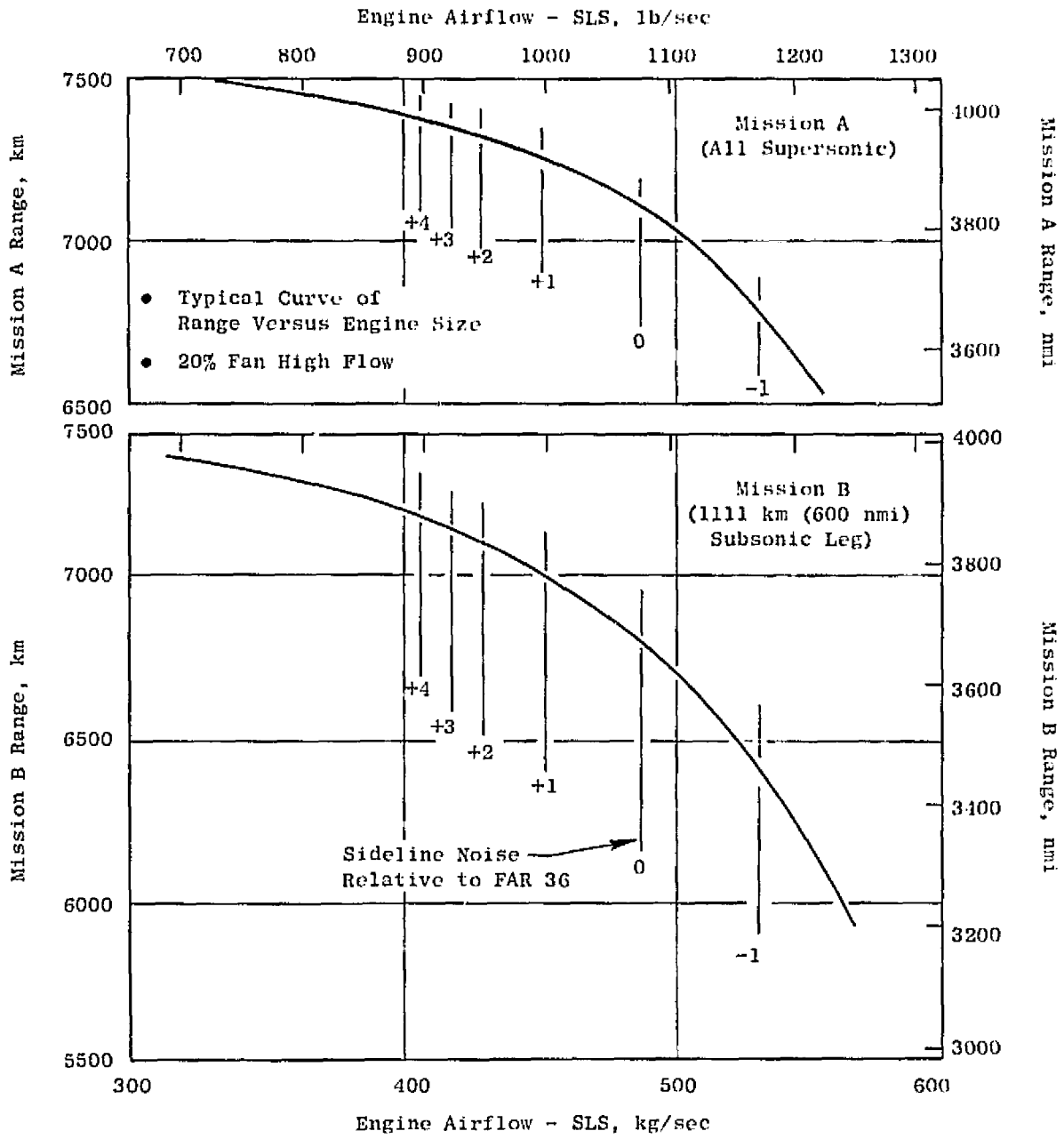
Figure 51. AST Mission Range Performance.

104

Table 21. Noise Characteristics for Engine Sized for Takeoff.

	Effects of Varying Exhaust Jet Velocity and Varying Amounts of Power Management			
Exhaust Jet Velocity, V_J – m/sec (ft/sec)	744 (2442)	762 (2500)	777 (2550)	792 (2600)
Airflow for 273110 N (61400 lbf) 7.0 Thrust – kg/sec (lb/sec)	528 (1164)	488 (1077)	467 (1029)	451 (994)
Peak Sideline Noise (Constant throttle climbout) EPNL dB	110.0	110.7	111.5	112.6
Peak Sideline Noise (Power Management) EPNL dB	110.0	110.0	110.0	110.0
Δ Range (Mission A) km (nmi)	(base)	+278 (+150)	+370 (+200)	+407 (+220)
Δ Range (Mission B) km (nmi)	(base)	+333 (+180)	+426 (+230)	+500 (+270)
Estimated Altitude at Community Point m (ft)	570 (1870)	562 (1843)	543 (1782)	523 (1716)
Estimated Community Noise (Cutback Thrust) EPNL dB	101.9	102.8	103.6	104.3
Traded Noise EPNL dB	108.0	108.0	108.0	108.0

4.3.3 Variable Bypass Engine (Supersonic Inflow Fan)

As part of the AST program the General Electric Co. conducted a short study to evaluate the variable bypass engine utilizing supersonic inflow. This engine had been proposed by Dr. A. Ferri of Advanced Technology Laboratories, Inc. as a candidate for the AST mission. The variable bypass engine is a nonaugmented, moderate-bypass, separated-flow turbofan which is supposed to provide dramatic improvements in weight and fuel consumption and improvements in aircraft range or takeoff gross weight (see Figure 52).

4.3.3.1 Analysis

The novel feature of the variable bypass engine is in the fan component. The fan of this engine obtains the desired pressure ratio in a single stage with essentially no static pressure rise. The fan accepts supersonic axial Mach numbers at supersonic flight speeds so that the conventional supersonic inlet is replaced by a simple fixed-geometry, external compression body faired into the fan hub. A description of this concept and an evaluation of the engine by Advanced Technology Laboratories, Inc. is presented in their report TR-201, "Study of Variable Cycle Engines Equipped with Supersonic Fans," by Horacio Trucco, September 1975 (issued as NASA CR-134777).

In the ATL report, two fan configurations are described: the IGV-rotor configuration and the rotor-stator version. The IGV-rotor system was chosen as the configuration for GE evaluation due to its generally better performance. The fan discharge Mach number is higher than the flight Mach number, making a rather elaborate supersonic inlet system necessary for the core compressor.

Throughout this GE study, component characteristics and system loss assumptions were chosen using consistently optimistic assumptions. This philosophy was followed so as to give the variable bypass engine the best possible level of performance.

Fan performance used for this study for the IGV-rotor configuration is presented in Figure 53 (taken from Figure 13 of ATL Report TR-201). A design-point fan pressure ratio of 3.5 was used, and this requires a design corrected tip speed of 402 m/sec (1320 ft/sec). The design-point fan discharge flow was split by the supersonic inlet lip for the core compressor at a point where the bypass ratio of 1.5 would result. The performance of the core inlet was based on a total pressure recovery of 90% accompanied by an 8% boundary layer bleed. This core inlet performance is probably optimistic considering the high level of boundary layer flow, velocity profile distortion, and swirl approaching this inlet. Thrust regain from the boundary layer bleed air was calculated on an ideal basis using a bleed air total pressure equal to the static pressure at a point in the core inlet where the local Mach number was 1.2.

106
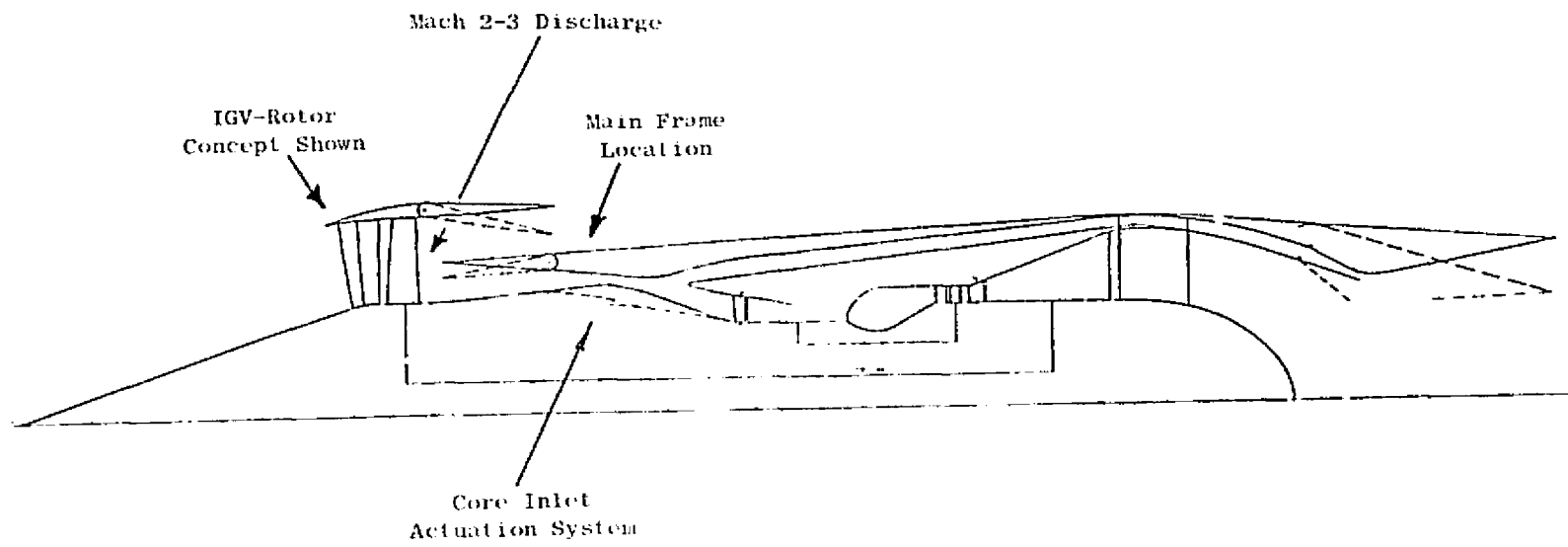
Figure 52.   Variable Bypass Engine Concept.
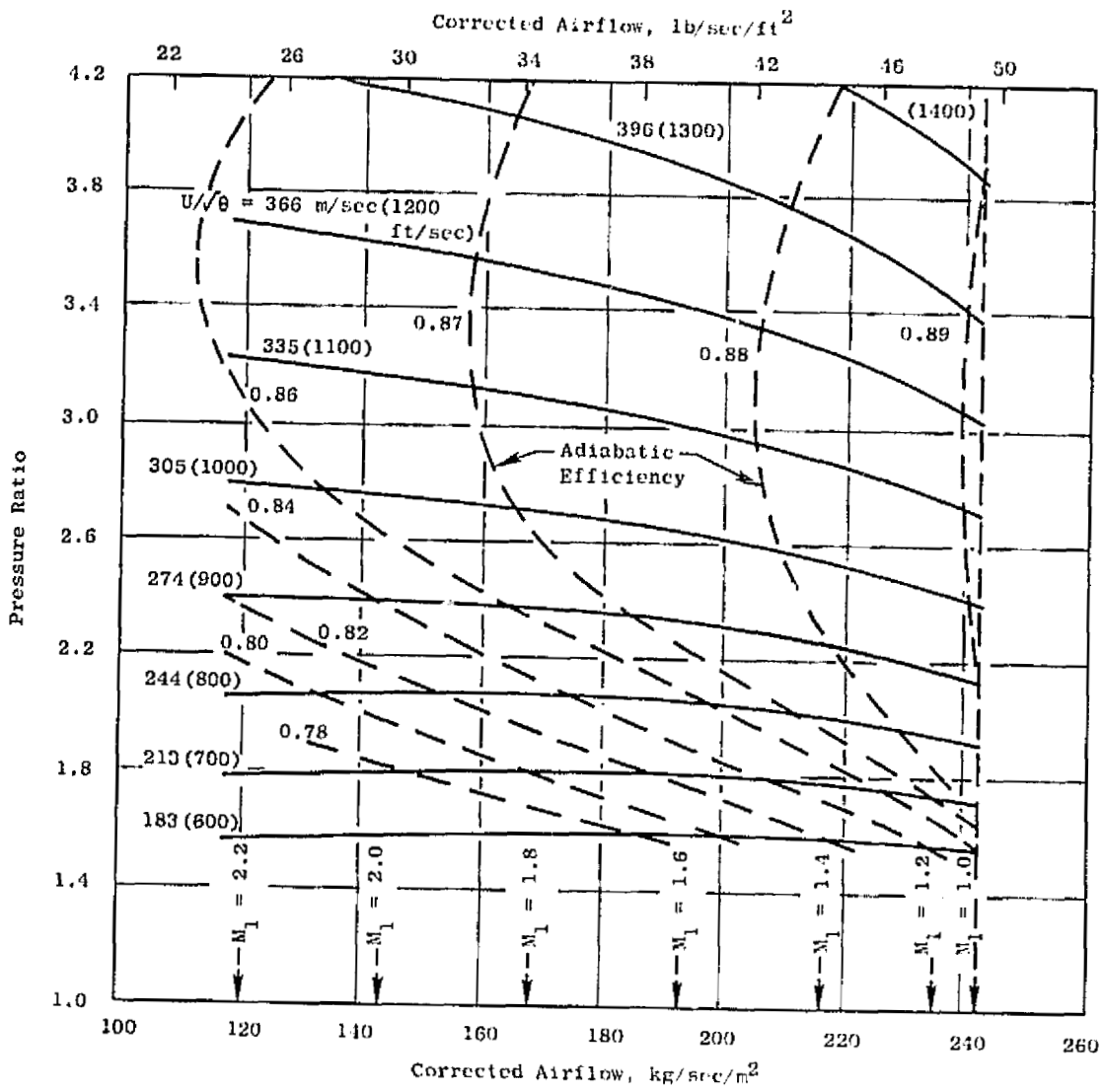
Figure 53. Supersonic Fan Map.

Because the core inlet Mach number is supersonic, a compressor/core inlet matching problem arises which is not present in a conventional turbofan engine. A subsonic bypass system, used to position the core inlet normal shock, is included in the GE configuration for off-design operation.

The core configuration was assumed to be similar to a scaled J101 high-pressure system. The pressure ratio of the core compressor is 5.3, which corresponds to the first six stages of the J101. The J101 flow/speed characteristic was used. However, the efficiency was increased in order to be consistent with AST cycle studies. The core peak efficiency line characteristics assumed are shown in Figure 54. The core design corrected airflow is 103.1 kg/sec (227.5 lb/sec). If the core inlet bleed flow is considered as bypass flow, then the design bypass ratio is 1.72 rather than 1.5.

A maximum cycle turbine inlet temperature T4, of 1538° C (2800° F) was selected for the turbine systems based on studies of another VCE with the same T41 and slightly higher cycle pressure ratio. The cooling flows assumed were:

Nonchargeable Compressor Discharge (CD) - 5.9%

High Pressure Turbine CD + Interstage · 5.1%

Low Pressure Turbine Interstage   - 6.2%

The cooling flows for the low pressure turbine were based on a previous study of single-stage configuration and are, therefore, highly optimistic for the present study. Constant turbine efficiencies of 90% for the high pressure turbine and 89.5% for the low pressure turbine were assumed throughout.

Nozzle gross thrust coefficients for all streams except the boundary layer bleed flow were assumed to be 98%. The boundary layer bleed flow gross thrust coefficient was assumed to be unity.

Engine airflow size was selected to be consistent with the ATL studies in which the fan inlet design capture area was set at 4.16 m² (44.8 ft²). This results in a design fan corrected airflow at sea level static of 725 kg/sec (1600 lb/sec).

In analyzing engine performance data it was found that the high pressure turbine was sized at sea level static, while the low pressure turbine was sized at supersonic cruise. For supersonic operation it was assumed that the fan could be run at its sea level design physical speed while the core was allowed a 5% increase in physical speed over the sea level design value.

The supersonic cruise condition was assumed to be Mach 2.32 at 16319 m (53540 ft) with T_{am} = ISA + 8° C (14.4° F). The maximum fan corrected tip speed at this flight condition is 316 m/sec (1038 ft/sec) at a design physical rpm of 3253. The rotor inlet specific corrected flow is 148.8 kg/sec/m² (30.43 lb/sec/ft²) which results in a fan pressure ratio of 2.92 at an adiabatic efficiency of 0.867 using the referenced fan map. Operating the core at 105% physical speed results in a core corrected speed of 85.1% and a

Variable Bypass Engine
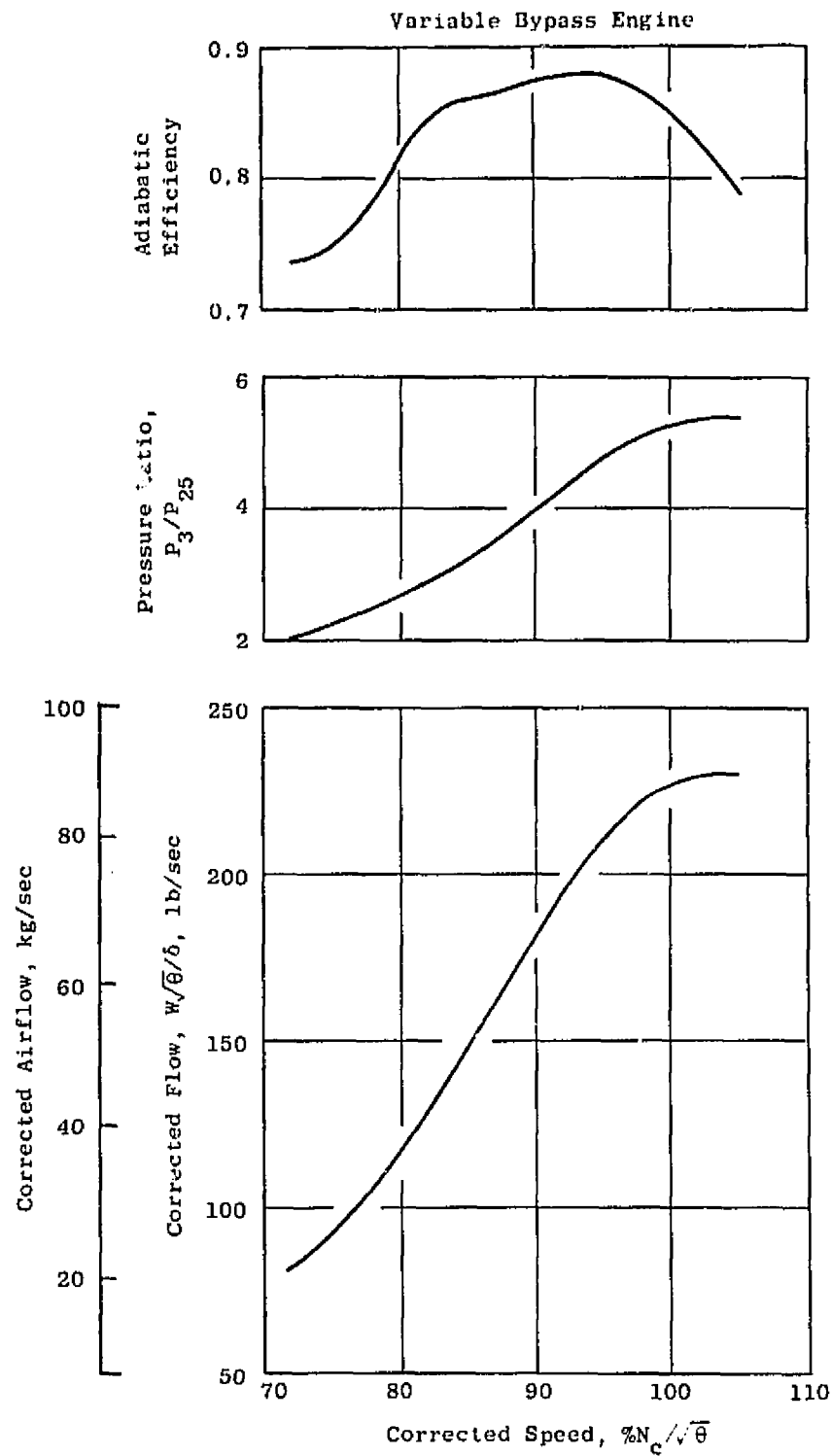
Figure 54. Assumed Core Aerothermo Characteristics.

core corrected flow of 66.7 kg/sec (147 lb/sec). The resulting minimum by-pass ratio is 2.01, compared to a sea level static design value of 1.72. The high fan pressure ratio, coupled with the high bypass ratio, results in very high power extraction required by the low pressure turbine. The turbine discharge annulus area resulting in a 0.5 discharge Mach number is 2.115 m^2 (3277 in.^{2}). Using a lower mechanical limit of turbine discharge radius ratio of 0.6, the low pressure turbine discharge diameter is 205.1 cm (80.75 in.). The turbine loading is such that four, or preferably five, low pressure turbine stages are required. This large low pressure turbine is the source of very high transonic nozzle drag, as the complete expansion nozzle area is much less than the turbine projected area.

A preliminary flowpath was constructed using cycle data (Figure 52). A variable cowl, shown on the core inlet, is used to reduce the degree of throat geometry variation in the starting process. The variable geometry fan cowl nozzle and core exhaust nozzle are shown in the extreme positions. The excess core bypass flow (if any) is discharged out a common exhaust area aft of the core nozzle throat.

A serious problem is the design of the mechanism required to vary the fan exhaust nozzle flaps. At takeoff a crushing load on this flap system of greater than 133440 N (30,000 lb) exists. Undoubtedly the structure and actuators to support this high load will require greater cowl thickness than is shown in the flowpath layout. This would result in even greater cowl pressure drag and boattail drag.

Another serious problem at takeoff is caused by the choked sharp lip inlet ahead of the fan rotor. Extensive flow separation from the inner cowl surface results in a total pressure recovery of less than 80% at static conditions. Since this region of separated flow will extend a good distance downstream of the inlet lip, the rotor blade tip will be affected and possibly will encounter severe rotor aeromechanical stability problems. In conventional engine/inlet systems the engine blading is located a great distance downstream of the inlet lip and separated regions can 'wash out' or else devices such as blow-in doors can be used to minimize sharp lip effects. Such approaches as these are not available in the present engine configuration due to the proximity of the fan rotor to the inlet lip.

Engine performance was calculated for an acceleration path using maximum power. Engine part-throttle performance was calculated for subsonic cruise, supersonic cruise, and subsonic hold conditions. Installation drag estimates were made at each performance point based on the positions of the geometry required. Additive drag was based on conical flow-field calculations for a 0.3141 rad (18°) half angle cone. Cowl pressure drag coefficients were estimated using an elliptical cowl having an initial angle of 0.322 rad (18.5°). Fan nozzle and core nozzle boattail drags were estimated using wind tunnel afterbody drag correlations for similar geometries. Friction drag was calculated using compressible friction coefficients with Reynolds numbers based on total engine shell length and shell surface area. Pressure drag on the conical main engine body was neglected. The component and combined drag

coefficients used are shown in Figure 55. The large transonic drags of the core and fan nozzles are evident in this figure.

The acceleration performance thrust characteristics are shown in Figure 56. Data are shown for both installed and uninstalled thrust. Shown also in this figure are the installed and uninstalled thrust of a 408 kg/sec (900 lb/sec) GE variable cycle engine (VCE). The inferior acceleration thrust of the 725 kg/sec (1600 lb/sec) variable bypass engine is evident.

Estimated supersonic cruise performance, both installed and uninstalled, of the variable bypass engine is shown in Figure 57. Also shown for reference is the performance of the 408 kg/sec (900 lb/sec) GE VCE. At a given thrust level the performance of the engine is inferior to the 408 kg/sec (900 lb/sec) VCE. If the engine size needs to be increased to improve acceleration performance, the cruise performance will deteriorate even more.

Shown in Figure 58 is the installed and uninstalled performance of this engine at subsonic cruise. It shows a small advantage in the 725 kg/sec (1600 lb/sec) size. Also shown for reference is the performance for the 408 kg/sec (900 lb/sec) VCE. Again, increased engine size would cause the performance to deteriorate.

An attempt was made to try to duplicate the parametric performance levels presented in Figure 19 of the Advanced Technology Laboratories' report TR-201 to see if differences in analytical modeling could be a source of conflicting results. The exact points taken from Figure 19 were run with the ATL component performance assumptions listed on page 32 of TR-201 (with the exception that the compressor bleed shown was eliminated). Values of bypass ratio used were the same as those used in the ATL report. Since ATL assumptions regarding turbine cooling air and second inlet bleed air were not listed, the optimistic values used in the GE anlaysis were retained. The results of this comparative analysis are shown in Figures 59 and 60. In Figure 59 there are large discrepancies between GE calculated performance and that quoted in TR-201. Shown at each of the performance points is the compressor discharge temperature (T3) in degrees F. The levels shown of T3 are excessive to the point where none of the cycles presented in Figure 59 is feasible. Even the compressor itself would have to be cooled at some of these temperature levels.

The performance points were rerun for an ideal situation in which all turbine cooling air and inlet bleed airflows were eliminated, and all tailpipe and duct pressure losses also were eliminated. The resulting performance is shown in Figure 60. The GE performance levels now begin to approach the values presented in TR-201. Performance points at Mach 2.2 and 2.7 were also run with the above idealized assumptions and the ATL TR-201 tabular performance was nearly duplicated. The compressor discharge temperatures of these two points also were excessive. No acoustic evaluation was conducted. Mission results are summarized in Table 22.
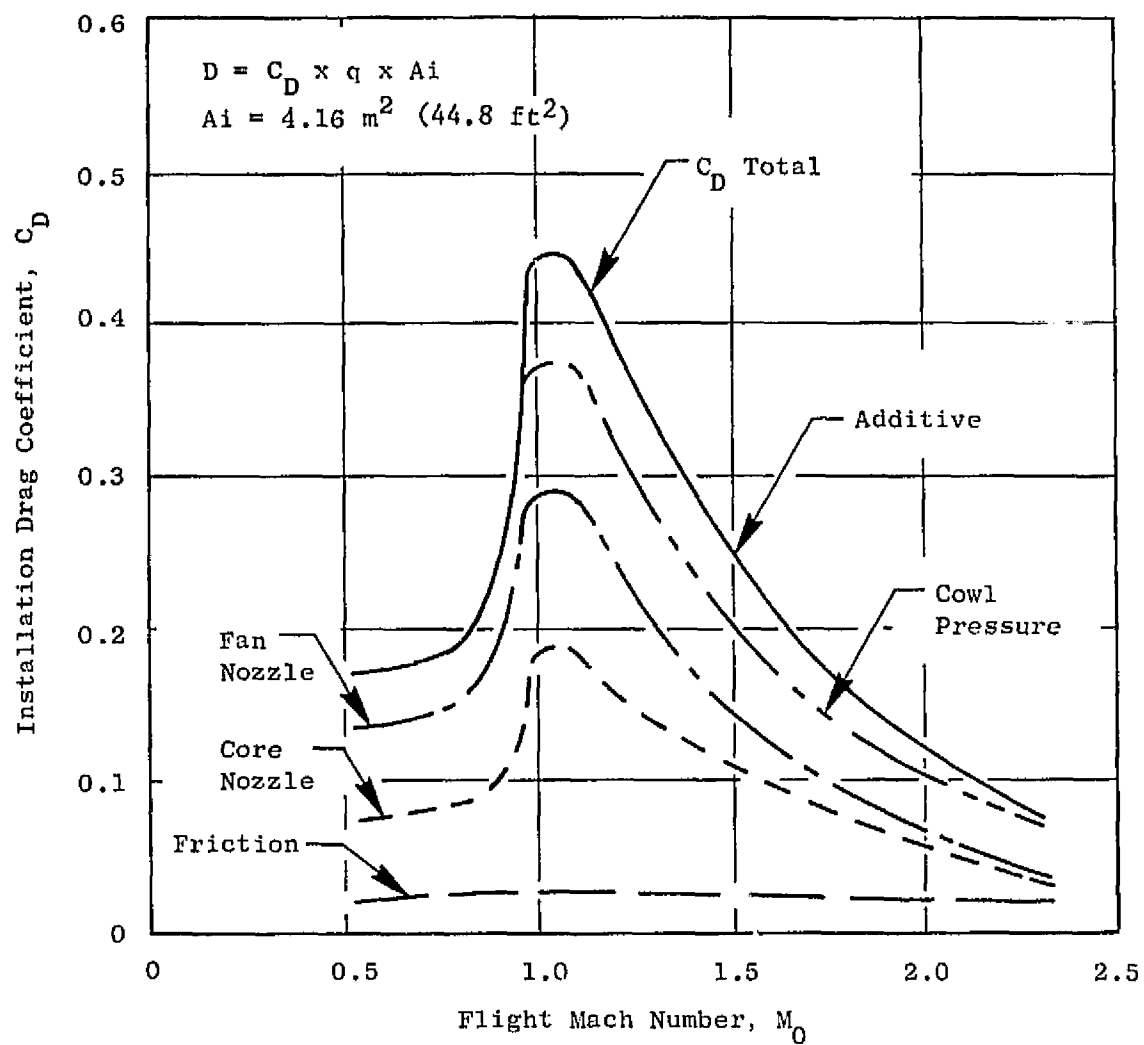
Figure 55. Installation Drag Summary, Variable Bypass Engine.
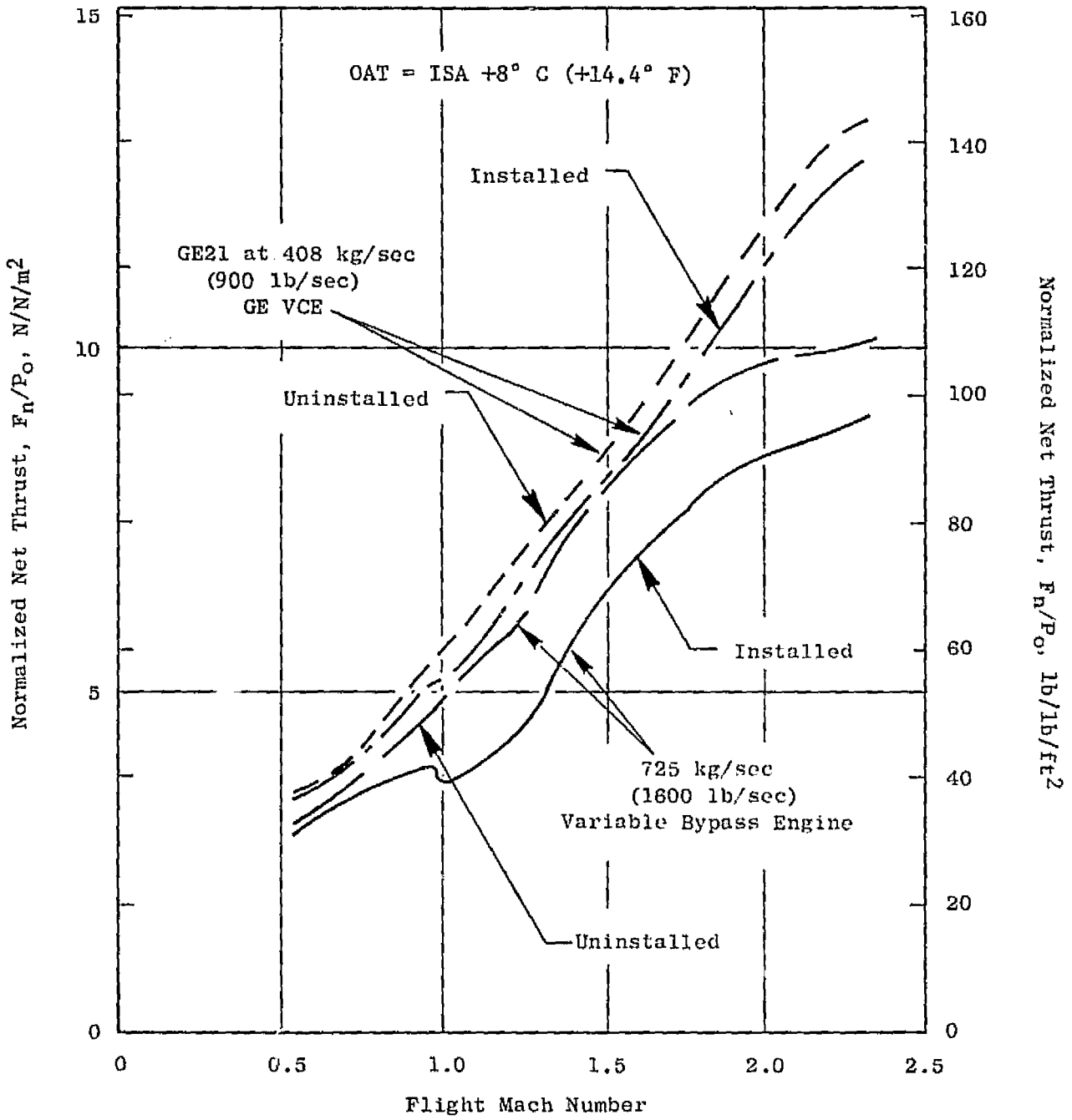
Figure 56. Acceleration Performance, Variable Bypass Engine.
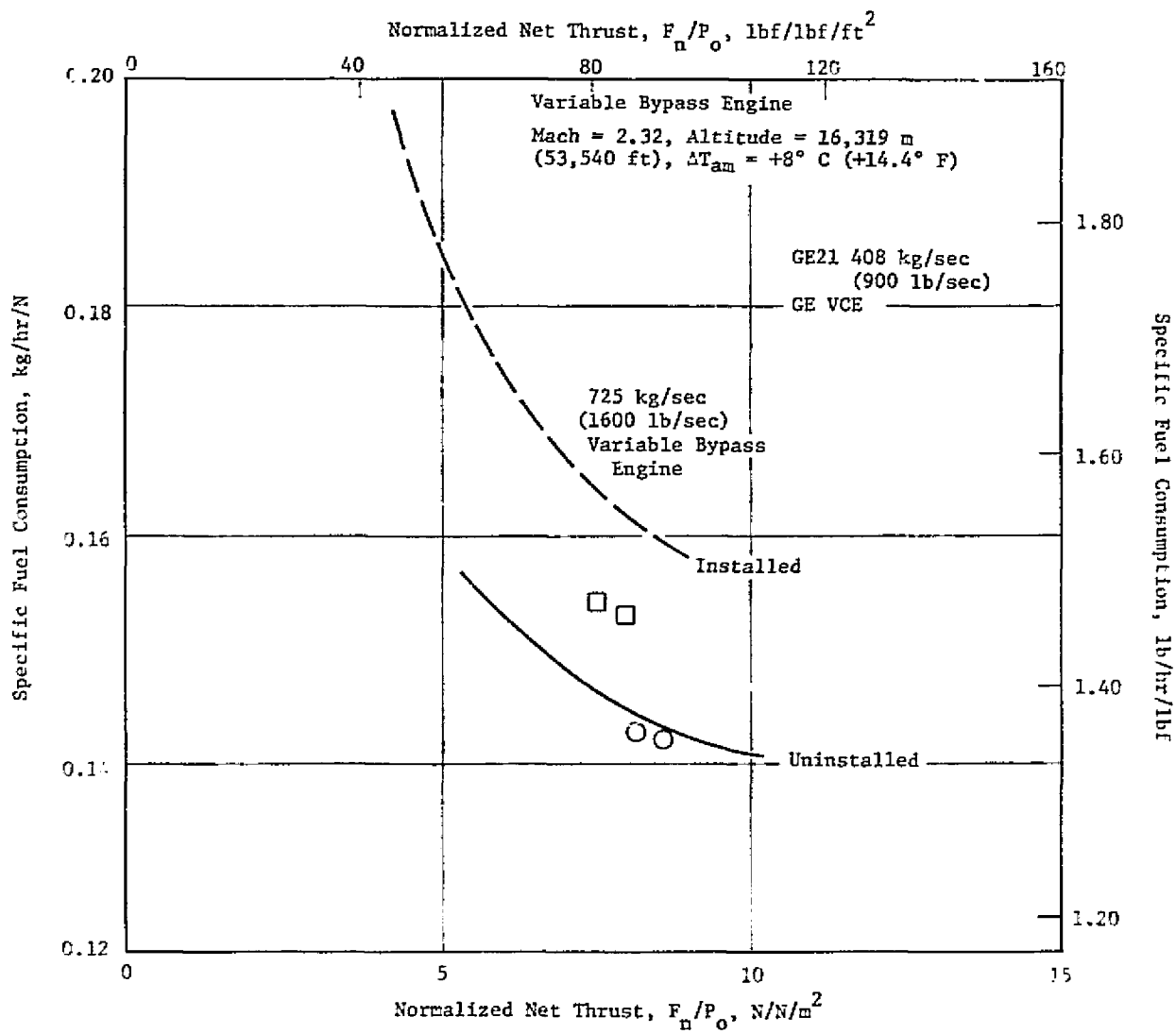
Figure 57. Supersonic Cruise Performance.

Normalized Net Thrust, F_n/P_o, lbf/lbf/ft^2

GE21 408 kg/sec
(900 lb/sec)
GE VCE ☐ Installed
○ Uninstalled

Variable Bypass Engine
$M_0 = 0.95$, Alt. = 10,668 m (35,000 ft)
$\Delta T_{am} = +8°$ C (+14.4° F)

725 kg/sec
(1600 lb/sec)
Variable Bypass
Engine

Installed

Uninstalled

Specific Fuel Consumption, kg/hr/N

Specific Fuel Consumption, kg/hr/N

Normalized Net Thrust, F_n/P_o, N/N/m^2
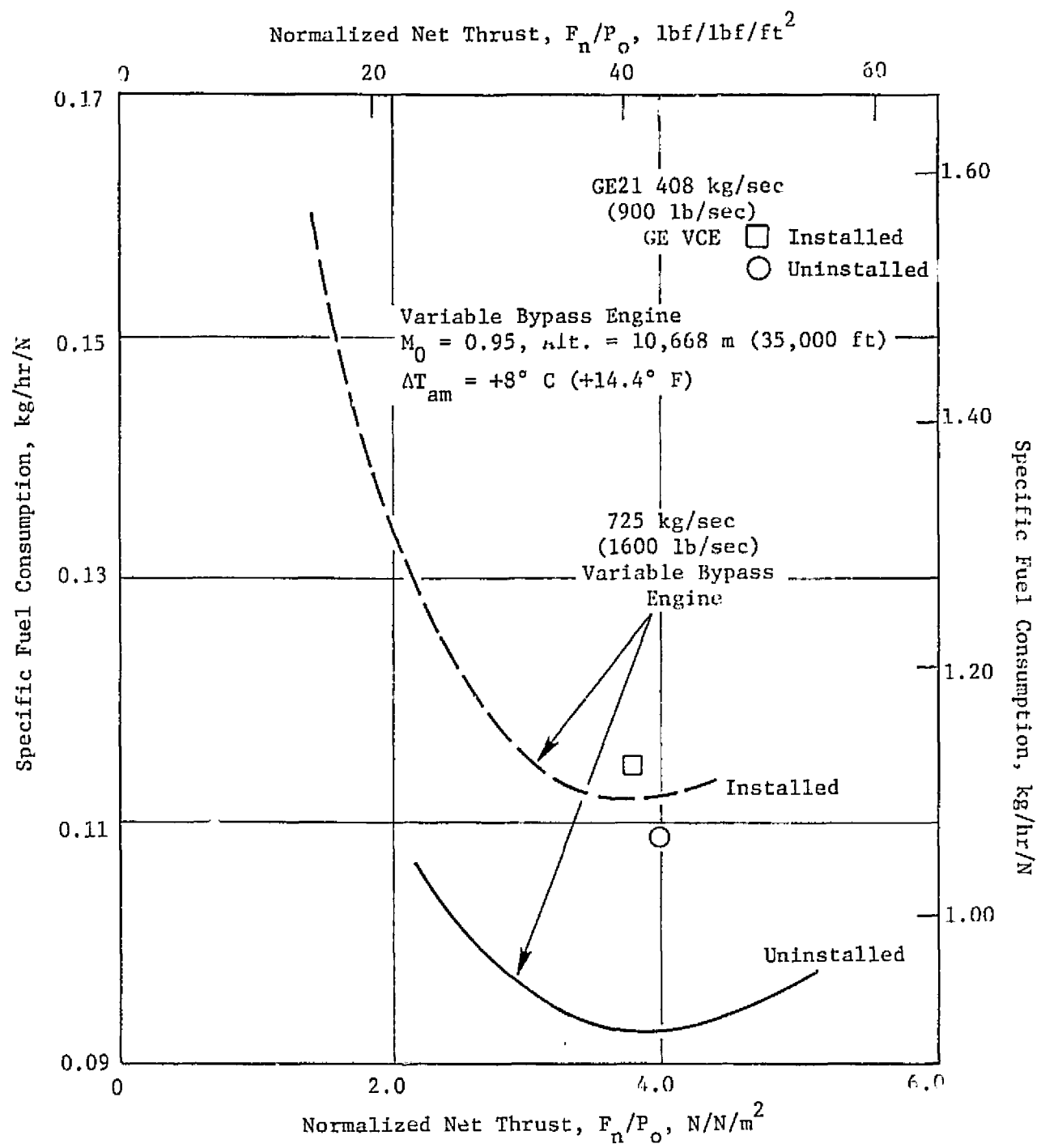
Figure 58. Subsonic Cruise Performance.

116
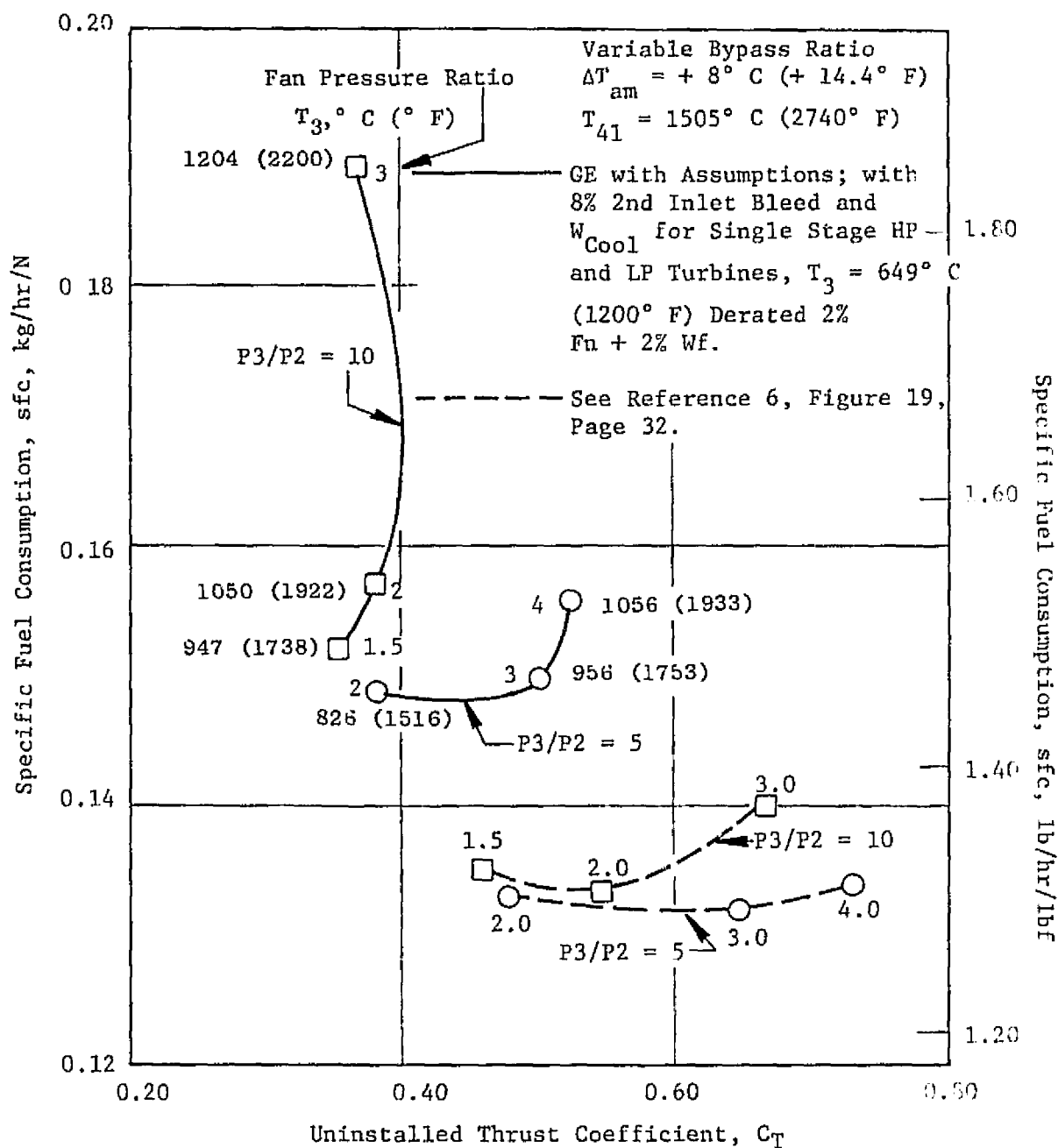
Figure 59. Comparison SFC, Mach 2.7 at 19812 m (65,000 ft).
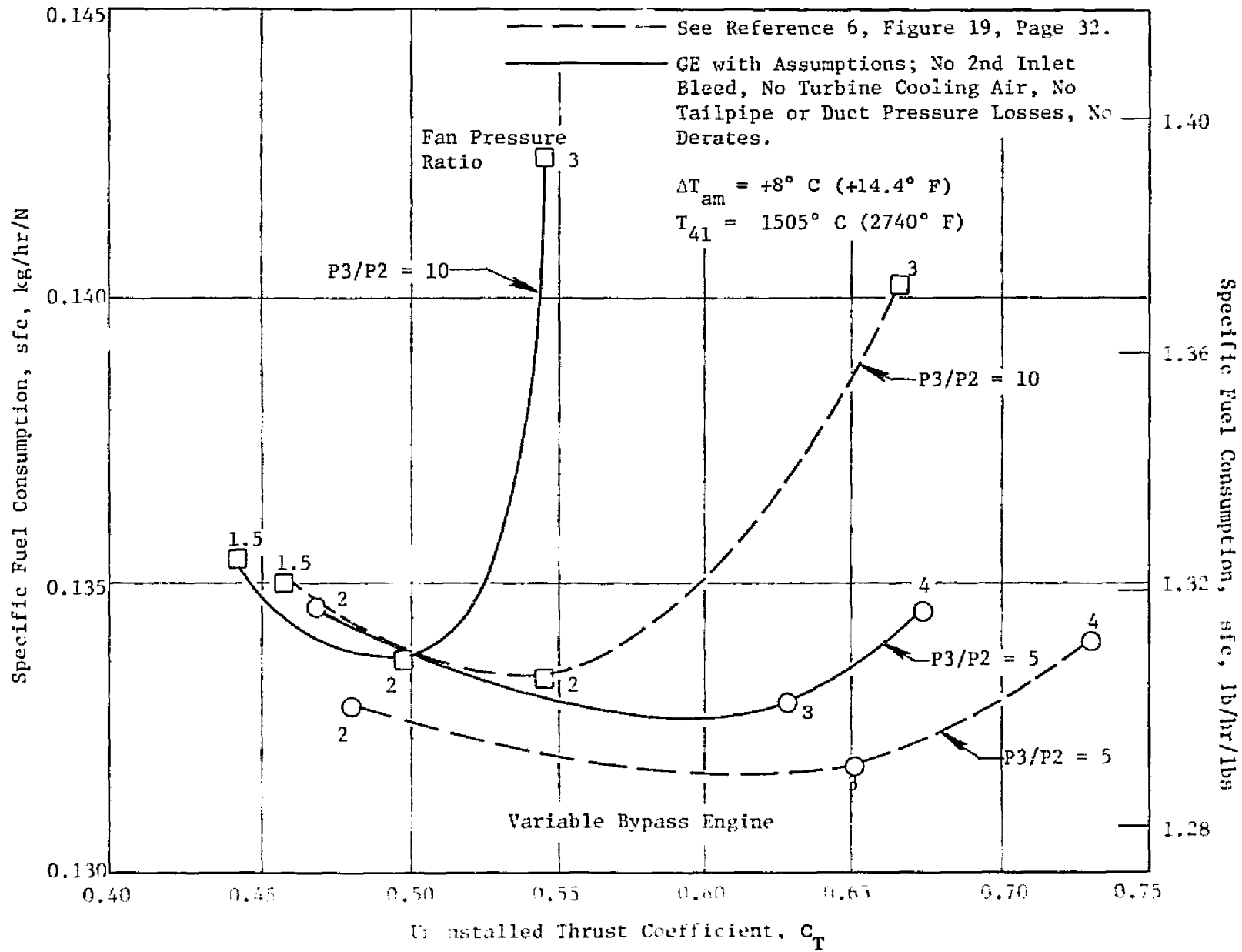
Figure 60. Optimistic SFC Comparison – Mach 2.7 at 19812 m (65,000 ft).

4.3.3.2 Conclusions

It is the conclusion of the General Electric Company that the encouraging performance characteristics presented in ATL Report TR-201 are due in part to the assumptions used regarding component performance and cooling air requirements. However, the scope of the General Electric study was not broad enough to draw firm conclusions regarding the inherent merits of the variable bypass engine cycle itself.

Table 22. Mission Results of Variable Bypass Engine.

- Ground Rules ~ 20% Thrust Margin Required at M = 2.32

- Engine Airflow Size ~ 816 kg/sec (1800 lb/sec)

  - Base NASA Weight 8392 kg (~18500 lb)
    Prime Mission Relative Range = 0.95

  - +25% Weight 10480 kg (~23100 lb)
    Prime Mission Relative Range = 0.85

4.4 PRELIMINARY DESIGN

The engine selected for preliminary design studies was the GE21/J11 Study B3 double-bypass variable cycle engine (VCE). This engine incorporates a 20% high-flow fan and is designed for Mach 2.4 cruise. The engine is:

Engine flow size (takeoff)	– 381 kg/sec (840 lb/sec)
Fan pressure ratio	– 4.0
Overall pressure ratio	– 17.3
Bypass Ratio	– 0.35
Turbine rotor inlet temperature, maximum	– 1538° C (2800° F)

The GE21/J11B3 VCE is a low bypass ratio (0.35), dual-rotor turbofan engine with a low temperature augmentor, designed for dry power supersonic cruise, using the augmentor for transonic climb and acceleration only. At takeoff high-flow conditions, the bypass ratio is almost twice the supersonic cruise level with airflow to provide acceptable FAR 36 noise levels and thrust. Figure 61 is a drawing of the double-bypass VCE concept. The basic differences between the VCE and a conventional turbofan engine are the separation of the fan into two blocks with an outer bypass duct between the fan blocks, and the normal bypass duct after the second fan block. For the low-noise, takeoff mode the front block of the fan is set at its maximum flow configuration. The second fan block is operated to adjust the jet exhaust velocity and flow to produce the desired thrust/noise relationships for takeoff. During subsonic cruise operation the front fan block is set to provide the best match between inlet spillage and internal performance. In this mode the second fan block is set to provide the proper cruise thrust. The desired high inlet airflow can be maintained down to the required subsonic cruise thrust requirement, which practically eliminates inlet spillage drag, and, because of the high flow, also reduces the afterbody drag. The effect of the increased bypass ratio and reduced installation drag is to decrease the installed specific fuel consumption (sfc) by about 15% as compared to a conventional turbofan engine which does not have the capability of holding airflow levels as thrust is reduced.

In the climb/acceleration and supersonic cruise modes, the front block fan is set to meet the aircraft inlet flow supply, and the rear block fan and high pressure compressor are set to pass all of the front block fan flow; and, the engine operates the same as the nominal 0.35 bypass ratio turbofan engine. Another advantage of the split fan configuration is that, to produce high takeoff airflow, only the design of the front block fan and low pressure turbine are affected. As a result, a large weight saving is realized over the weight of a conventional turbofan engine sized for the same takeoff airflow and noise level. (See Section 4.1 for a more detailed explanation.)

A major effort has been made to simplify the engine and the exhaust system in order to reduce cost and weight and to increase reliability. The cycle was established for dry (nonafterburning) takeoff and supersonic cruise, and to require only two turbine stages. The choice of a mixed-flow arrangement eliminates the need for a sophisticated high-performance duct

120
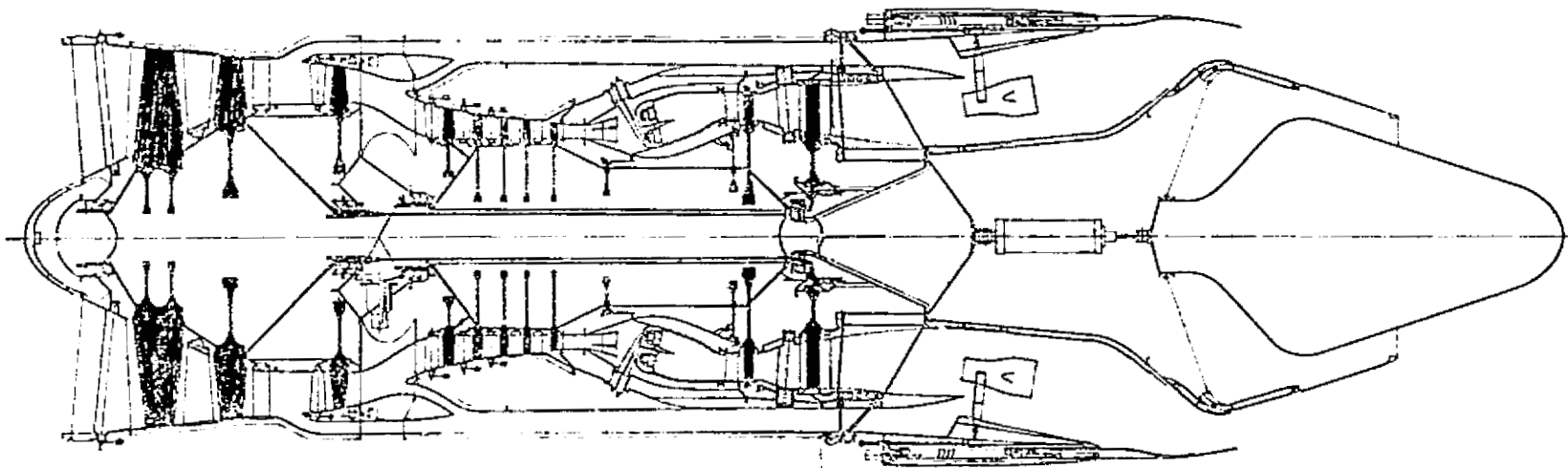
Figure 61. Double-Bypass Variable Cycle Engine Concept.

burner and requires only a very simple climb/acceleration low temperature-rise augmentor. The low bypass ratio, mixed-flow selection for supersonic operation also assures inlet compatibility. The use of the annular jet noise suppression concept in the VCE design resulted in a simpler, lighter weight exhaust system with fewer movable parts and actuation systems. These and other improvements have resulted in a lighter, more reliable engine. A continuing effort on weight reduction, cost reduction, and increased reliability through simpler design is expected to show further improvements in the future.

The preliminary design of the GE21/J11 Study B3 basic engine included aerodynamic definition of components, mechanical design, stress analysis, and material selection of all rotating and stationary engine parts. The feasibility of the design and confirmation of preliminary weight estimates were a major output of this study. Further effort will be required for more detailed analysis and design, as improvements continue to be made in performance and in the mechanical and aerodynamic layout of the variable cycle engines.

4.4.1 Basic Engine Preliminary Design

Low Pressure Compressor

The low pressure compressor is a 3-stage axial flow design consisting of two sections or "Blocks". Block I has two stages with variable inlet guide vanes and fixed stators; Block II has variable inlet guide vanes. The characteristics of the low pressure compressor are:

Front Block

```
Number of stages    - 2
Inlet radius ratio - 0.4 to 0.45
Material            - Boron Aluminum
```

Second Block

```
Number of stages    - 1
Inlet radius ratio - 0.6 to 0.7
Material            - Titanium
```

High Pressure Compressor

The high pressure compressor is a five-stage axial flow design with a constant hub radius. The front stages are titanium, and the aft stages are steel. The characteristics of the high pressure compressor are:

```
Number of stages       - 5
Inlet radius ratio    - 0.7 to 0.8
Material               - Titanium/steel
```

122

Main Combustor

The main combustor is a dou.ie-annular design for low emissions, which is a direct development of the low emission combustor f-om the NASA Experimental Clean Combustor Program. See Section 4.4.2.1 for a detailed review of this combustor.

High Pressure Turbine

The high pressure turbine is a single-stage design utilizing advanced cooling techniques derived from the USAF Advanced Turbine Er-;ine Gas Generator (ATEGG) Program.

```
Number of stages          - 1
Rotor inlet temperature;
  Maximum                 - 1538° C (2800° F)
  Cruise                  - 1482° C (2700° F)
  Blade material          - Directional Solidified Eutectic
```

Low Pressure Turbine

The low pressure turbine is a single-stage design with cooled rotor blades. The rotor blades are a lightweight, high-aspect-ratio type with a tip shroud for optimum aero performance.

```
Number of stages          - 1
Rotor inlet temperature   - 1371° C (2500° F)
Blade material            - Directional Solidified Eutectic
```

Exhaust Nozzle

See Section 4.4.2.2.

4.4.2 Component Preliminary Design

Two components were selected for more detailed discussion: combustors, exhaust nozzles. Each is discussed in the following sections.

4.4.2.1 Combustor Design Studies

Low Emissions Double-Annular Combustor

The double-annular combustor concept, as illustrated in Figure 62, is derived from the low emissions, double-annular combustor developed for the GE Experimental Clean Combustor Program (ECCP) sponsored by NASA. The GE21 combustion system is a short-length version of this concept that has the
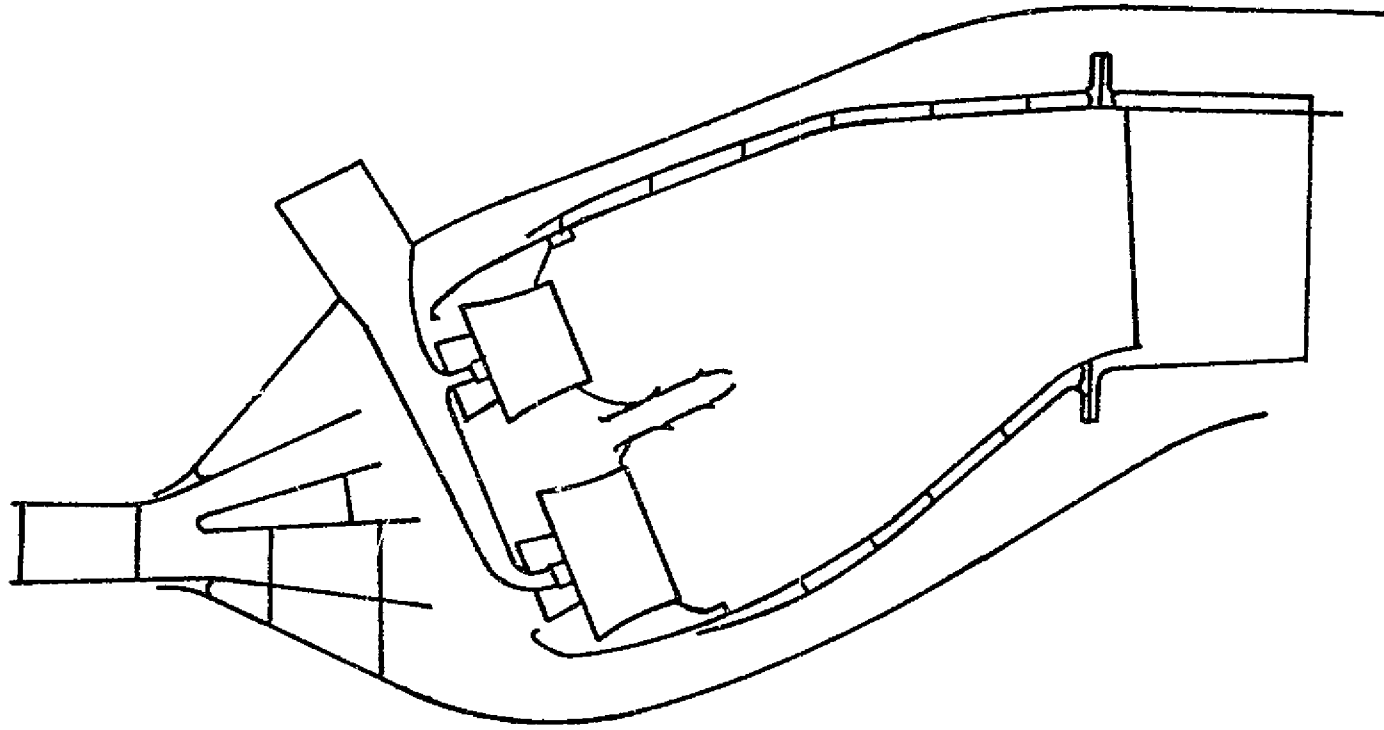
Figure 62.   Double-Annular Combustor Design GE21/J11 3 VCE.

potential for meeting all requirements with good performance and low emissions over a wide operating range. At light-off and low-power operating conditions, all of the burning takes place in the outer annulus, which is a low-velocity pilot combustion zone that is designed to have low CO and hydrocarbon emissions at idle and other low power conditions. At takeoff and other high-power operating conditions, a major proportion of the fuel is burned in the inner annulus, which is a high-velocity main combustion zone that is designed to produce low NO_x emissions at these airport conditions.

Test results of a double-annular combustion system similar to the one illustrated in Figure 62 have demonstrated very low emission levels and indicate the potential with further development -- of meeting all of the Federal airport emissions requirements. The double-annular systems is designed to operate on only one annulus, preferably the outer annulus, at ground idle conditions where the required heat addition is small and the airflow must be small with low average velocities to achieve a fairly rich mixture and high combustion efficiency. With high combustion efficiency, the hydrocarbon and carbon monoxide emissions are low. Also, this mode of operation is used for light-off at engine starting conditions, where excellent light-off characteristics are obtained due to this low-velocity design.

As engine speed is increased above the idle condition, fuel is admitted to the other annulus, preferably the inner annulus, which is designed to admit a large proportion (50% to 70%) of the total airflow with a very high-velocity dome flow pattern. This fresh mixture in the high-velocity annulus is ignited or "piloted" by the hot combustion gases from the outer, or low-velocity annulus. At full-speed, full-thrust conditions, the larger proportion of the fuel is burned in the high-velocity annulus. The lean mixture in the high-velocity annulus results in greatly reduced formation rates for the oxides of nitrogen. In addition, the high average velocity reduces the "residence time" of this reaction which results in very low emission levels for the oxides of nitrogen at takeoff conditions. This combustion system has demonstrated very high combustion efficiencies and very good performance at takeoff operating conditions.

To reduce the length of the combustion system and to improve the flow distribution ahead of the combustor domes, the combustor inlet diffuser for the double-annular combustion system has an annular splitter vane as an integral part of the prediffuser casting. This splitter vane has a dual purpose. For the same value of area ratio, the length of the prediffuser can be reduced by about 40%, and the splitter vane may be contoured to direct high-energy flow leaving the prediffuser exit plane into each of the annular dome regions. A single splitter vane, as shown in Figure 62, divides the prediffuser into two parallel diffusers, each of which has a length-to-inlet-height ratio that meets the no-stall criterion of the Stanford diffuser test and flow regime correlations. Without the splitter vane, the same criterion would require a much longer diffuser.

AST Combustor Design Layout Studies

Geometric design parameters for the GE21/J11B3 double-annular combustion system were determined from detailed aerodynamic design studies. These parameters, which include combustor liner length, outer and inner dome heights, and center-body length were based on design parameters for the NASA ECCP double-annular combustion system. Combustor dome swirl cup size and fuel nozzle size were selected to provide the correct fuel and airflow proportions entering the dome regions. Thirty-two fuel injector-swirl cup assemblies were selected for each of the two dome annuli. This number provides a good balance between fuel system complexity and turbine inlet temperature distribution requirements.

Design studies for the combustor inlet prediffuser design were based on the results of the Stanford diffuser test programs and flow regime correlations. This design, with a central splitter vane, has a short length and low pressure loss and is carefully matched, aerodynamically, to the combustor dome and cowling design.

A detailed aeromechanical design layout drawing of the GE21/J11B3 double-annular combustion system is illustrated in Figure 62. The results of stress analysis and heat transfer studies of this system show that the stress levels and predicted liner life are acceptable. The combustor liners are impingement cooled. The impingement air is also used for film cooling of the inner liner surfaces. The forward end of the combustor is supported by streamlined struts which are fastened to the outer casing by thirty-two radial pins. The aft ends of the outer and inner liners are bolted to flanges that project forward from the turbine diaphragm section. Machined axial and radial slip joints behind these flanges accommodate axial thermal growth of the combustor liners and differential radial thermal growth of the liners and turbine diaphragm.

Each of the thirty-two fuel nozzle stems is a streamlined integral design which carries the inner and outer annulus fuel nozzles on the same assembly. This fuel nozzle stem assembly, which also carries the flow divider valves at the top end, can be removed and replaced as a unit.

Emissions estimates for the GE21/J11B3 engine cycle with the double-annular combustion system (as shown in Table 23) are based on the results of the NASA Experimental Clean Combustor Program. A GE computer program, "EICAL", was prepared to use the relationships for the emissions correlations developed for the ECCP program to predict the emissions indices for new double-annular combustion system designs that operate at different cycle conditions. The index values are then used in another computer program, "EPATS", to predict the integrated cycle emissions, or EPA parameters, as shown in Table 23 for the GE21/J11B3 double-annular combustion system. As illustrated by this table, the GE21/J11B3 double-annular combustion system is expected to meet the 1984 EPA airport emissions requirements for Class T5 engines.

126

Table 23. Double-Annular Combustor Estimated Emissions.

	GE21/ J11B3	1984 Standard T5 Engines	% Reduction Required
CO kg/1000 N Thrust-hr/Cycle	15.5(7.7)	15.7(7.8)	0
C_x/Hy (1b/1000 lbf fn-hr/Cycle)	1.6(0.8)	2.0(1.0)	0
NO_x	7.5(3.7)	10.1(5.0)	0

Estimated Cruise NO_x = 13.5 kg/1000 kg of Fuel (13.5 1b/1000 lb of Fuel)

Premixing Combustion Systems

If the stringent standards proposed (in Table 14) to control the emissions of NO_x during high-altitude cruise are made requirements, additional major combustor design technology advances appear to be needed. Specifically, it is anticipated that combustors will be required in which the fuel flow entering the combustion system is prevaporized and premixed with the combustion air to a relatively low equivalence ratio before entering the combustion zone.

Experimental results have shown that it is feasible to reduce NO_x emissions to low levels at AST cruise conditions by sufficient premixing of the fuel and air upstream of the combustion zone.

The variable geometry premixing combustion system design illustrated in Figure 63 is an advanced concept that is expected to have low NO_x emissions at high-altitude cruise conditions and has the potential for low emissions at all of the operating conditions. At cruise conditions and at other high-power operating conditions, the fuel is premixed with the combustion air in short, high-velocity premixing ducts. At low-power operating conditions, premixing is unnecessary and high-flow through the premixing ducts would provide fuel-air mixtures that are too lean for good performance. Therefore, at these conditions a variable valve arrangement is used to reduce the duct airflow and increase the airflow through the dome swirl cups; and, all of the fuel is injected through conventional fuel nozzles directly into the dome region.

This premixing-combustor concept represents a major departure from existing combustion system design technology. It will require extensive development efforts to evolve a practical system that meets all of the combustion system design requirements and one which will meet proposed emissions requirements.

A variable geometry, premixing combustion system design was prepared for the GE21/J11B3 engine cycle (shown in Figure 63) having evolved from a series of aeromechanical design studies. This system is designed to have very low NO_x emissions at high-altitude cruise conditions and also meet all of the engine combustion system performance requirements.

The premixer section for this design consists of thirty-two separate premixer ducts that are circular in shape for a length of about two duct diameters and then transition into two rectangular ducts that carry the premixer flow into the combustor dome region. The premixer ducts are positioned over the compressor exit flowpath to reduce engine length. Each duct has a mechanically-actuated poppet valve at the inlet to the premixer. These valves will be closed at idle conditions and open at takeoff and cruise conditions. Fuel is injected into the premixer ducts through pressure atomizing fuel nozzles that are positioned in the center of each valve head.

Thirty-two fuel nozzles and swirl cups are used in the pilot dome of this combustion system. The combustor liners are designed for impingement
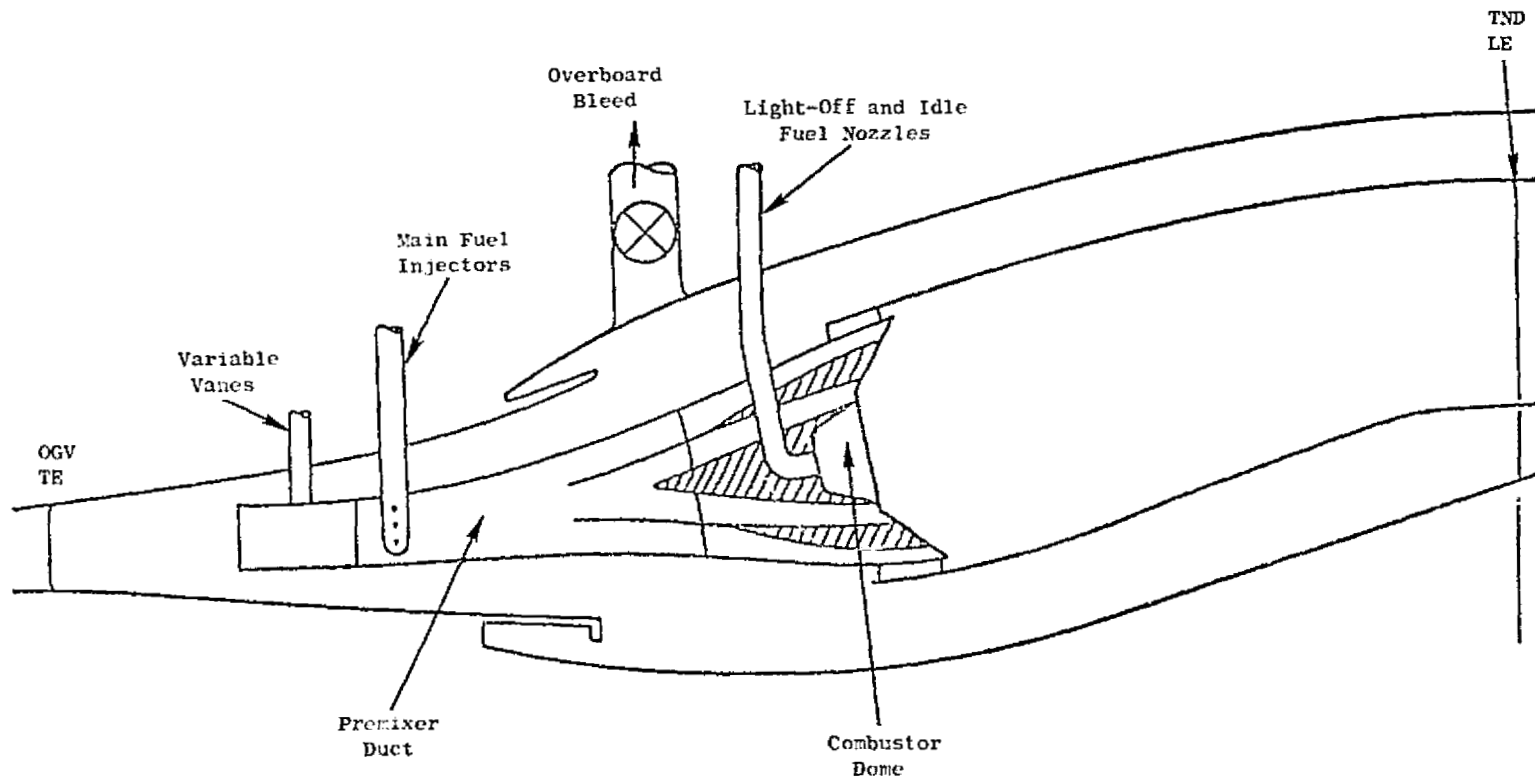
Figure 63. Premixing Combustor Design Concept – AST VCE.

cooling and are attached to the turbine diaphragm section through radial and axial slip joints that can accommodate differential thermal growth of these parts.

Emissions predictions for this design are based on single-annular combustor test results for idle and other low power conditions. At high power conditions, the emissions from the premixing system are based on additional test results. As a result of these studies, the EPA emission parameters for the premixing combustion systems have been estimated (as shown in Table 24). The predicted value for NO_x emissions at cruise conditions is considerably less than that for the double-annular system, and the predicted EPA parameters for NO_x and hydrocarbons are lower than the 1984 standards for Class T5 engines. However, the predicted value for carbon monoxide emissions is somewhat higher than the 1984 standards. Some development effort will probably be required to reduce the CO emissions to the 1984 standard levels. In addition, additional research is required to bring altitude cruise NO_x levels down to the proposed CIAP target level.

4.4.2.2 Exhaust Nozzles

Background

During Phase II of the advanced supersonic propulsion system technology study, a variable plug, single stream, chute-suppressed exhaust system was studied for the double-bypass variable cycle turbofan engine. A low temperature augmentor and a cascade thrust reverser were incorporated in this exhaust system. Figure 64 shows the GE21/J9 study B1 exhaust system designed to the Phase II requirements. This exhaust system is relatively complex and therefore heavy. Seven actuation systems are used to control the various moving components required to meet all operational modes: reverser cover, translating A9 shroud, outer bypass mixer, inner bypass mixer, A8 throat flaps, suppressor cover door and chute suppressor. A primary objective of the Phase III program was to simplify the design and reduce the weight of the AST exhaust system.

Annular Suppression

Near the end of the Phase II contract, acoustic tests conducted at the General Electric Company acoustic test facility under the Duct-Burning Turbofan (DBTF) contract with NASA (NAS3-18008) showed dramatic noise reductions were obtained with an annular exhaust arrangement. This arrangement consisted of a high temperature, high velocity outer stream at a high radius ratio ($R_i/R_o \doteq 0.85$) and a low temperature, low velocity inner stream. These velocity and temperature profiles are shown schematically in Figure 65. Phase III exhaust systems were designed to take advantage of this annular suppression characteristic.

130

Table 24. Premixing Combustor Estimated Emissions.

	GE21 J11B3	1984 Standard T5 Engines	% Reduction Required
CO kg/1000 N Thrust-hr/Cycle	17.8(8.8)	15.7(7.8)	12
C_xHy (lb/1000 lbf fn-hr/Cycle)	1.2(0.6)	2.0(1.0)	0
NO_x	9.5(4.7)	10.1(5.0)	0

Est. Cruise NO_x = 4.4 kg/1000 kg of Fuel (4.4 lb/1000 lb of Fuel)
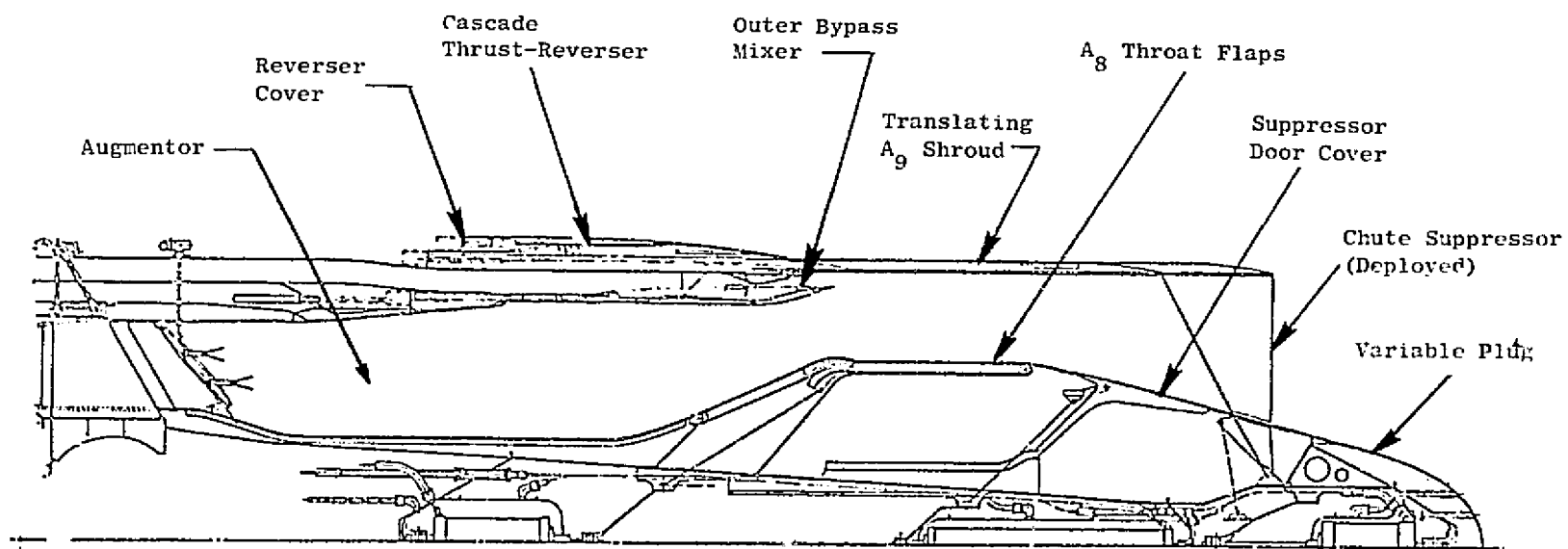
Phase II Exhaust System
GE 21/J9 Study B1

Figure 64. Baseline Double-Bypass Nozzle Configuration.

V Outer

V Inner

T_t Outer

T_t Inner
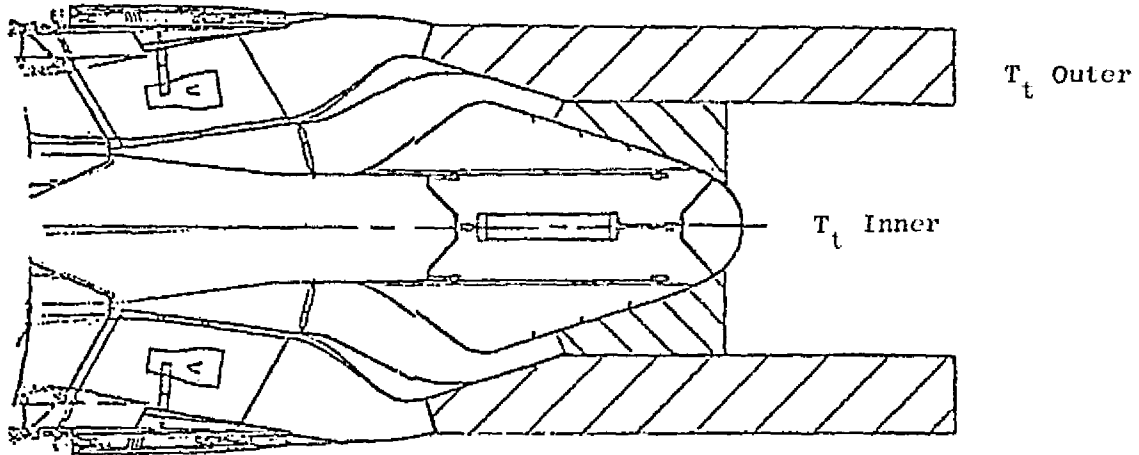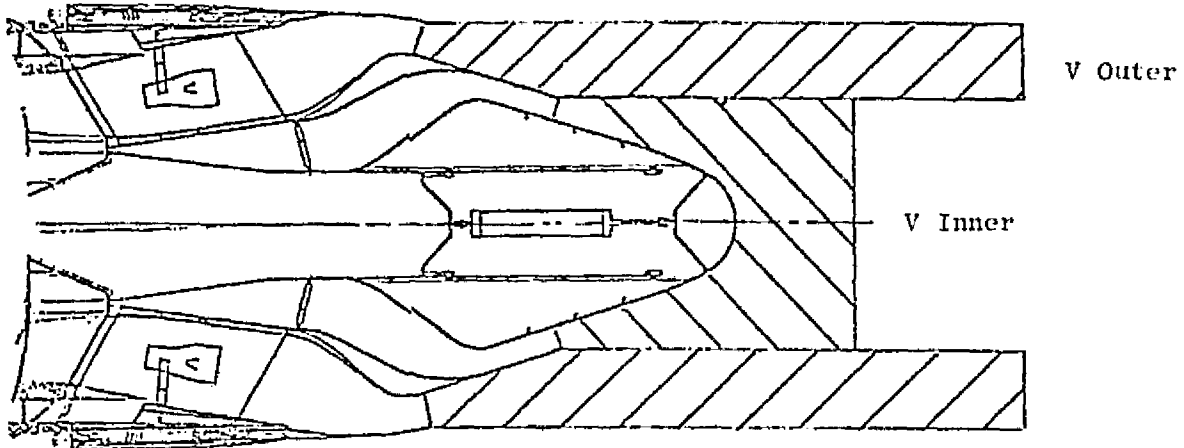
Figure 65. Annular Suppression Velocity and Exhaust Temperature Proportions.

Phase III Exhaust Systems

Several different exhaust systems were evaluated in Phase III. Each is discussed below.

Low-Flow Inner-Stream Exhaust Nozzle

The first annular suppression exhaust system designs were based on use of low inner nozzle flows because model test results showed that suppression could be achieved with the low-temperature center flow being 10% or less of the high-temperature outer-stream flow. Fan flow is directed from the outer ducts through the turbine frame to the plug support beam and thence to the fan nozzle. Figures 66 and 67 show this system applied to separated flow double-bypass engines and to mixed flow double-bypass engines. The annular system is shown on top compared to the GE21/J9B1 nozzle on the bottom respectively. To obtain the high radius ratio (≈ 0.85) on the outer exhaust stream and still keep the nozzle diameter small, the outer stream area (A_8) must be small. A_8 is sized for the high temperature core engine flow during suppressed operation and the excess low velocity fan flow is discharged through a forward fan nozzle. During unsuppressed operation, the forward nozzle is closed, the aft inner nozzle is closed, and the fan air is mixed with the core flow and discharged through the outer nozzle. Although these were attractive systems from the standpoint of utilizing annular suppression, they were still complex and heavy. Six actuation systems are required in each of these exhaust systems. To further simplify and lighten the exhaust system as well as the airplane installation the forward nozzle was eliminated.

High-Flow Inner-Stream Exhaust Nozzle

The fixed-primary plug nozzle (shown in Figure 68 compared to the GE21/J9B1 nozzle) resulted from the high-flow inner-stream design studies. The forward nozzle is eliminated and the mixed double bypass flow is ducted though turbine frame extension struts to the inner duct and exhausted through the center nozzle. Some of the bypass air is mixed with the core flow and exhausted through the outer nozzle. The combination of the variable area center nozzle and the outer stream mixer allows the airflow in the outer stream to match the outer stream exhaust area and thus eliminate the variable area plug crown flaps and its actuation system. The outer shroud is contoured to provide some outer nozzle throat area variation but since the shroud is positioned axially to obtain the exit area required for best performance at any pressure ratio, the outer stream throat area is fixed at any particular operating condition. The thrust reverser cascades and blocker doors are integrated in the translating outer shroud. This design approach resulted in a greatly simplified and lightweight exhaust system. Only three actuation systems are required to perform the nozzle area variation, flow mixing, internal area ratio adjustment, thrust reversing and annular suppression functions. In addition, the suppression characteristics are maintained through power cutback at the community noise monitoring condition because the high radius ratio and annular suppression characteristics are not changed by exhaust flow area changes.

134

Low-Flow Inner Stream
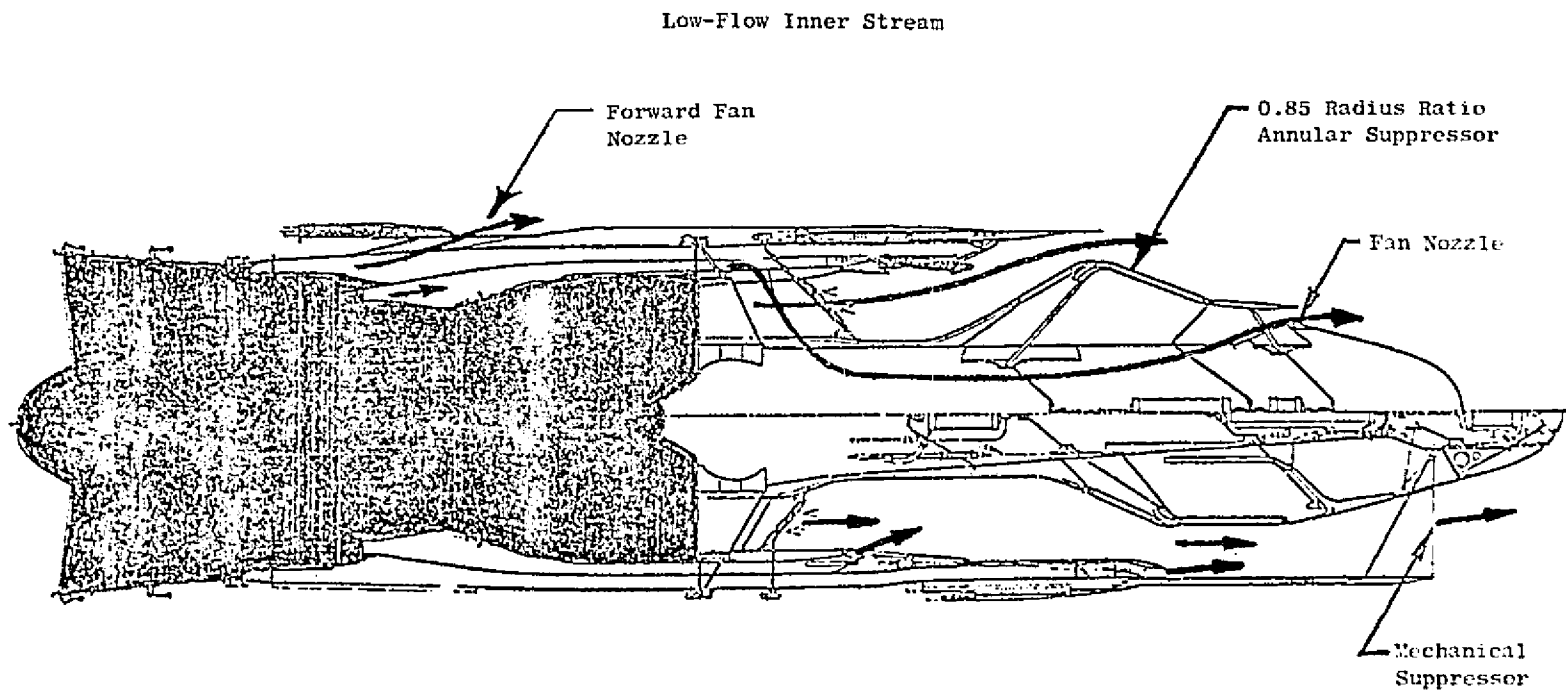
Figure 66. Baseline Separated Double-Bypass Configuration.
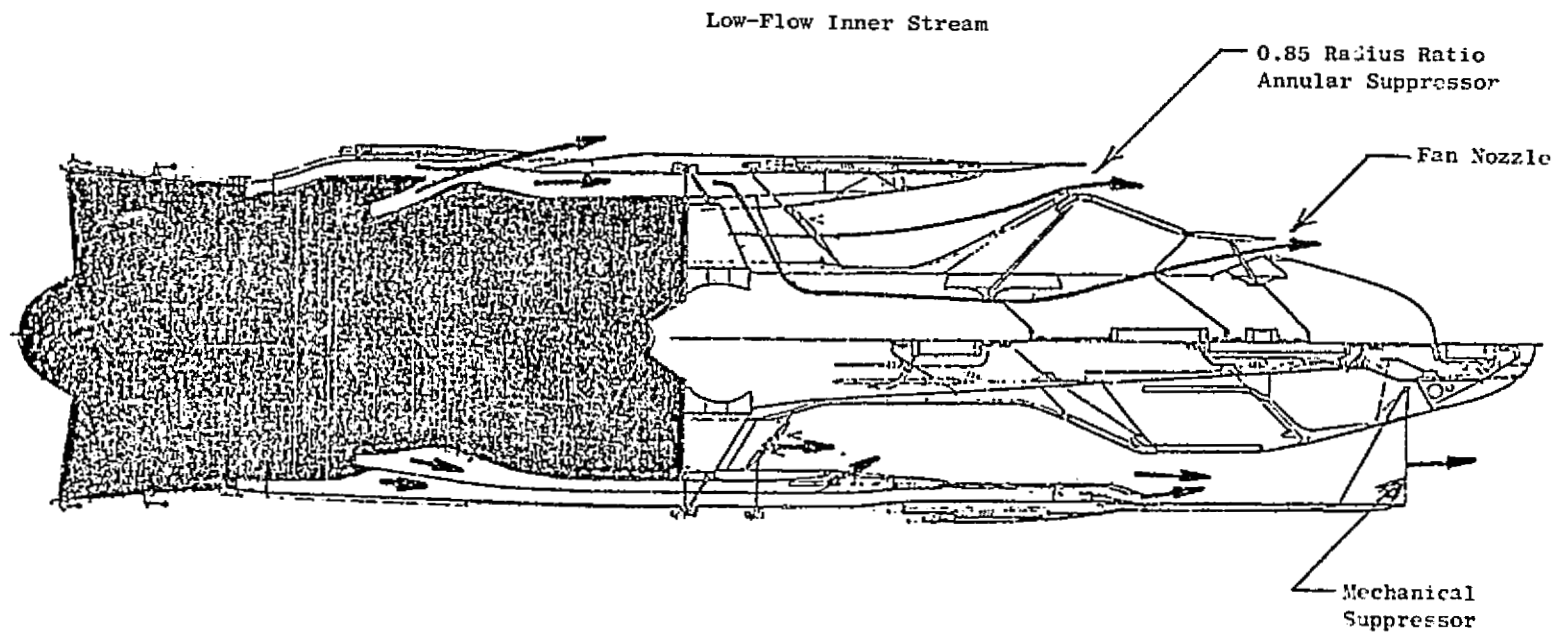
Figure 67.   Baseline Mixed Double-Bypass Configuration.
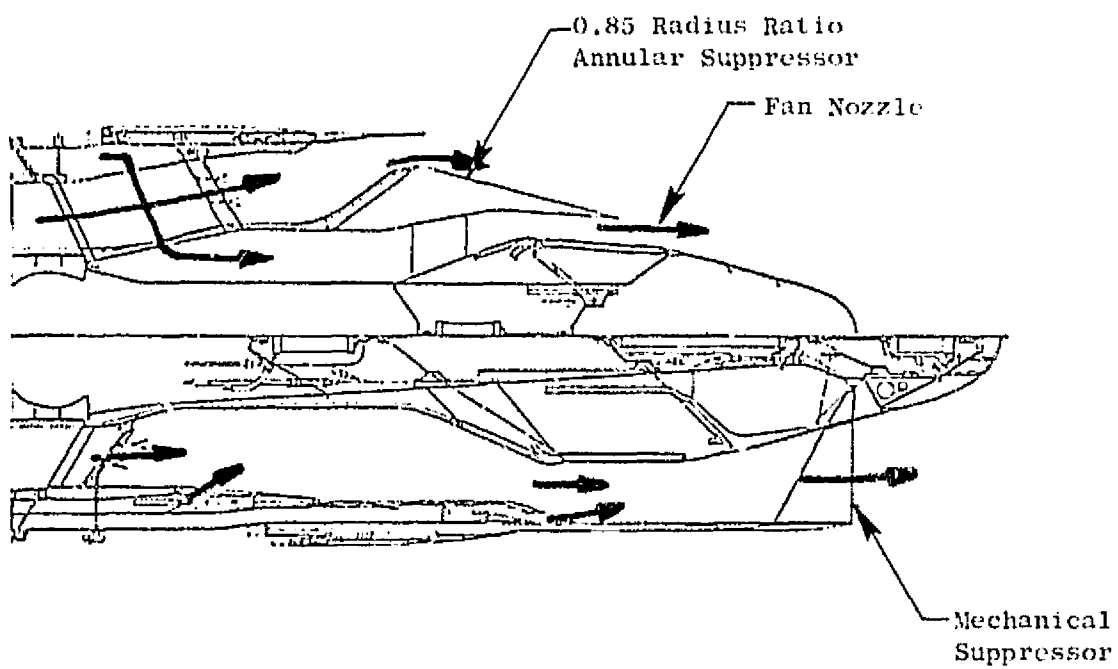
Figure 68. Baseline Interim Fixed Primary Double-Bypass Configuration.

The first fixed-primary exhaust system designs used flaps for changing the center nozzle area as shown in Figure 68. In the later Phase III fixed primary designs, a translating plug is used for the center nozzle and the nozzle is shortened. This change further simplifies the structural design and reduced weight. This nozzle is shown in Figure 69 in the takeoff mode on top and in the reverse mode on the bottom. Figure 70 shows the relative positions of the translating plug and translating shroud for the major operating modes of the fixed-primary exhaust nozzle.

Preliminary Design Exhaust Nozzle

The Phase III preliminary design exhaust nozzle is the GE23/J9 Study B3, shown in Figure 69. The major features of this exhaust system are as follows:

1. A translating cylindrical shroud to optimize the internal area ratio for best aerodynamic performance.

2. Integration of the reverser cascades and blocker doors into the translating shroud to minimize actuation requirements. Actuated internal or external cover doors or separate blocker systems are not required.

3. A fixed plug crown. Due to the unique flow control system provided by the translating center nozzle and the bypass mixer, plug crown flaps are not required. This fixed structure reduces weight, reduces leakage, and eliminates the maintenance and reliability problems associated with flaps and seals.

4. Eight duct-strut extensions of the turbine frame struts to duct bypass air to the inner nozzle.

5. A translating center plug nozzle for control of the bypass airflow throat area. Again, in this area the undesirable features of flaps and seals for commercial application are eliminated.

6. Bypass flow mixers located between the eight duct-struts for mixing the bypass flow with the core flow for good performance.

7. A low temperature [1038° C (1900° F) maximum] augmentor for thrust augmentation during climb conditions.

An in-depth study of the exhaust system design has been made. The airflow passages have been sized for good performance at appropriate flow Mach numbers, diffusion rates, and convergence rates. The plug and outer shroud contours have been optimized for good performance and low weight, resulting in a shorter lightweight plug. Peak actuator forces and stresses of major components have been determined. Table 25 summarizes the operating temperatures, material selections and component lifes expected in the major components. The cascade-type thrust reverser provides for 'tailoring' of the exhaust efflux to prevent reingestion or impingement on the aircraft.

138

8 Strut-Ducts

Translating Shroud

0.85 Radius Ratio Annular Suppressor

Take-Off Mode

Fan Nozzle

Translating Inner Plug

Reverse Mode

Blocker Doors

Cascade Reverser
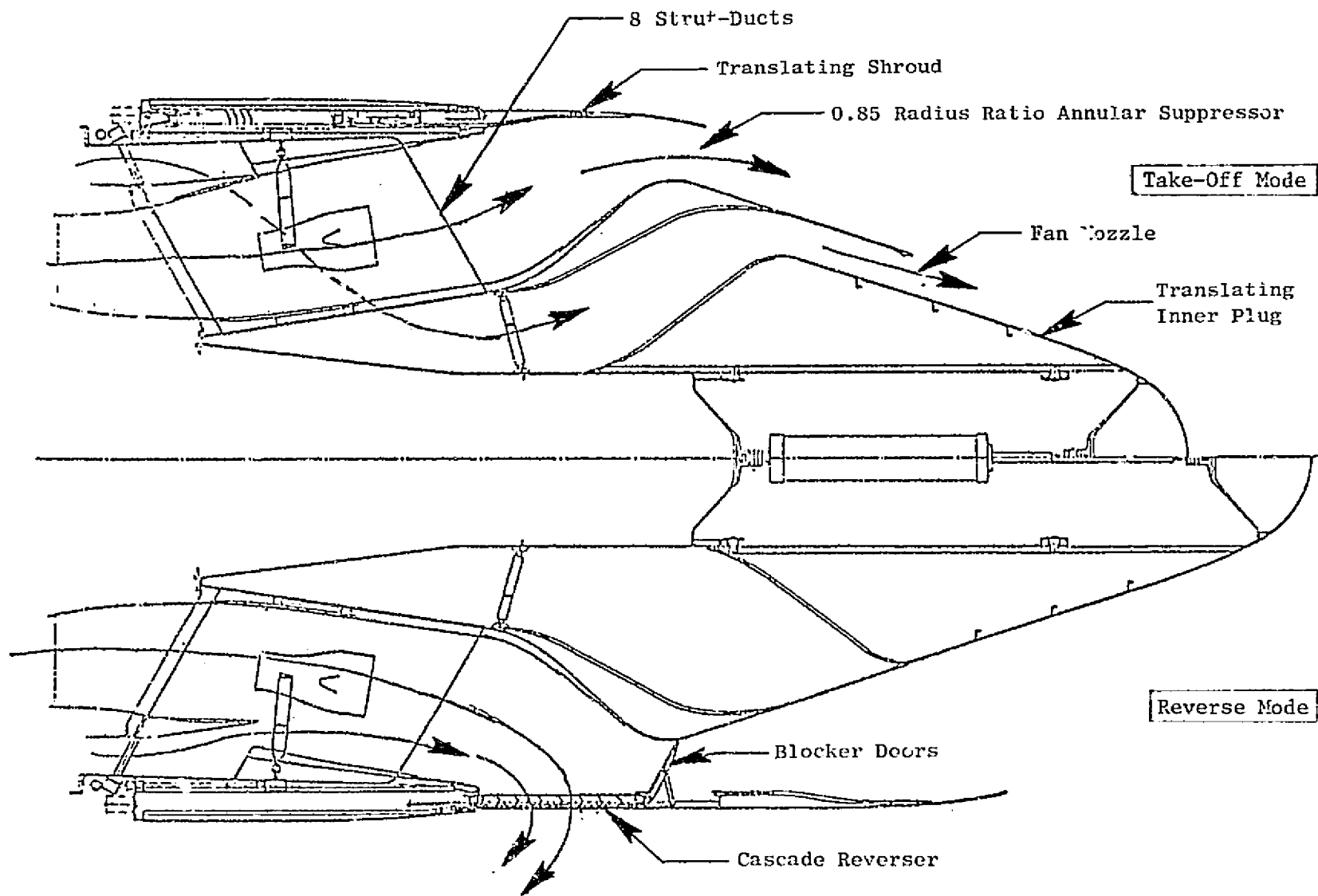
Figure 69. Fixed Primary Exhaust System, GE21/J11 Study B3.

TAKEOFF

SUBSONIC CRUISE

ACCELERATION

SUPERSONIC CRUISE

REVERSE
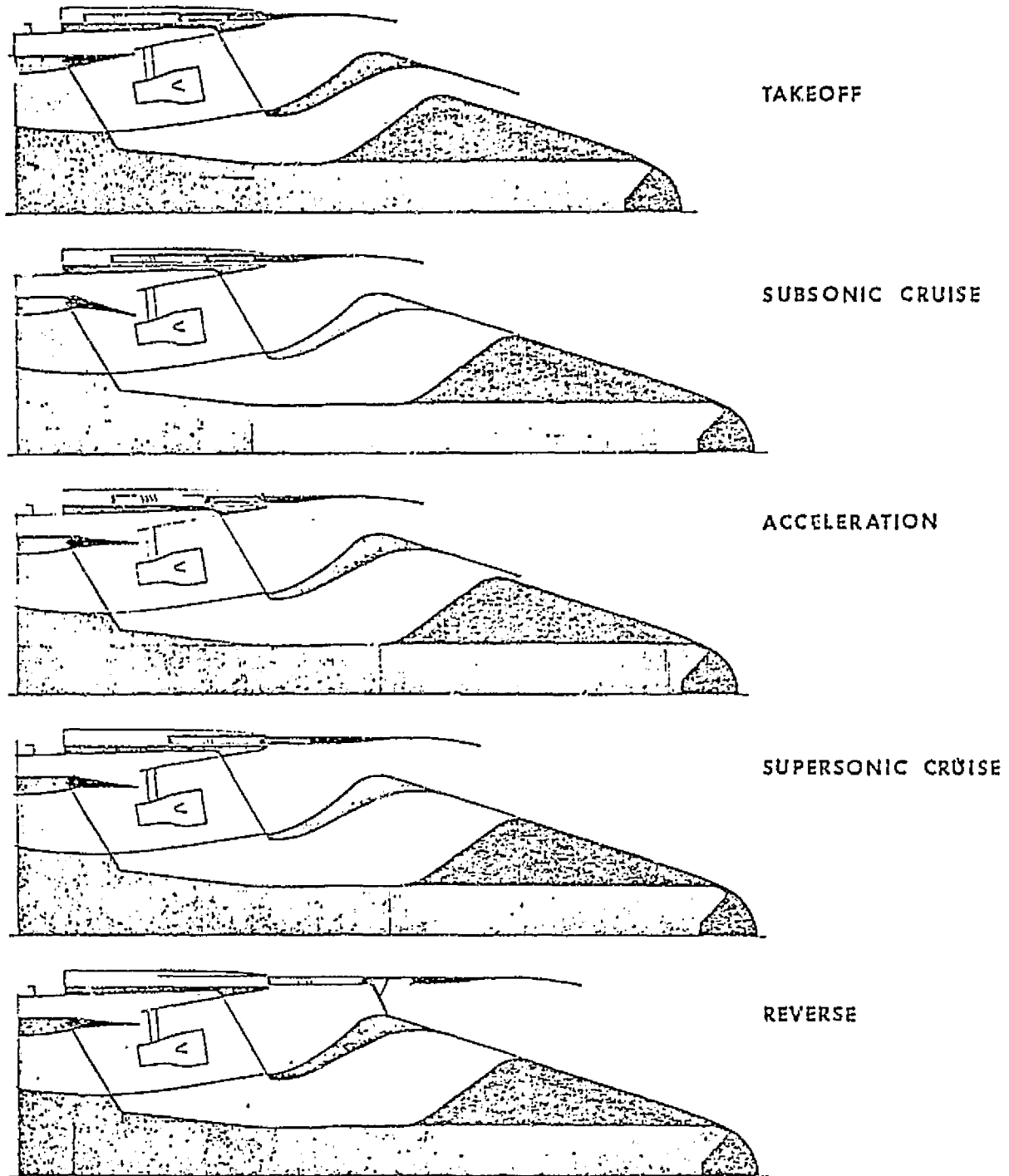
Figure 70. Fixed Primary Operational Modes.

Table 25. Mechanical Design Summary.

Component	Temperature °C (°F)	Material	Component Life Hours (Without Repair/ With Repair)
Structure Outer	760(1400)	René 63/In 718	12,000/36,000
Structure Inner	338(640)	Ti-6Al-2Sn-4Zr-2Mo/R41C	12,000/36,000
Struts	427(800)	René 63	8,000/18,000
Outer Plug	871(1600)	René 63	12,000/36,000
Translating Plug	343 649(650 1200)	Ti/René 63	12,000/36,000
Translating Shroud	760(1400)	René 63/Ni76XBC*	4,000/12,000
Liners	760 954(1400 1750)	HS-188 and Ni76XVS**	4,000/12,000
Mixer	338 954(640 1750)	In 718/Ni76XVS**	4,000/12,000
Augmentor Structure	954(1750)	Ni76XVS**	4,000/12,000
Flameholder	1038(1900)	Ceramic	4,000/12,000
C&A	---	---	---

* Blade Cast
** Vane Sheet

Chute and Annular Suppression

If additional suppression above that obtained by the annular suppression effect is required, a relatively simple shallow chute arrangement can be added to the high-temperature outer stream. The shallow chutes form the outer plug surface in the stowed position so that a cover is not required. This exhaust system has a total of four actuation systems. The shallow chute suppressed fixed-primary exhaust nozzle design details are shown in Table 26.

Summary

Considerable improvement in the exhaust system has been made in Phase III. Weight has been reduced by about 30% in the 408 kg/sec (900 lb/sec) airflow size. The number of actuation systems have been reduced from 7 to 3. Along with the reduction in actuation systems, there has been a considerable reduction in moving parts which results in large improvement in reliability and maintainability. Exhaust system leakage has been reduced to a point where it is practically negligible. The leakage area/A_8 in the fixed primary nozzle is only about 10% of that in the GE4 TSEN exhaust system. These improvements in simplicity make the supersonic AST exhaust system design comparable to present-day subsonic commercial exhaust systems, in that the nozzle is fixed and has a single cascade-type thrust reverser. Furthermore, the plug port in the nozzle is "bathed" in cooler air (i.e., fan air). Furthermore, no mechanical noise suppressor is required.

Table 26. Phase III Exhaust Systems Summary.

Engine Airflow Size – 408 kg/sec (900 lb/sec)

	Weight kg (lb)	ΔWt. kg (lb)	No. of Actuation Systems	Diameter cm (in.)	Length cm (in.)	Cfg (Takeoff)	Cfg (Cruise)
GE21/J9/B1	2812(6200)	(-) (-)	7	214.4(84.4)	497.8(196)	0.91-0.93	0.97-0.98
Low Bleed Double Bypass	2517(5550)	-295(-650)	6	226.3(89.1)	408.9(161)	0.91-0.94	0.96-0.97
Low Bleed Mixed Double Bypass	2427(5350)	-385(-850)	6	216.7(85.3)	386.1(152)	0.92-0.94	0.97-0.98
First Fixed Primary	1996(4400)	-816(-1800)	3	216.4(85.2)	424.2(167)	0.96-0.98	0.97-0.98
GE21/J9/B3 Fixed Primary	1905(4200)	-907(-2000)	3	226.8(89.3)	345.4(136)	0.96-0.98	0.96-0.97
Fixed Primary with Shallow Chute Suppressor	2313(5100)	-499(-1100)	4	236.5(93.1)	358.1(141)	0.90-0.92	0.96-0.97

4.5 AIRFRAME RELATED STUDIES

Due to the importance of powerplant/airframe integration, airframe con-
tractors were requested to carry out inlet and nacelle integration studies.
Lockheed, McDonnell Douglas, and Boeing carried out separate analyses. These
studies have been documented in the final reports listed here:

Lockheed Report LR-27854, "Supersonic Cruise Vehicle Inlet Design For
Variable Cycle Engines," November 5, 1976.

Lockheed Report LR-28071, "Advanced Supersonic Engine/Airframe Inte-
gration Study," February 21, 1977.

McDonnell Douglas Report MDC-J4562, "Nacelle Integration Study," March
1977.

Boeing Report D6-44513, "Advanced Supersonic Propulsion Study-Engine/
Nacelle/Airframe Integration Studies," (undated).

The material included below consists of edited abridgements of the study
results of each of these airframe subcontractors, using portions of text ma-
terial from their reports. Conclusions stated and recommendations made are
those of the airframe companies.

The Lockheed VCE Inlet Concept Study is discussed in Section 4.5.1
below. The Lockheed, McDonnell Douglas, and Boeing Nacelle Integration
Studies are discussed in Sections 4.5.2.1, 4.5.2.2, and 4.5.2.3, respectively
(below).

4.5.1 Variable Cycle Engine Inlet Concept Study

Introduction

The supersonic cruise vehicle inlet studies were performed by the
Lockheed-California Company for the General Electric Company. The results
were obtained in a six-month program, which was conducted from April to
October 1976.

With the advent of variable cycle engines, which are capable of ingest-
ing much higher airflows at transonic speeds than the earlier predominantly
fixed geometry engines, close matching between inlet and engine airflows over
the entire Mach number range becomes extremely important. If higher airflows
could be handled at speeds below the nominal cruise Mach number, two advan-
tages would accrue. First, the installed performance would be improved
because of the reduction in inlet spillage and nozzle boattail drags. Second,
the available maximum thrust would increase, giving more flexibility in the
selection of optimum climb profiles.

As the engine designer introduces special features to change airflow in specific Mach number regions, the inlet design also must include the capability for area variations in order to take advantage of the increased engine flexibility. This requirement has led to a number of variations from the simple translating-spike axisymmetric inlet design, including translating centerbody barrel sections and auxiliary modulated loors which are kept open well into the low supersonic Mach number range. Since a two-dimensional inlet intrinsically has a greater capability to match arbitrary airflow schedules than the translating-spike axisymmetric inlet, it is more probable that a conventional two-dimensional inlet design could be made to match higher transonic flows without the requirement for the addition of complex devices. However, this design is still liable to be heavier than even the complicated axisymmetric inlet.

The primary objectives of this study are to select first the most appropriate inlet which is best matched to a given General Electric variable cycle engine, and then to refine the definition of the selected inlet through more detailed analyses.

Mission and Aircraft Design

The supersonic cruise vehicle mission profile selected for the study is shown in Figure 71. The mission involves climb to optimum altitude for Mach 2.55 cruise followed by deceleration and descent. Because a majority of the fuel (53%) is used during supersonic cruise, the major emphasis of the study is at the supersonic cruise point. However, because 31% of the fuel is consumed during takeoff and climb, inlet performance and the associated airflow matching problems at takeoff and at transonic speeds also are included in the analysis.

The aircraft used in the study is the Lockheed-California CL 1609-1 supersonic cruise vehicle with over-wing and under-wing powerplant nacelles, as shown in Figure 72. This aircraft is designed for Mach 2.55 cruise on a hot day and has a takeoff gross weight of 268,530 kg (592,000 lb). The over/under nacelle arrangement results in an over-wing inlet local Mach number of 2.75 and under-wing inlet local Mach number of 2.51 at a typical supersonic cruise life coefficient.

Engine Type

The General Electric Company GE21/J11 double-bypass variable cycle engine with a 20% high-flowed fan was selected for the study. A schematic of the engine installation is shown in Figure 73. The engine, which has a sea level Mach 0.3 hot day thrust of 181,000 N (40,700 lb), was selected because of its high ratio of transonic to cruise corrected airflow and its airflow flexibility provided by the variable geometry and digital controls.

146
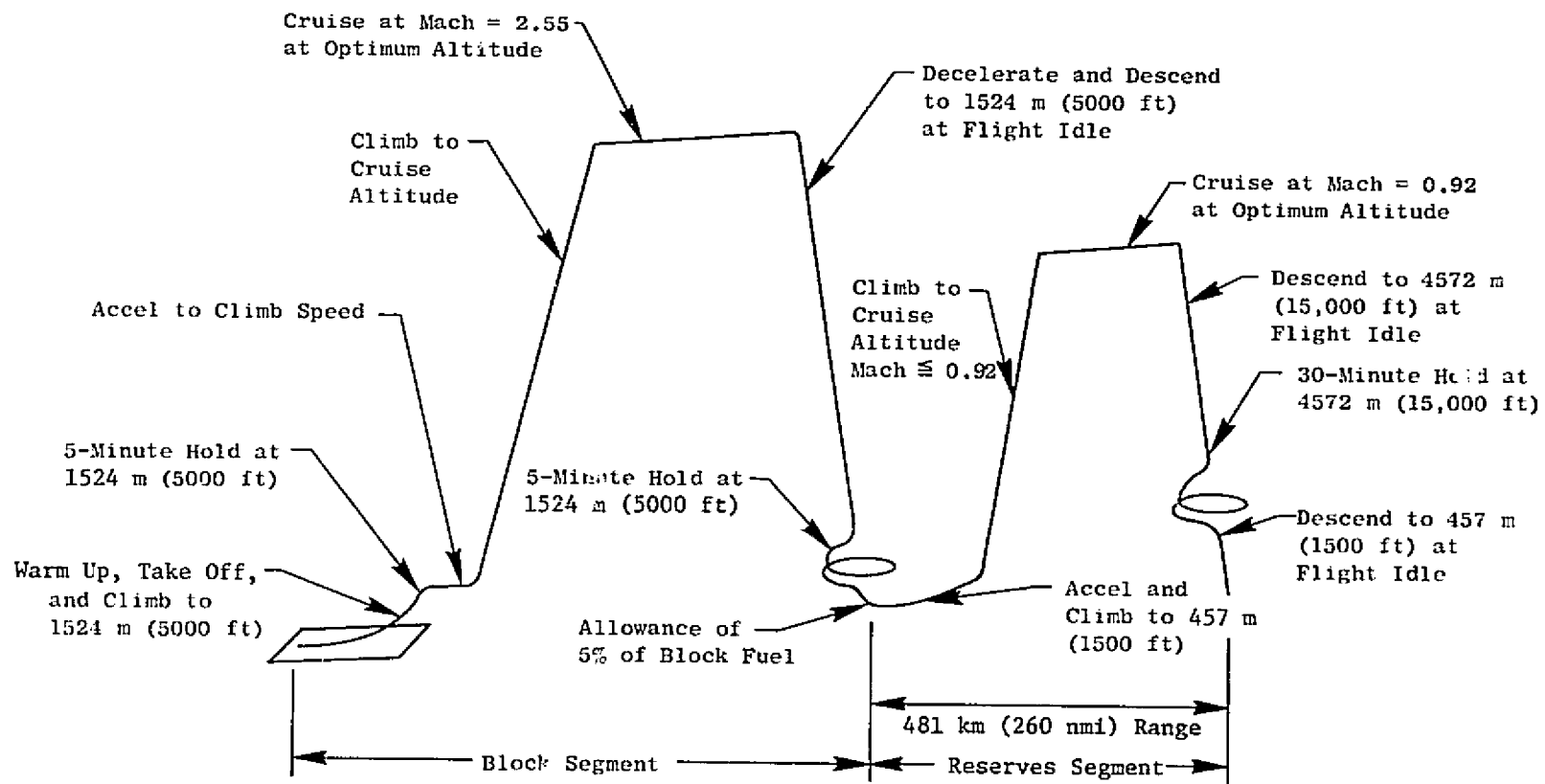
Figure 71. Mission Profile.

WING		TAIL	
TIP FOLDED	TIP EXTENDED	HORIZONTAL	VERTICAL
617.19 (7215.5)	617.45 (7400)	45.32 (530.2)	11.05 (130.0)
1.72	8.07	1.707	0.507
39.559 (135.13)	37.753 (123.87)	3.512 (30.12)	2.475 (8.108)
10.156 (1727.1)		1.746 (144.35)	7.795 (305.5)
5.111 (201.95)	3.795 (115.25)	2.032 (73.21)	3.733 (79.11)
0.1157		0.23	0.57
25.513 (1055.9)		5.850 (899.90)	5.414 (211.2)
2.271(73.02)/3.235(59.66)/1.013(00.02)	1.005 (30.72)	1.897 (95.51)
3.031		3.0	3.0
6.117		1.0	3.0

:SS HEIGHT - 268.525 KG (592.000 LBS)

.ER PLANT (4) G.E. GE 21/J11B4 DUAL CYCLE VCE

:TALLED THRUST - 181.000 NEWTONS (40.700 LBS) M 0.3 SL 30 DEG C

6.35 m (20.85 ft)

33.97 m (111.85 ft)

37.757 m (123.87 ft)

38.
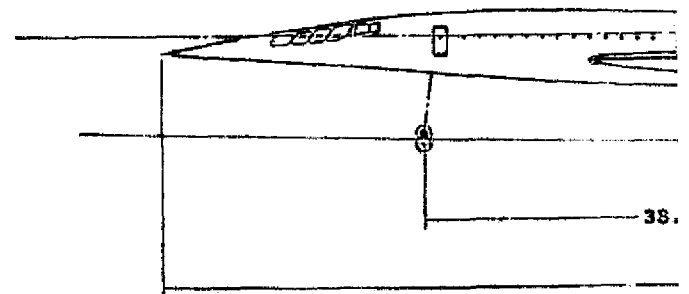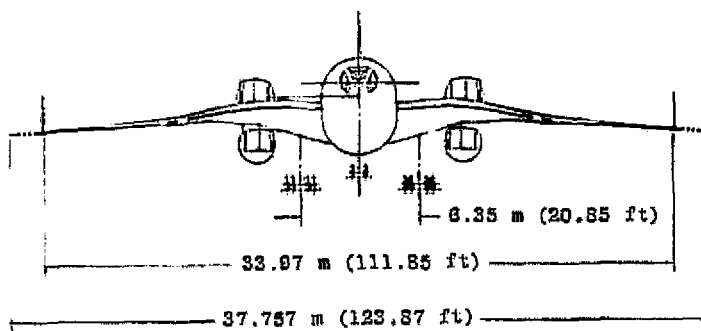
Figure 72. Supersonic Cruise Vehicle General Ar..

SCALE-METRES
SCALE-FEET

10.6 m (34.79 ft)

38.618 m (126.67 ft)

89.51 m (293.67 ft)

Vehicle General Arrangement (Lockheed—California Company).

149

Mach 2.55 Double-Bypass Variable Cycle Engine

Fn = 181033 N (40,700lb) at Sea Level; Mach 0.3 Std Day

+15° C (+27° F)

All Dimensions in cm (inches)

Engine Airflow = 288-345 kg/sec (633-760 lb/sec)

164.8 (64.89)   164.5 (64.77)   175.8 (69.22)   190.3 (74.92)

360.2 (141.82)   669.5 (263.6)
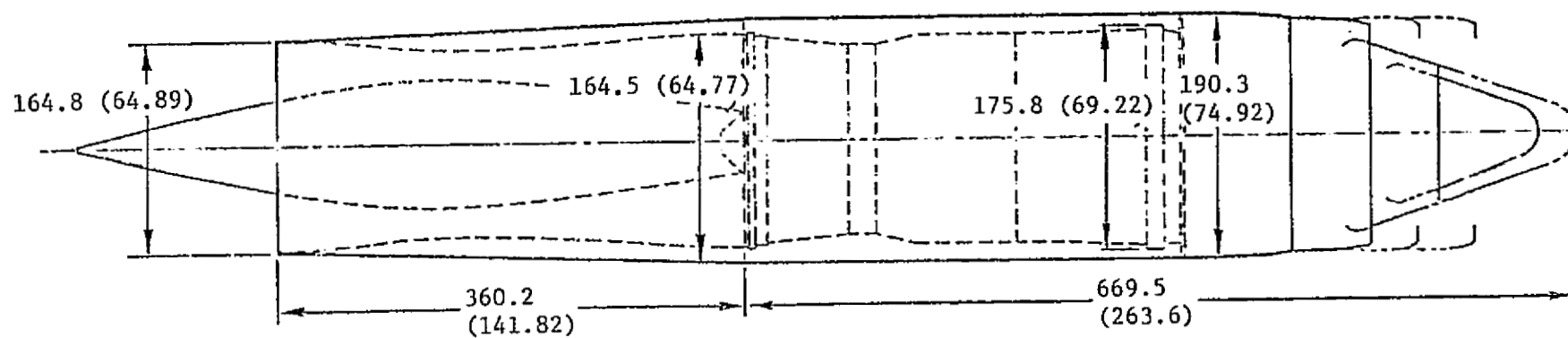
Figure 73.   Pod Arrangement (GE21/J11 VCE).

Inlet Design

The inlet screening and selection procedure consists of a cruise-point parametric design study, a transonic and takeoff airflow matching study, and an evaluation of several additional factors such as inlet aerodynamic and hardware commonality, self-starting capability, and aircraft installation. The cruise-point parametric design study involves developing a family of two-dimensional and axisymmetric inlets using as the independent variables inlet pressure recovery, throat Mach number, and percent internal contraction.

An analysis to obtain families of supersonic cruise-point designs two-dimensional and axisymmetric inlets has been developed. The inlet design parameters which have been used in the analysis consist of the local Mach number, throat Mach number, throat pressure recovery, percent internal contraction, initial cone or wedge angle, subsonic diffuser wall angle, aspect ratio (for the two-dimensional inlets), engine compressor face dimensions, and engine corrected airflow. The analysis procedure then yields the cowl lip internal angle, supersonic diffuser length, subsonic diffuser length, throat area, bleed mass flow rate, capture area, and approximate inlet contours.

The basic approach of the analysis is to obtain flow conditions along the centerbody and internal cowl surfaces from a simple application of the method of characteristics and shock theory, such that the throat Mach numbers on the cowl and centerbody are equal. Having a uniform throat Mach number minimizes flow distortion and is one of the primary design constraints. For the two-dimensional inlet, all external compression on the centerbody beyond that due to the initial wedge is done by isentropic compression with the compression waves focused at the cowl lip. For the axisymmetric inlet, two-dimensional isentropic compression is used from the initial cone to the final conical ramp, and two-dimensional flow is assumed aft of the cowl lip station, where the local Mach number at the cowl lip station is the average between the surface Mach number on the final conical ramp and the Mach number at the cowl lip.

The inlet geometry ground rules for the two-dimensional and axisymmetric inlets are illustrated in Figure 74. The 0.05235 rad (3°) initial wedge angle and 0.1745 rad (10°) initial cone angle were selected to give a small total pressure loss across the initial shock waves of both inlets. A 0.08725 rad (5°) inlet cowl lip thickness was assumed for which structural integrity can be assured. The total included subsonic diffuser angles are 0.08376 rad (4.8°) and 0.16578 rad (9.5°) for the two-dimensional and the axisymmetric inlets, respectively.

Two-Dimensional Inlets

The overall approach employed in the analysis of the two-dimensional inlets consisted of applying the approximate methods of characteristics and shock theory to eliminate the shock reflection point, α_3, (see Figure 75) as

0.08725 Rad (5°) Minimum Lip Thickness

0.999 Recovery

0.08376 Rad (4.8°)

0.0523 Rad (3°)

Symmetrical Vertical Ramp

1.6 Capture Aspect Ratio

Two-Dimensional Inlet

0.08725 Rad (5°) Minimum Lip Thickness

0.999 Recovery

0.1658 Rad (9.5°)

0.1745 Rad (10°)

Axisymmetric Inlet
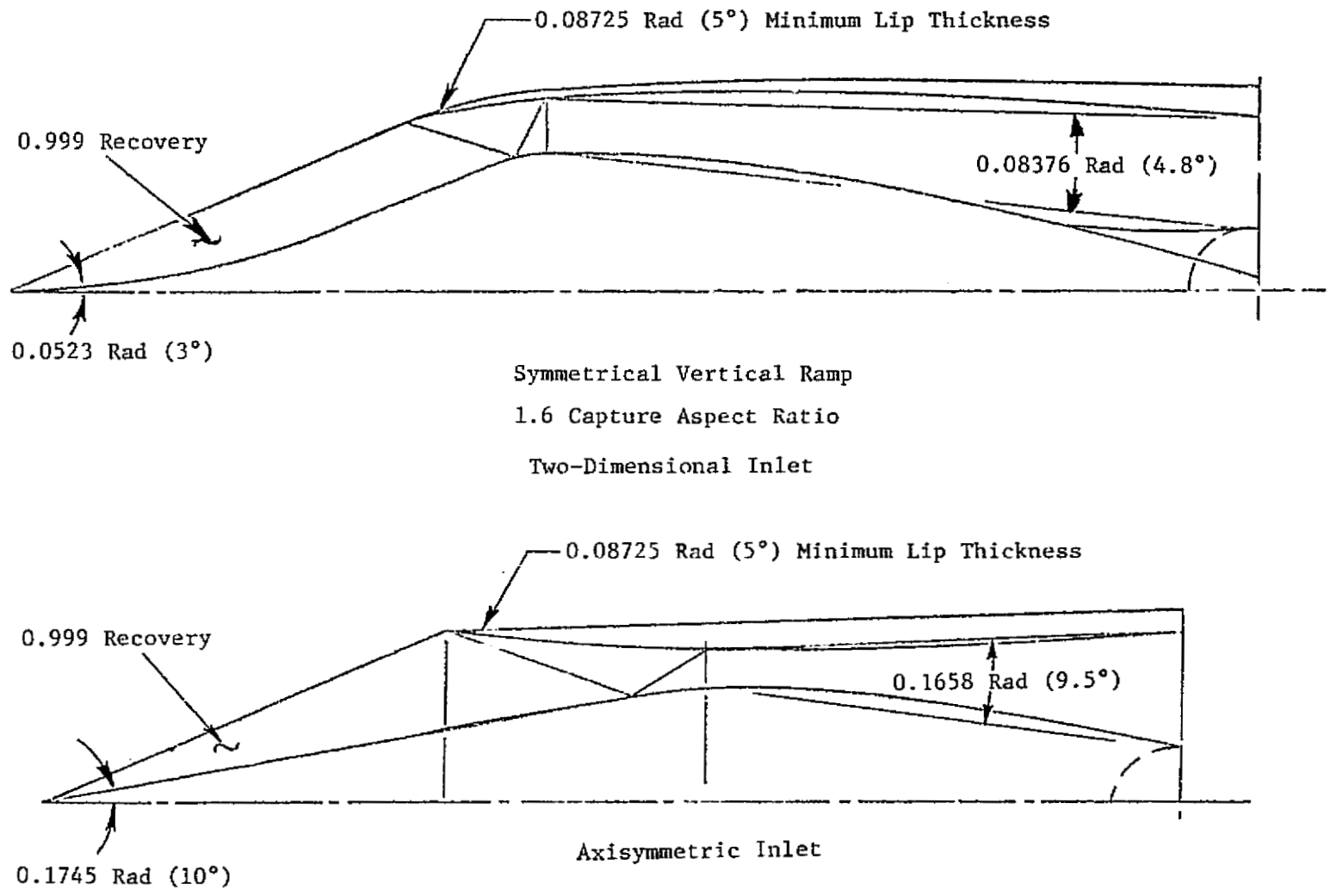
Figure 74.   Inlet Design Ground Rules.

α_1 = Initial Wedge Angle

α_2 = Final Ramp Angle

α_3 = Shock Reflection Point Angle

α_4 = Cowl Lip Internal Angle

α_5 = Throat Angle
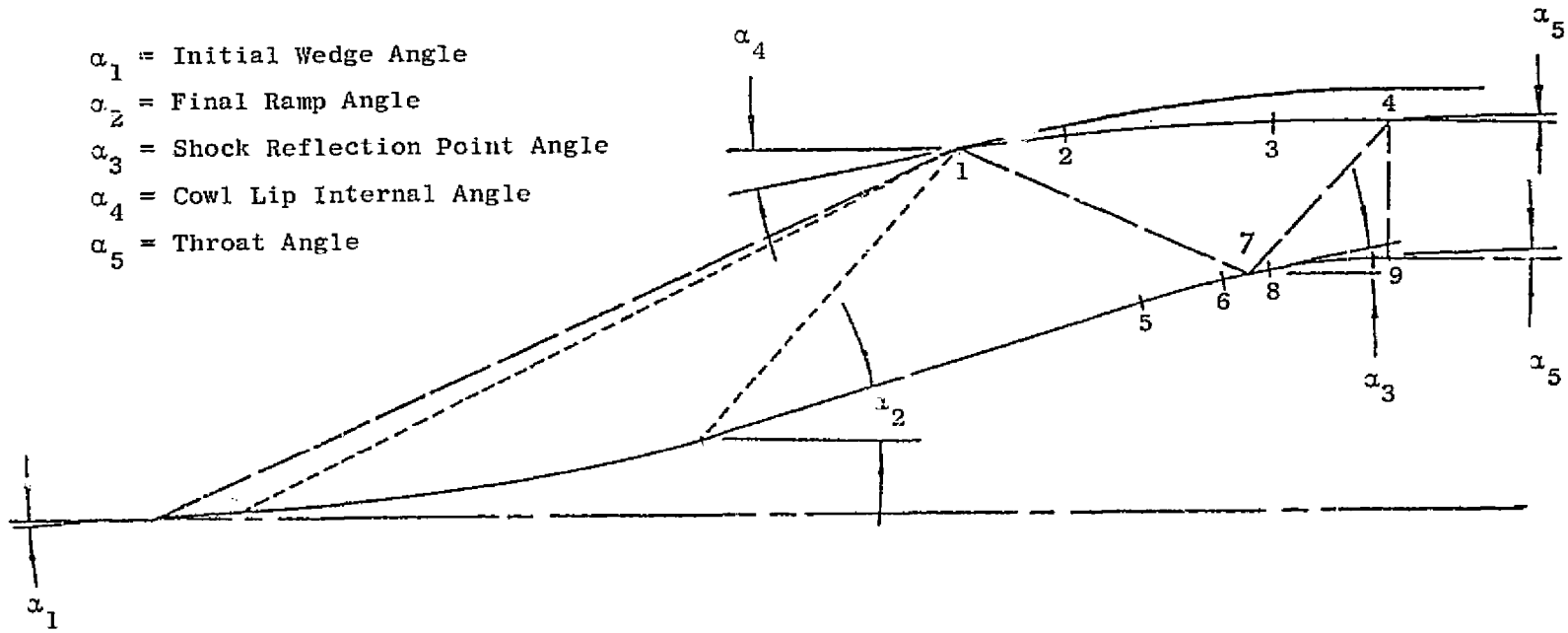
Figure 75. Inlet Angles Definition, Two-Dimensional Inlet.

an explicit variable, of finding the final ramp angle, α_2, and cowl internal angle, α_4, which are consistent with the given design parameters, and of determining from the known geometry the supersonic and subsonic diffuser lengths, and approximate inlet contours.

The analysis was used to determine approximate inlet contours, inlet lengths, and cowl internal lip angles for two-dimensional inlets designed for the GE21/J11 variable cycle engines installed on the Lockheed CL 1609-1 Mach 2.55 cruise vehicle. The GE21/J11 engine net installed thrust of 197,490 N (44,000 lb) at sea level, Mach 0.3 on a standard +15° C (+27° F) day corresponds to an engine face diameter of 175.8 cm (69.21 in.) and a nacelle maximum diameter of 197.9 cm (77.91 in.).

Approximate two-dimensional inlet contours and shock wave patterns were determined from the analysis for the design Mach number of 2.75 and three different internal contractions and are shown in Figure 76.

Axisymmetric Inlets

The approach used in the analysis for axisymmetric inlets is almost identical to that for two-dimensional inlets except that the Prantl-Meyer compression starts on the cone surface using the cone Mach number, and the local Mach number at the cowl lip station is the average between the surface Mach number on the final conical ramp and the Mach number at the cowl lip. Also, the angle of the flow approaching the cowl lip is the average between the angles of the flow at the cowl lip and the final conical ramp. The bleed mass flow rates were again found for axisymmetric inlets.

The analysis procedure discussed above was used to determine approximate inlet contours, inlet lengths, and cowl internal lip angles for axisymmetric inlets designed for GE21/J11 variable cycle engines installed on the Mach 2.55 Lockheed CL 1609-1 cruise vehicle. Approximate axisymmetric inlet contours and shock wave patterns were determined from the analysis for the design Mach number of 2.75 and three different levels of internal contraction and are shown in Figure 77. The effect of varying percent internal contraction on inlet length and cowl internal lip angle for throat recoveries from 0.90 to 0.96 and throat Mach numbers from 1.25 to 1.40 have been determined.

Analysis

The inlet width, W, for a two-dimensional inlet with an aspect ratio equal to 1.6 is approximately equal to the diameter, D, for an axisymmetric inlet. The total length for the two-dimensional inlet is about 50% longer than that of the axisymmetric inlet for the same percent internal contraction and throat conditions. This is due primarily to the smaller subsonic diffuser wall angle selected for the two-dimensional inlet than for axisymmetric inlet (as discussed previously) and the larger throat height for the two-dimensional inlet.

0.92 Throat Recovery-- 1.35 Throat Mach Number

Figure 7C. Inlet Contours, Two-Dimensional Inlets.
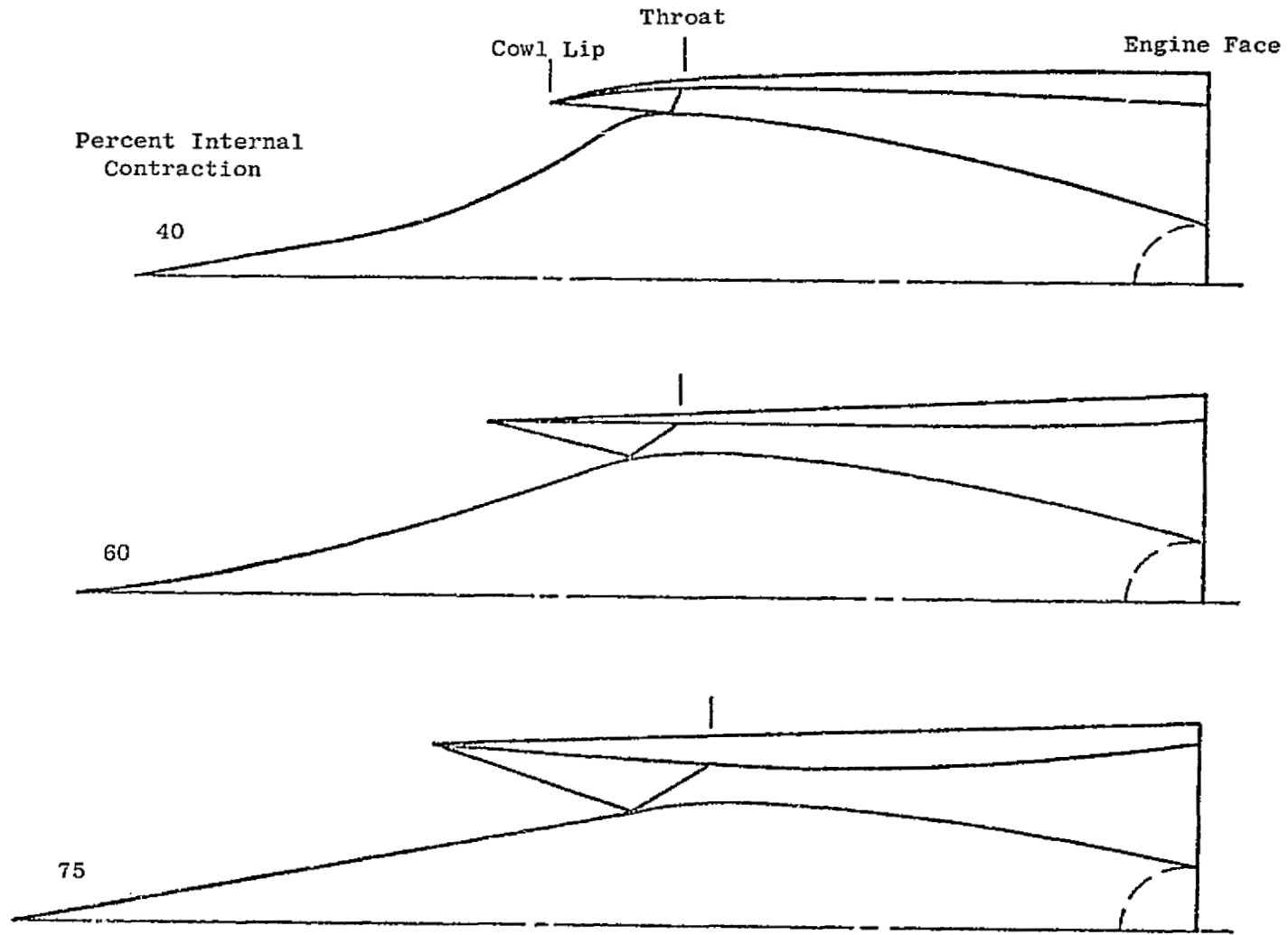
Figure 77. Inlet Contours, Axisymmetric Inlets.

Installed Performance

The installation losses for superonic cruise consist of cowl friction drag, cowl wave drag, and bleed drag. The cowl friction drag was determined from correlations using the inlet layouts and lengths presented in Figures 76 and 77 for the two-dimensional and axisymmetric inlets. The cowl wave drag was found from correlations using the inlet layouts and cowl angles for the two-dimensional inlets and for the axisymmetric inlets. For the two-dimensional inlets, the external cowl lip angle for the horizontal top and bottom plates was taken to equal 0.08275 rad (5°). Inlet bleed mass flow ratios for both two-dimensional and axisymmetric inlets were based on previous calculations. The bleed drag coefficient based on bleed capture stream tube area is taken to equal unity. This corresponds to a bleed exit total pressure recovery of about 0.15 for a Mach number of 2.5. The resulting cowl friction drag, cowl wave drag, bleed drag, and total drag as functions of percent internal contraction for throat recoveries from 0.90 to 0.96 and a throat Mach number of 1.35 are presented in Figures 78 and 79 for the two-dimensional and axisymmetric inlets, respectively. The drag coefficients in these figures are for both pairs of over-wing and under-wing inlets and are based on a freestream dynamic pressure at Mach 2.55 and an aircraft wing area of 62,458 m^2 (6720 ft^2). As seen from these drag results, the bleed drag is quite significant, particularly for the higher percent internal contractions. Similar drag results were calculated for two-dimensional and axisymmetric inlets having the inlet throat Mach numbers varying from 1.25 to 1.40 for a throat recovery of 0.92. The effect of throat Mach number on drag was found to be small.

Structures and Weights

The weight estimates of the two-dimensional and axisymmetric inlet families were developed by assessment of relative differences based on fundamental relationships. Results of prior Lockheed inlet studies, including the Lockheed L-2000 SST and YF-12 development programs, and work performed during the Supersonic Cruise Aircraft Research (SCAR) contracts were also utilized to develop the weight estimating techniques. The inlet weights were determined as functions of geometry and loads. These results were then combined with the influence of the inlet performance variables (percent internal contraction, throat recovery ratio, and throat Mach number) on inlet geometry and loads to yield the inlet weights as functions of inlet performance variables. The comparison of inlet weights given in Figure 80 shows that the two-dimensional inlet is about 55% heavier than the axisymmetric inlet; 30% of this increment is due to the length and 25% is due to structural differences. There is a significant increase in weight with an increase in throat recovery for a given percent internal contraction and throat Mach number. This increase in weight is a result of the combined increase in duct design pressure, inlet total length to diameter ratio, inlet capture area, and inlet total length, with increase in throat recovery. The data of Figure 80 is for a fixed value of throat Mach number 1.35. The influence of this variable was investigated, and the inlet weights were found to be essentially insensitive over the range of throat Mach numbers from 1.25 to 1.40.
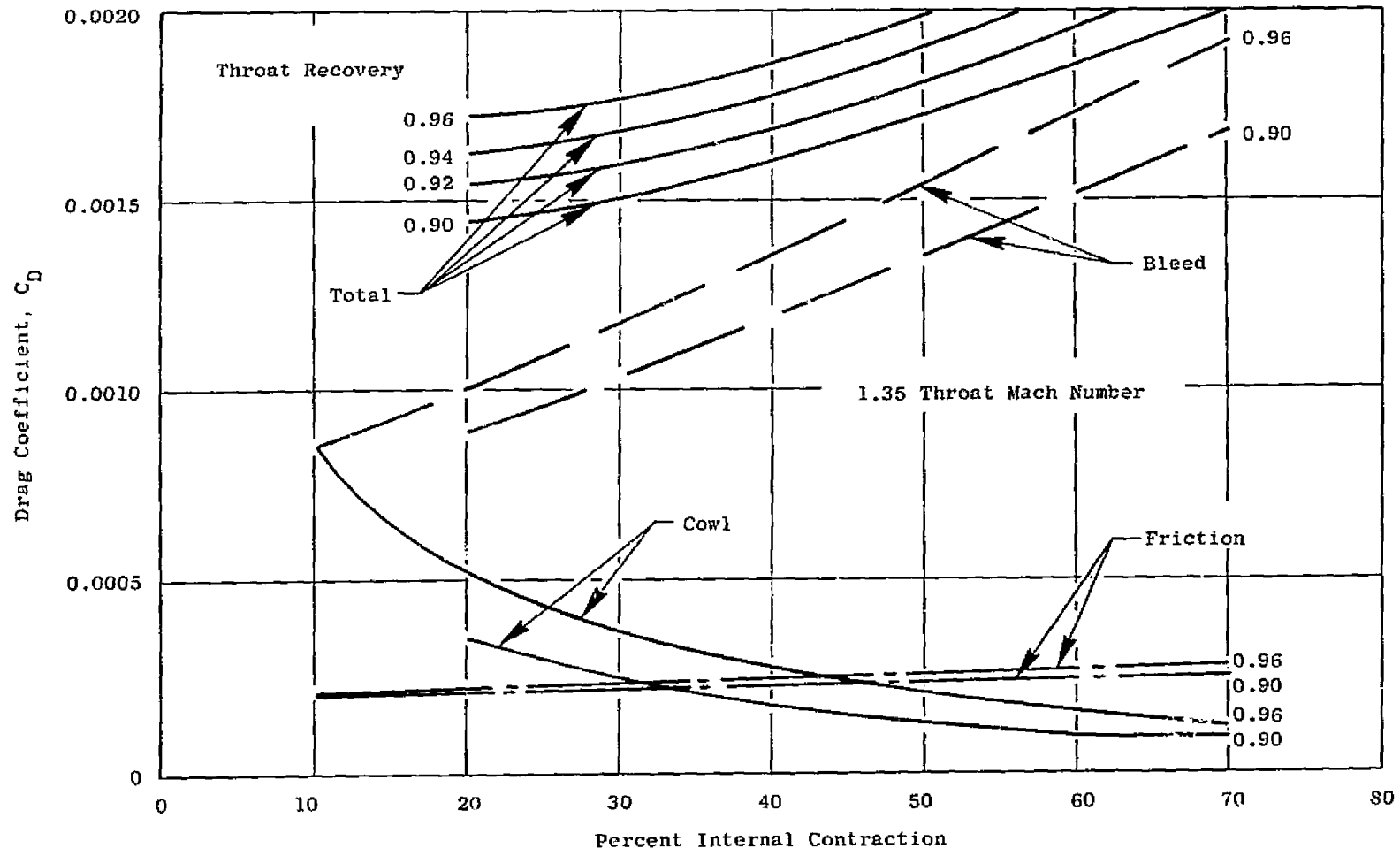
Figure 78. Drag Forces, Two-Dimensional Inlets.
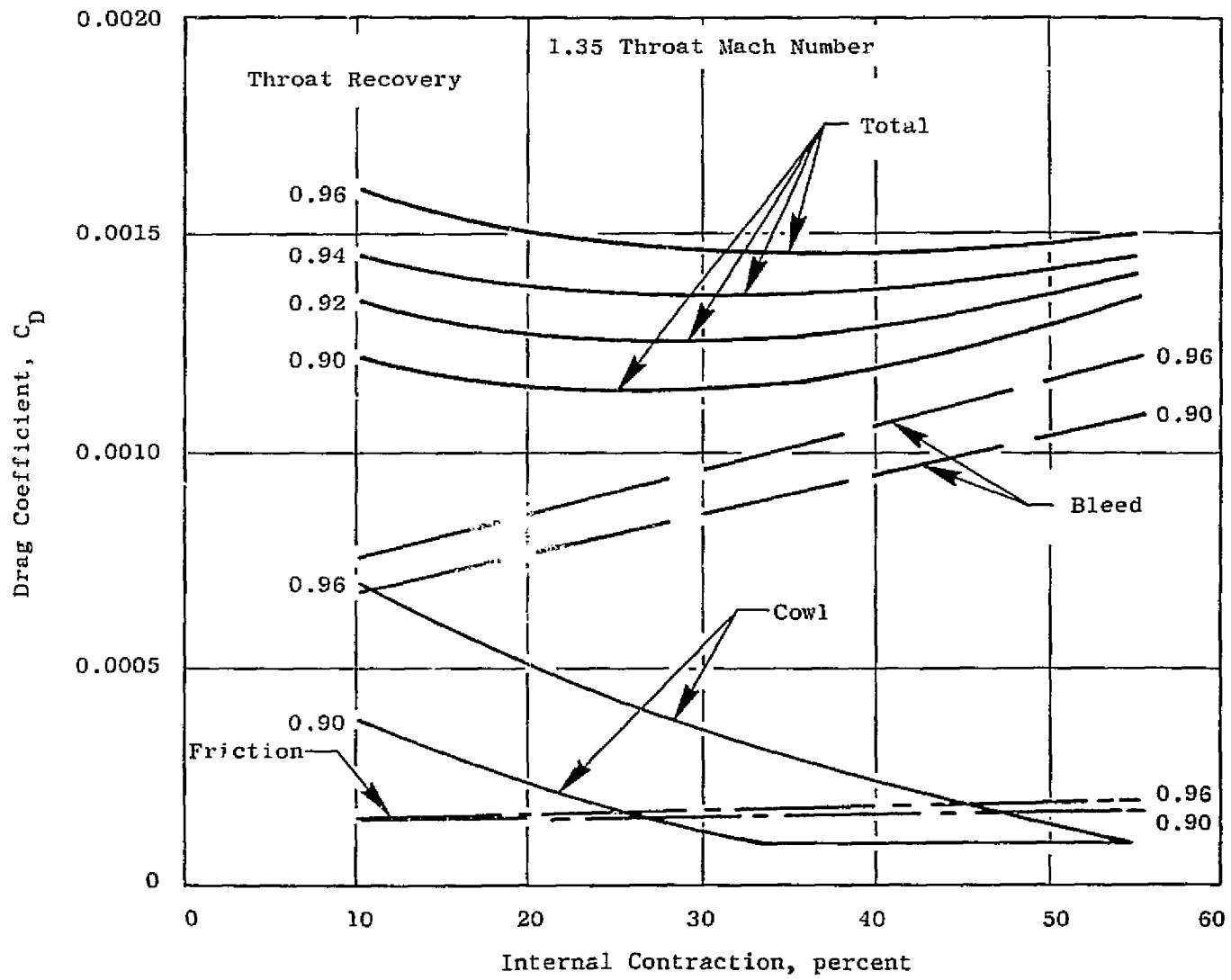
Figure 79. Drag Forces, Axisymmetric Inlets.
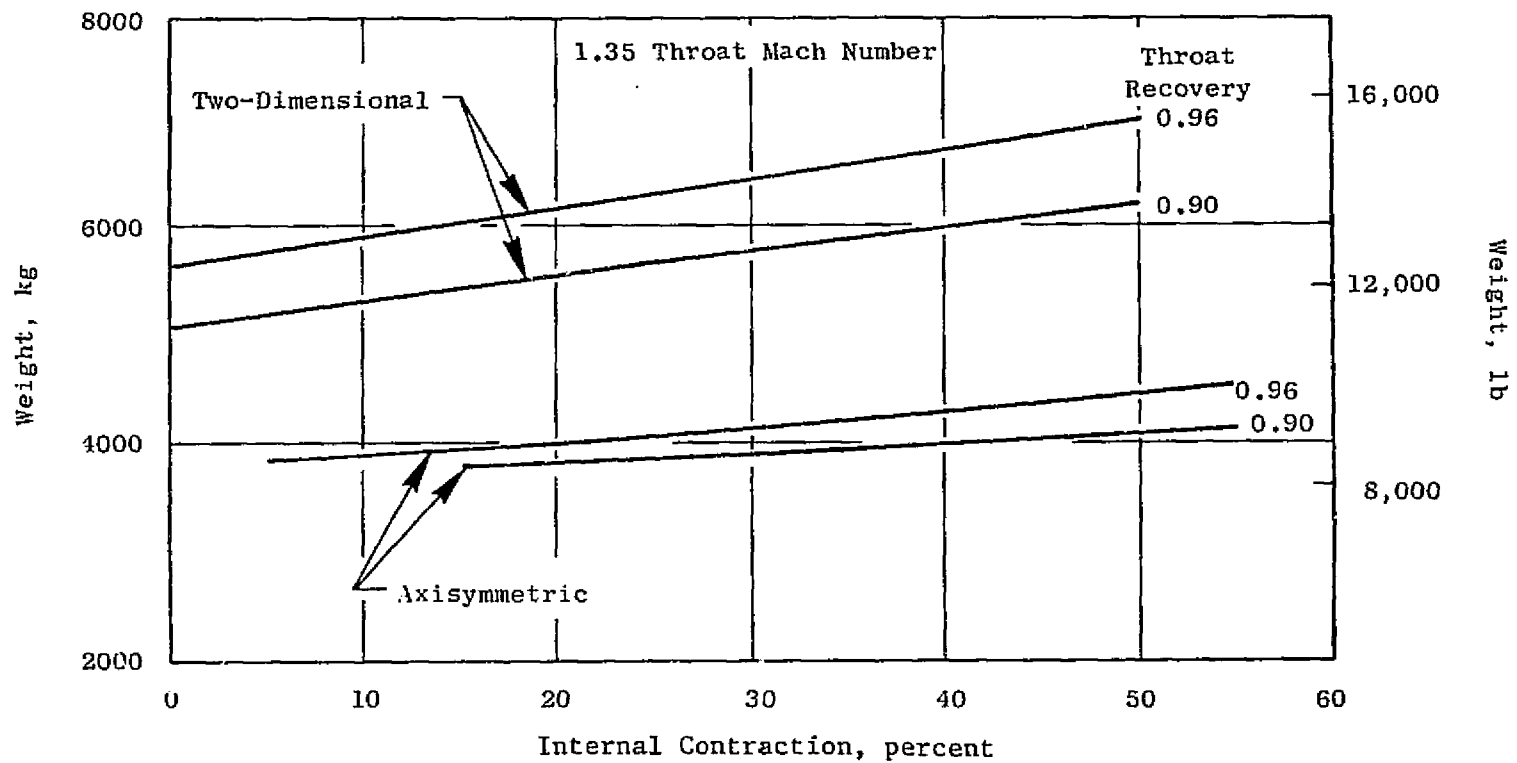
Figure 80.   Inlet Weight (Ship-Set).

Design Comparison

The influence of inlet design variations on aircraft supersonic cruise range is presented in Figures 81 and 82 in terms of the range decrement relative to a datum inlet design (defined as a 30% internal contraction axisymmetric inlet with a 1.35 throat Mach number and a 0.90 throat recovery). These results are for the Lockheed CL 1609-1 aircraft configuration which employs over-wing and under-wing inlets. Results are given in Figure 81 for throat recoveries from 0.90 to 0.96 at a throat Mach number of 1.35 and in Figure 82 for throat Mach numbers from 1.25 to 1.40 at a throat recovery of 0.92. Range decrements are presented for two-dimensional and axisymmetric inlets as functions of percent internal contraction.

The optimum two-dimensional inlet has about 120 nmi less range than the optimum axisymmetric inlet. The optimum two-dimensional inlet has a low internal contraction of 20%; whereas, the optimum axisymmetric inlet has a large internal contraction of about 50%. The inlets were designed for a local Mach number of 2.75 corresponding to the overwing inlet. The range increments for the inlets are relatively insensitive to both pressure recovery and throat Mach number. Increasing the pressure recovery decreases the engine specific fuel consumption. However, this is almost exactly offset by the inlet weight increase associated with increased design pressure and the slightly increased inlet wetted area. The variation of throat Mach number has almost no effect on inlet weight. The associated drag forces for two-dimensional and axisymmetric inlets indicate that there are compensating effects of cowl drag and bleed drag. The effects of cowl auxiliary inlet area on pressure recovery at Mach 0, 0.3, and 0.5 have been evaluated for both two-dimensional and axisymmetric overwing inlets. The higher pressure recovery for the two-dimensional inlet relative to the axisymmetric inlet is due to the larger throat of the two-dimensional inlet. In these studies a maximum throat to capture area ratio of 0.70 was used for the two-dimensional inlets.

It is clear that the axisymmetric inlets must have a large percent internal contraction to be competitive with the two-dimensional inlet. To provide takeoff recoveries comparable to those of the two-dimensional inlets, the axisymmetric inlet must have a substantially greater auxiliary inlet area. This will result in a weight advantage increment for the two-dimensional inlet which is not included in the aircraft range comparisons shown in Figures 81 and 82.

The results of this evaluation are presented in Figure 83 and show the effect of free-stream Mach number and ratio of auxiliary inlet area to capture area on pressure recovery for competitive two-dimensional and axisymmetric inlets. Again, the advantages of the two-dimensional inlet in terms of auxiliary inlet area and pressure recovery is apparent.

Sufficient throat area variation exists for the two-dimensional inlet to provide good transonic and cruise airflow matching; however, a significant performance penalty exists for the best axisymmetric inlet determined from the supersonic cruise study. In order to reduce this penalty, axisymmetric

162
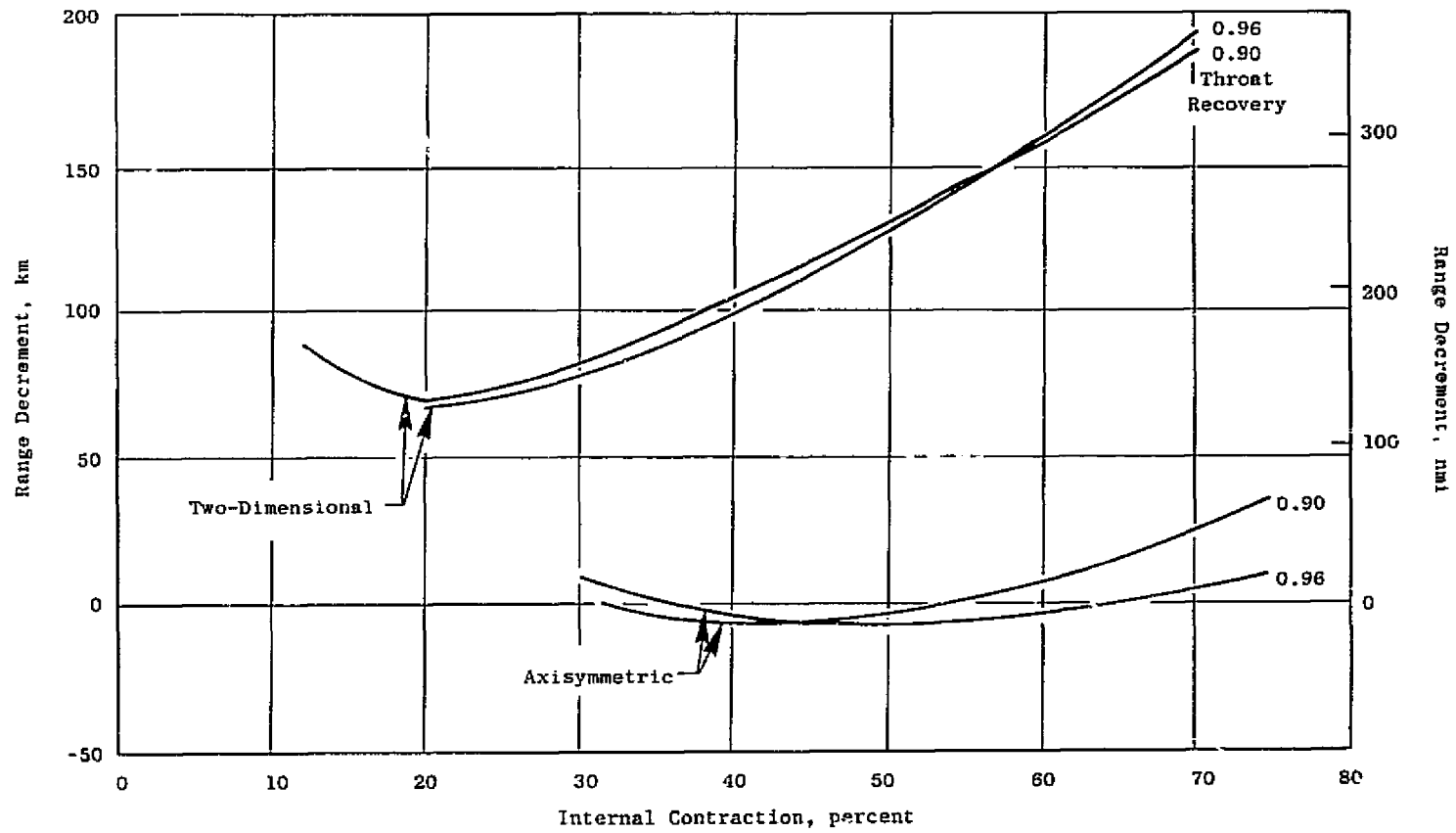
Figure 81. Range Comparison, 1.35 Throat Mach Number.
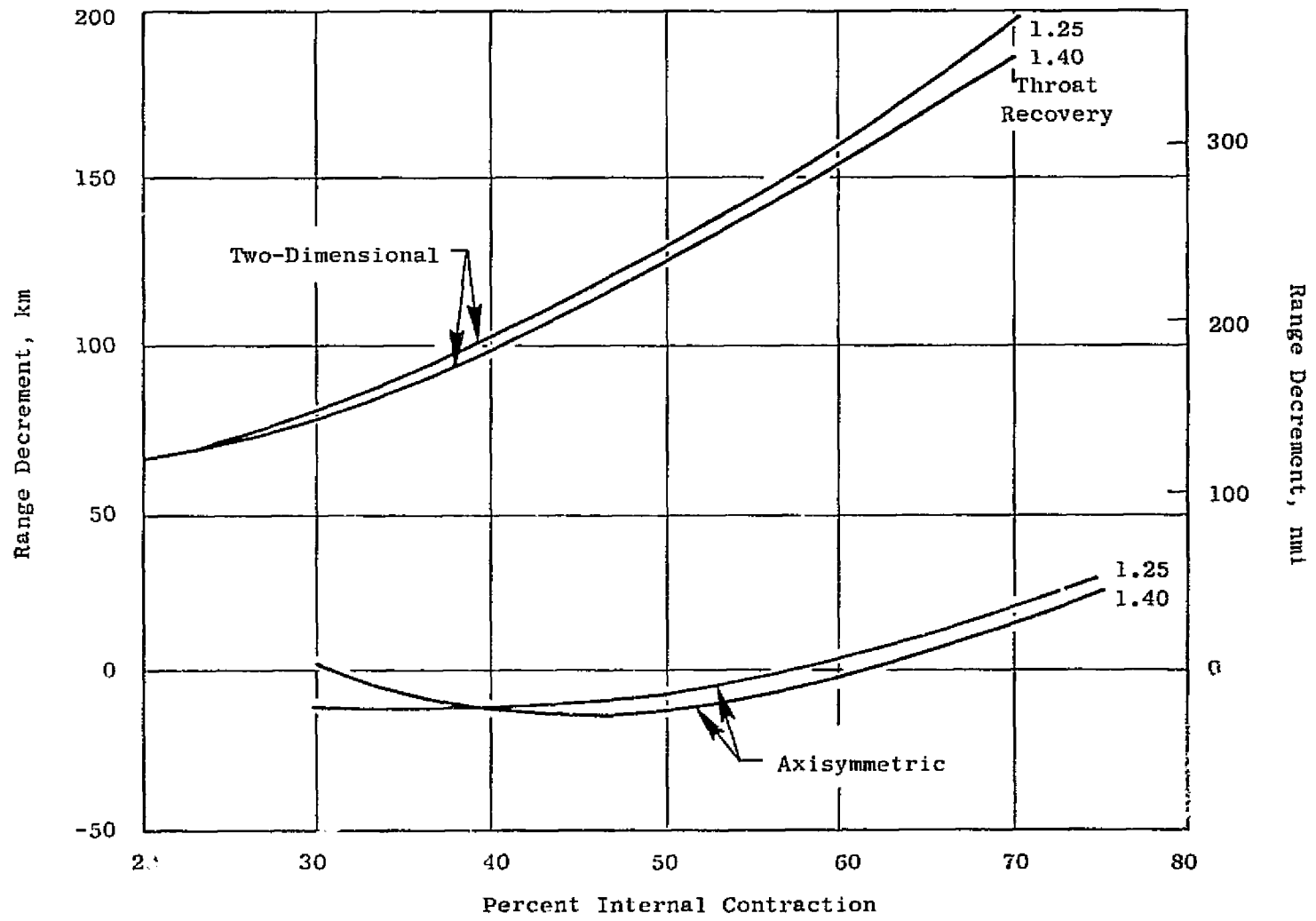
Figure 82. Range Comparison, 0.92 Throat Mach Number.
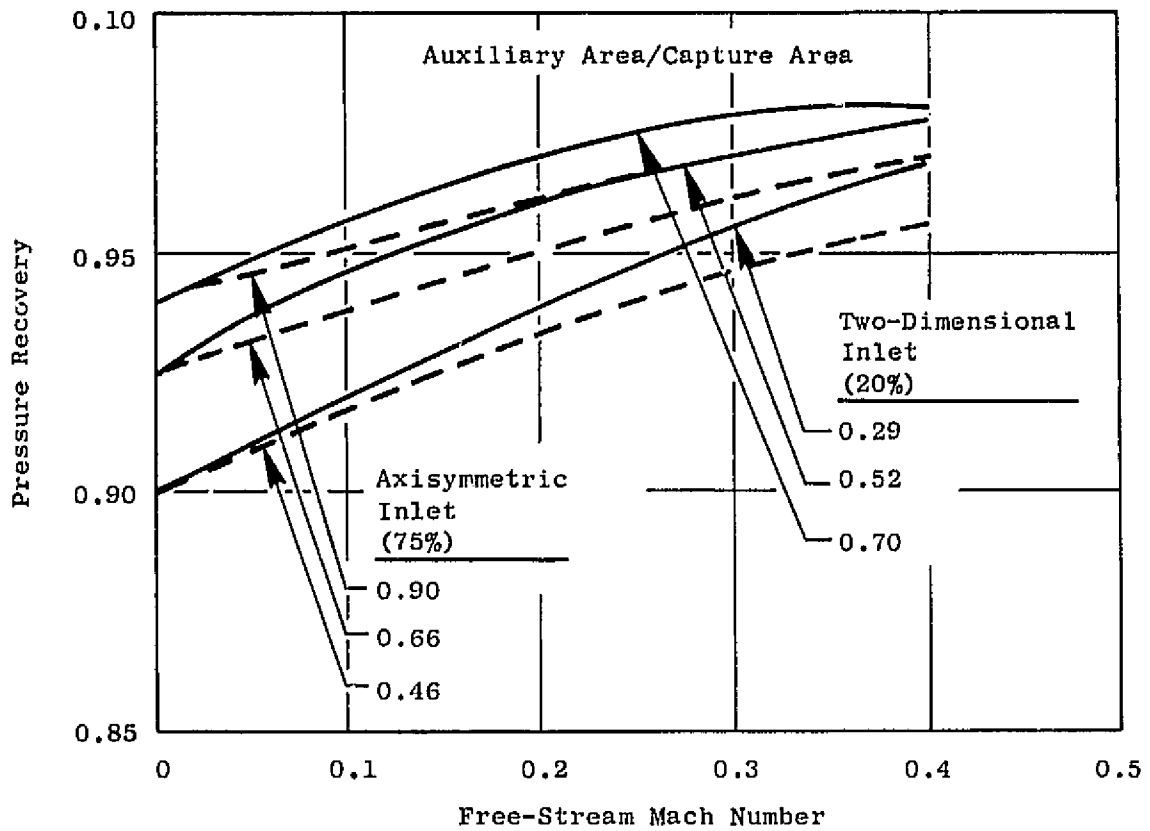
Figure 83. Takeoff Inlet Pressure Recoveries.

inlets with a higher percent internal contraction with certerbody auxiliary inlets were investigated. Flush-mounted cowl auxiliary inlets were employed for both inlet types for takeoff conditions.

The estimated pressure recoveries at Mach 0.9 for axisymmetric overwing inlets with and without centerbody auxiliary inlets are presented in Figures 84, 85, and 86 for engine corrected airflows of 226.8 kg/sec (500 lb/sec), 288 kg/sec (635 lb/sec), and 324.8 kg/sec (716 lb/sec), respectively. Engine corrected airflows of 226.8 kg/sec (500 lb/sec) and 324.8 kg/sec (716 lb/sec) correspond to Mach 0.9 cruise and climb conditions, respectively. Substantial inlet supercritical pressure recovery losses occur even for the lowest engine airflow for values of about 60% internal contraction and lower, because of the restriction in maximum throat to capture area ratios.

These restrictions in area are for axisymmetric inlets with translating centerbodies only, and the maximum throat area occurs when the maximum diameter of the centerbody is positioned at the cowl lip. Although the use of centerbody auxiliary inlets, which have an auxiliary throat area equal to one-tenth that of the basic inlet capture area, significantly improved the recovery at the low percent internal contractions, the pressure recoveries are still too low except at the low corrected airflows where an engine cycle performance penalty is incurred. Cowl auxiliary inlets could be considered. However, transonic operation of such auxiliary inlets is considered a high development risk because of compressor face distortion effects.

The conclusion is reached that the axisymmetric inlet must be designed for high internal contraction and will therefore not be self-starting. By contrast, the greater flexibility of the articulated centerbody of the two-dimensional inlet can provide sufficient throat area even at low values of internal contraction. It can therefore be designed for self-starting.

Inlet Selection

As a result of the above-described analysis, a low contraction-ratio, self-starting, two-dimensional inlet was selected as the most appropriate inlet for the General Electric Company GE21/J11 variable cycle engine installed on the Lockheed-California Company CL 1609-1 aircraft configuration with over/underwing powerplant installations. The competitive axisymmetric inlet with a 75% internal contraction and the two-dimensional inlet installation selected have virtually the same aircraft range with comparable degrees of over-wing and under-wing inlet hardware commonality. However, the two-dimensional inlet requires substantially less auxiliary inlet area to satisfy the engine takeoff airflow requirements. Further, due to its low contraction ratio, the two-dimensional inlet provides a self-starting capability at all supersonic speeds and thereby minimizes the undesirable effects of an accidental inlet unstart. Also, the inherent flexibility of the engine provided by variable geometry and digital controls, in combination with the flexibility provided by the articulated centerbody compatible with the two-dimensional design, is expected to permit virtual elimination of inlet subcritical transonic spillage drag.

166
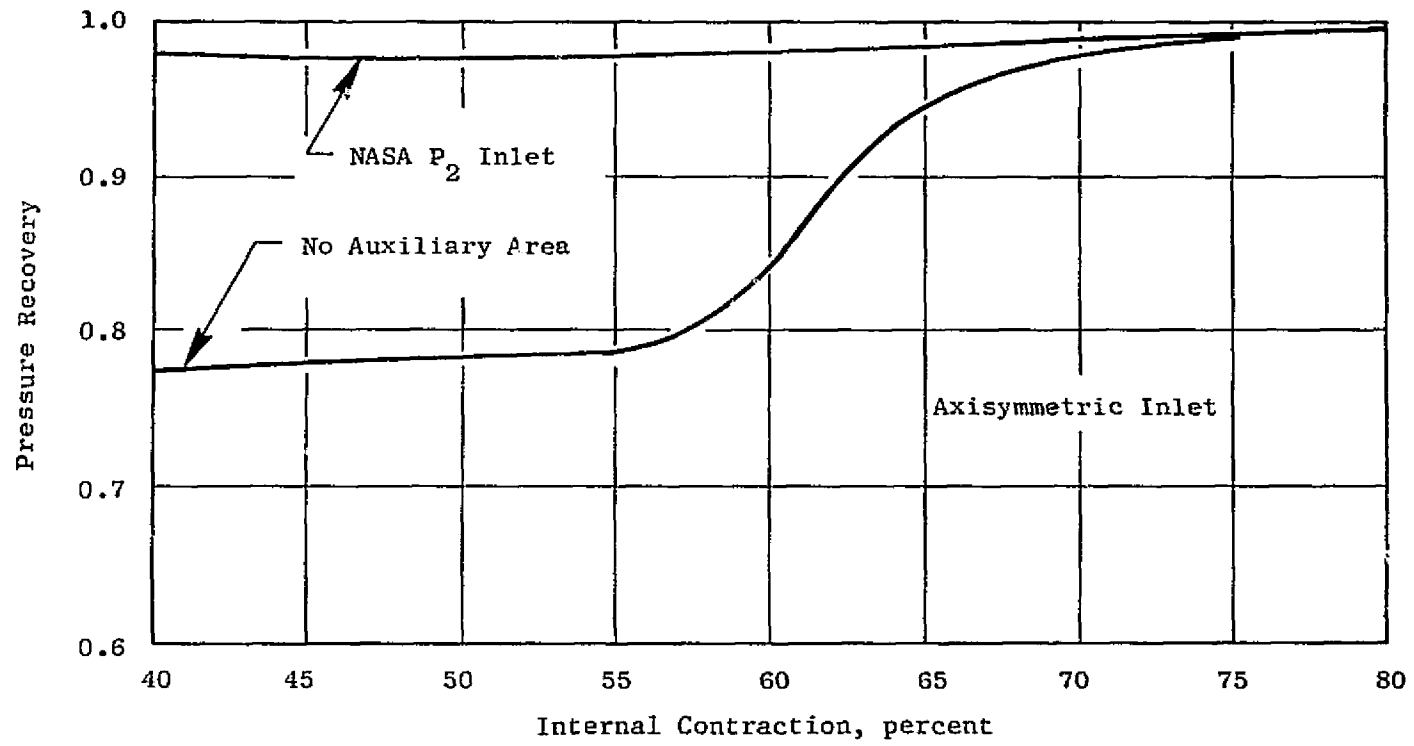
Figure 84. Pressure Recoveries at Mach 0.9, 227 kg/sec (500 lb/sec) Engine Airflow.
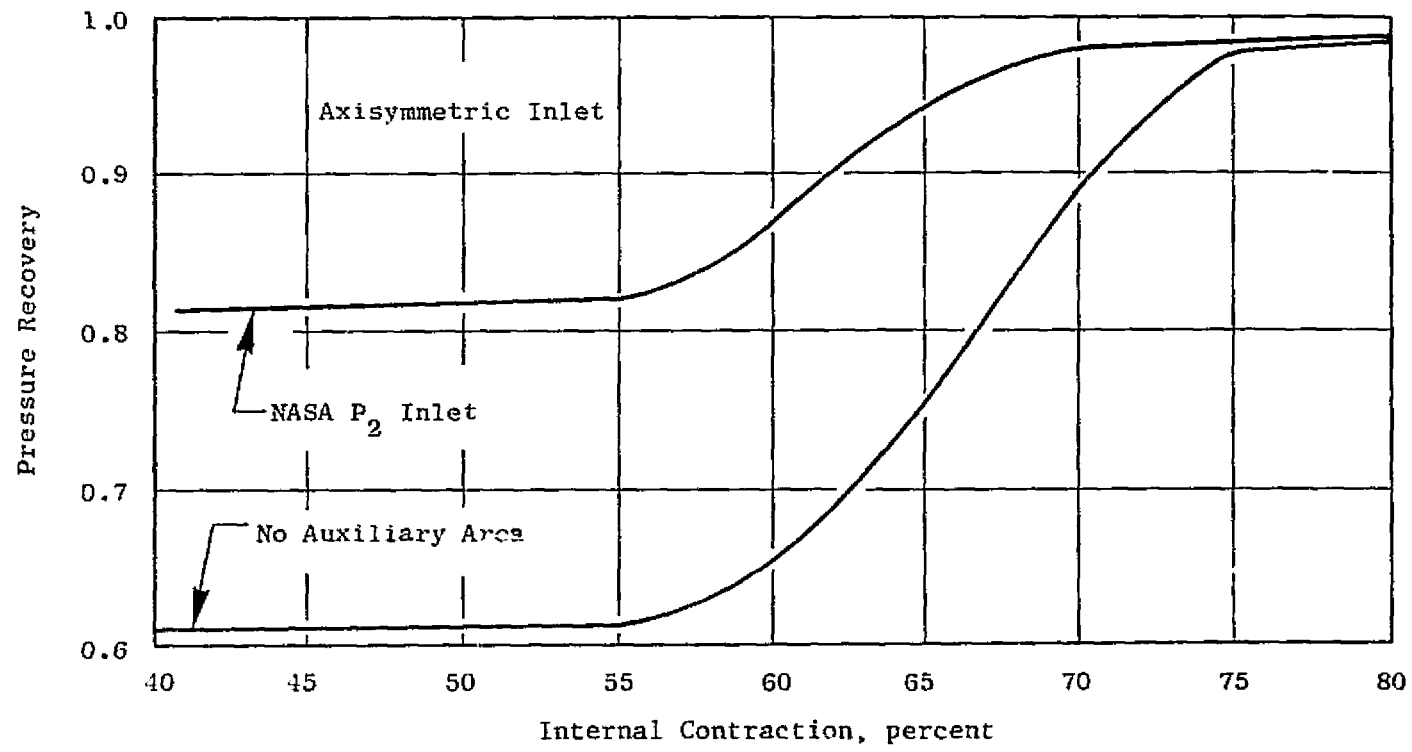
Figure 85. Pressure Recoveries at Mach 0.9, 288 kg/sec (635 lb/sec) Engine Airflow.

Axisymmetric Inlet
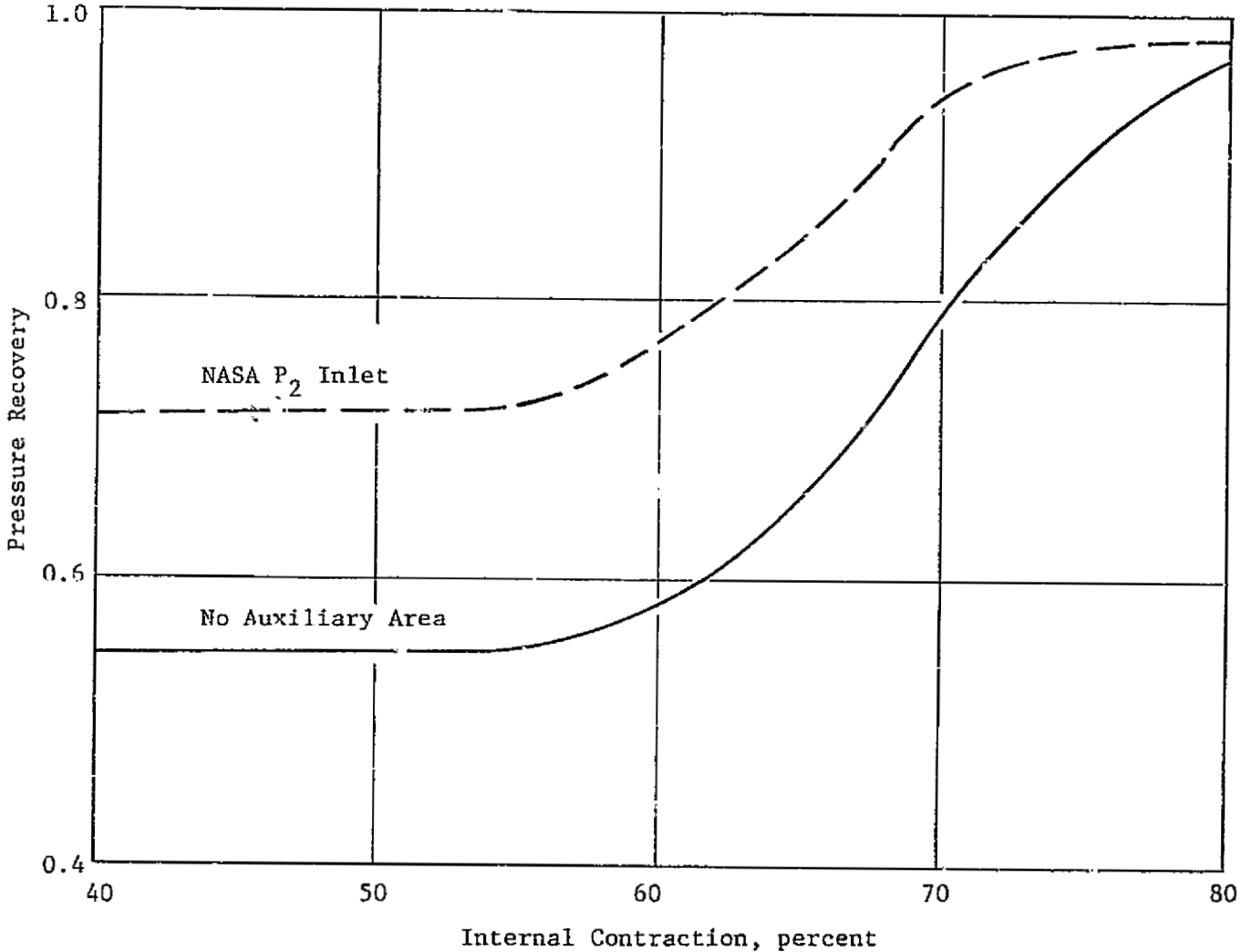
Figure 86. Pressure Recoveries at Mach 0.9, 325 kg/sec (716 lb/sec) Engine Airflow.

Detailed Inlet Design

Detailed design analyses of the selected two-dimensional inlet with 20% internal contraction have been conducted for the purpose of refining the inlet definition and of detailing the mechanical design.

Installation drawings showing the general layout of the selected two-dimensional inlet with the General Electric GE21/J11 engine are shown in Figures 87, 88, and 89. Figure 87 shows the plan view and side view of the over-wing and under-wing nacelles. The nacelles are integrated with the wing contours to give a small nozzle/exhaust spacing ratio and to minimize the boundary layer diverter frontal area. The under-wing inlet structural details are shown in Figure 88, and the inlet cross sections are given in Figure 89. The inlet has a supersonic and subsonic diffuser divided into two isolated ducts by a variable geometry centerbody. The centerbody incorporates a simple operating linkage that provides good supersonic diffuser contours for off-design Mach numbers and variable duct areas for the complete range of flight conditions. The subsonic diffuser makes a smooth transition from a rectangular cross section at the throat to a circular cross section at the engine face. Cowl auxiliary inlets are incorporated to augment the duct airflow pressure recovery during takeoff and at low speed. A system of dynamically controlled bypass doors and valves is used for positioning the inlet terminal shock wave when the inlet is started and for minimizing drag at lower speeds. A bleed system is also employed to increase pressure recovery and to extend the range of stable inlet flow.

Structural analysis was conducted on all components of the inlet system including centerbody, shell structures, bypass doors, and auxiliary inlet doors.

A detailed weight analysis was conducted on the two-dimensional inlet configuration shown in Figure 88. The results of the weight analysis are tabulated below:

Component	Weight	
	kg/Aircraft	(lb/Aircraft)
Centerbody	1,034	2,280
Shell Structure	2,647	5,835
Doors (Auxiliary and Bypass)	515	1,135
Controls, Valves, Mechanism	649	1,430
Total	4,845	10,680

These weights reflect the utilization of advanced composite materials of 42% in the centerbody, 41% in shell structure, and 81% in the bypass and auxiliary doors. A resulting 13.1% weight reduction over an all-metal inlet was achieved.

170

SCALE-METRES
SCALE-FEET
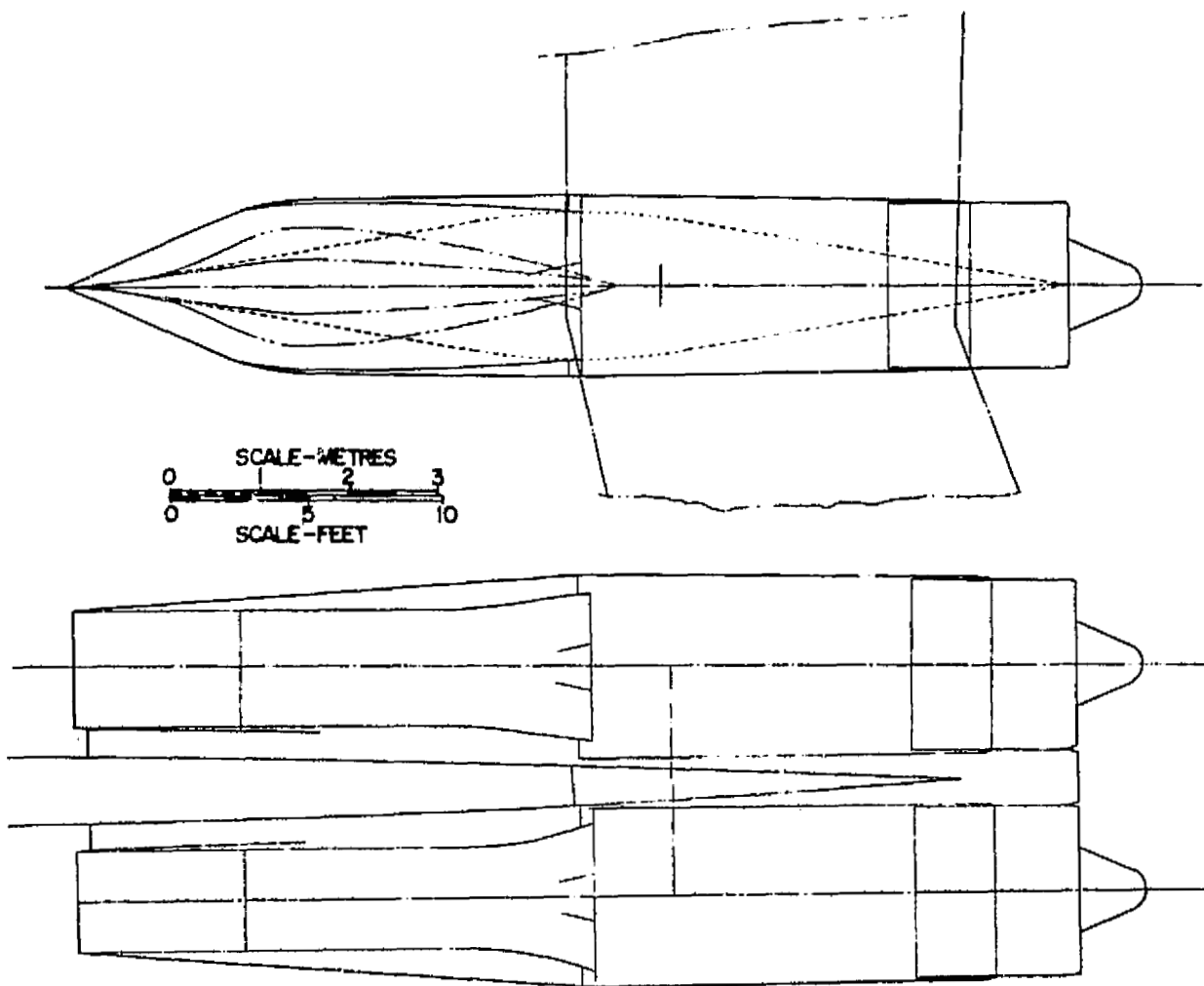
Figure 87. Installation Drawing, Engine Nacelle.

Figure 88.   Installation Drawing, Structural Detai

ng, Structural Details, Under-Wing Inlet.

173

Section J-J

Engine Face

Section H-H

Section F-F

Throat

SCALE-METERS
5   10   15

SCALE-INCHES
0   10 20   40   60
0   1   2   3   4   5
SCALE-FEET

Section I-I

Section G-G

Section E-E

Cowl Lip
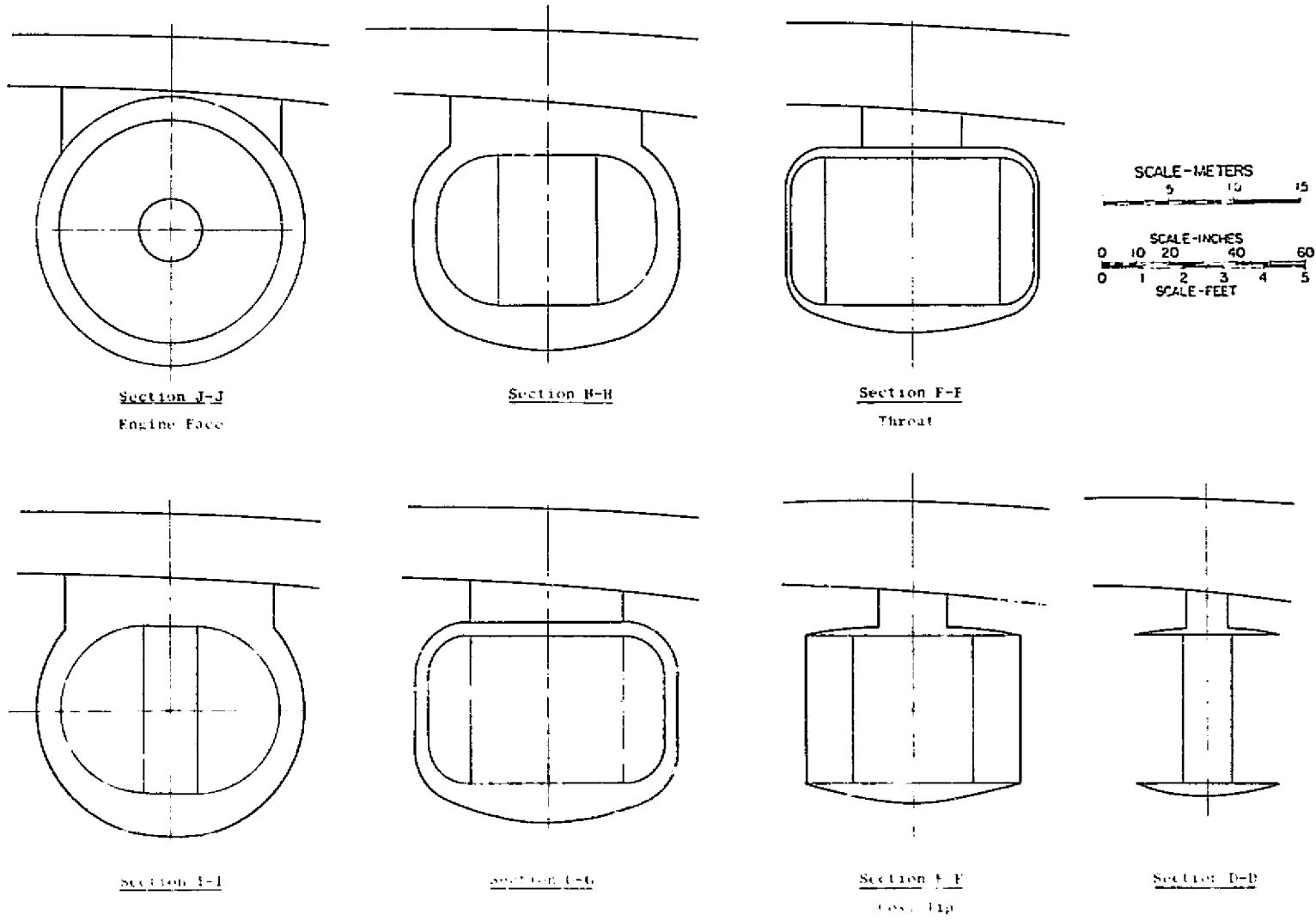
Section D-D

Figure 89.   Installation Drawing Cross Sections, Under-Wing Inlet.

Evaluation of Selected Inlet Designs

The mission performance of the Lockheed CL 1609-1 supersonic cruise vehicle with the General Electric GE21/J11 engines and the selected two-dimensional inlet installed has been computed. The GE21/J11B1 and GE21/J11B4 engines are installed over and under the wing, respectively, and are identical except for different controls software.

The variation of critical pressure recovery and mass flow with inlet local Mach number are given in Figures 90 and 91 and are applicable to both over-wing and under-wing inlets. The pressure recovery and mass flow ratio schedules with local Mach number were based on the experience with the Lockheed L-2000 inlet. The inlet bleed mass flow ratio is assumed linear with the local Mach number and is equal to 0.0685 at Mach 2.75 and zero at Mach 1.0.

The installation losses are grouped into internal losses and external losses. The internal losses have a direct effect upon engine cycle performance and include inlet pressure recovery, compressor bleed, accessory power extraction, and exhaust nozzle performance. The exhaust nozzle performance including the nozzle boattail drag was supplied by the General Electric Company.

The external losses are related to the nacelle location and aerodynamic shape of the inlet and include inlet spillage drag, inlet bleed drag, bypass drag, and cowl drag. The inlet critical additive drag as a function of local Mach number was determined from a Lockheed in-house inlet computer program. Because the variable cycle engine airflow is made to match the inlet by means of engine control software, no subcritical spillage or bypass penalties are included. Inlet bleed drag was calculated using a unity bleed drag coefficient based on the bleed stream tube capture area. The inlet cowl drag is accounted for in the airplane wave drag.

The thrust and fuel flow for the GE21/J11 engine was obtained from an installed engine performance computer deck supplied by General Electric. The engines are sized for an aircraft thrust-to-weight ratio of 0.275 at Mach 0.3 and for a 20% high-flow front block. The net installed thrust at sea level Mach 0.3 was 181,030 N (40,700 lb) for a +15° C (+27° F) hot day.

The aerodynamic performance of the Lockheed CL 1609 supersonic cruise vehicle was determined. Drags used in determining performance capability are based on NASA wind tunnel tests of a modified SCAT 15F model. A method is used to build up the drag from the wind tunnel data base to the full-scale CL 1609-1 configuration.

The mission analysis results are summarized in Table 27. For the flight profile of Figure 71, the results show that the CL 1609-1 airplane with a takeoff gross weight of 268,530 kg (592,000 lb) which includes a payload of 26,309 kg (58,000 lb) has a range of 6326 km (3416 nmi).

176
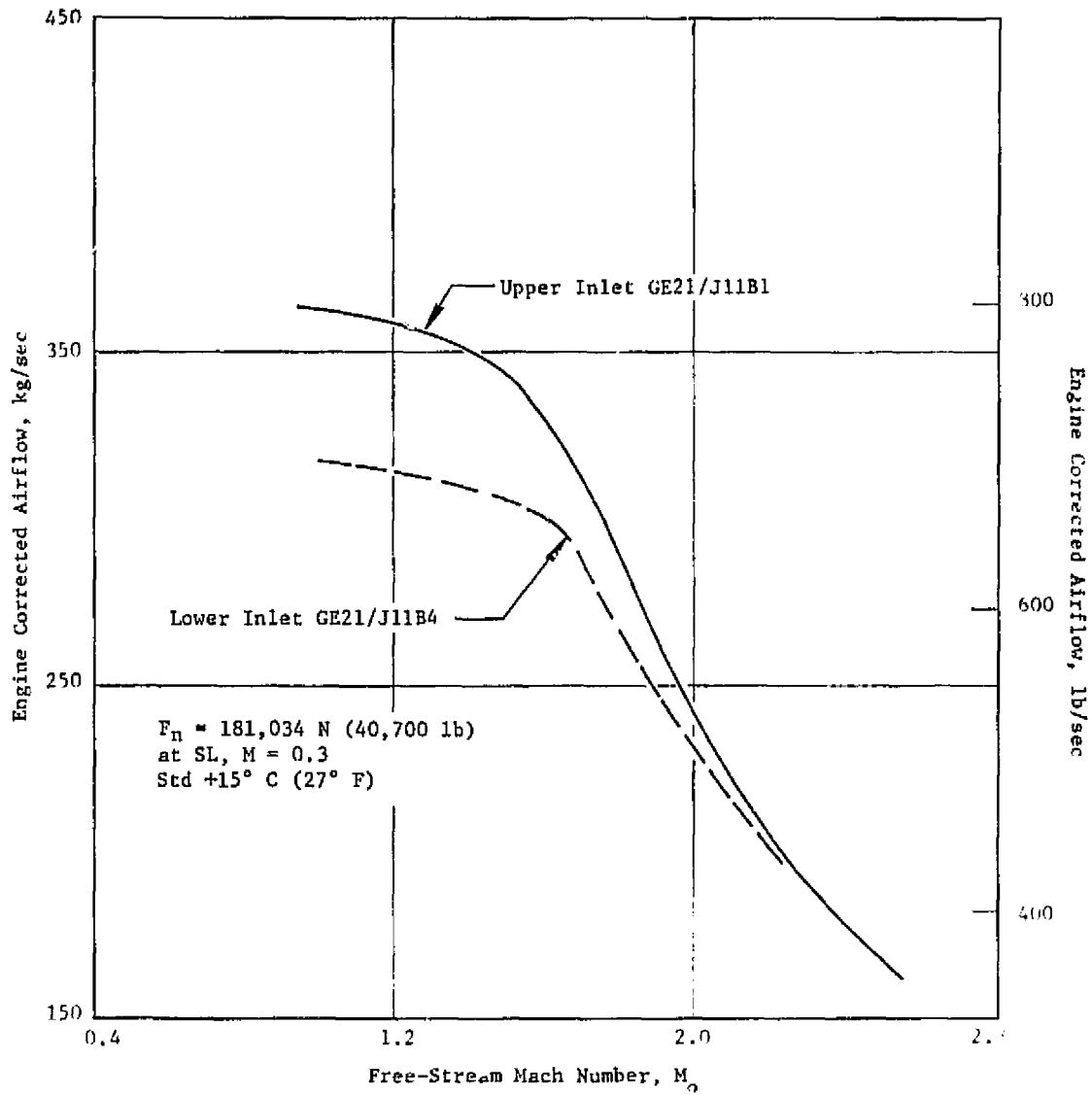
Figure 90. Engine Airflow Characteristics, Two-Dimensional Inlet.
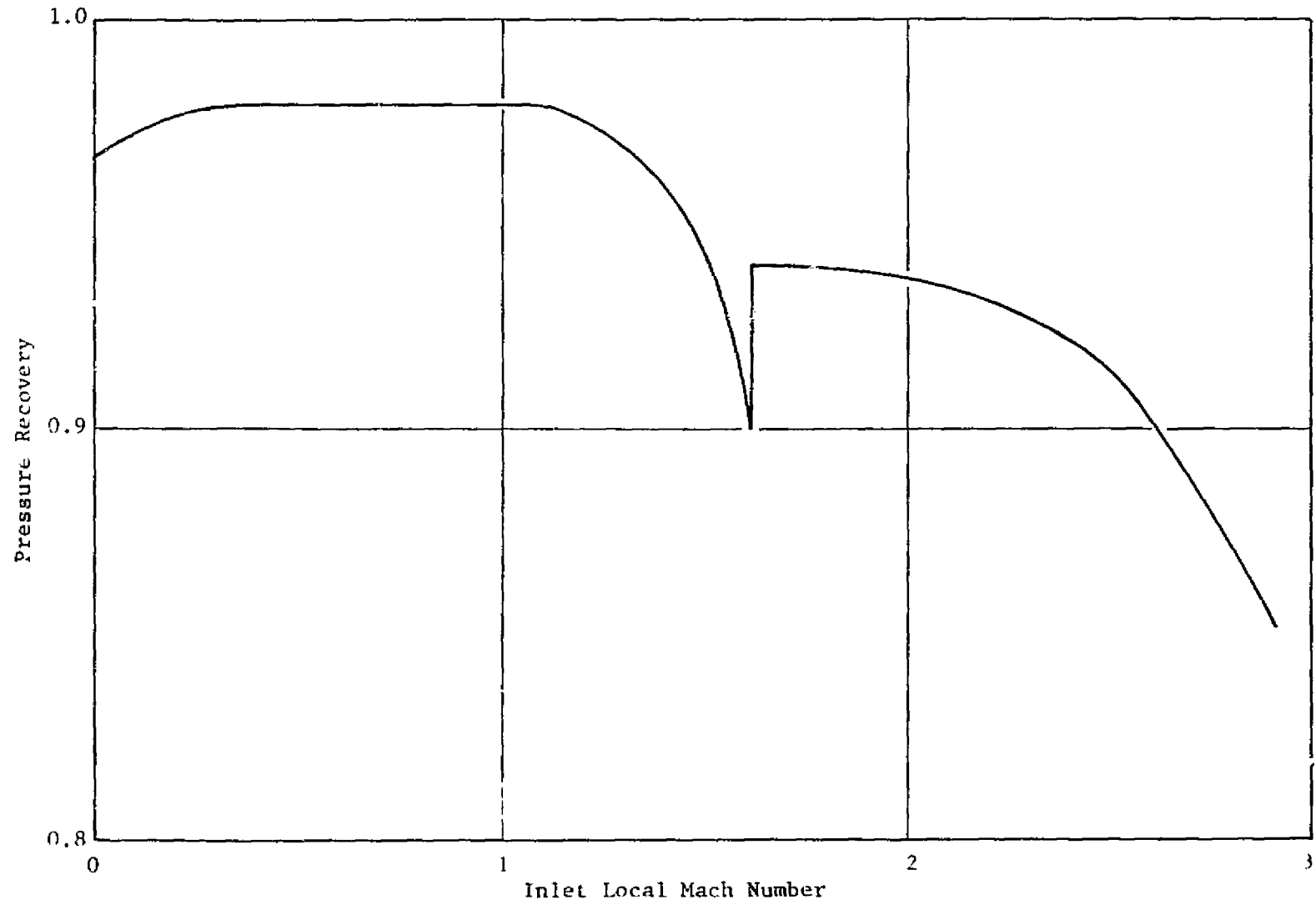
Figure 91.   Inlet Pressure Recovery, 2-D Inlet.

Table 27. Mission Performance Summary for
Supersonic Cruise Vehicle.

Engine	GE21/J11B1,B4
Cruise Mach Number	2.55
T/W, Lift-off	0.275
Cruise L/D	8.21
Cruise sfc (avg.) kg/hr/N (lb/hr/lbf)	0.163 (1.595)
Zero Fuel Weight, kg (lb)	141298 (311503)
Cruise Fuel - Percent	53
Climb Fuel - Percent	23
Takeoff and Subsonic Fuel - (Block Segment) Percent	8
Reserves - Percent	16
Range - km (nmi)	6326 (3416)

From the parametric design study of the two-dimensional and axisymmetric inlets the following conclusions are drawn:

- The length of the two-dimensional inlet is approximately 50% greater than that of an axisymmetric inlet having the same design parameters, with about 37% being attributed to the subsonic diffuser.

- The weight of the two-dimensional inlet is approximately 55% greater than that of an axisymmetric inlet having the same design parameters, with about 30% being due to length changes and the remaining 25% being due to structural differences.

- The cowl friction drag, inlet bleed drag, and inlet weight increase and the cowl wave drag decrease with increasing internal contraction such that a maximum supersonic cruise range exists at an internal contraction of 20% for the two-dimensional inlet and 50% for the axisymmetric inlet.

- When no performance penalties were assessed for commonality of over- and under-wing inlets, the best supersonic cruise range for the two-dimensional inlet installation is about 120 nmi less than that for the axisymmetric inlet installation.

- Sufficient throat area variation exists for the two-dimensional inlet to provide good transonic cruise airflow matching.

- When centerbody auxiliary inlets are utilized with the axisymmetric inlet, the transonic recovery is significantly improved at low internal contractions but is still not acceptable except at the low engine corrected airflows where a cycle performance penalty is incurred.

- Cowl auxiliary inlets are required for both the inlet types at takeoff conditions.

A self-starting, two-dimensional inlet having 20% internal contraction and cowl auxiliary doors for takeoff was selected over the best axisymmetric inlet which had a 75% internal contraction, cowl auxiliary inlets for takeoff, and no centerbody auxiliary inlets.

4.5.2 Engine/Nacelle/Airplane Integration Studies

Three airframe contractors (Lockheed-California, McDonnell Douglas, and Boeing) conducted studies in which General Electric double-bypass variable cycle engines were installed in nacelles and installed performance was calculated. Results of the studies carried out by these three contractors are

180

summarized in the following sections. The material below is taken largely from:

1. Lockheed Report LR-28071, "Advanced Supersonic Engine/Airframe Integration Study," February 21, 1977.

2. McDonnell Douglas Report MDC-J4562, "Nacelle Integration Study," March 1977.

3. Boeing Report D6-44513, "Advanced Supersonic Propulsion Study Engine/Nacelle/Airframe Integration Studies," (undated).

4.5.2.1 Nacelle Integration Study (Lockheed-California Company)

Introduction

The objective of the engine/airframe integration study described below is to provide refined installation definitions and validation of the design performance of a General Electric GE21 double-bypass variable cycle engine installed in an over/under nacelle arrangement on the Lockheed CL 1609 Mach 2.55 supersonic cruise vehicle. The GE21/J11B4 was chosen for the study as being a representative example of the VCE concept. It was not planned that comparisons between different engines be included in the analysis.

With the inherent airflow flexibility of variable cycle engines, matching of the engine and inlet airflows becomes extremely important for realization of the advantages of the advanced engine cycles. The variable geometry features of variable cycle engines allow the engine airflow to be scheduled and varied for maximum installed performance. This requires minimizing the effect of inlet recovery loss, spillage, and nozzle boattail drag. The benefits of these new engine and inlet designs yield large improvements in aircraft performance, compared to earlier supersonic aircraft.

Aircraft Selection

The aircraft used in this study is the Lockheed-California Co. CL 1609 supersonic cruise vehicle with over-wing and under-wing powerplant nacelles. This aircraft is designed to cruise at Mach 2.55 on a hot day (ISA +8° C (+14.4° F)). See Figure 92.

For the integration study, the vehicle takeoff gross weight and payload were held constant at 268,527 kg (592,000 lb) and 26,308 kg (58,000 lb), respectively. A matrix of candidate thrust-to-weight (T/W) and wing loading (W/S) ratios was evaluated (see Figure 93). Airport field length characteristics based on FAA regulations were also generated as a function of thrust-weight and wing loading. These characteristics were used to define the constraints based on requirements for second segment climb gradient, takeoff field length, sideline and flyover noise levels, and landing approach speed. The selected aircraft configuration is defined in terms of thrust-weight and
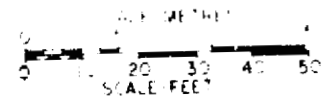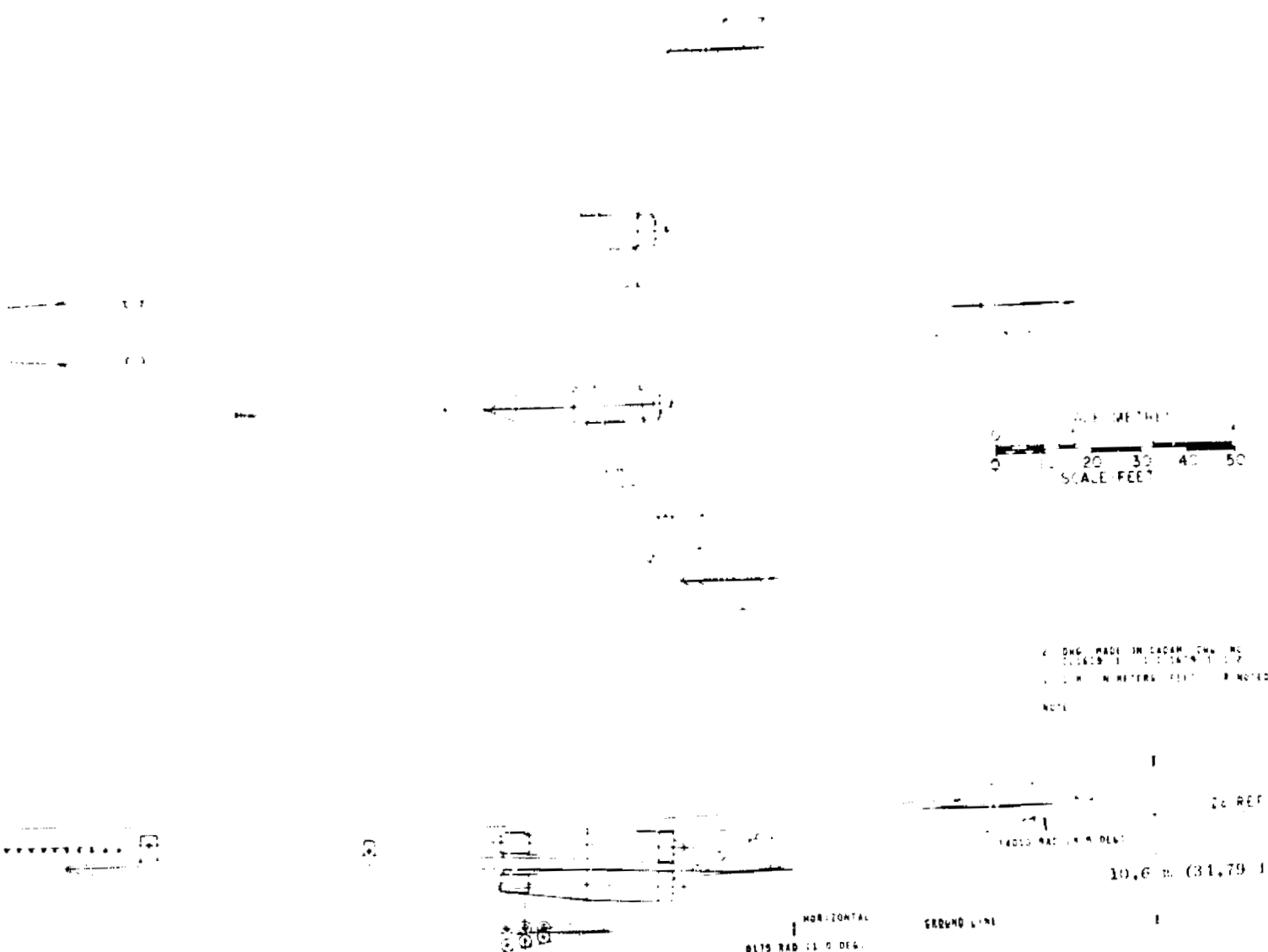
—— 6.35 m (20.85 ft)

33.97 m (111.85 ft)

37.757 m (123.87 ft)

Figure 92. General Arrangement, Lockheed S

ALT. METERS

0   20   30   40   50
SCALE FEET

NOTE

Z REF PLANE

10.6 m (31.79 ft)

HORIZONTAL

GROUND LINE

BLTS RAD (1.0 DEG)

38.618 m (126.67 ft)

89.51 m (293.67 ft)

rrangement, Lockheed SCAR Vehicle.

183
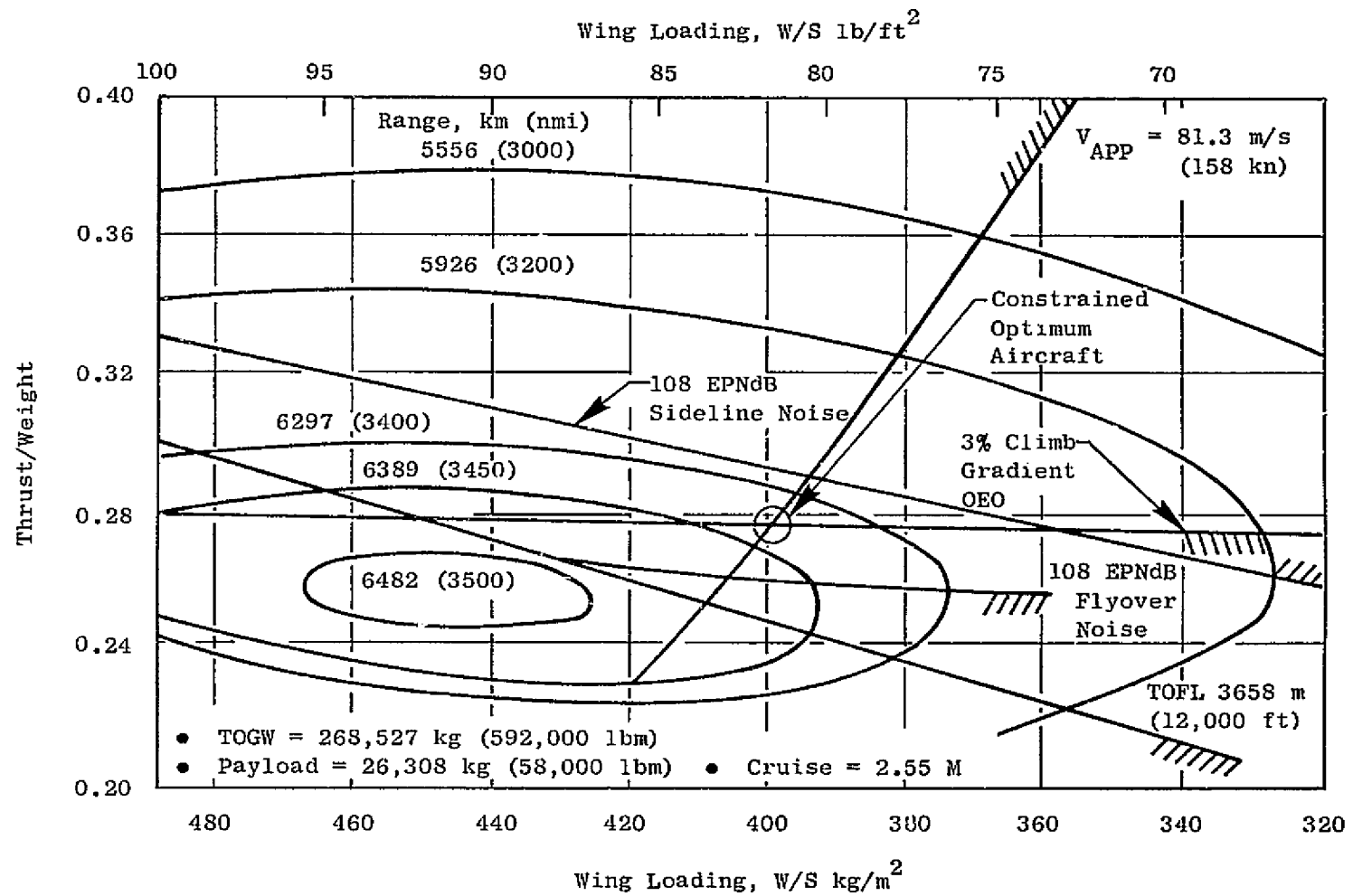
Figure 93. Aircraft Parametric Design Analysis (GE21/J11/B4 VCE).

wing loading as that which results in maximum range and still meets the airport performance constraints. The most critical constraints limiting the selection of the aircraft are (1) landing approach speed and (2) second segment climb gradient. The resulting constrained optimum aircraft configuration has a wing loading of 400 kg/m^2 (82 kg/ft^2) at takeoff and a thrust-to-weight ratio of 0.275 at lift-off. The wing area is 647 m^2 (7200 ft^2). The engine thrust size is 181,000 N (40,700 lb) and nominal airflow size is 288 kg/sec (633 lbm/sec).

Mission

Mission performance analyses were conducted using an IBM 370 digital computer program. The flight profile is shown in Figure 94. The basic part of the profile (block segment) consists of the initial warmup, takeoff, and climb to cruise altitude, cruise at design cruise Mach number, descent to 1524 m (5000 ft), and then loiter at that altitude for 5 minutes. The reserves' segment consists of an allowance of 5% of block fuel, a subsonic cruise to an alternate airport of 482 km (260 nmi) distance, and holding there for 30 minutes. Range in each case is the total distance credited during each block segment. Warmup consists of 10 minutes at partial power with a total engine thrust corresponding to 5% of aircraft gross mass, while takeoff and climb to 1524 m (5000 ft) are comprised of a one-minute allowance plus time required to climb to 1524 m (5000 ft), both at maximum dry takeoff power. Climb to supersonic cruise altitude follows a specified speed schedule which is optimum within the placard limitations of the aircraft (see Figure 95). The five-minute hold at the end of the block segment allows for some holding maneuvers prior to landing, plus descent to touchdown.

Engine

The engine selected for the propulsion system integration study is the General Electric GE21/J11B4, a Mach 2.55 double-bypass, augmented variable cycle engine (VCE). The engine is based upon material and component performance technology projected for the 1985 time period. It is equipped with a single-stage, moderate temperature-rise augmentor. In order to minimize noise, the engine is operated at dry power during takeoff. The augmentor is utilized only during the acceleration and climb segments of the mission. Maximum augmentor temperature is 1293° C (2360° F).

The nozzle is comprised of a convergent-divergent plug nozzle with a fixed primary nozzle and variable fan nozzle. The cylindrical outer shroud translates axially to provide nozzle area control. Thrust reverser cascades are incorporated in the nozzle shroud. During takeoff a portion of the lower energy fan air is ducted to the inner annular plug to provide a nozzle configuration capable of taking advantage of annular noise suppression.

186
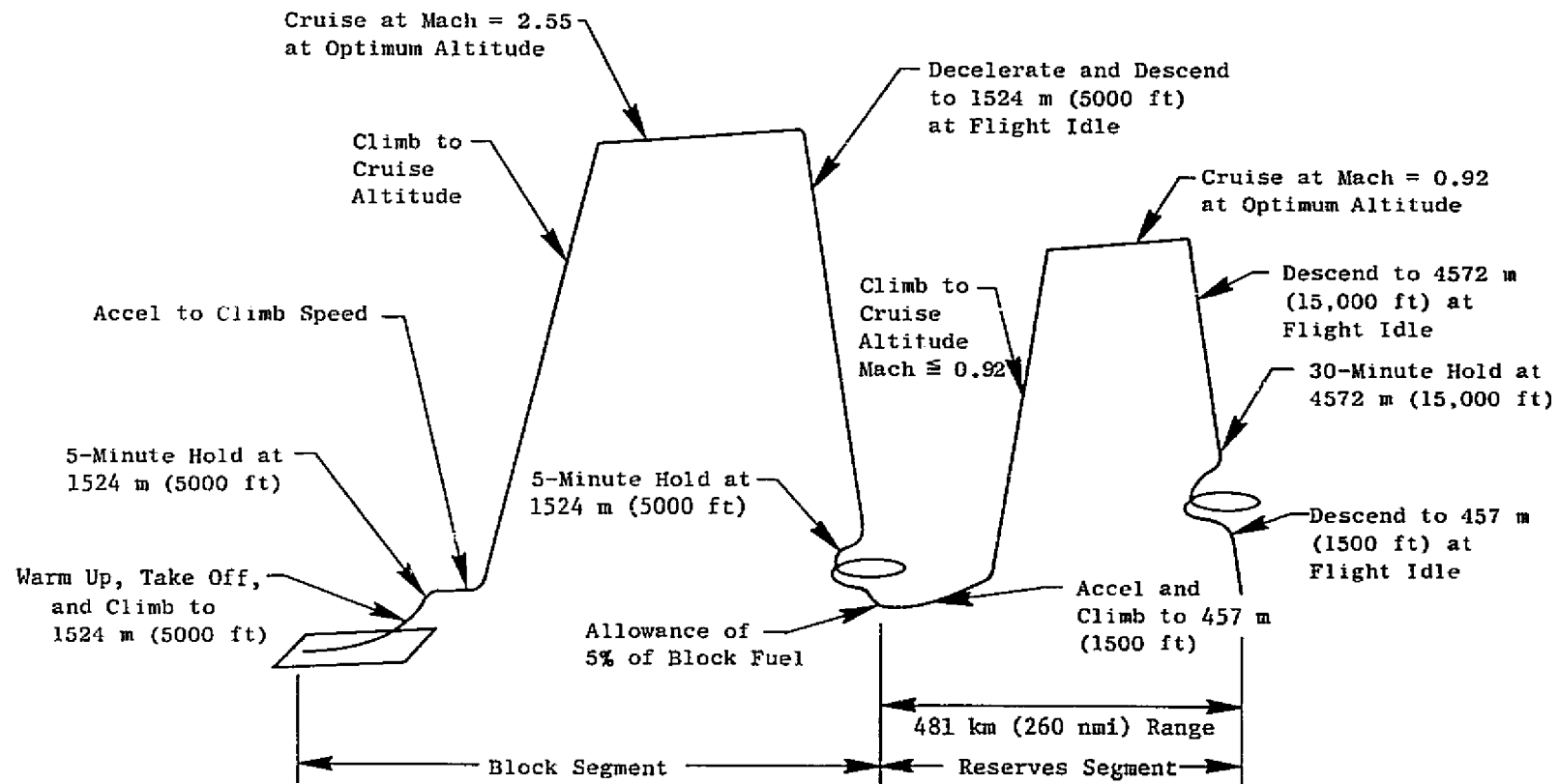
Figure 94. Mission Profile.
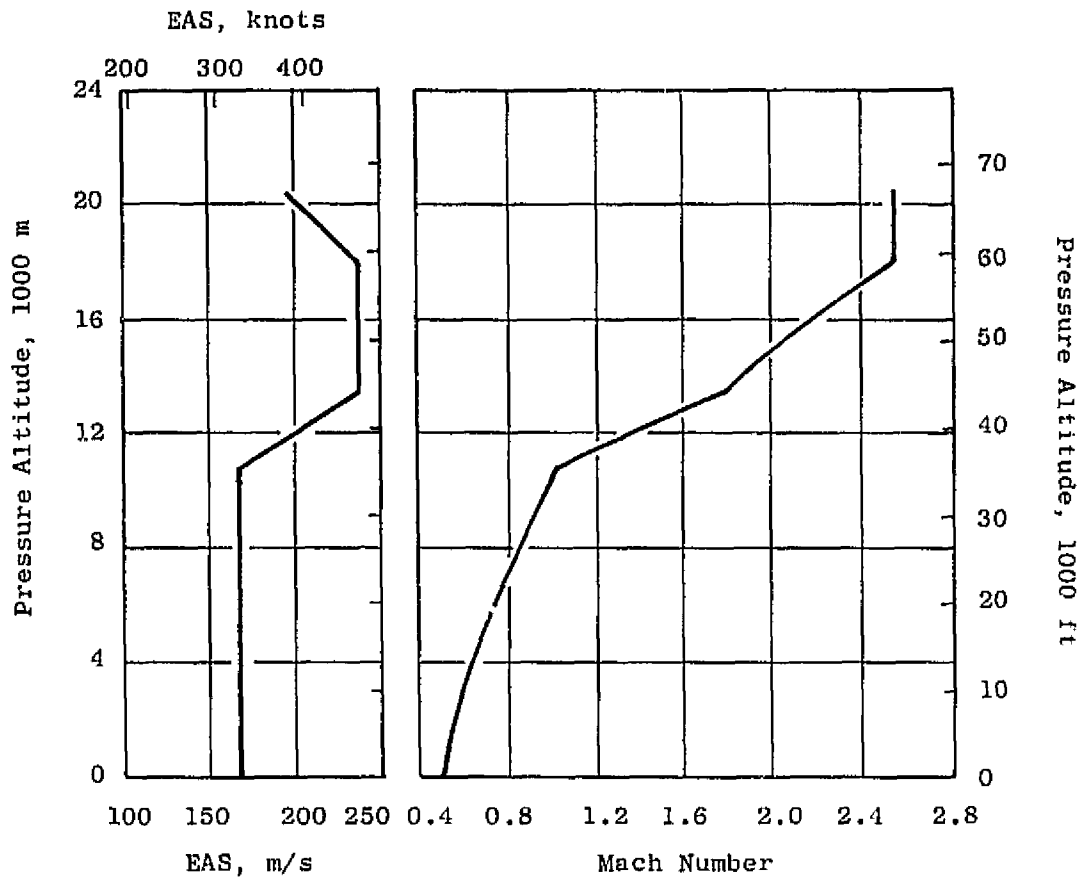
Figure 95. Climb-Speed Schedule.

Engine Size Selection

The GE21/J11B4 engine was sized to produce 181,000 N (40,700 lb) thrust at the sea level, Mach = 0.3, ISA +15° C (+27° F) lift-off condition. This thrust size is consistent with a 287 kg/sec (633 lbm/sec) sea level static airflow. The selected airflow size is near optimum in terms of payload/range performance. The selected airflow size also meets the Lockheed requirements of 3658 m (12,000 ft) takeoff field length, 81.3 m/s (158 knots) approach speed, and traded FAR 36 noise levels.

Nacelle Location

The results of a previous engine nacelle location study have shown that an over/under nacelle arrangement is an attractive alternative to a four-engine under-wing arrangement. The following potential advantages of the over/under configuration have been identified:

1. Jet noise shielding, which allows engine size to be optimized for a slight range advantage.

2. High-lift enhancement as a result of increased flap span.

3. Inlet unstart isolation provided by wing shielding.

4. Weight reduction, which results from a more efficient engine support structure.

5. Reduced vertical tail size due to movement inboard of the critical engine-out moment arm.

This nacelle general configuration is given in Figure 96.

Nacelle Designs

During the engine/airframe integration study the basic shape, location, and drag characteristics of a number of nacelle concepts were defined and evaluated using the Lockheed SCAR arrow wing over/under nacelle aircraft arrangement.

This study included consideration of both the axisymmetric and the two-dimensional inlet configurations. In order to evaluate the impact of accessories on the nacelle shape and performance, nacelle concepts were developed with and without accessories. The four nacelle configurations evaluated in the integration study are listed below:
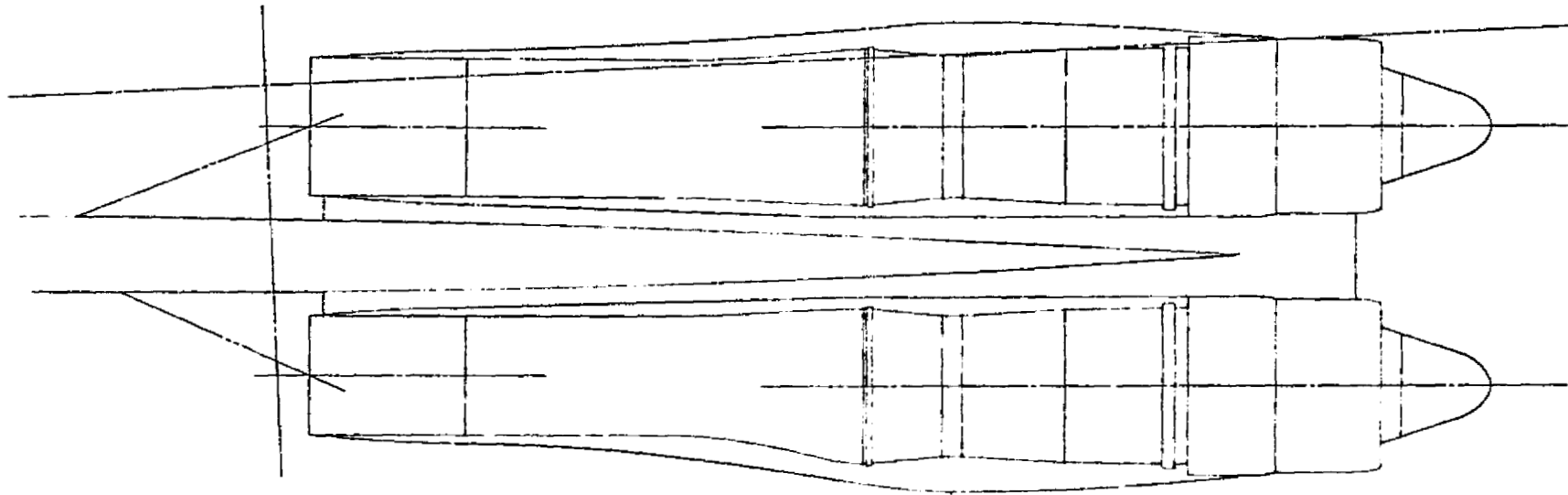
Figure 96. Nacelle Configuration, SCAR Two-Dimensional Inlet.

CL 1609-2	Axisymmetric	No Accessory Impact
CL 1609-3D	2-D Inlet	No Accessory Impact
CL 1609-4A	Axisymmetric Inlet	Accessories within Nacelle
CL 1609-5A	2-D Inlet	Accessories within Nacelle

The aerodynamic nacelle drag, mass properties, acoustic characteristics, and aircraft mission performance of these four nacelle concepts were evaluated so as to select the optimum nacelle configuration for the GE21/J11B4 engine. Results are presented in Figure 97 and Table 28.

The advantage in range of the axisymmetric inlet was lost when accessories were integrated in the nacelle. This occurred because the nacelle drag advantages of the axisymmetric inlet were substantially reduced when accessories impact:d the nacelle contours. The range penalty for integrating accessories in the nacelle was 28 km (15 nmi) with the 2-D inlet and 104 km (56 nmi) for the axisymmetric inle...

In summary, a relatively minor range difference was shown between the axisymmetric and 2-D inlet configurations. Thus, the 2-D inlet was selected primarily because of self-starting capability of the low contraction ratio inlet design.

At the completion of the evaluation, the two-dimensional inlet concept was selected for further propulsion installation design study. Since the range differences between the different configurations are relatively minor, the two-dimensional inlet remains the preferred inlet type for the GE21/J11B4 engine installation.

Inlet Configuration (Two-Dimensional Design)

The selected two-dimensional inlet configuration with the General Electric GE21/J11B4 engine is shown in Figures 98 and 99. The inlet is composed of a supersonic and subsonic diffuser divided into two isolated ducts by a variable geometry centerbody. The centerbody incorporates a simple operating linkage that provides good supersonic diffuser contours for off-design Mach numbers and variable duct areas for the complete range of flight conditions. The subsonic diffuser makes a smooth transition from a rectangular cross section at the throat to a circular cross section at the engine face.

Auxiliary cowl doors are incorporated to augment the inlet pressure recovery during takeoff. The large inward-opening doors are located on each side of the inlet and have a curved lip section along the ...t edge of the
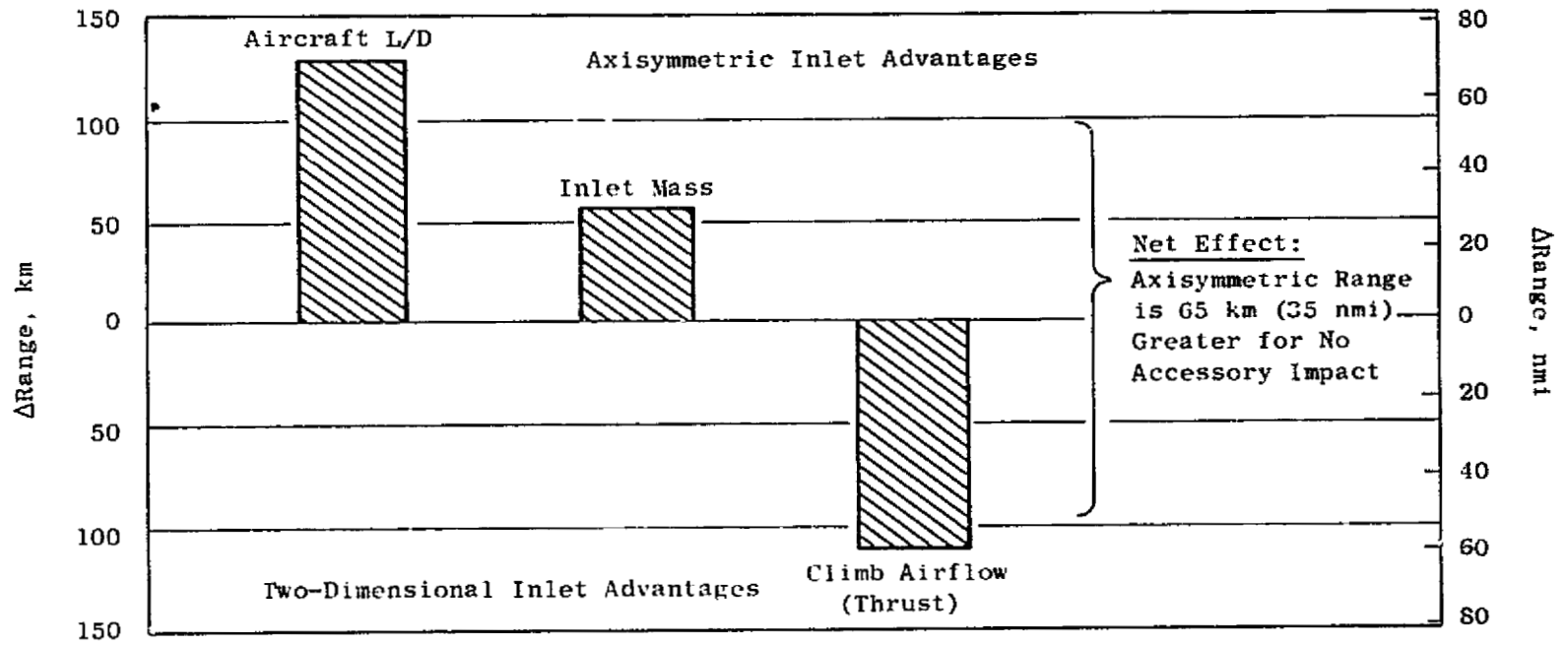
Figure 97. Factors Affecting Range Differences.

Table 28. Mission Performance Comparison.

TOGW = 267,527 kg (592,000 lbm)

	CL 1609-2 Axisymmetric No Impact		CL 1609-3D 2-D No Access Impact		CL 1609-4A Axisymmetric Nacelle Access		CL 1609-5A 2-D Nacelle Access	
Zero Fuel Mass kg (lbm)	140,902	(310,636	141,520	(311,999)	140,948	(310,737)	141,566	(312,100)
Cruise Mach = 2.55								
Avg. L/D	8.28		8.09		8.22		8.08	
Avg. sfc kg/hr/daN (lbm/hr/lb)	1.635	(1.603)	1.636	(1.604)	1.636	(1.604)	1.637	(1.605)
Avg. S.R. km/kg (nmi/lbm)	0.0743	(0.0182)	0.0727	(0.0178)	0.0739	(0.0181)	0.0727	(0.0178)
Fuel kg (lbm)	62,861	(138,585)	64,447	(142,082)	61,324	(135,197)	64,080	(141,272)
Climb Mach = 1.2, h = 11,491 m (37,700 ft								
Thrust N (lb)	309,329	(69,540)	404,441	(90,922)	309,312	(69,536)	404,339	(90,899)
Drag N (lb)	228,172	(51,295)	241,881	(54,377)	235,222	(52,880)	246,391	(55,391)
sfc kg/hr/daN (lbm/hr/lb)	1.586	(1.555)	1.452	(1.424)	1.586	(1.555)	1.452	(1.424)
Total Climb Fuel kg (lbm)	34,004	(74,967)	31,839	(70,194)	35,350	(77,934)	32,128	(70,830)
Hold at 4572 m (15,000 ft)								
Avg. L/D	12.83		12.76		12.81		12.74	
Avg. sfc kg/hr/daN (lbm/hr/lb)	1.170	(1.147)	1.165	(1.142)	1.169	(1.146)	1.163	(1.141)
Avg. Fuel Flow kg/hr (lbm/hr)	12,824	(28,272)	12,895	(28,428)	12,843	(28,314)	12,908	(28,458)
WUTO + Subsonic Fuel kg (lbm)	10,559	(23,278)	10,629	(23,432)	10,679	(23,543)	10,629	(23,434)
Reserve Fuel kg (lbm)	20,200	(44,534)	20,140	(44,402)	20,224	(44,586)	20,159	(44,443)
Range Difference km (nmi)	Base	(Base)	-65	(-35)	-104	(-56)	-93	(-50)

0.0174 Rad (1.0°)

Y = 5.50 m (216.628 in.)

0.0218 Rad (1.25°)

Triple-Unit Fuel Pump

Alternator

ECS Compressor

Y = 5.50 m (

Y = 5.50 m (216.628 in.)

Full Authority Digital Electronic Control (FADEC)

PTO Shaft

Heat Exchanger

Hydraulic Pump

Oil Lube and Scavenge Pump

X = 50 m (2000 in.)

SECTION A-A

Oil Tank

GE21/J11B4 Engine

SECTION A-A

SCALE 1:15   Y = 5.50 m (216.628 in.)

Plane

Oil Lube and Scavenge Pump

SECTION C-C
SCALE 1:15

SECTION B-B
(INLET UP)

Figure 98.   Engine Installation, GE21/J11B4 ar

Fuel Pump

Y = 5.50 m (216.636 in.)

Y = 5.50 m (216.636 in.)

Y = 5.50 m (216.636 in.)

Y = 5.50 m (216.636

essor

draulic Pump

SCALE-METRES

SCALE-FEET

SECTION C-C
SCALE 1/10
(FRONT ENGINE MOUNTS)

SECTION D-D
SCALE 1/10
(ENGINE ACCESSORIES)

PRELIMINARY

SECTION E-E
SCALE 1/10
(REAR ENGINE MOUNTS)

SECT ON

:ion, GE21/J11B4 and Two-Dimensional Inlet.

195

auxiliary inlet openings. These doors are located approximately one-duct diameter upstream of the engine face for mixing of the main inlet and auxiliary inlet airflows. The auxiliary doors remain open during takeoff and low-speed flight.

Dynamically controlled bypass doors and valves, used for positioning the inlet terminal shock wave and for minimizing drag at lower speeds, are shown in Sections A-A and View K-K of Figure 99. These overboard bypass doors are also to be used for engine-out operation. The firewall valves are for ventilation airflow into the engine compartment. The ventilation airflow is exhausted through louvers at the aft end of the engine compartment. The bypass air exhausts through six doors, two on each side shown in Section A-A and two in the lower shell structure shown in View K-K of Figure 99. The lower bypass doors are fed by air from the centerbody aft compartment.

The inlet bleed system is used to increase the pressure recovery and to extend the range of stable inlet flow. The bleed is taken in the region of internal shock waves in the supersonic diffuser. The cowl bleed exhausts through fixed nozzles on the cowl and spring-loaded cowl doors. Centerbody, top-wall, and bottom-wall bleed exhausts through fixed forward louvers and controlled doors, both on the bottom plate of the inlet. At supersonic cruise, some of the centerbody bleed passes into the cowl structure and through the firewall valves to the engine compartment.

Inlet Selection (Two-Dimensional Design)

A self-starting, two-dimensional inlet, having 20% internal contraction and an axisymmetric inlet having 76% internal contraction, were selected as the most appropriate inlet designs for the General Electric GE21/J11B4 engine when installed on the Lockheed-California CL 1609 supersonic cruise aircraft. These inlet design selections were based upon parametric analyses at supersonic cruise, transonic, and takeoff conditions as reported in the inlet design study conducted for GE (see Section 4.5.1).

The inlet capture area, which was computed at the supersonic cruise point, is a function of engine corrected airflow and inlet local Mach number. The over-wing and under-wing inlets were sized for the cruise engine corrected airflow and the individual inlet local Mach numbers. This results in the under-wing inlet being smaller than the over-the-wing inlet.

The two-dimensional over-wing and under-wing inlets have substantial inlet commonality. This is accomplished by having identical plan view contours for both inlets and providing the lower required capture area of the under-wing inlet with a smaller height as shown in the two side views of Figure 100. The centerbody is shown in the supersonic cruise and the fully contracted positions in Figure 100. The over-wing and under-wing inlet capture areas were determined using the supersonic cruise engine corrected airflow, the inlet local Mach numbers, assumed critical mass flow ratios, and assumed bleed mass flow rates.

197

AUXILIARY INLET OPEN
FOR TAKE OFF

BYPASS DOOR CLOSED

BLE

BLEED HOLE PATTERN

FIREWALL VALVE CLOSED

FORWARD TRANSLATION JOINT

SECOND RAMP

FIRST RAMP

FIREWALL BULKHEAD

AUXILIARY INLET CLOSED

VORTEX GENERATORS

FIREWALL VALVE OPEN

BYPASS DOOR SHOWN AT MAXIMUM
OPENING DURING DESCENT

SECTION B-B
SHOWING CENTERBODY CONTRACTED

PRESSURE

VIEW C-C
PLAN VIEW OF DIVERTER CONTOUR

BLEED EXIT LOUVERS
REMOVABLE FOR ACCESS

BLEED EXIT LOU
AT SHUT
OPEN AT LOW SU
SONIC SPEEDS

Figure 99. Structural Details, Unde

BLEED EXIT DOORS

AFT TRANSLATION JOINT

BYPASS DOOR ACTUATORS

BLEED HOLE PATTERN

STANCHION (4 PLACES)

CENTERBODY ACTUATORS

SECOND RAMP

FIRST RAMP

CENTERBODY HINGE

FIREWALL VALVES

SIDE LIP

SIDE BYPASS DOOR AT CRUISE POSITION

PRESSURE PROBES

BLEED EXIT NOZZLES

AUXILIARY INLET CLOSED

CENTERBODY PANEL
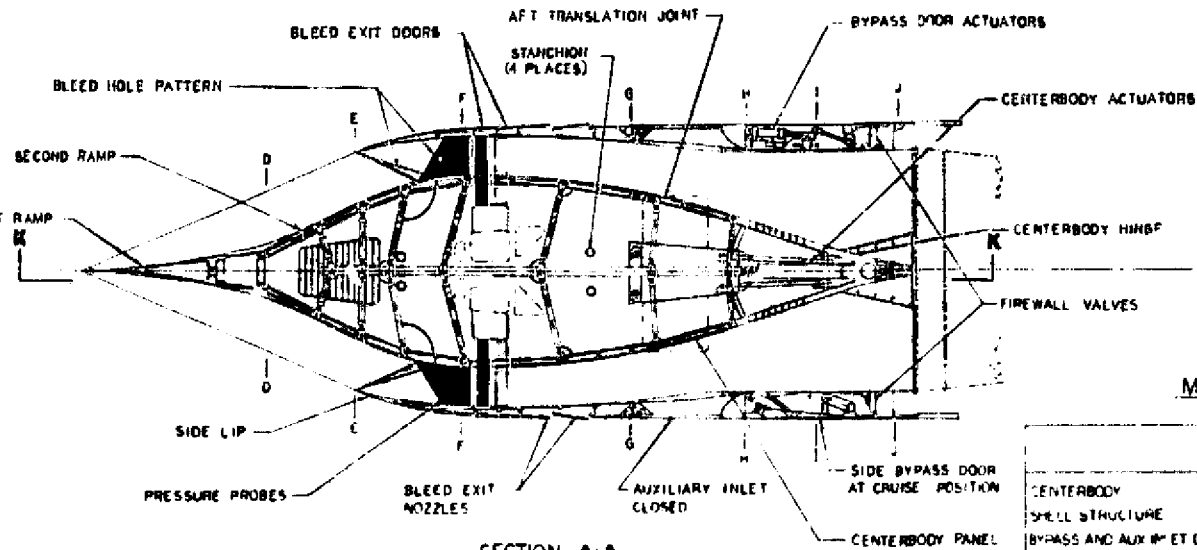
SECTION A-A
SHOWING CENTERBODY EXPANDED
CUT ADJUSTED THRU BYPASS DOORS ON LEFT SIDE & ACTUATOR OPPOSITE

MATERIALS

	GRAPHITE POLYIMIDE (Gr/NR-15082)	TITANIUM ALLOY (Ti 6Al-4V)
CENTERBODY	42%	58%
SHELL STRUCTURE	41%	59%
BYPASS AND AUX INLET DOORS	81%	19%
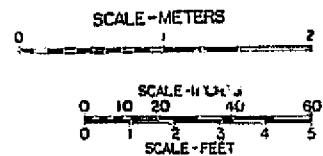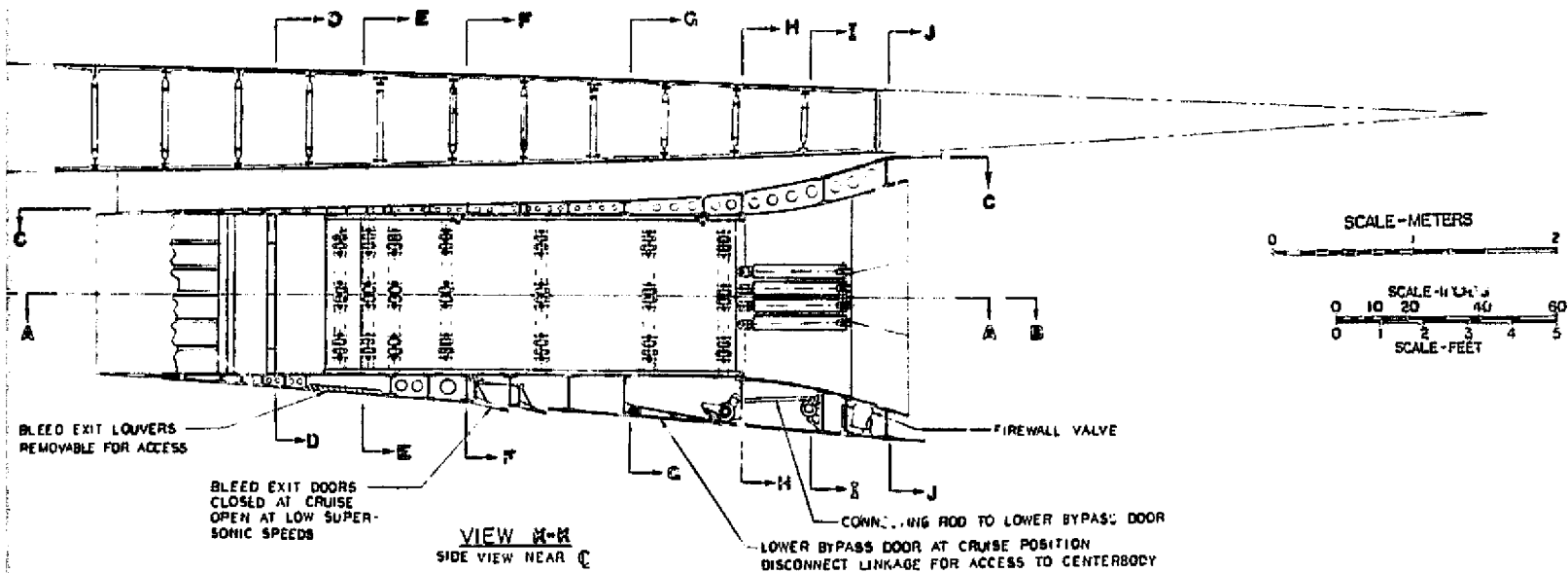
BLEED EXIT LOUVERS REMOVABLE FOR ACCESS

FIREWALL VALVE

BLEED EXIT DOORS CLOSED AT CRUISE OPEN AT LOW SUPERSONIC SPEEDS

VIEW K-K
SIDE VIEW NEAR ℄

CONNECTING ROD TO LOWER BYPASS DOOR

LOWER BYPASS DOOR AT CRUISE POSITION
DISCONNECT LINKAGE FOR ACCESS TO CENTERBODY

SCALE-METERS
0   1   2

SCALE-INCHES
0 10 20   40   60

SCALE-FEET
0 1 2 3 4 5

Structural Details, Under-Wing Inlet.

199
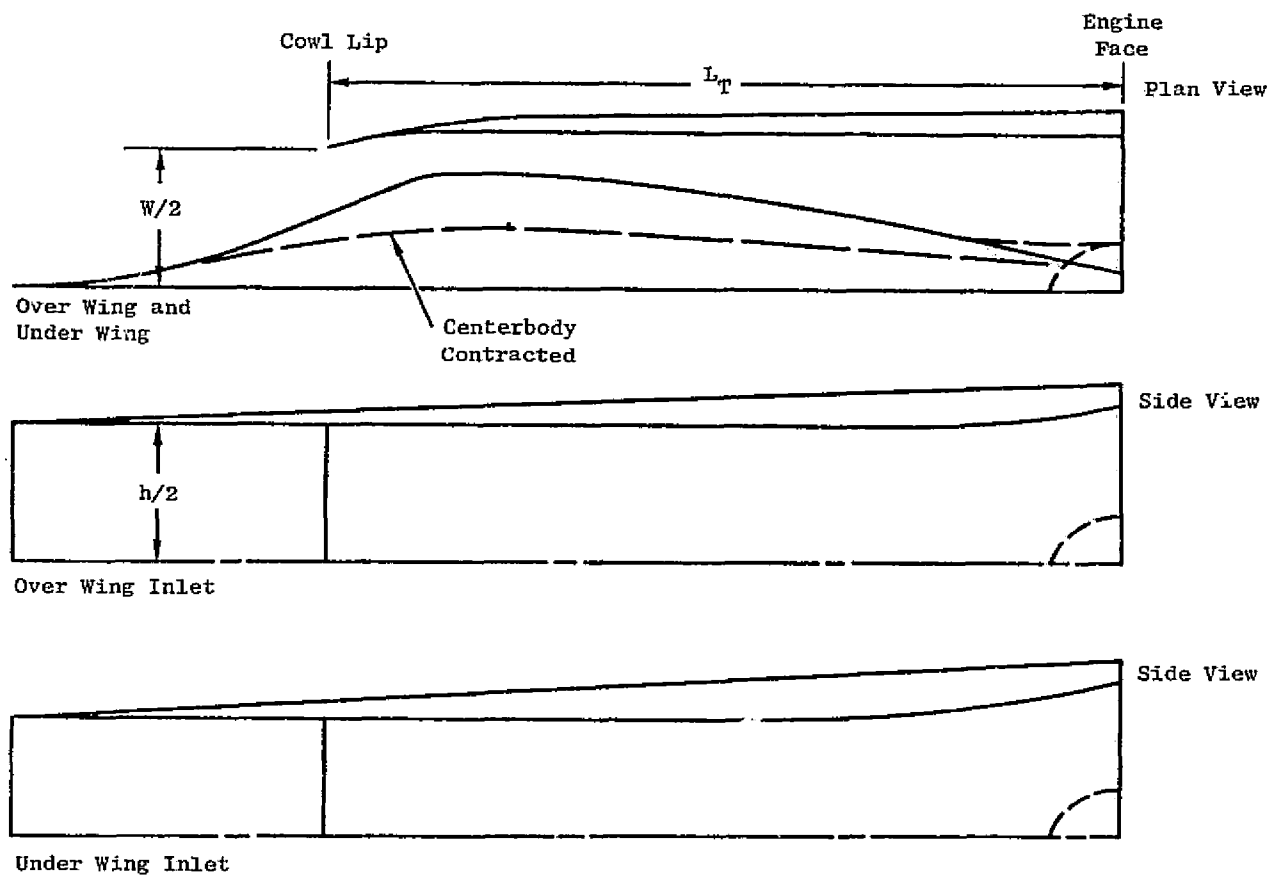
Inlet	Capture Area m^2 (ft^2)	W/2 m (ft)	Aspect Ratio	L_T/(W/2)
Over Wing	2.110 (22.719)	0.726 (2.383)	2.00	5.841
Under Wing	1.873 (20.165)	0.726 (2.383)	1.746	5.841

GE21/J11/B4 Engines
Fn = 181 kN (40,700 lb)
Sea Level, M = 0.3,
Std +15° C (27° F)

Figure 100. Typical Two-Dimensional Inlet Contours.

Inlet Performance and Airflow Matching

The inlet performance and inlet engine airflow matching for the selected two-dimensional and axisymmetric inlets are determined as a function of flight conditions. The critical inlet pressure recovery and mass flow ratio as functions of inlet local Mach numbers are given in Figures 101 and 102 for the selected two-dimensional and axisymmetric inlets, respectively. Because of common inlet aerodynamics, these results are applicable to both over-wing and under-wing inlets. The pressure recovery and mass flow ratio variation with local Mach number are based on the previous Lockheed L-2000 inlet study results for the two-dimensional inlet and on NASA inlet tests for the axisymmetric inlet. Using the two-dimensional and axisymmetric inlet performance shown in Figures 101 and 102, the inlet corrected airflow schedules of Figure 103 were obtained. These inlet corrected airflows match the corresponding GE21/J11 engine corrected airflow schedules used in the performance analysis. The over-wing and under-wing engine-corrected airflows are different (except for cruise) in order to match the corresponding inlets and are accommodated with identical engine hardware utilizing different control software. The two-dimensional inlet can supply more airflow than the axisymmetric inlet at off-design speeds due to its ability to provide larger off-design throat areas. This results in significantly higher installed thrust levels for the two-dimensional inlet compared to those of the axisymmetric inlet.

Nacelle Structural Concept and Mounting

The nacelles and adjacent wing structure are proposed to be designed to provide integrated load paths and to allow for structural interaction of loads and deflections. The inlet shell structure is attached to the wing through an interchangeable joint. The engine is supported from a beam structure cantilevered aft of the wing box structure and the inlet through a fail-safe mount system which is designed to isolate the engine from loads induced by structural deflections. The nacelle concept development includes consideration for (1) static strength at overspeed conditions, (2) fail-safe requirements for both structure and mechanism, and (3) design stress levels selected to provide the required fatigue life. The nacelle structural concept incorporates provisions for doors; however, a detail design of doors, links, and mechanisms was not included. For nacelle design these details are important and will require consideration of items incorporating wear resistant and/or replaceable elements to assure life and maintainability appropriate for airline service.

The GE21/J11B4 engine is attached to the airframe structure by a four-point mounting system as shown in Figure 104. Thrust fittings and a vertical link are attached to identical engine mounting bosses at the forward ring. Two radial links are attached to the aft-engine mount ring. Engine loads and mounts are reacted as follows:

202
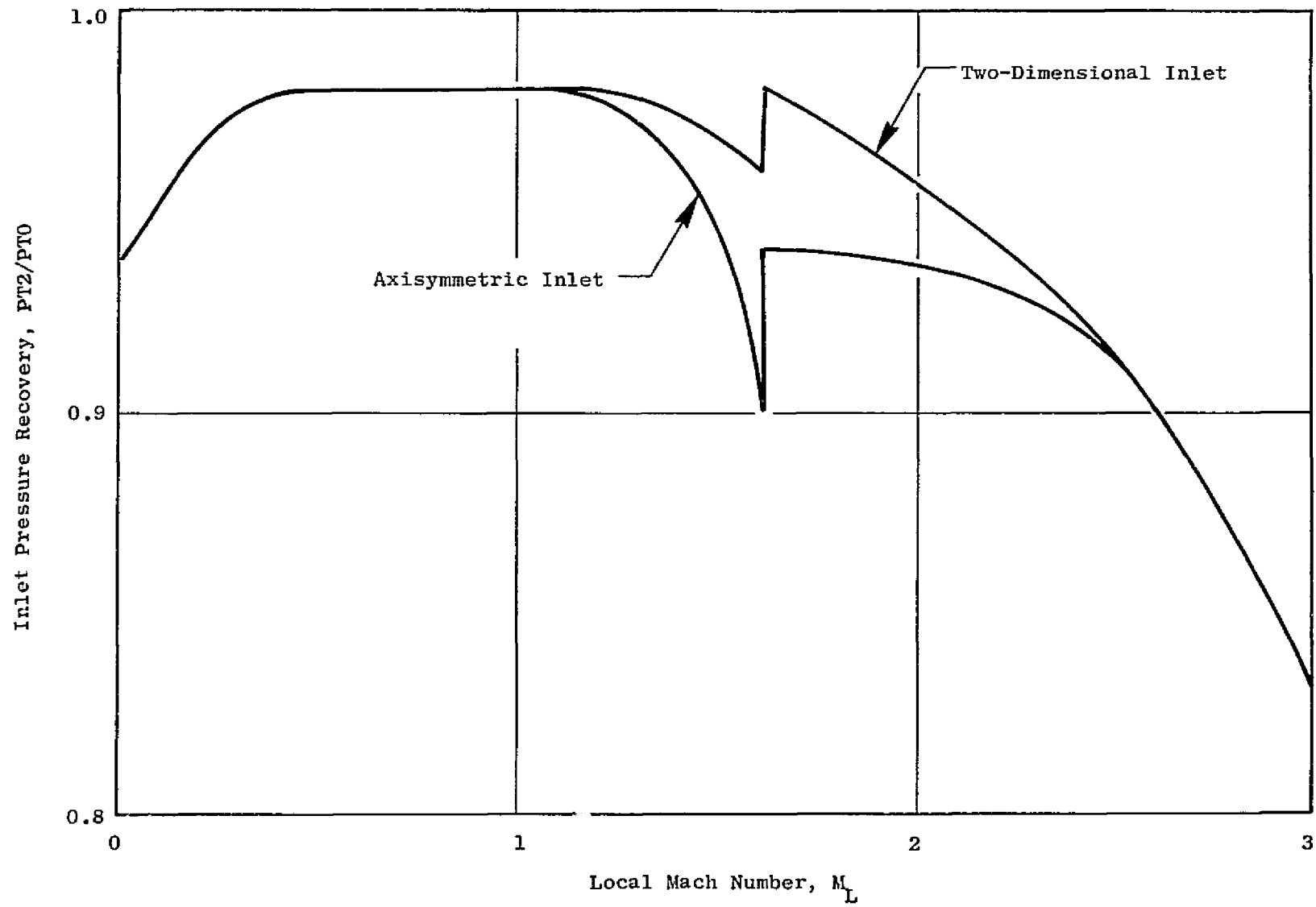
Figure 101. Critical Inlet Pressure Recovery.
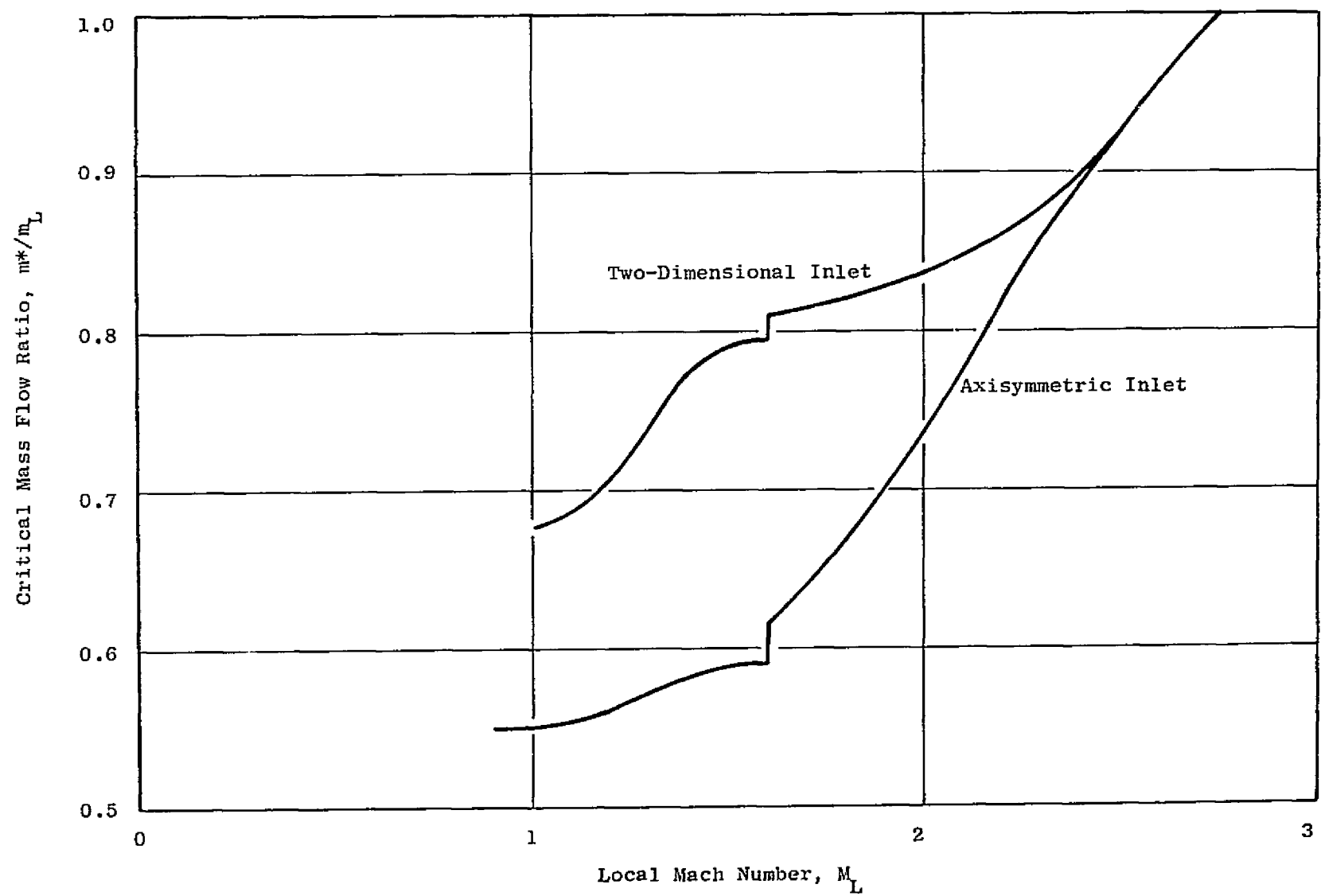
Figure 102. Critical Mass-Flow Ratio.
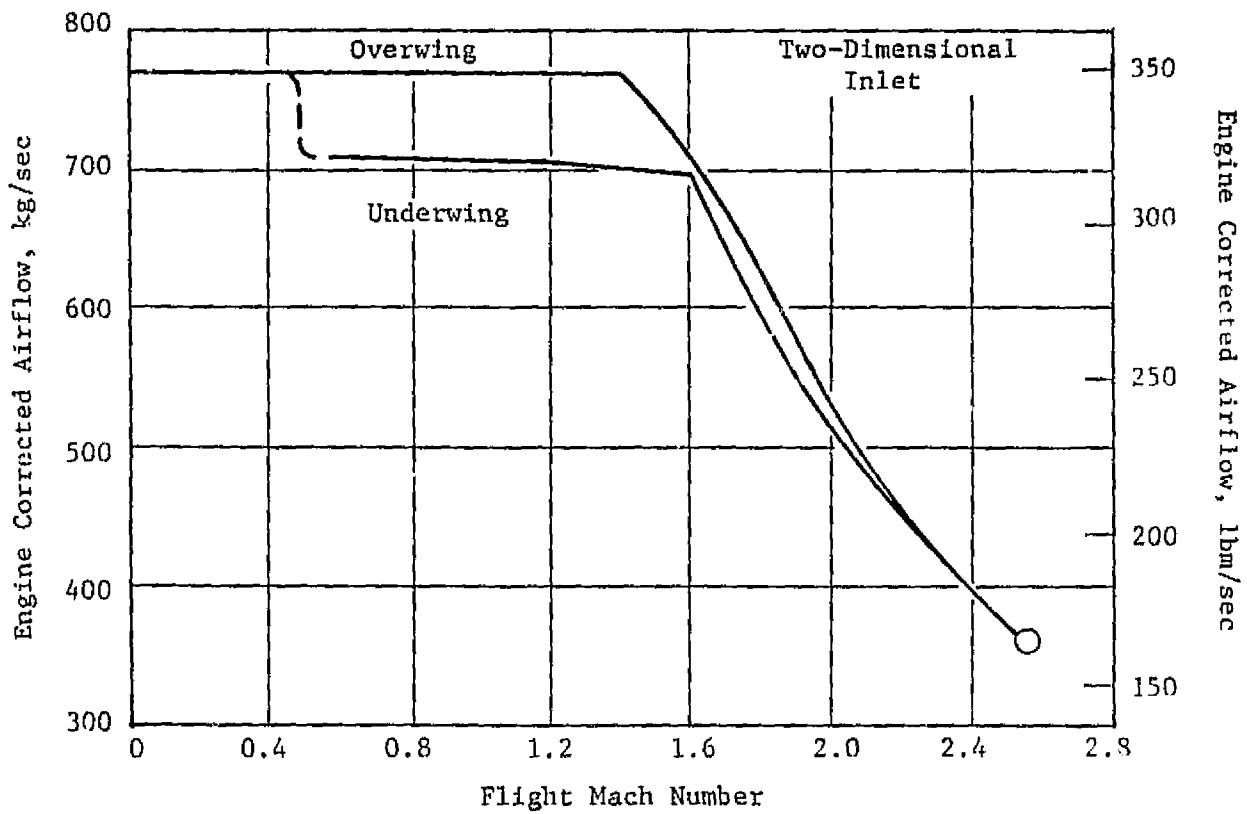
Figure 103. Engine Airflow with Two-Dimensional Inlets, GE21/J11B4 VCE.

Upper Engine

Rear Mount Link

Inbd

Fwd

Lower Engine

Forward Thrust, Side and
Vertical Load

Forward Thrust and Vertical Load
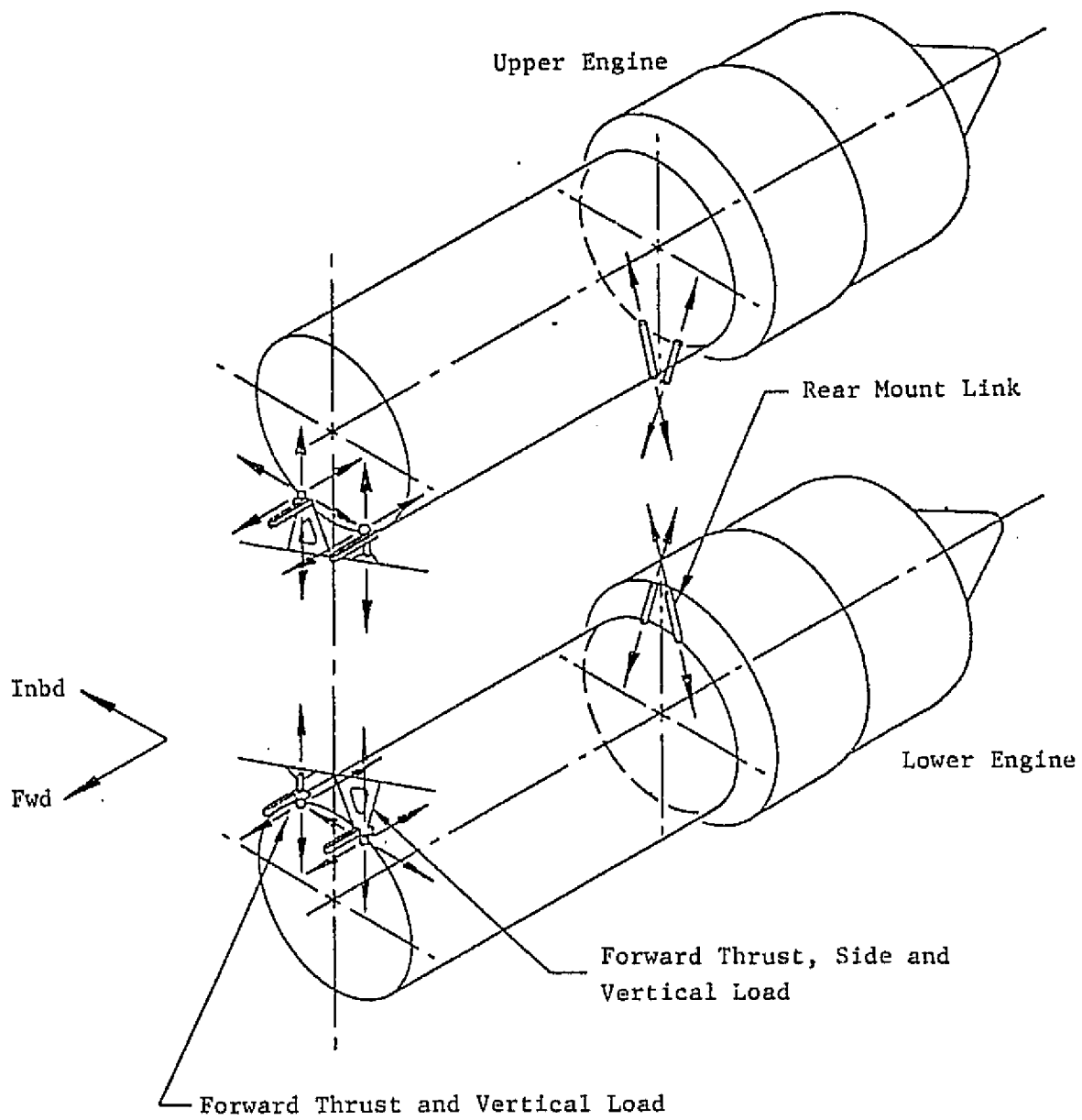
Figure 104. Engine Mount Load Diagram.

Drag and thrust, forward thrust fittings

Side load, yawing moment, forward inboard upper and forward outboard lower thrust fitting and aft links

Vertical load, pitching moment, all four mount points

Rolling moment, forward thrust fitting and link

The cowling is essentially a pressurized cylinder which encloses the engine and connects the inlet to the engine nozzle as shown in Figure 105. The engine cowling consists of four curved panels (per engine) that are approximately 3.7 m (144 in.) long (combined length). The forward cowl door is 2.16 m (85 in.) in length, with the aft cowl door being 1.42 m (56 in.).

Other Design Configurations

The GE21/J11B4 engine accessories are located between the wing and each engine as shown in Figure 99. All aircraft accessories (with the exception of the ECS system) are located in the aft section of the wing. One engine-driven aircraft accessory gearbox is located inboard of the inlets, the other outboard. The ECS system compressor, heat exchanger, and accompanying ducts are aft of the engine accessories.

The upper engine gearbox is located in the pylon below the engine as shown in Section G-G of Figure 99. The gearbox drives the engine high-pressure hydraulic pump, ECS compressor, engine alternator, triple-unit fuel pump, PTO shaft, and the oil lube and scavenge pump. The lower engine accessory gearbox is in the pylon above the engine, as shown in Section A-A of Figure 99. The same gearbox is used on both engines by designing the lubrication system to permit the gearbox to be turned 3.14 rad (180°) from one engine to the other. The oil lube pump pad is covered on the lower engine accessory gearbox. The oil lube and scavenge pump are located below the engine on a separate engine driven gearbox.

Analysis of engine control systems lead to the conclusion that full-authority electronic control systems and advanced accessories should be developed.

Fire protection provisions are incorporated for the prevention, control, and containment of fires and the thermal protection of structure. Engine compartment cooling and ventilation are necessary to reduce the relatively high-temperature environment encountered in the nacelle of a supersonic cruise vehicle and to prevent the buildup of harmful vapors.

Engine maintainability features are incorporated in the nacelle design, considering access for on-board maintenance, engine removal, and ground handling.

FOLDOUT FRAME 1.
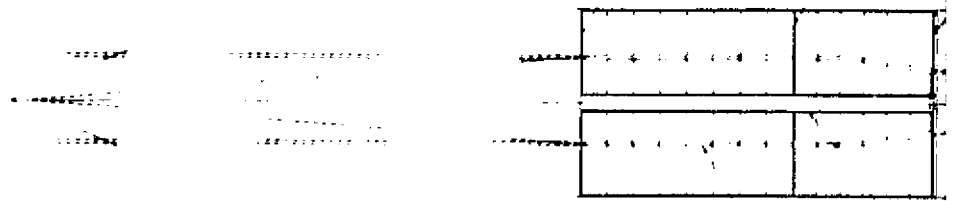
View A

X = 50.80 m (2000 in.)
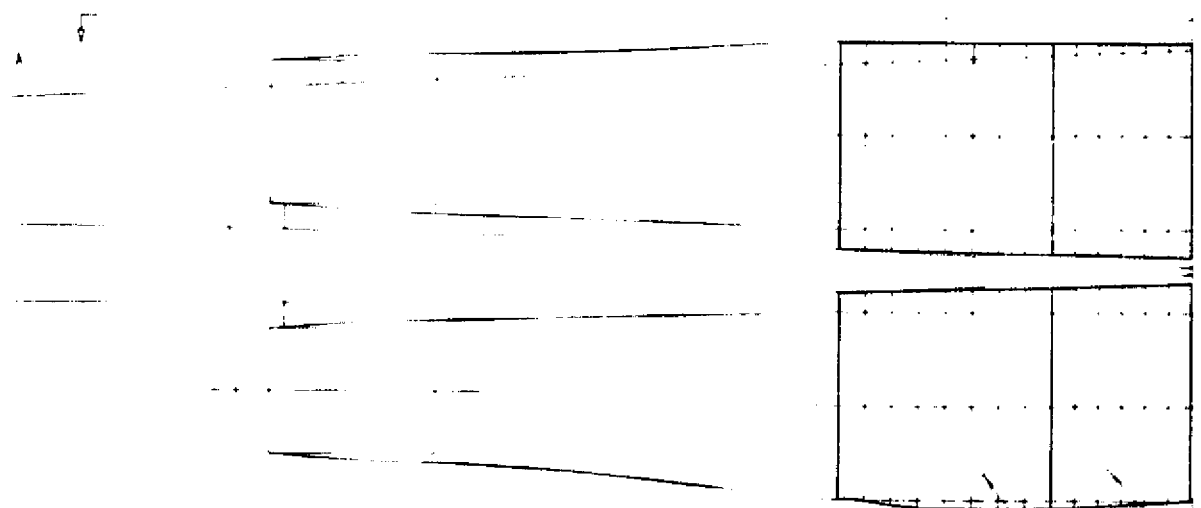
Figure 105. Nacelle Structural Arrange

SCALE-METRES

SCALE-FEET

$X = 5.30$ r $(216.628$ in.$)$

Structural Arrangement.

209
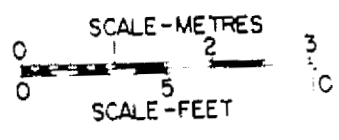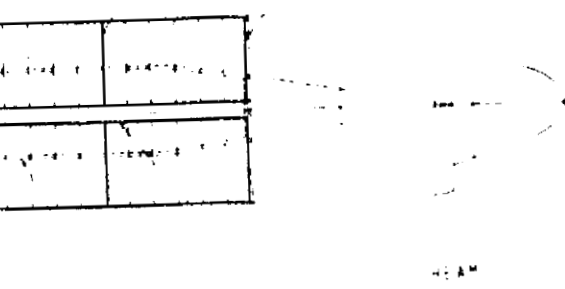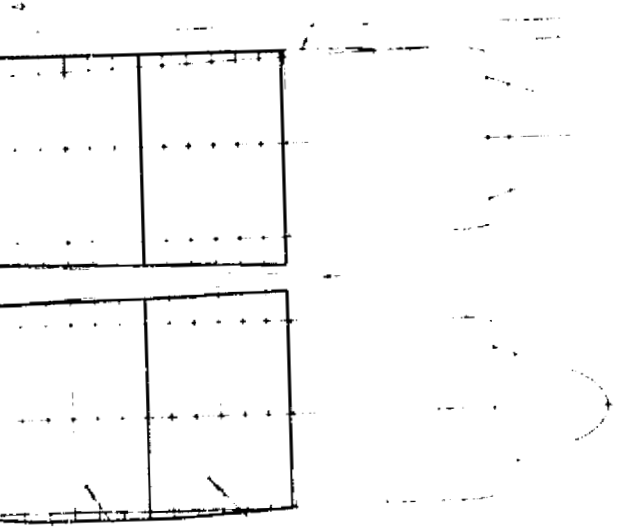
Installation Losses

The engine installation losses accounted for in the propulsion system analysis are grouped into two categories: internal losses and external losses. The internal losses, which have a direct effect upon engine cycle performance, include inlet pressure recovery, compressor bleed, accessory power extraction, and exhaust nozzle performance. The exhaust nozzle performance, including the nozzle boattail drag, was supplied by General Electric. The critical inlet pressure recovery and mass flow ratio for the two-dimensional and axisymmetric inlets are given in Figures 101, 102, and 103. The engine compressor bleed flow rate was 0.41 kg/sec (0.90 lbm/sec) and the assumed accessory power extraction was 135 kW (181 hp), both per engine.

The external losses, which are related to the nacelle location and aerodynamic shape of the inlet, include inlet spillage drag, inlet bleed drag, bypass drag, and cowl drag. The inlet spillage and bleed drags and the nozzle boattail drags are given in Figure 106 for the selected two-dimensional inlets. The inlet spillage drags were obtained from a Lockheed-developed inlet computer program. Because the variable cycle engine airflow matches the inlets by means of engine control software, no subcritical spillage or bypass penalties are included. The inlet cowl drag is accounted for in the airplane wave drag routine.

The inlet bleed mass flow ratios for both inlet types at supersonic cruise were obtained from previous correlations and are assumed linear with local Mach number between Mach 1.0, where the bleed mass flow ratio was assumed to be zero, and Mach 2.75, where the value was set equal to the assumed correlation value. At cruise, the upper inlet bleed mass flow ratio was 0.068 for the two-dimensional inlet and 0.083 for the axisymmetric inlet. The lower bleed mass flow ratio for the two-dimensional inlet is due to the lower wetted area of the supersonic diffuser (as a consequence of lower internal contraction) compared to that of the axisymmetric inlet. The inlet bleed drags were computed for sonic axial overboard discharge with estimated bleed recoveries.

Acoustic Analysis

An acoustic analysis was conducted to estimate the jet noise levels of the GE21/J11B4 engine installed in the Lockheed CL 1609-8 over/under nacelle arrangement. The engine jet noise was estimated for two different lift-off thrust sizes, as shown in Table 29. The first column of the table gives noise levels for a thrust size of 197,500 N (44,400 lb) at Mach = 0.3, and a flyover altitude of 549 m (1800 ft). The second column gives flight conditions and noise levels for the CL 1609-8 aircraft with the engines sized for lift-off T/W = 0.275. The approach noise was assumed to be 106.6 EPNdB.

Noise reductions for the annular effect and the over/under engine effect shown in the table are based on small model test data. Power cutback noise reductions are based on preliminary analyses. Consequently, additional studies are required to verify the reductions assumed.
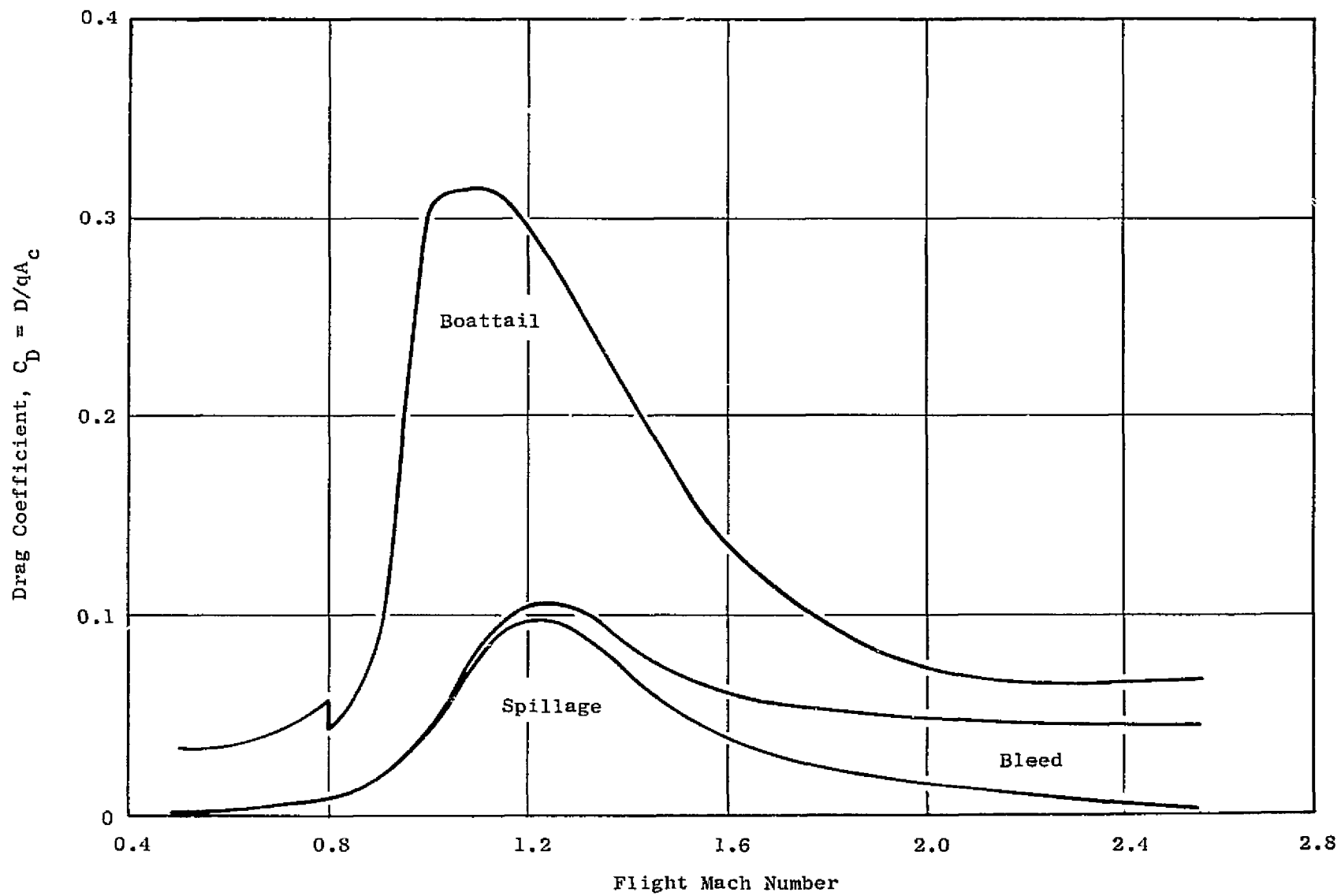
Figure 106.   Installation Drags, Two-Dimensional Inlet.

Table 29. Engine Jet Noise Analysis.

	Comparison Standard	Aircraft (GE21/J11B4)
Thrust, kN (lb)	197.5 (44,400)	181 (40,700)
Aircraft Mach Number	0.3	0.3
Flyover Altitude, m (ft)	549 (1800)	549 (1800)
Flyover Noise, EPNdB	121.3	121.3
Annular Effect, EPNdB	-8.3	-8.3
Over/Under Engine Effect, EPNdB	-3.0	-3.0
Power Cutback, EPNdB	-6.4	-6.4
Net Flyover Noise, EPNdB	104.1	103.6
Sideline Maximum Noise Position		
Altitude, m (ft)	381 (1250)	381 (1250)
Sideline Distance, m (ft)	649 (2128)	649 (2128)
Sideline Noise, EPNdB	116.2	115.9
Annular Effect, EPNdB	-8.3	-8.3
Net Sideline Noise, EPNdB	107.9	107.6
Net Approach Noise, EPNdB	106.6	106.6

Twin-jet noise tests show that noise radiated by simple, round nozzle jets to be directionally oriented. Noise in a plane passing through the jet axes is less than noise in a plane 1.57 rad (90°) to the jet axes plane. This phenomenon provides a method for reducing aircraft community noise. Figure 107 gives a comparison of noise for aircraft with four engines under the wing and for over/under engine arrangements. Although a potential reduction of up to 5 dB has been shown to exist by model tests, reductions of only 3 dB have been assumed in the CL 1609-8 noise analyses. Acoustic tests need to be performed with coaxial nozzles using inverse velocity profiles to verify that noise-shielding is a valid concept for reduction of community noise levels.

Technology Assessments

The GE21/J11B4 engine definition was based on materials and component performance levels projected for a 1985 development start. During this contract, the effect of not meeting assumed technology levels was investigated by General Electric and Lockheed. GE estimated the effects of technology level on various cycle parameters, engine performance, and weight. The changes in technology levels shown in Table 30 represent GE's estimates of the maximum uncertainty of the assumed technology for that time period. Lockheed took the GE engine performance and mass changes and utilized aircraft mission sensitivities to evaluate the effect upon aircraft range. The results of the study are summarized in Table 30.

As shown, the largest effect upon aircraft range results from the 0.01 reduction in exhaust nozzle thrust coefficient, 224 kn (121 nmi). The aircraft performance was also found to be sensitive to the amount of turbine cooling flow required, as indicated by the 111 km (60 nmi) range loss for a 2% increase in cooling airflow (defined as a percentage of core airflow). Technology assumptions for component efficiency are indicated to have a relatively minor effect upon aircraft performance.

Conclusions and Recommendations (Lockheed-California Co.)

Based upon the results of the engine/airframe integration study of the General Electric GE21/J11B4 engine, the following conclusions were reached and recommendations offered:

1. No major installation problems have been identified to date with the over/under installation of the GE21/J11B4 double-bypass variable cycle engine in the Lockheed CL 1609 aircraft. Continued study is desired to verify the overall merits of this concept relative to the more conventional under-wing installation.

214
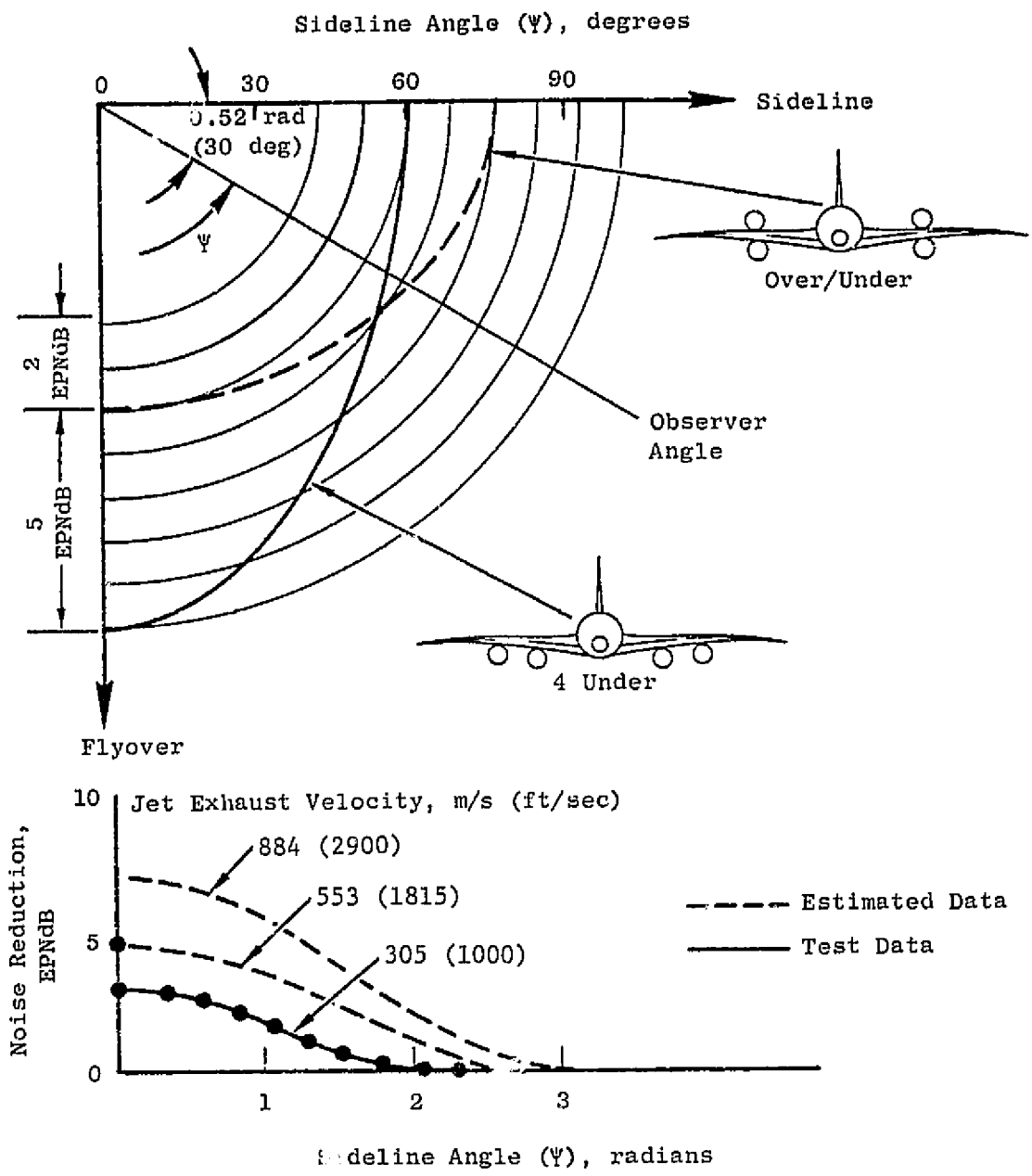
Figure 107. Comparison of Noise Levels Under the Wing Versus Over/Under Engine Arrangement.

Table 30. Effect of Engine Technology on Performance and Range.

Affected Item	Technology Delta	Engine Performance Effect Δsfc at Constant FN, %		Mission Range ΔR ~km (nmi)
		Supersonic Cruise	Subsonic Cruise	
1. Front Block Fan Efficiency	$-0.01\ \eta_{F1}$	+0.40	+0.38	-28 (15)
2. 2nd Block Fan Efficiency	$-0.01\ \eta_{F2}$	+0.20	+0.05	-11 (6)
3. HP Compressor Efficiency	$-0.01\ \eta_{HPC}$	+0.44	+0.25	-30 (16)
4. HP Turbine Efficiency	$-0.01\ \eta_{HPT}$	+0.50	+0.32	-33 (18)
5. LP Turbine Efficiency	$-0.01\ \eta_{LPT}$	+0.20	+0.29	-15 (8)
6. Turbine Cooling Flow	+2% W2	+1.70	+0.70	-111 (60)
7. Exhaust Nozzle Thrust Coefficient	$-0.01\ CF_G$	+3.28	-1.9	-224 (121)
8. Composite Front Fan vs. Titanium	$-0.005\ \eta_F$	+0.20	+0.19	-14 (7.5)
9. Composite Structures	1% Engine Mass	---	---	-19 (10.5)
10. VCE Concept: (Core to LPT Driven 3rd Stage)				
(a) Engine Weight	+5.9%	---	---	-115 (62)
(b) Cooling Flow	+1.4% W2	+1.22	+0.50	-72 (39)
(c) LP Turbine Efficiency	$-0.02\ \eta_{LPT}$	+0.44	+0.58	-33 (180
				-220 (119)
				(Item to Total)

2. The two-dimensional inlet appears to have several key advantages including increased airflow supply capability during climb and the self-starting feature. Nevertheless, it may be possible to develop an axisymmetric inlet design which provides better overall aircraft performance than the 2-D inlet. Thus, both types of inlet should remain under consideration.

3. In order to realize the benefits of the airflow flexibility of variable cycle engines, attention must be given to matching of inlet and engine airflow schedules for optimized installed performance along the flight path.

4. Continued design evaluation of the over/under engine arrangement is required, with emphasis upon selecting an accessory arrangement which represents the best possible trade between engine replacement, maintainability and performance requirements.

5. Integration of accessories on the engine has a minor influence upon aircraft mission performance, particularly with the 2-D inlet.

6. Additional effort is desirable to determine the effect of advanced accessories on the engine installation (the current study was conducted with 1970 GE4 engine technology accessory definitions).

7. Further cooperative study is recommended to establish a mutually satisfactory mount system to provide better access to engine accessories.

8. Additional noise tests and analyses are required to establish the level of jet noise shielding which is obtained by virtue of the over/under arrangement.

9. More detailed analyses should be conducted to determine the impact of fan noise transmitted through the inlet auxiliary doors and, if necessary, devise noise reduction techniques which will be effective in reducing fan noise to acceptable levels.

10. Based upon the results of technology sensitivity studies conducted for the GE21/711 variable-cycle engine, it appears that the primary research effort should be concentrated in the areas of exhaust nozzle development, turbine cooling technology, and toward demonstration of the present VCE concept.

4.5.2.2 Nacelle Integration Study (McDonnell Douglas)

Introduction

The approach utilized was to select an attractive GE engine, refine the nacelle configuration, refine the selected engine, and assess propulsion technology.

The subtasks included in the study are as follows:

- Engine selection

- Engine sizing

- Structural nacelle trade study

- Engine mount location

- Engine component sensitivity

- Engine refinement

- Airplane performance evaluation

The preliminary integration analysis was carried out using the GE21/J11B2 and B6 engines. The results were refined to fit the characteristics of the GE21/J11B10 engine. Results presented below summarize the second (final) phase of the study in which the GE21/J11B10 engine is used.

Aircraft and Mission

The aircraft layout used in McDonnell Douglas studies is illustrated in Figure 108. It is a conventional aircraft design with four engines located in four separate under-wing pods. The takeoff gross weight is 340,200 kg (750,000 lb). It is designed for cruise at 2.2 Mach number on a standard day. The mission is described in Figure 109.

Engine

The GE21/J11B10 double-bypass variable cycle engine is a twin-spool configuration consisting of a multistage fan, high-pressure compressor, primary burner, high-pressure turbine, low-pressure turbine, augmentor, an annular convergent-divergent plug nozzle with translating shroud (for inherent sound suppression), and a thrust reverser. The nozzle has a fixed primary nozzle, variable fan exhaust nozzle, and a translating cylindrical shroud to provide the internal area ratio for expansion of the exhaust gases. Cooling of the nozzle is by fan discharge air. No secondary airflow is required for cooling purposes and no provisions are incorporated to handle secondary airflow from the intake duct.

The GE21/J11B10 represents a refinemenet of the J11B2 and J11B6 engine cycles. The cruise airflow is increased, takeoff thrust is increased, boat-tail drag is decreased without an engine weight penalty. The basic engine cycle is nonaugmented, but an option is provided for a low-temperature augmentor. An option is also provided for a 5 PNdB mechanical suppressor.

218

Characteristics			
Item	Wing	Horizontal Stabilizer	Vertical Stabilizer
Area ft^2	10,000	780	700
Aspect Ratio	1.84	2.0	0.9
Taper Ratio	0.128 (Trap)	0.16	0.25
Sweep of LE	71° and 57°	50°	50°
Dihedral	0 at TE	0	———
T C % C	2.25-3.00	3.5	25
Tail Vol Coef	———	0.118	0.044

Payload Capacity

   Mixed Class

      First Class - 3 and 4 Abreast - 38 Pitch -

      Tourist Class - 4, 5, and 6 Abreast - 34 P

Cargo Volume

Forward	1500 ft^3
Aft	750 ft^3
Total	2250 ft^3

Section Y_c = 1100

Section Y_c = 1760
Spar No. 2

Section Y_c = 2320
Spar No. 4

Section Y_c = 2000
Spar No. 3

Section Y_c = 2600
Rear Spar No. 5
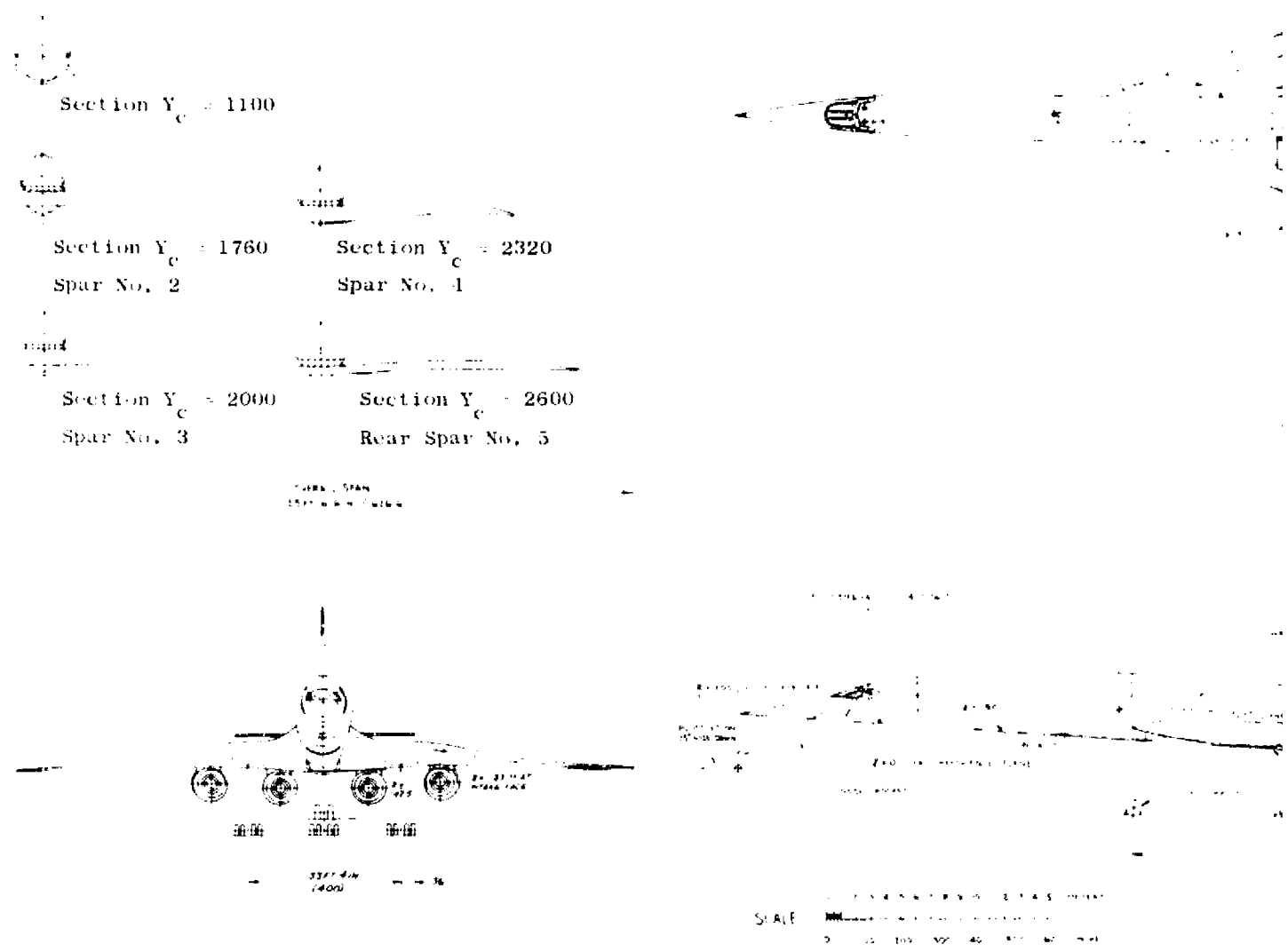
Figure 108. Aircraft General Arrangeme

M2.2 Supersonic Cruise Altitude >
15,240 m (50,000 ft)

Decelerate to 180 m/sec EAS

Descend at
Constant 180 m/sec EAS

Climb from
M=1.0 to M=2.2

Climb at Constant
180 m/sec EAS
to M=1.0

Decelerate to 129 m/sec
EAS at 3048 m (10,000 ft)

1524 m (5000 ft) Acelerate to 185 m/sec EAS

15 Minute Allowable | Climb at 118 m/sec EAS

Enroute Fuel
Allowance (7% Trip Fuel)

Cruise at 9144 m (30,000 ft) Long Range

Descend at
168 m/sec EAS

Climb at
185 m/sec EAS
to Cruise M

30 Minute Hold
at 4572 m (15,000 ft)

Accelerate to
3048 m (10,000 ft)
185 m/sec EAS

Decelerate to 3048 m
(10,000 ft) 129 m/sec EAS

Climb at 118 m/sec EAS

Descend at
129 m/sec EAS

Range

Range 370 km (200 nmi)

Trip Fuel

Block Time and Fuel
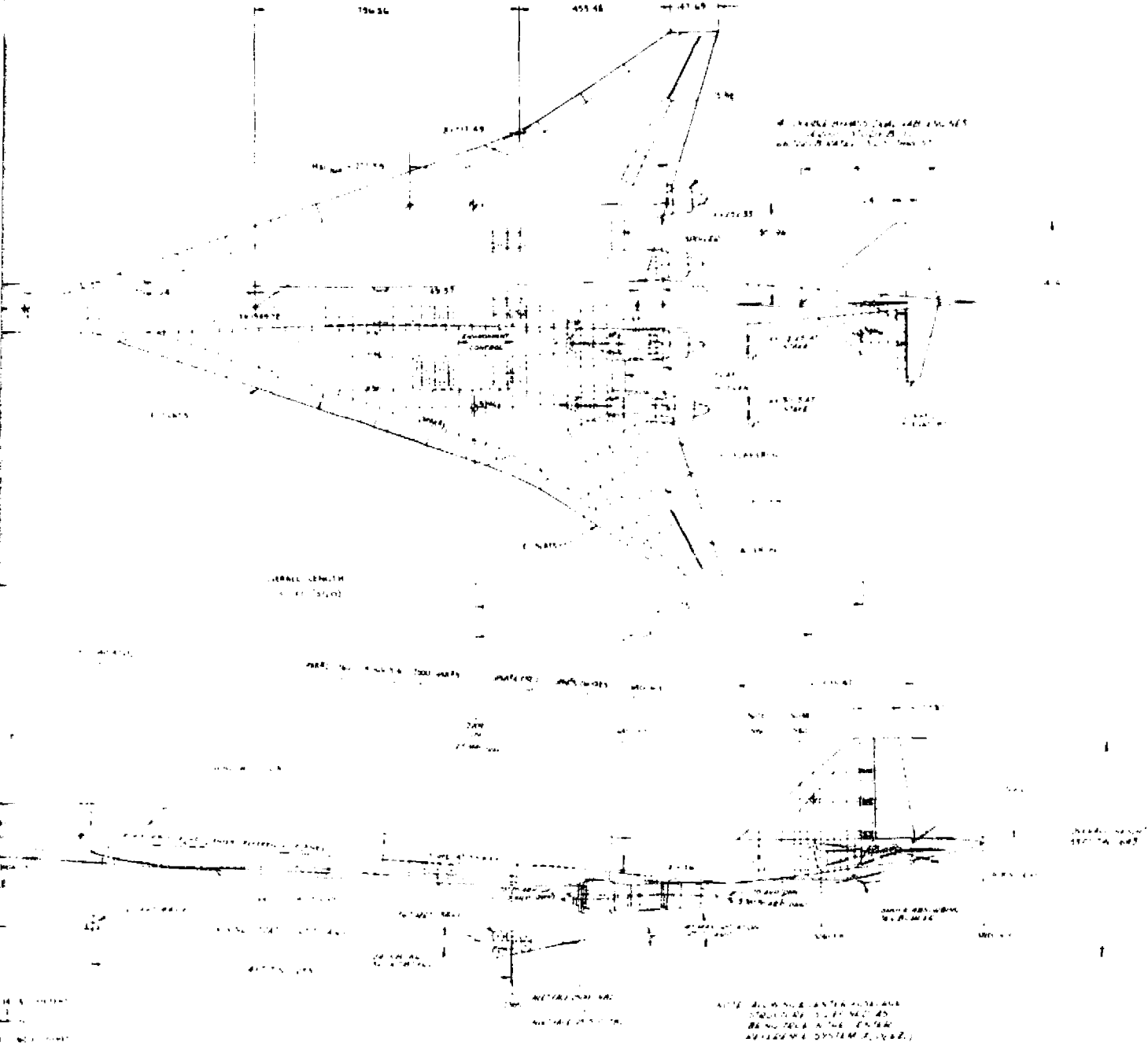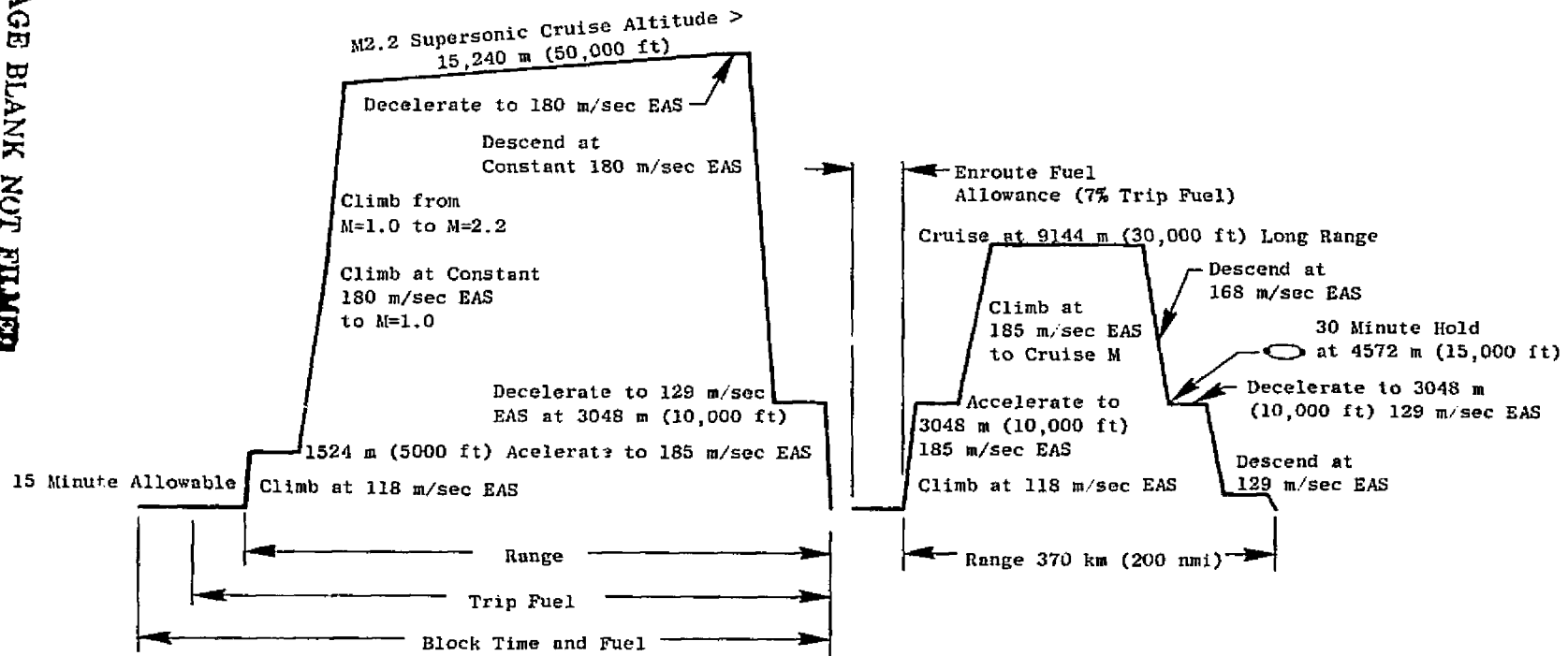
Figure 109. Mission Profile.

The uninstalled performance data are obtained by utilizing the GE supplied data package based on and corrected as required to include the effects of:

- U.S. 1962 model atmosphere

- Inlet recovery

- GE-supplied internal nozzle velocity coefficient

- Customer compressor air bleed – 0.454 kg/sec (1 lb/sec)

- Customer power extraction – 149 kW (200 hp)

- Jet "A" fuel, lower heating value – 4.34×10^7 J/kg (18,400 Btu/lb)

- No losses for acoustic treatment

Engine Size Selection and Acoustics

The GE21/J11B10 data pack supplied by GE is run utilizing the McAir requirements, i.e., pressure recovery, airflow schedule, Mach 2.2 cruise and standard day. Sizing criteria for this engine are takeoff thrust [231,300 N (52,000 lb) at Mach 0.3, sea level, standard +10° C (+18° F) day per engine, uninstalled, no external drag] and FAR Part 36 noise requirements [381m (1250 ft) altitude, Mach 0.3, 692 m (2270 ft) sideline, and 381 m, (1250 ft) Mach 0.3, takeoff/cutback, standard 10° C (+ 18° F) day]. This level of takeoff thrust should result in a takeoff field length of 3353-3505 m (11,000-11,500 ft) at sea level ISA + 10° C (+18° F) day. Cutback thrust is 147,900 N (33,250 lb).

Figure 110 illustrates the engine sizing logic based on GE data. Data are shown for four engine suppressed noise (GE calculations with annular-type nozzle) for sideline at 381m (1250 ft) altitude and takeoff/cutback at 381m (1250 ft) altitude over the monitor. Also shown on Figure 110 is the engine size required for both sideline and takeoff/cutback. The resulting engine size to meet both thrust and FAR 36 noise requirements is 433 kg/sec (955 lb/sec) engine inlet corrected airflow (see Figure 110). The sideline suppressed noise is 108 EPNdB and the takeoff/cutback noise is 108 EPNdB at an aircraft altitude of 381m (1250 ft) over the 6.5 km (3.5 nmi) noise monitor.

Figure 111 illustrates the engine sizing logic, based on GE data, for an engine utilizing a mechanical suppressor together with the annular nozzle. If the nominal suppressed noise is used, an engine size of 387 kg/sec (853 lb/sec) engine inlet corrected airflow results and meets both thrust and FAR 36 noise requirements. The sideline suppressed noise is 103.8 EPNdB and the takeoff/cutback noise is 109.7 EPNdB at an aircraft altitude of 381m (1250 ft) over the 6.5 km (3.5 nmi) noise monitor. The delta weight of the suppressor is 215 kg (474 lb).
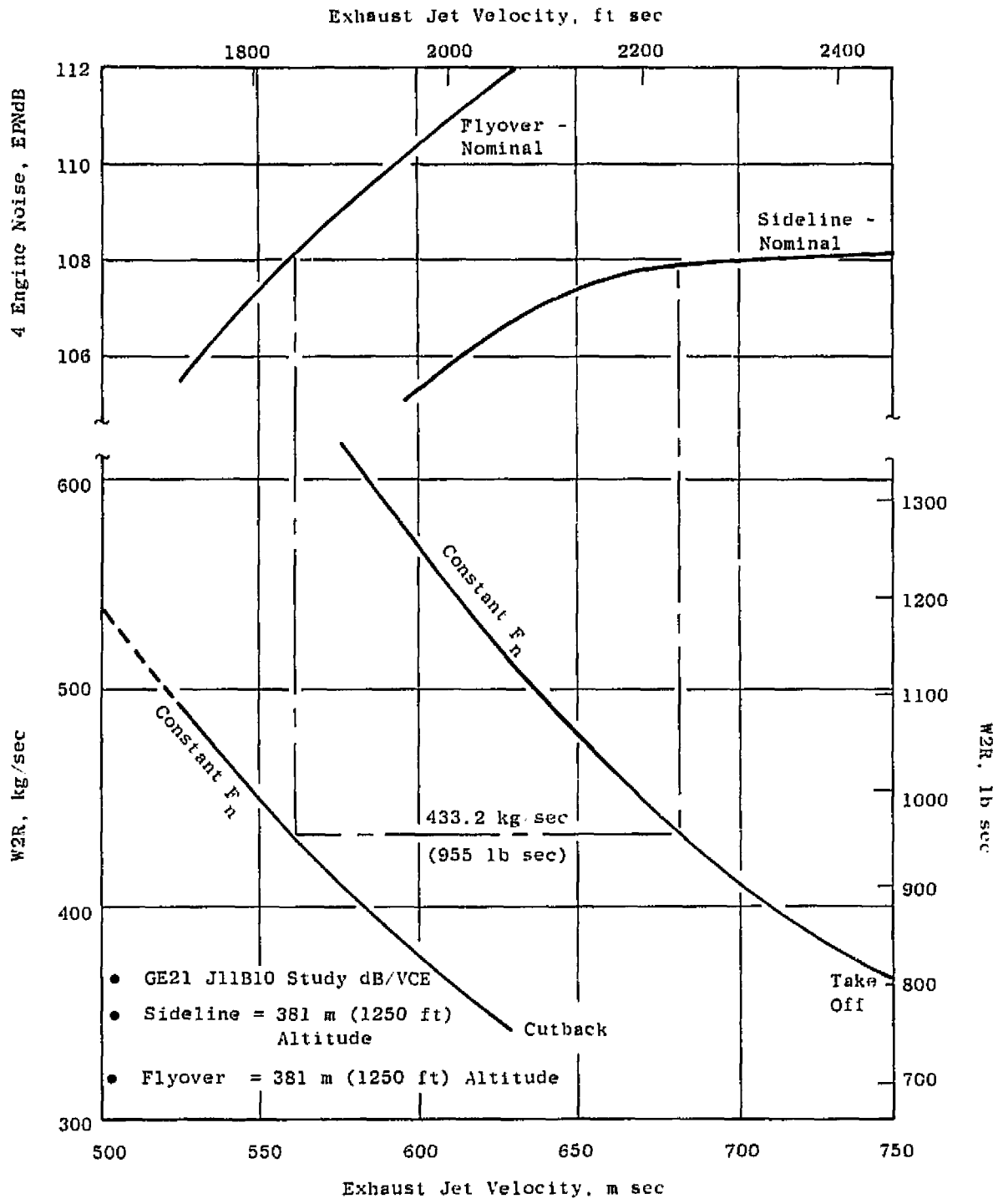
Figure 110. Engine Sizing - Annular Nozzle.

Exhaust Jet Velocity, ft sec
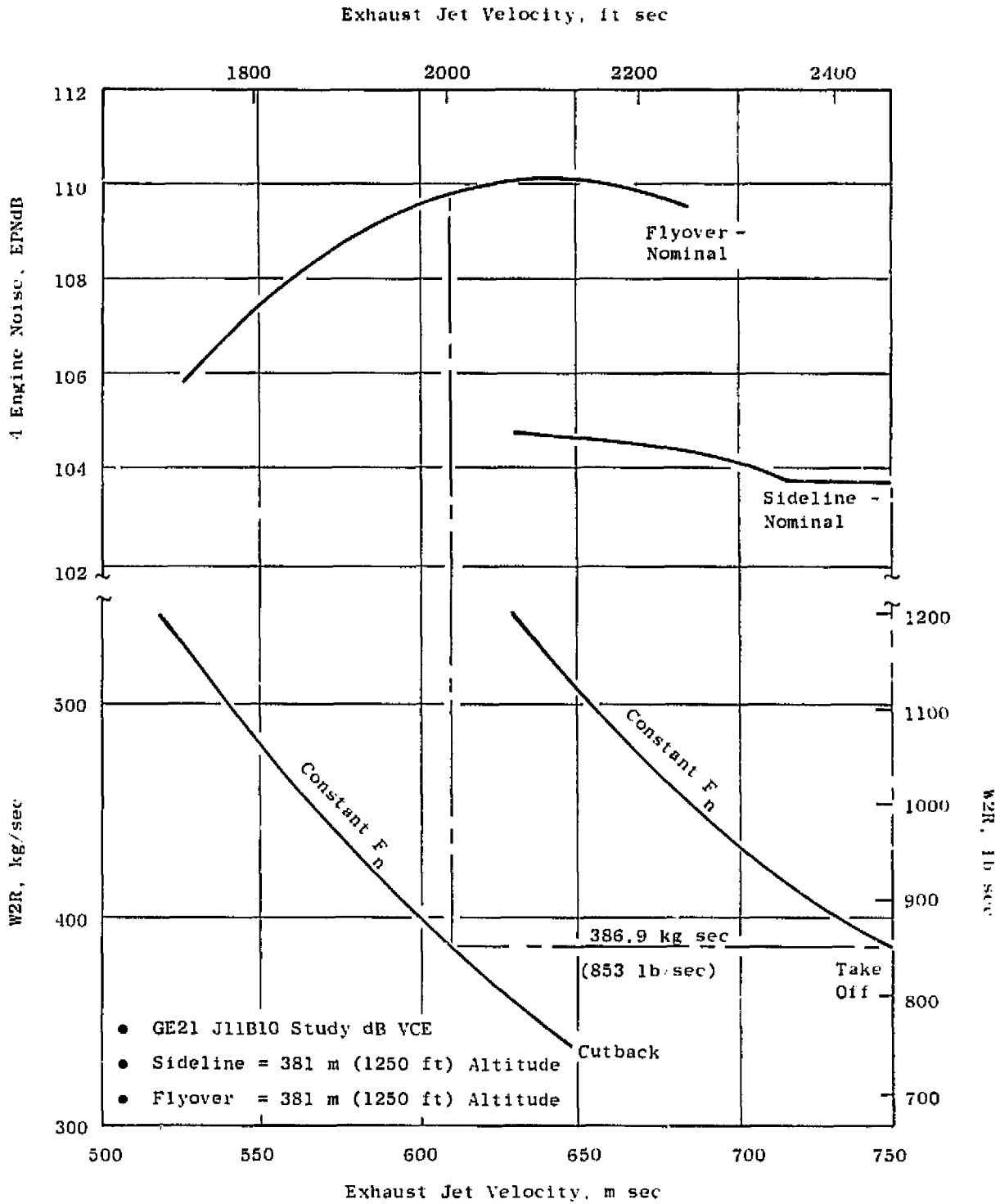
Figure 111. Engine Sizing, Annular Nozzle with Mechanical Suppressor.

Engine operation is controlled through the scheduling of fan speed, duct Mach number, and fan exhaust nozzle throat area. At takeoff, a selected reduced thrust level is achieved with maximum engine speed and corrected airflow.

The installed engine/nacelle arrangement is shown in Figure 112.

Nacelle Location and Design

Installation of the GE21/J11B10 engine in four axisymmetric nacelles for the baseline airframe is shown in Figure 113. The forward and aft locations have been determined analytically from inputs by aerodynamics, structural mechanics, acoustics, and propulsion technologies.

The location of engines on the wing does not allow usage of the full-circumferential opening for thrust reversing proposed by the engine manufacturer. Thrust reversing is only achievable in local areas [1.57 rad (90°) above and 2.62 rad (150°) beneath the engine nozzle] to clear deployed wing flaps in the landing configuration. Th locations as shown on the three-view drawing (Figure 108) provide the best solution to the requirements of the previously established criteria.

Engine/Nacelle Attachment to the Wing

A previous study of structural versus nonstructural nacelle concepts indicated substantial weight savings to be realized by the choice of a structural nacelle design (see Figure 114). This integration study reflects such a philosophy. The upper segment of the nacelle is composed of semihoop frames skinned with titanium/honeycomb sandwich panels. This structure is integral with a pylon/box beam cantilevered aft of the rear spar of the wing main torque box. The lower closing longeron of the structural nacelle segment carries hinged nonstructural access panels forming the lower segment of the engine nacelle.

The engine is mounted to the pylon/nacelle structure by means of links. The forward mounting links carry thrust, side, and vertical loads. The aft-mounting links carry vertical, side, and torque loads and translate for engine axial growth under operating temperatures.

The axisymmetrical intakes are mounted to a full-hoop frame on the front of the nacelle structure. Flexible seals are provided to allow for relative movement between intake and engine faces. The boundary layer diverter is integrated into the engine nacelle/wing fairing.

Two alternate nacelle configurations were studied in which the forward mount was moved from the horizontal centerline to 0.26 rad (15°) and to 0.52 rad (30°) above the horizontal centerline. The engine manufacturer determined that there would be no weight penalty to relocate the main mount.
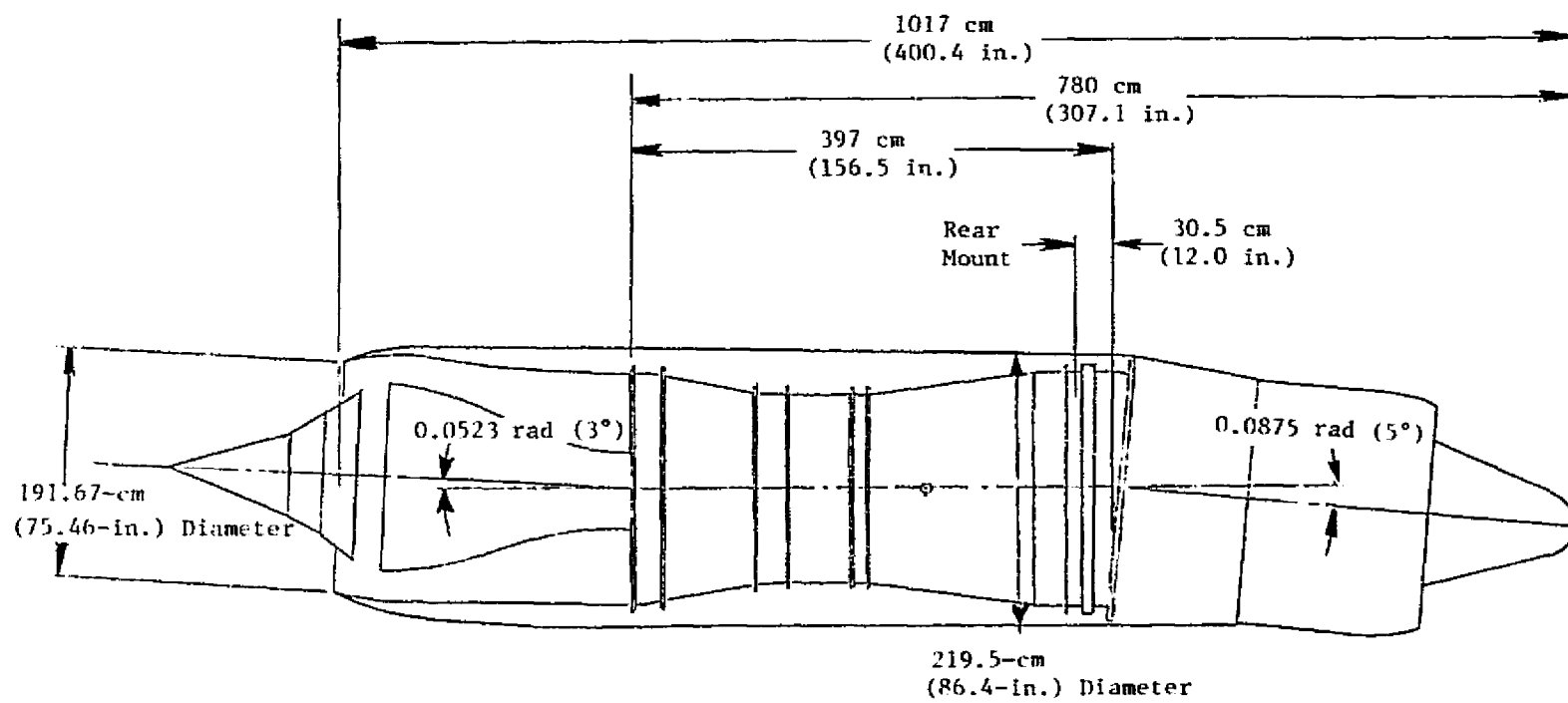
GE Double-Bypass
GE21/J11B10 Study
Airflow, 433 kg/sec (95 5 lb/sec)

Figure 112. Engine Pod Arrangement.

Figure 113.   Engine Ins

PLAN VIEW

SIDE VIEW

SCALE

Figure 113.   Engine Installation.

Centimeters

0	100	200	300	400	500

0	100	200

Inches
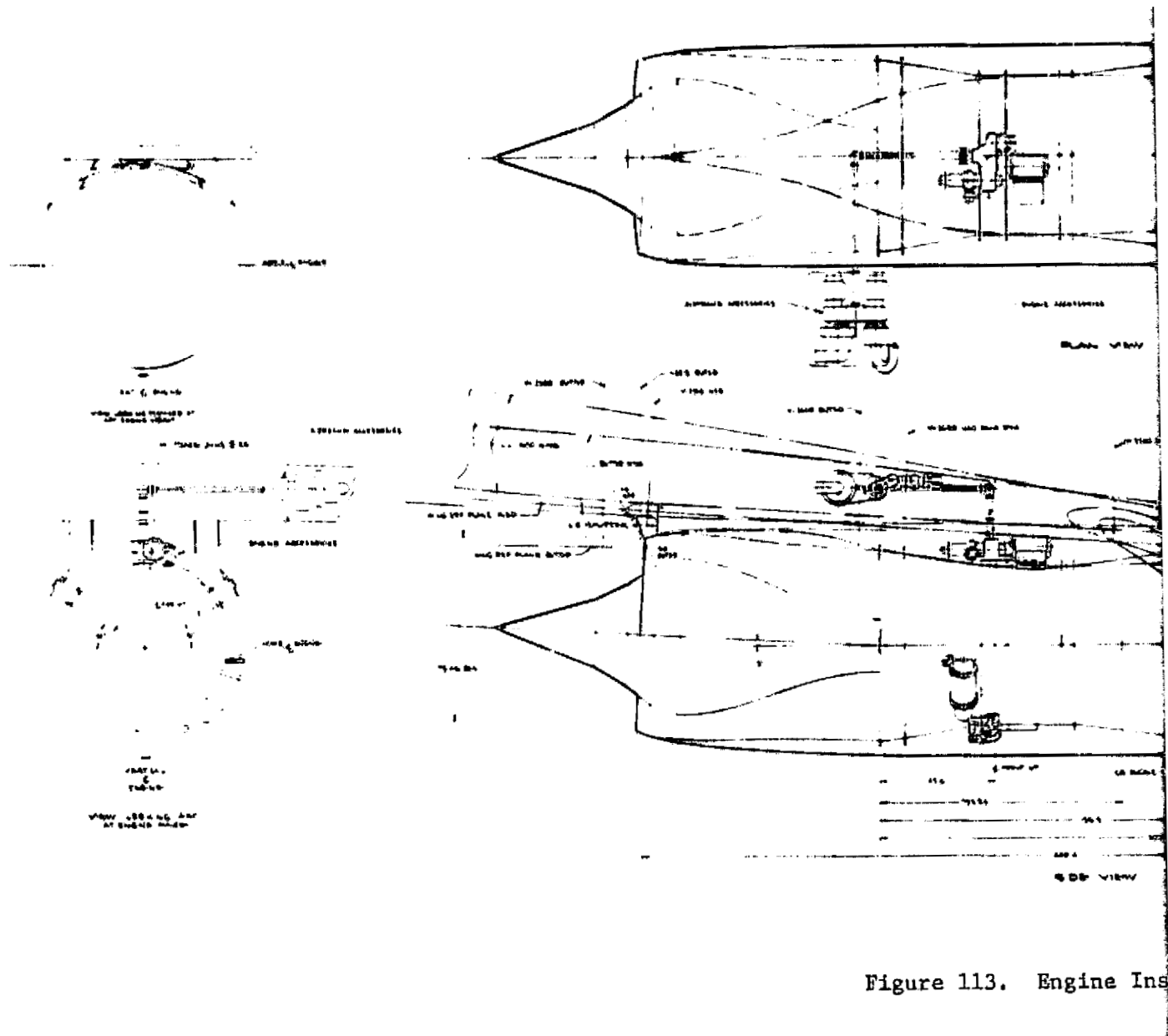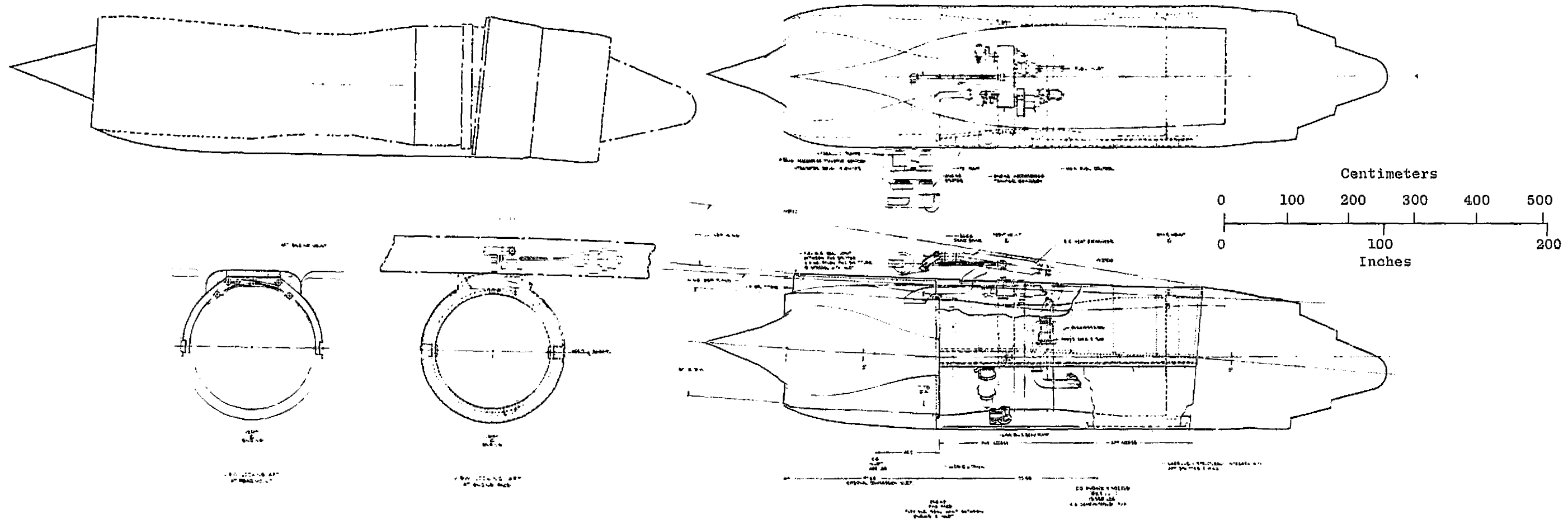
Figure 114. Details of Structural Nacelle Concept.

228

This study indicated that the nacelle weight can be decreased by raising the mount to a location 0.52 rad (30°) above the horizontal engine centerline. Figure 115 describes the final mount arrangement.

The inlet total pressure recovery variation is shown in Figure 116. Also shown in the figure is the variation of inlet critical mass flow ratio and the inlet cone schedule. The mass flow ratio for the inlet boundary layer bleed airflow is shown in Figure 117.

The engine inlet airflow schedule for the GE21/J11B10 engine is also shown in Figure 117. The installed inlet performance for the engine is shown in Figure 118. As shown by the upper graph in the figure, the inlet airflow supply provides an adequate match with the engine airflow demand. The three-cone, axisymmetric, external compression inlet is sized at the design point of Mach 2.2. The sized capture area is $2.88m^2$ (31.05 ft^2). The engine cooling airflow (environmental cooling and engine compartment ventilation) is estimated at 2% of inlet capture air at Mach 2.2 cruise (same as for the other McAir – evaluated GE advanced technology engines).

Installed Performance

The analysis of the propulsion system performance included the determination of the inlet performance and drag characteristics and an estimation of the nacelle drag characteristics which, when combined with the installed engine performance, produce the installed propulsion system performance. The inlet performance and the nacelle analysis include an evaluation of the following items:

- Inlet spillage drag

- Inlet bypass drag

- Engine compartment ventilation and environmental control system (ECS) cooling airflow drag

- Nacelle skin friction drag

- Nacelle afterbody drag

- Nacelle wave drag

Nacelle Structures

Engine installed weight calculations were made including assessment of the following items:

- Inlet length

- Engine length and diameter

Figure 115. Selected Nacelle Confi[

Centimeters

0   100   200   300   400   5(

100

Inches
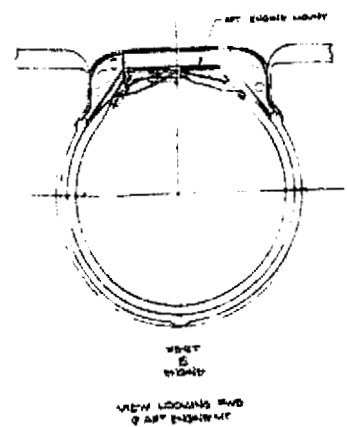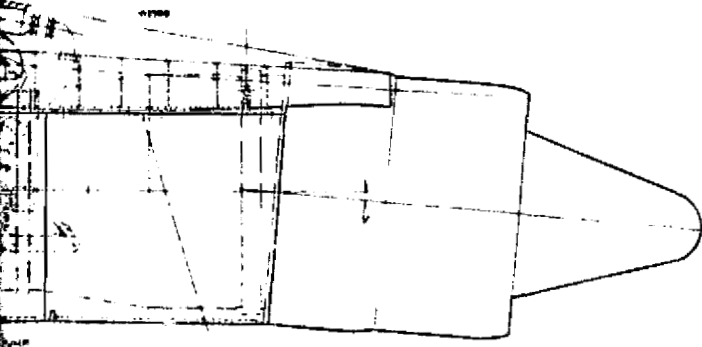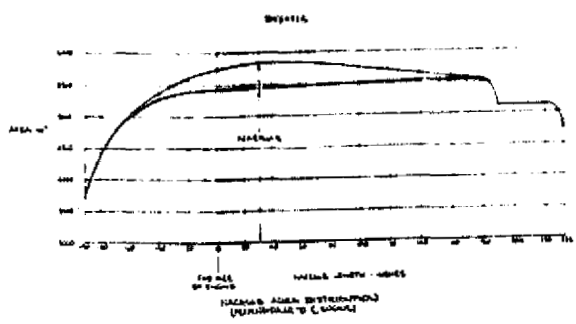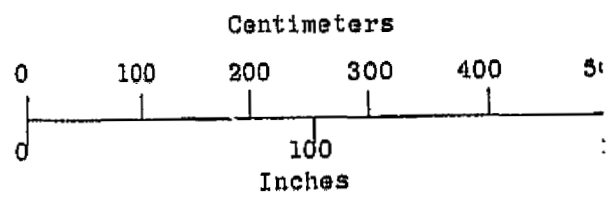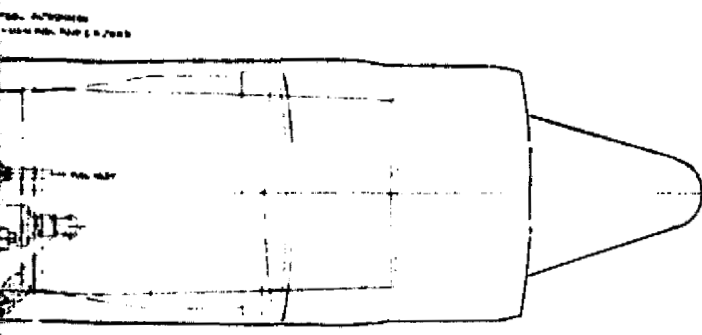
lected Nacelle Configuration.

231
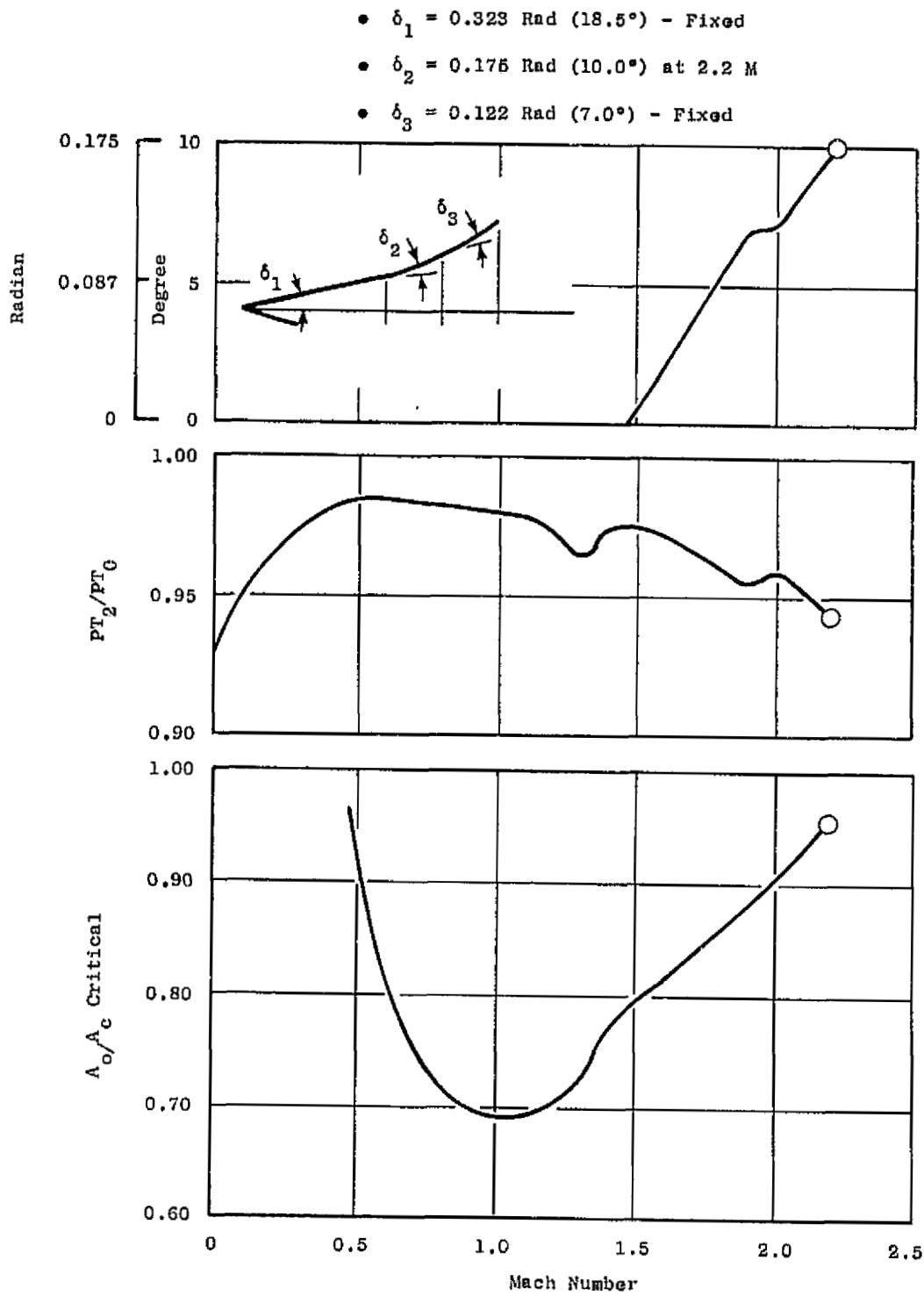
Figure 116.   Inlet Performance.

GE21/J11 B10
STD DAY
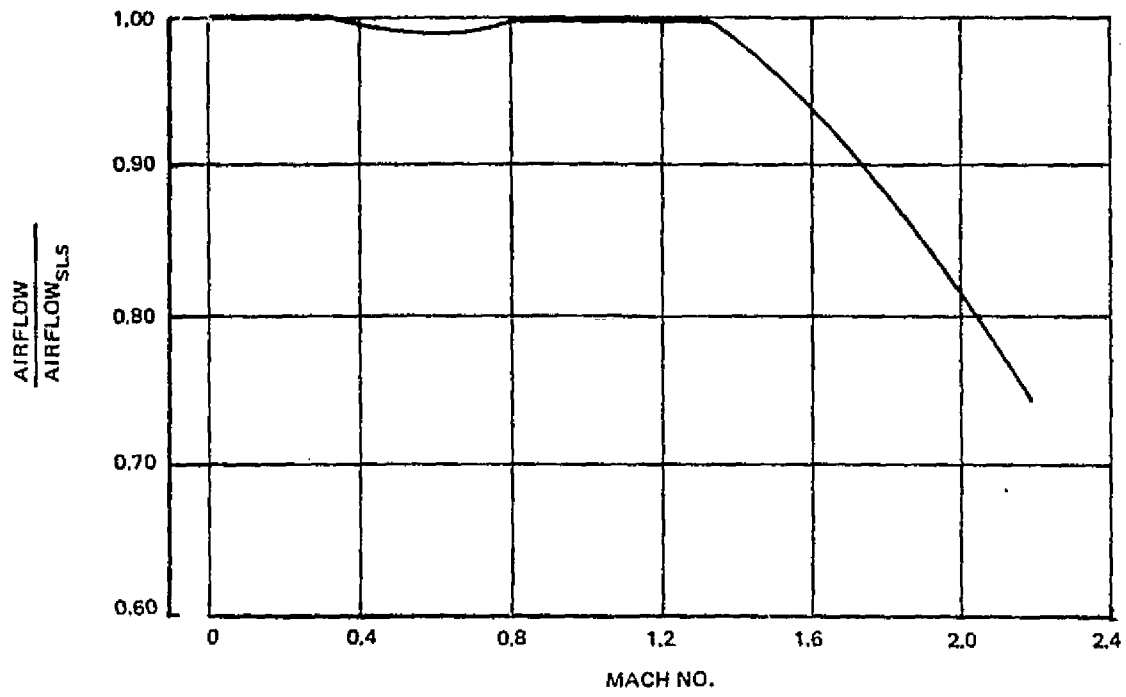
Figure 117. Airflow Schedule.

234

- GE21/J11B10 Engines
- WAT_2 = 433 kg/sec (955 lb/sec)
- A_c = 2.88 m^2 (31.05 ft^2)
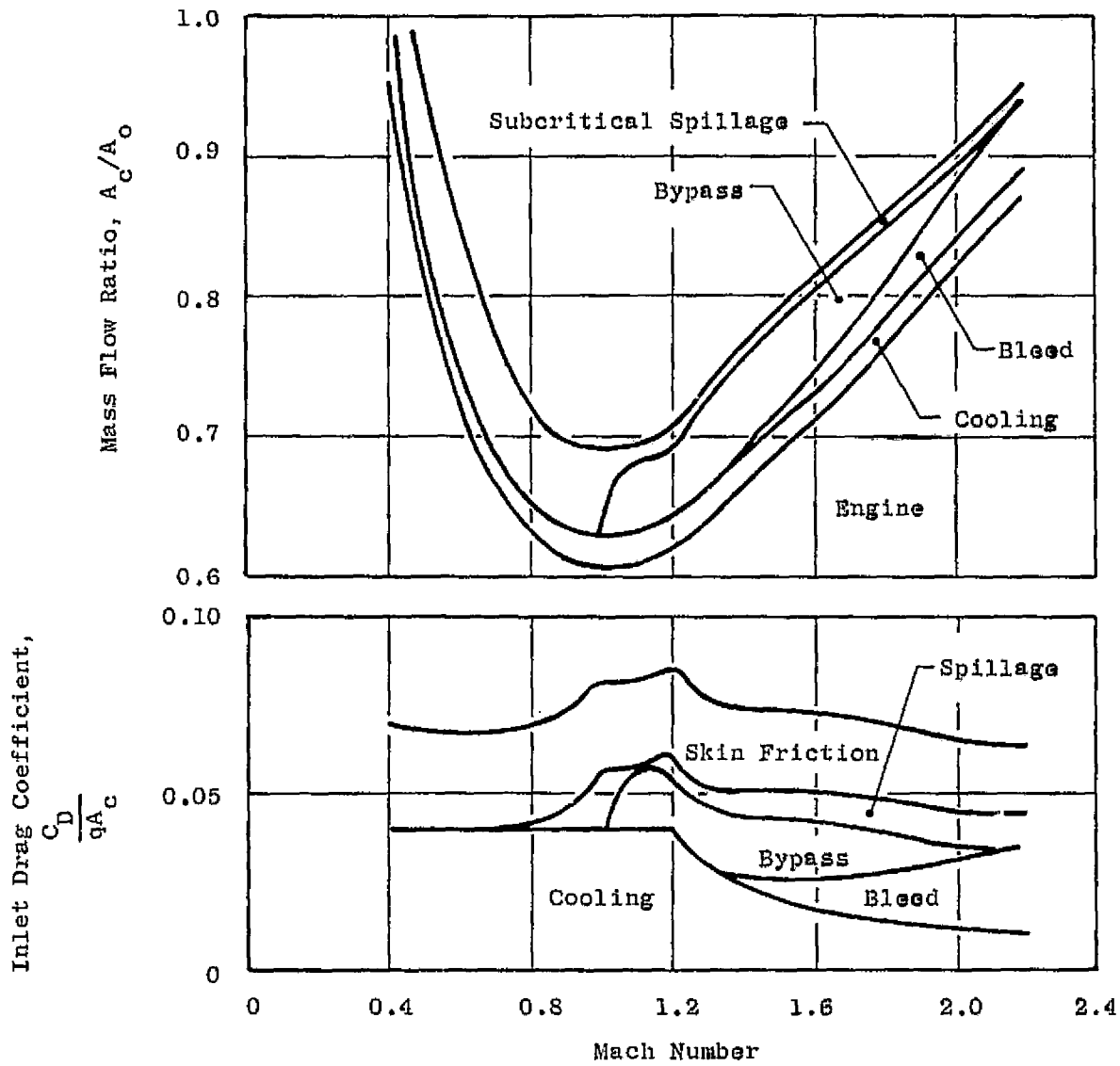
Figure 118. Installed Inlet Performance.

- Flutter and aeroelasticity

- Ground clearance (and landing gear length)

- Airframe structure and loads

- Engine and pod center of gravity

- Engine airflow size

Certain other nacelle trade studies were carried out during the preliminary phase of the studies, including alternate materials for nacelle construction and improved accessories.

Results of these additional trade studies were incorporated into the final phase of studies in which the GE21/J11B10 engine was evaluated.

Acoustic Analysis

The acoustic analysis, conducted for the aircraft configuration powered by the GE21/J11B10 engine, consists of the calculation of estimated jet noise in conjunction with engine sizing studies. Engine cycle data have been employed to estimate the jet noise at aircraft Mach numbers and altitudes representative of the three FAR Part 36 measuring conditions. After the engine size had been determined, the flightpath for the improved double-bypass, dual-cycle engine powered aircraft configuration was calculated and engine cycle data at the above conditions were defined. The noise levels for the three conditions are then estimated using the McAir gas turbine engine noise (GTEN) computer program. The standard climb profile incorporates a thrust cutback over the takeoff (community) measuring station.

The engine size for noise and takeoff thrust is 383.3 kg/sec (845 lb/sec) engine inlet corrected airflow. The required jet noise suppression is provided by the annular nozzles with suppressed noise levels as estimated by GE.

The jet noise levels for the J11B10 engine without mechanical suppression in the baseline airplane are based on specific engine conditions for the calculated takeoff and approach trajectories as estimated with the McAir GTEN program described below:

FAR Part 36 Measuring Station	Distance, m (ft)	Total Noise EPNL, EPNdB
Sideline	692 (2270)	108.1
Takeoff/Cutback	375 (1230)	110.0
Approach	113 (370)	104.6

This selected engine sized for noise [383.3 kg/sec (845 lb/sec)] is the minimum size which will meet FAR Part 36 noise requirements and takeoff thrust requirements.

The data presented in Figure 119 account for the changes in engine size and nacelle weight, and inlet and nacelle drags, but neglect the changes in aircraft wave drag. For a 10% change in engine size, the wave drag effect is quite small.

Figure 119 shows that, with the engine sized as described above to take advantage of noise trading, the range increases to 9001 km (4,860 nmi) and is very near the optimum engine size for cruise.

Noise levels for the engine which uses the 5dB suppressor were calculated. The results are for an engine of 387 kg/sec (853 lb/sec) size:

Sideline	103.8
Takeoff/Cutback	109.7
Approach	105 (approx.)

Aircraft Performance

The trimmed lift and drag characteristics for the GE21/J11B10 powered aircraft are obtained by adjusting the wave drag of the previous baseline aircraft for the difference due to the revised nacelles. The difference in nacelle skin friction drag is accounted for in the installed propulsion system performance. The supersonic wave drag for the J11B10 configuration is estimated to be 4.1 drag counts (ΔC_D = 0.00041) less than the baseline configuration. The characteristics used to determine the mission performance for the J11B10 powered aircraft are obtained by subtracting this increment from the wave drag of the baseline aircraft.

Estimated performance characteristics for the GE21/J11B10 powered aircraft are presented in Figures 119 and 120 as a function of engine size. The mission profile and fuel reserve ground rules are the same as used for the baseline turbojet aircraft (Figure 109). The takeoff gross weight is held constant at 340,194 kg (750,000 lb) and the payload is fixed at 25,385 kg (55,965 lb).

Figure 115 presents the takeoff characteristics and the height above the runway at 6.5 km (3.5 nmi) from the start of takeoff with the throttle cut back to meet the 4% all-engine climb gradient requirement of FAR Part 36. The variation of the aircraft characteristics with the engine size are indicated on the figure. The performance of the baseline aircraft is also shown for reference. Figure 119 presents the variation of operating empty weight with engine size used for the mission performance calculations, the altitude for maximum range factor at the start of the Mach 2.2 cruise, and the mission range.

GE21/J11 Study B10 DB/VCE
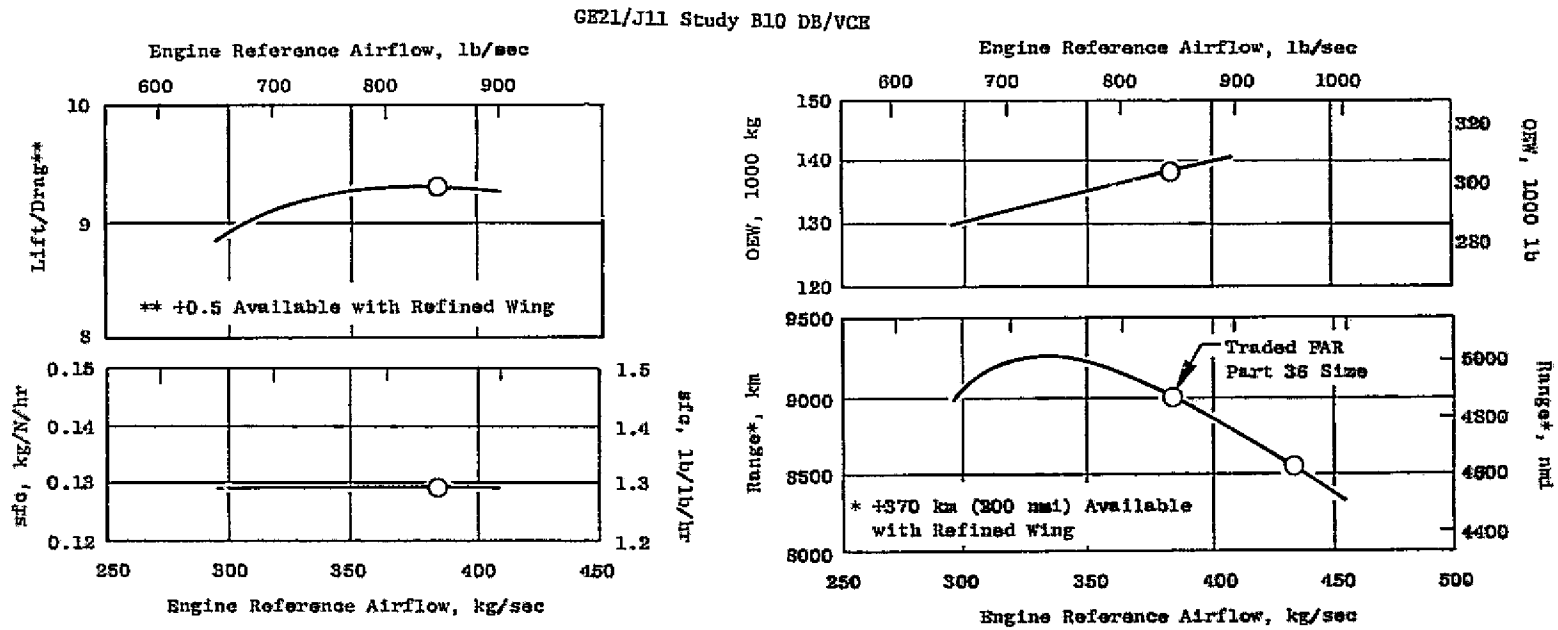
Figure 119. Effect of Engine Size on Mission Performance.

- GE21/J11B10 Engines
- Take-Off Gross Weight = 340,194 kg (750,000 lb)
- Sea Level Standard Day +10° C (+18° F)
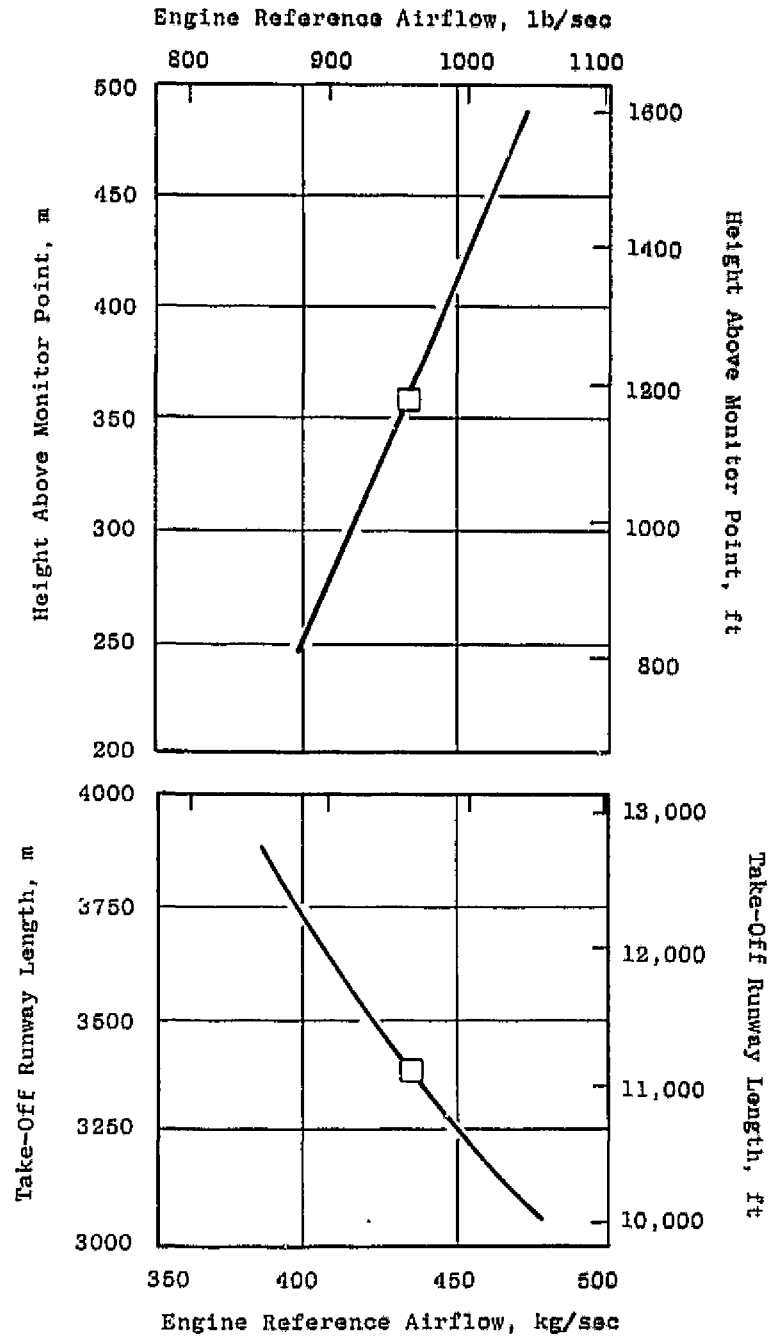
Figure 120. Effect of Engine Size on Takeoff Performance.

Engine Performance Comparison

As mentioned in previous discussion, an engine/airplane integration and a mission analysis has been accomplished on three versions of the GE double-bypass VCE installed in the McAir Mach 2.2 baseline airplane. The results of the mission analysis are shown in Figure 121. The optimum engine size based on takeoff thrust and noise requirements is shown. Also shown for comparison is the baseline McAir turbojet engine.

Technology Assessment

GE has made an assessment of the critical technology items including component efficiency, cooling air and weight. The McAir baseline aircraft powered by the GE21/J11 study B10 sized for noise and takeoff thrust at 383.3 kg/sec (845 lb/sec) has the following sensitivity factors:

Weight	—	41 km/452 kg (22 nmi/1000 lb)
Cruise sfc	—	81 km (44 nmi)/% change in sfc
Cruise Fn	—	0
Cruise Drag	—	56 km (30 nmi)/drag count
Subsonic sfc	—	9 km (5 nmi)/% change in sfc

Figure 110 shows the effect of changes in noise goals on engine size to meet FAR Part 36.

Figure 122 shows the impact of reduced annular suppression on engine size and the subsequent range reduction due to increasing engine size. The main area is identified as trade area (approach). It is bounded by takeoff thrust required, 110 EPNdB cutback, 110 EPNdB sideline, maximum annular effect and sideline/cutback traded noise equal to zero. If approach noise is 105.9 EPNdB (2.1 PNdB below FAR Part 36) then the required engine size is 383.3 kg/sec (845 lb/sec) for maximum annular effect. If approach noise is 108 EPNdB then the required ending size is 433 kg/sec (955 lb/sec) for a maximum annular effect. The corresponding loss in range is 439 km (237 nmi).

Figure 123 shows the impact of reduced annular suppression on engine size for an engine utilizing both the annular effect and a 5 PNdB mechanical suppressor.

Conclusions and Recommendations (McDonnell Douglas)

The following conclusions were reached:

1. An attractive inlet/nacelle arrangement can be designed for the GE21/J11B10 double bypass variable cycle engine.
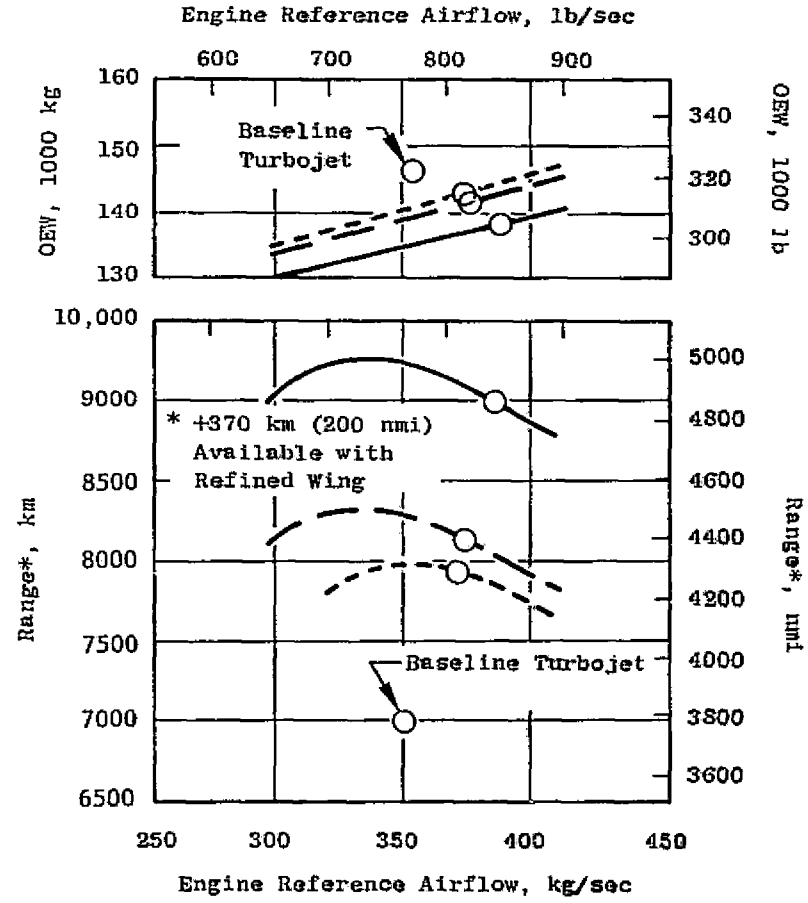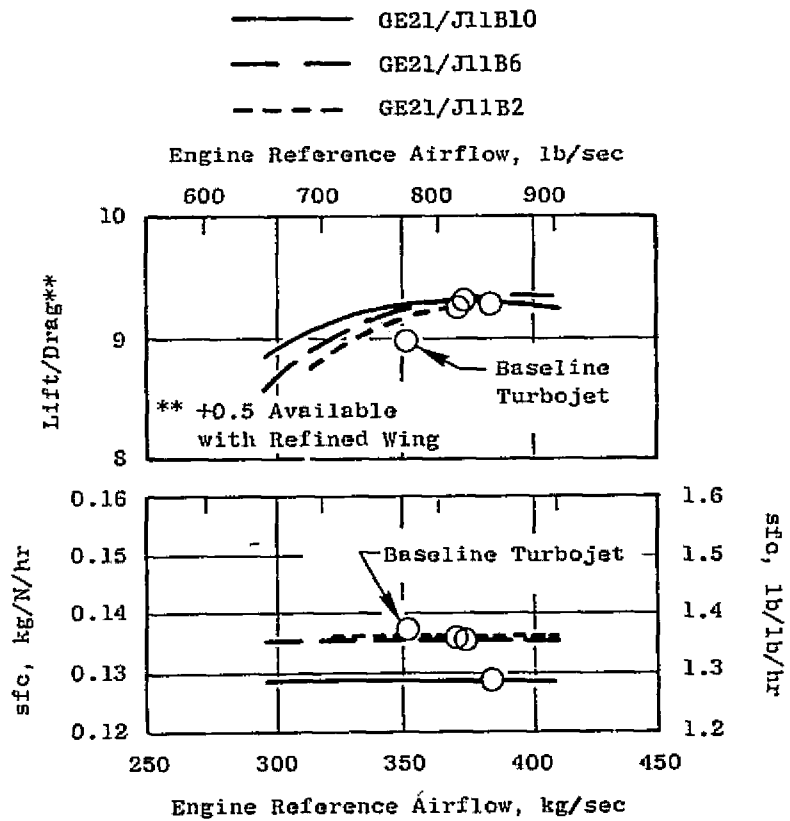
Figure 121.   Mission Performance Comparison.
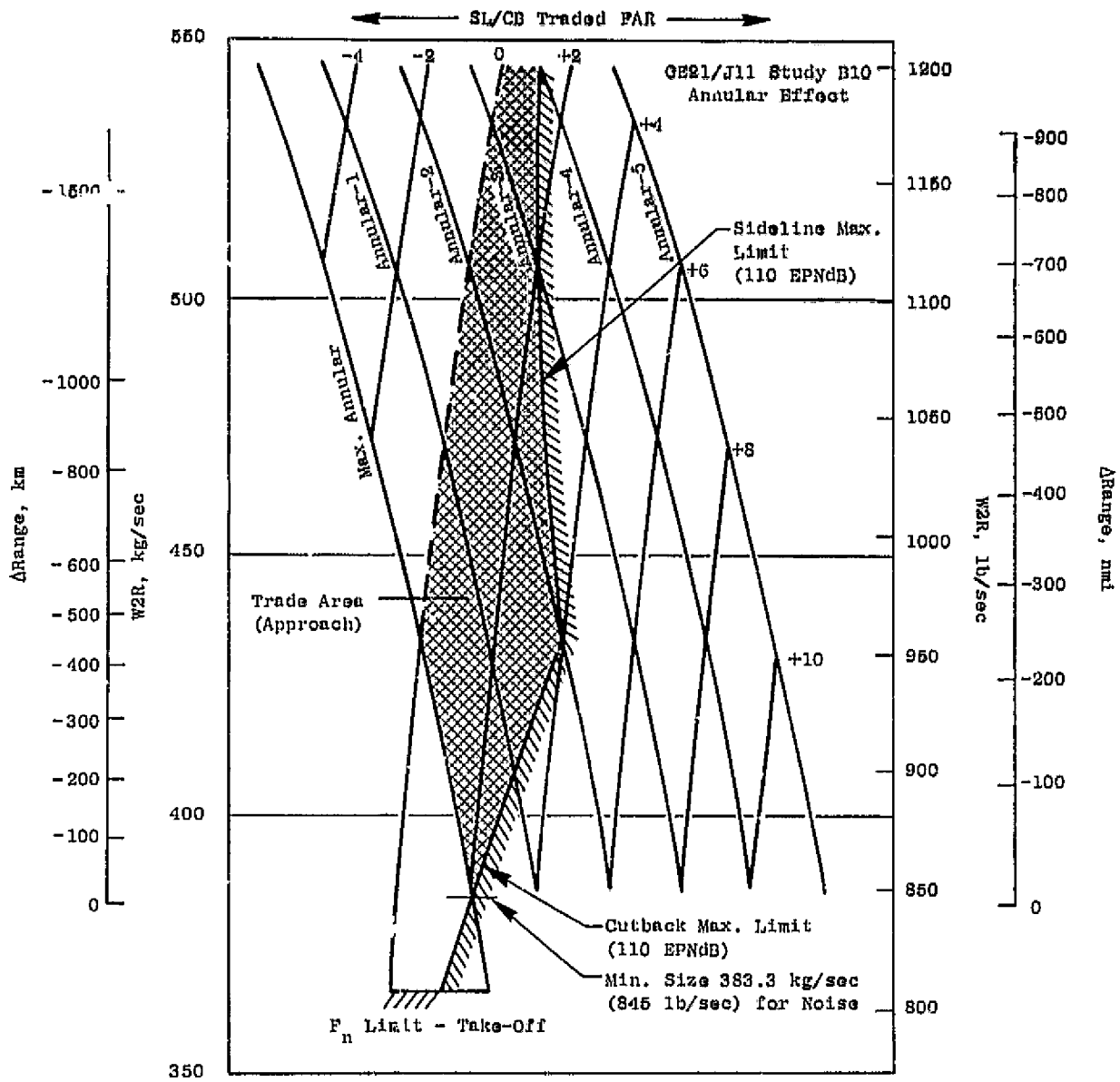
Figure 122. Range Change, Annular Nozzle.

242
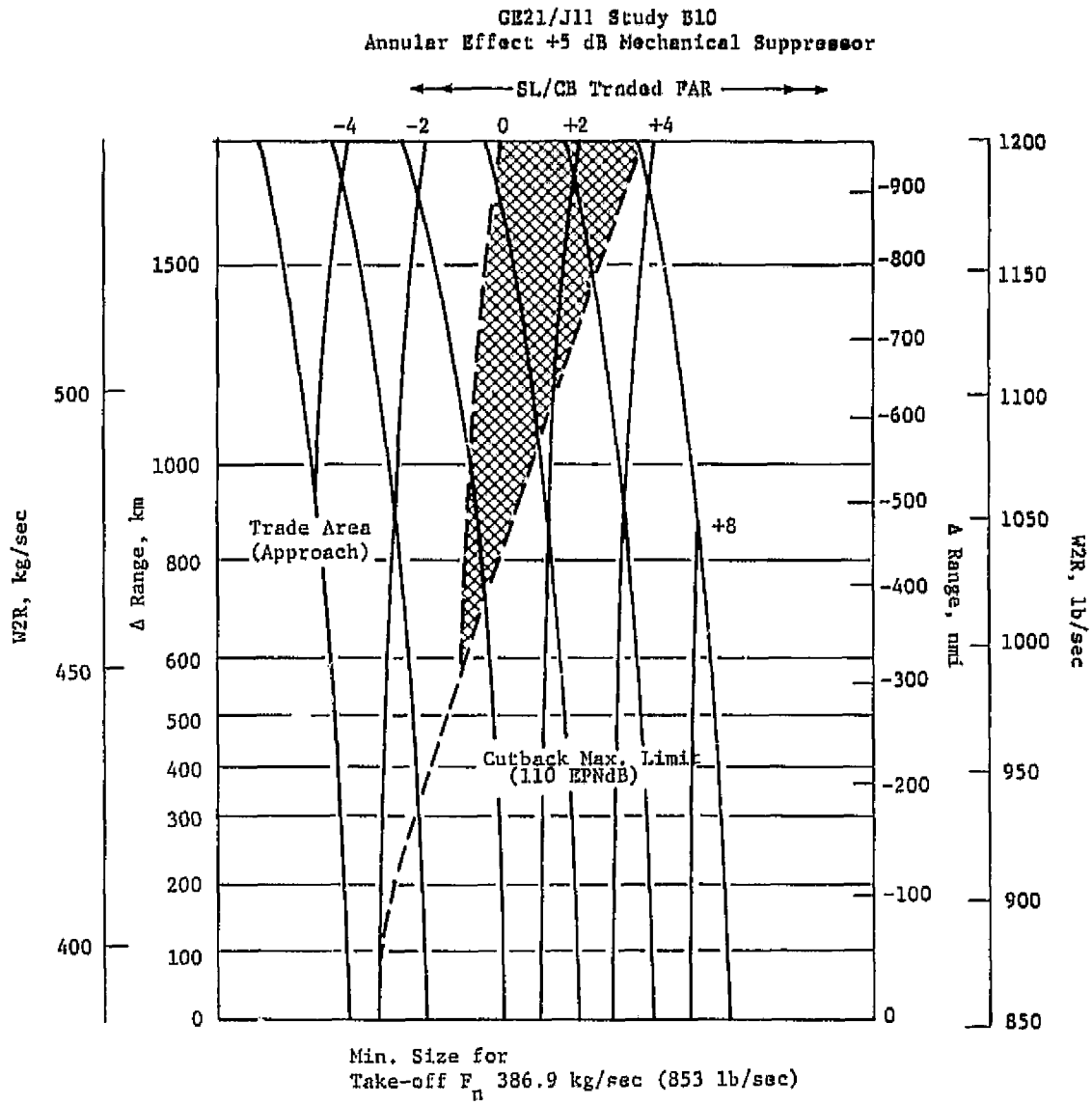
Figure 123.   Range Change, Annular Nozzle with Mechanical Suppressor.

2. The structural nacelle (engine inlet supported directly by the wing rather than from the engine front flange) results in a weight saving, per pod over the engine mount located on the engine horizontal centerline.

3. Engine mount relocation to 0.524 rad (30° C) above the engine horizontal centerline results in a weight saving versus the engine mount located on the engine horizontal centerline.

4. Engine and airplane accessories can be packaged efficiently to permit easy access for inspection and removal.

5. Engine component and airplane sensitivity studies show that the airplane range is most sensitive to noise constraints and noise technology, exhaust nozzle thrust coefficient, and engine weight.

6. The study revealed that the GE21/J11B10 double-bypass variable cycle engine is a viable candidate engine. This engine results in a 10% longer range than the GE21/J11B6 and a 13% longer range than the GE21/J11B2.

Based on the results of this study, the following recommendations are made:

1. Further refinements of the GE21/J11B10 engine cycle should be investigated in order to further improve range capability utilizing the McAir Mach 2.2 baseline supersonic cruise transport.

2. Further critical engine technology projections in greater depth should be accomplished to better define engine performance level as a function of engine development start date.

3. Areas recommended for future effort based on technology assessments are:

   • Noise suppression

   • Exhaust nozzle thrust coefficient

   • Engine weight

   • Turbine cooling air

   • Nacelle design and integration

244

4.5.2.3 Nacelle Integration Study (Boeing)

Introduction

This section summarizes the work performed by the Boeing Commercial Airplane Co. for support of the General Electric Co./NASA Contract NAS3-19544. This study has identified critical areas and characteristics of a propulsion system installation which is compatible with the GE21/J11 engine and a highly efficient supersonic cruise airplane configuration. The primary purpose of the study was to evaluate the GE21/J11 Study B5 cycle and improvements to the B5 cycle which would lead to improved AST airplane performance. Another purpose was to design and evaluate a structurally integrated nacelle installation for the best available engine definition. The cycle definition and installation integration were accomplished through a close working relationship and timely exchange of data and study results between The Boeing Co. and General Electric.

GE had evolved an augmented double-bypass variable cycle engine designated GE21/J11 Study B5. At the initiation of the nacelle integration study, the B5 appeared to be the engine best suited to the airplane, and it was selected as the basis for the preliminary installation analysis. Further engine improvements were identified and evaluated and were consolidated in a new engine definition, the GE21/J11 Study B9. The evaluation of this B9 engine is summarized in this section.

Airplane and Mission Characteristics

Mission analysis were used to evaluate the performance merits of each engine model. A parametric approach was used and the following assumptions form the basis of this study: (1) the reference wing area was 715 m^2 (7700 ft^2), (2) the maximum taxi weight (MTW) was 340,200 kg (750,000 lb), (3) a payload of 273 passengers 25,881 kg (57,057 lb) was carried, (4) operating temperature was for a standard +8° C (+14.4° F) day, and (5) the OEW minus engine pod weight was kept constant at 123,342 kg (271,920 lb). Engine pod weight was varied with engine size. This analysis did not include noise aspects of engine/airframe matching.

Engine size was parametrically varied to determine the airflow for optimum range while achieving a minimum transonic climb thrust margin of 0.30 and a time to climb to cruise altitude and Mach number no greater than 0.75 hours.

Engine Cycle and Size Selection

The GE21/J11 variable cycle engine (VCE) is defined with propulsion technology projected to be available in the 1985 period. The engine is designed for Mach 2.4 cruise at 16,764 m (55,000 ft) altitude with a steady-state inlet temperature limit of 193° C (840° R).

The exhaust system for the GE21/J11 engine consists of an annular, translating shroud, convergent-divergent plug configuration. The nozzle has a fixed primary nozzle, variable fan exhaust nozzle and a translating cylindrical shroud to provide the internal area ratio for expansion of the exhaust gases. Cooling of the nozzle is by fan discharge air. No secondary airflow is required for cooling purposes and no provisions are incorporated to handle secondary airflow from the intake duct. The variable geometry fan exhaust nozzle and fixed primary nozzle, in combination with the translating cylindrical shroud, provide excellent supersonic cruise performance and good performance at subsonic flight conditions.

Thrust reversing is achieved by the diverting of the exhaust gas flow through a series of cascades mounted in the nozzle shroud. This will yield approximately 44,480 N (10,000 lb) gross thrust in the forward direction for a 317 kg/sec (700 lb/sec) engine size.

The annular plug nozzle is assumed to provide approximately 9 PNdB static jet sound suppression from annular jet sound suppression effects. No mechanical jet sound suppressor is included.

Thrust augmentation is provided by a single-stage burner designed to yield moderate temperature levels [maximum of 1038° C (1900° F)] to adequately meet the mission propulsion requirements.

Engine Cycle and Size Selection (Cost)

The initial studies were based on GE21/J11B5 engine characteristics (shown in Table 31) for nominal SLS standard day conditions. During the course of this study certain engine improvements were made and resulted in the Boeing designation of B5A and B5B engines. The first of these variations, the B5A, has 5% higher supersonic airflow, increased specific thrust, reduced sfc's and boattail drags, and a 295 kg (650 lb) pod weight reduction. The second, the B5B, has a lower BPR (0.25 versus 0.35) relative to the B5A which results in 8% higher supersonic thrust, 2% higher subsonic sfc's, and 3% increase in pod weight. A small increase in inlet diameter and overall length causes a +0.001 increase in cruise drag coefficient (M = 2.32) and a 0.0001 reduction in transonic drag coefficient (M = 1.1) for these engines.

The progressive engine improvements were consolidated in a new GE engine definition, the GE21/J11 Study B9. An improved airflow schedule for the B9 engine was identified which was well-matched to the Boeing axisymmetric inlet supply airflow. The GE21/J11B9 engine has the same BPR as the B5B engine but a lower third-stage FPR (1.36 versus 1.48) and a higher cruise airflow. These B9 characteristics result in an increased supersonic cruise thrust (≈4%) and a lower subsonic cruise sfc (≈2%). Supersonic climb thrust varies from -10% at M = 1.1 to +13% at M = 2.0, while supersonic climb sfc varies from -1% at M = 1.1 to +1% at M = 2.0. A comparative tabulation of the GE21/J11 Study B5, B5A, B5B, and B9 engines are shown in Table 32 for a supersonic cruise condition.

246

Table 31. GE21/J11 Study B5 Characteristics.

SLS Standard Day Conditions

Total Corrected Engine Airflow kg/sec (lb/sec)	317.5	(700)
Cycle Pressure Ratio (Nominal)	17.30	
Bypass Ratio	0.35	
Net Installed Thrust, N (lb)	265,630	(59,720)
Net Installed sfc, kg/hr/N (lb/hr/lbf)	0.122	(1.19)
Estimated Dry Weight, kg (lb)	5806	(12,800)
Maximum Envelope Diameter, cm (in.)	200.1	(78.80)
Overall Length, cm (in.)	682.5	(268.70)

Table 32. GE21/J11 Engine Comparisons.

Altitude = 16,319 m (53,540 ft)
Mach = 2.32
Standard Temperature = ISA +8° C (+14.4° F)
$W2R_{SLS}$ = 317-349 kg/sec (700-770 lb/sec)

Engine Type	B5		B5A		B5B		B9	
Thrust N (lb)	73,390	(16,500)	79,840	(17,950)	86,290	(19,400)	90,070	(20,250)
sfc kg/hr/N (lb/hr/lbf)	0.142	(1.386)	0.138	(1.355)	0.138	(1.355)	0.137	(1.340)
BPR	0.35		0.35		0.25		0.25	
(P/P) Fan 2nd Blk	1.48		1.48		1.48		1.36	
$W2R_{2.32M}$ kg/sec (lb/sec)	214	(472)	224	(494)	224~	(494)	231	(510)
Engine Weight kg (lb)	5806	(12,800)	5466	(12,050)	5693	(12,550)	5693	(12,550)

Figure 124 shows how the improvements in the B5 cycle, and the resultant B9 definition, are reflected in the airplane range capability. The cycle changes included increases in supersonic cruise airflow, and consequently improvements in inlet/engine airflow matching characteristics. The airflow schedule of the B9 engine is well matched to the current inlet definition over most of the operating range.

Installed Engine Performance and Weight

Figures 125 through 127 compare the installed thrust and sfc of the B9 with the three B5 variants. The data show the B9 to have improvements relative to the B5(B), with the exception of lower supersonic climb thrust to Mach 1.8.

The B9 geometry is essentially the same as the B5, with the exception of small changes in the nozzle external lines. The installed performance data do not reflect any change in nozzle drag relative to the B5(B).

The propulsion pod weight for the GE21/J11B5 and B9 engines at the 317 kg/sec (700 lb/sec) baseline size is shown in Table 33.

Inlet/Engine Airflow Match

Concurrent with this cycle selection study, an inlet design study was in progress, under the sponsorship of NASA-Langley. Figure 128 shows the mass flow characteristics of this inlet and how it matches the demand flow of the B9 engine. Inlet mass flow free-stream area to local flow area ratio is plotted versus local Mach number for a free-stream design Mach number of 2.4. The inlet captive mass flow is shown as a solid line and the flow available to the engine is shown as a dashed line. The increment between these curves represents the bleed, vortex valve control flow, and leakage. The airflow schedule of the B9 engine is well-matched to the current inlet definition over most of the operating range. A small down-trim of airflow in the transonic flight regime is required to provide a fully matched definition.

Mission Analysis Results

Through the process of iterative cycle change and evaluation of airplane range effects, the B5 engine evolved into the B9, with a resultant range improvement of over 852 km (260 nmi) (see Figure 124). The improvements in engine specific weight and the reduced engine size requirements resulted in a total reduction in propulsion system weight of approximately 6804 kg (15000 lb). This weight reduction has significant implications in terms of the ability to balance the airplane, and minimize flutter stiffness penalties.
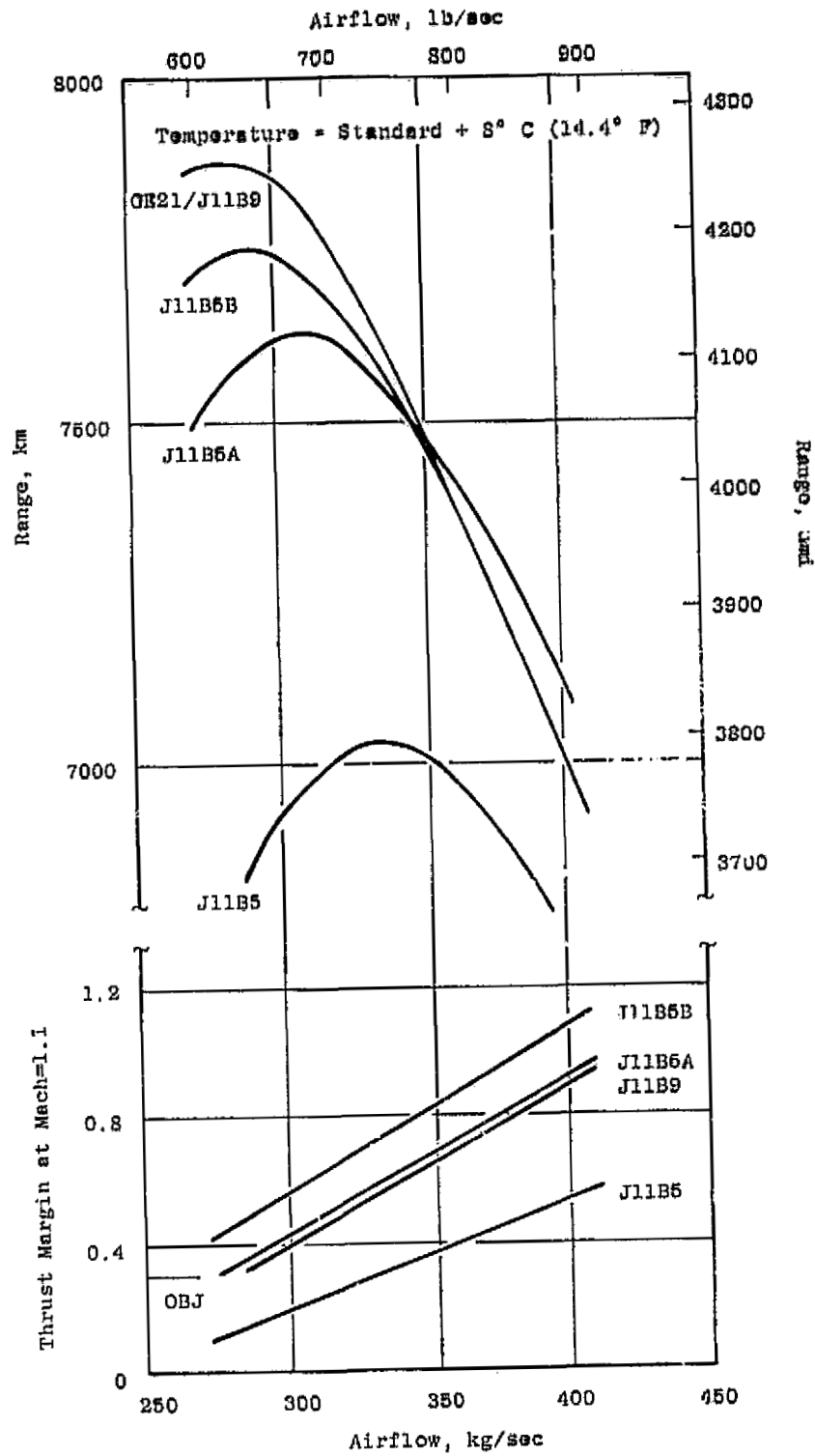
Figure 124. Performance of GE21/J11 Variants.
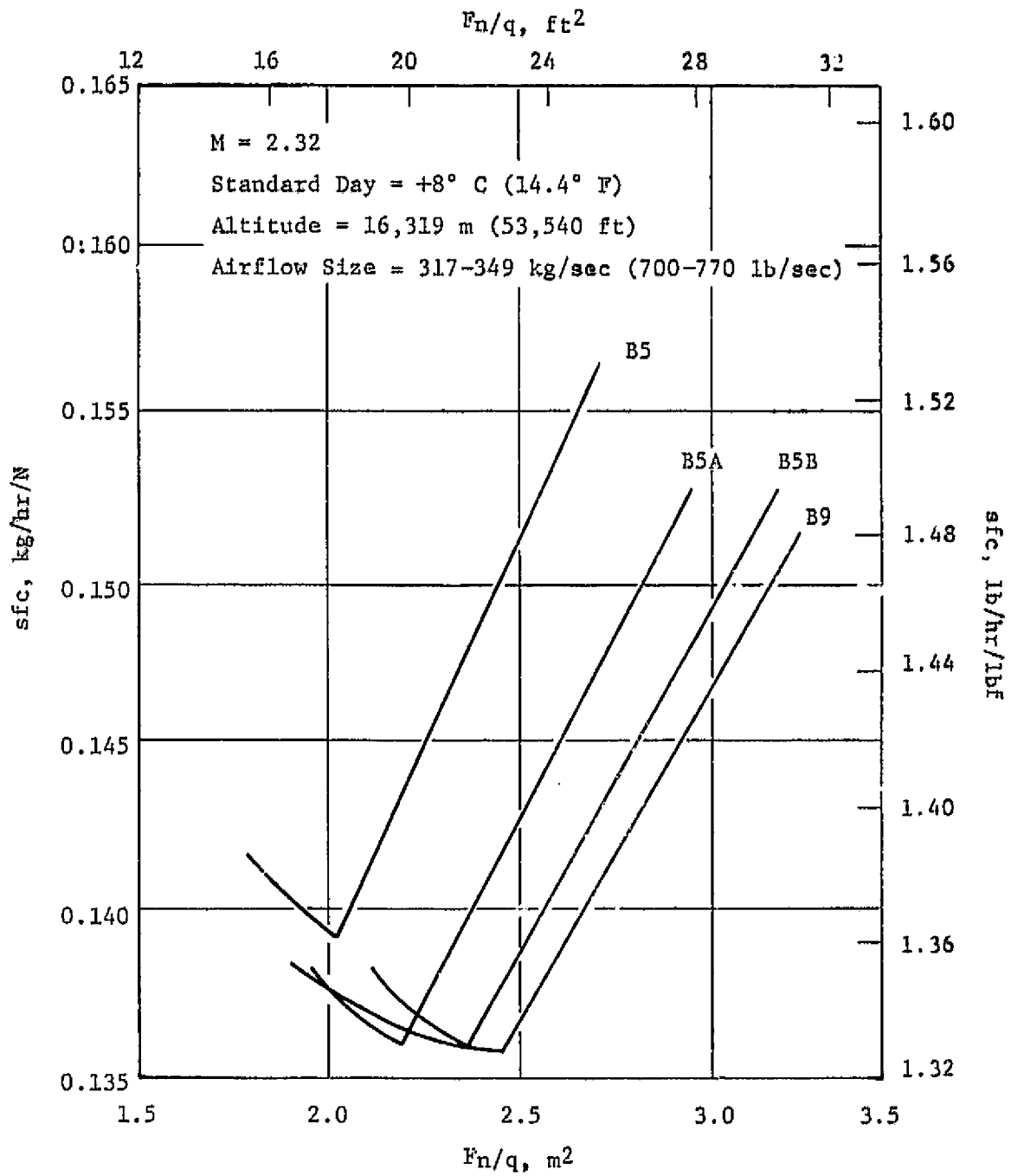
Figure 125. Installed Thrust Performance Comparisons of GE21/J11 Engines.
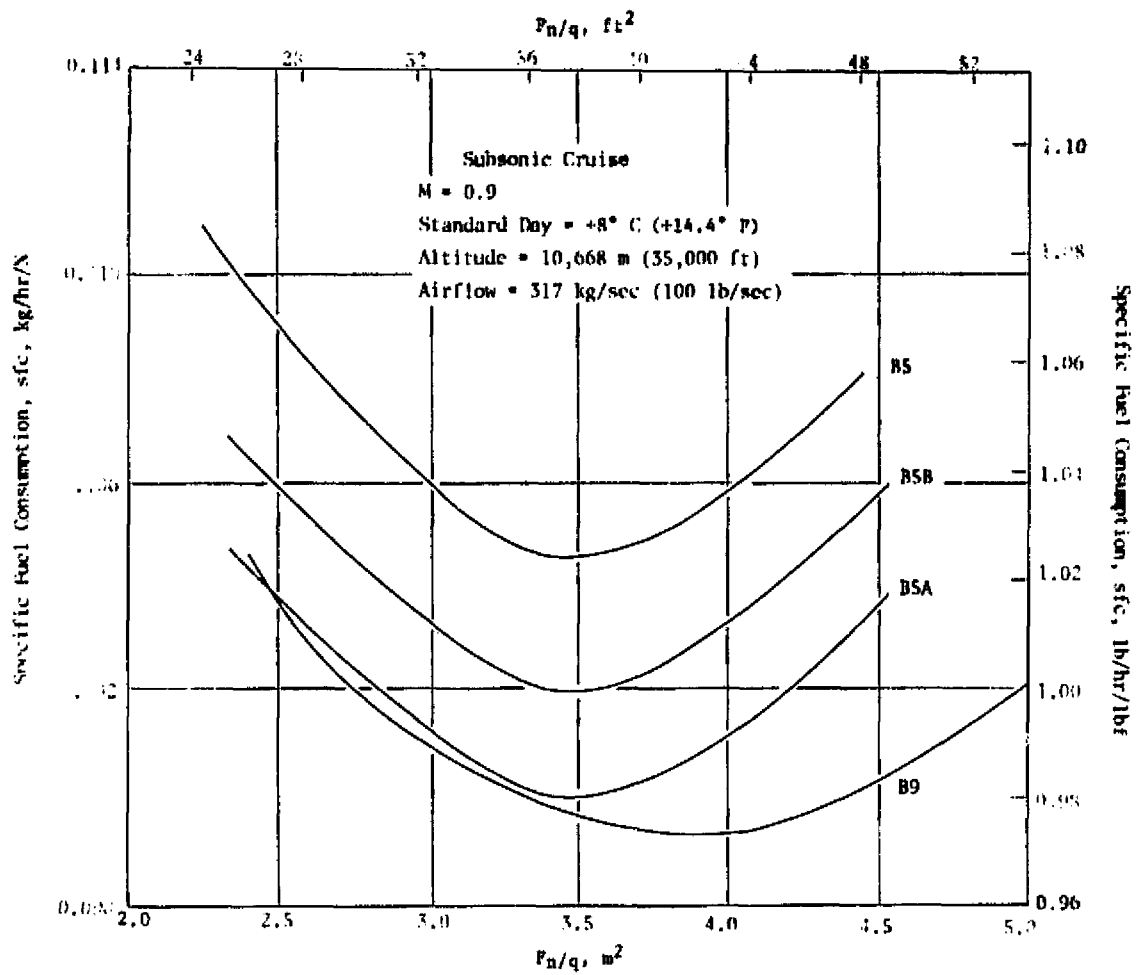
Figure 126. Installed SFC Performance Comparisons of GP21/J11 Engines.
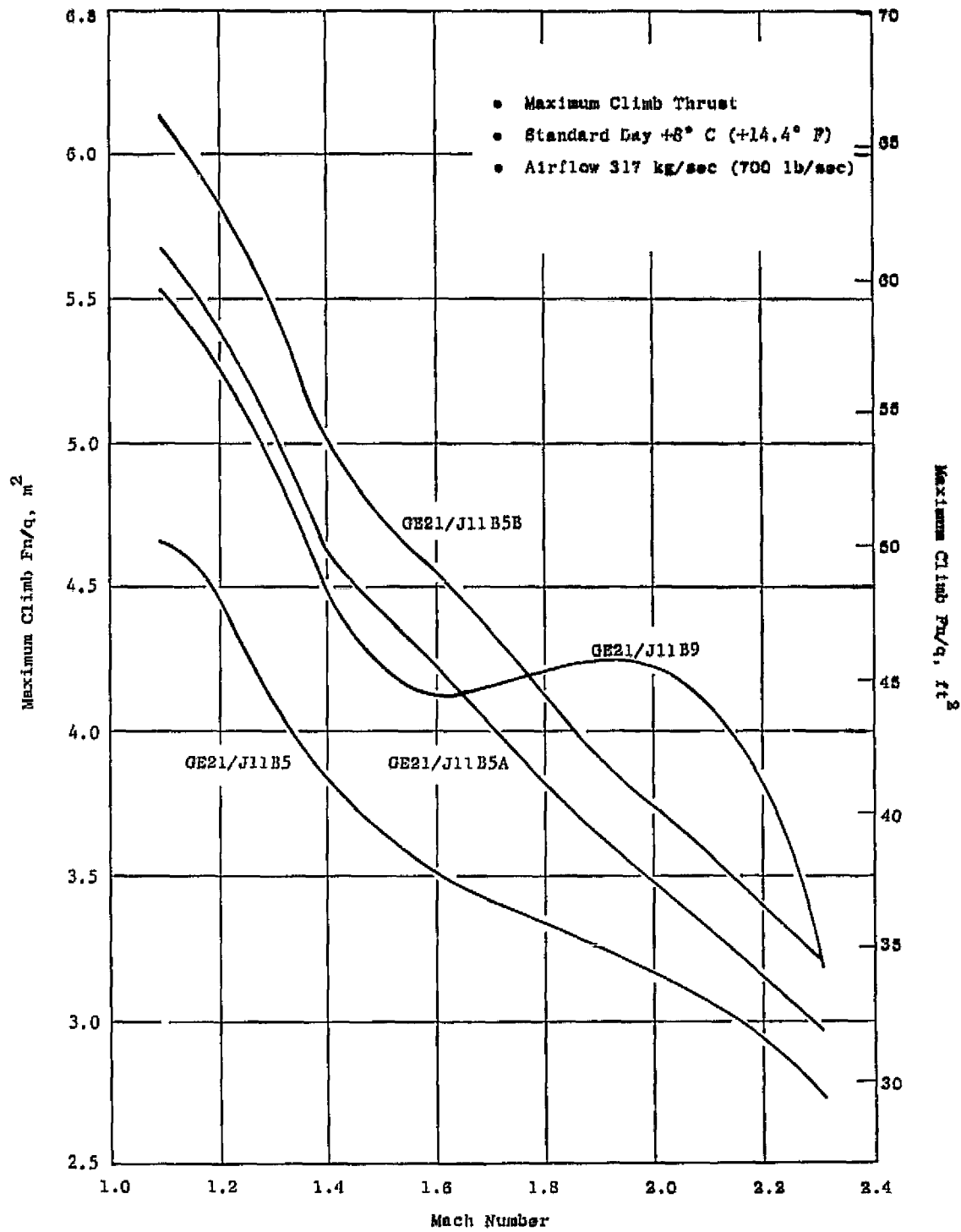
Figure 127. Installed Climb Thrust Performance Comparisons.

Table 33. GE21/J11B5 and B9 Pod Weights.

Baseline Airflow = 317 kg/sec (700 lb/sec)

	kg	(lb)
Engine and Nozzle	5806	(12,800)
Inlet (2.4-1)	1256	(2770)
Cowl	395	(870)
Support Structure	390	(860)
Total Pod	7847	(17,300)
Total Airplane	31,388	(69,200)
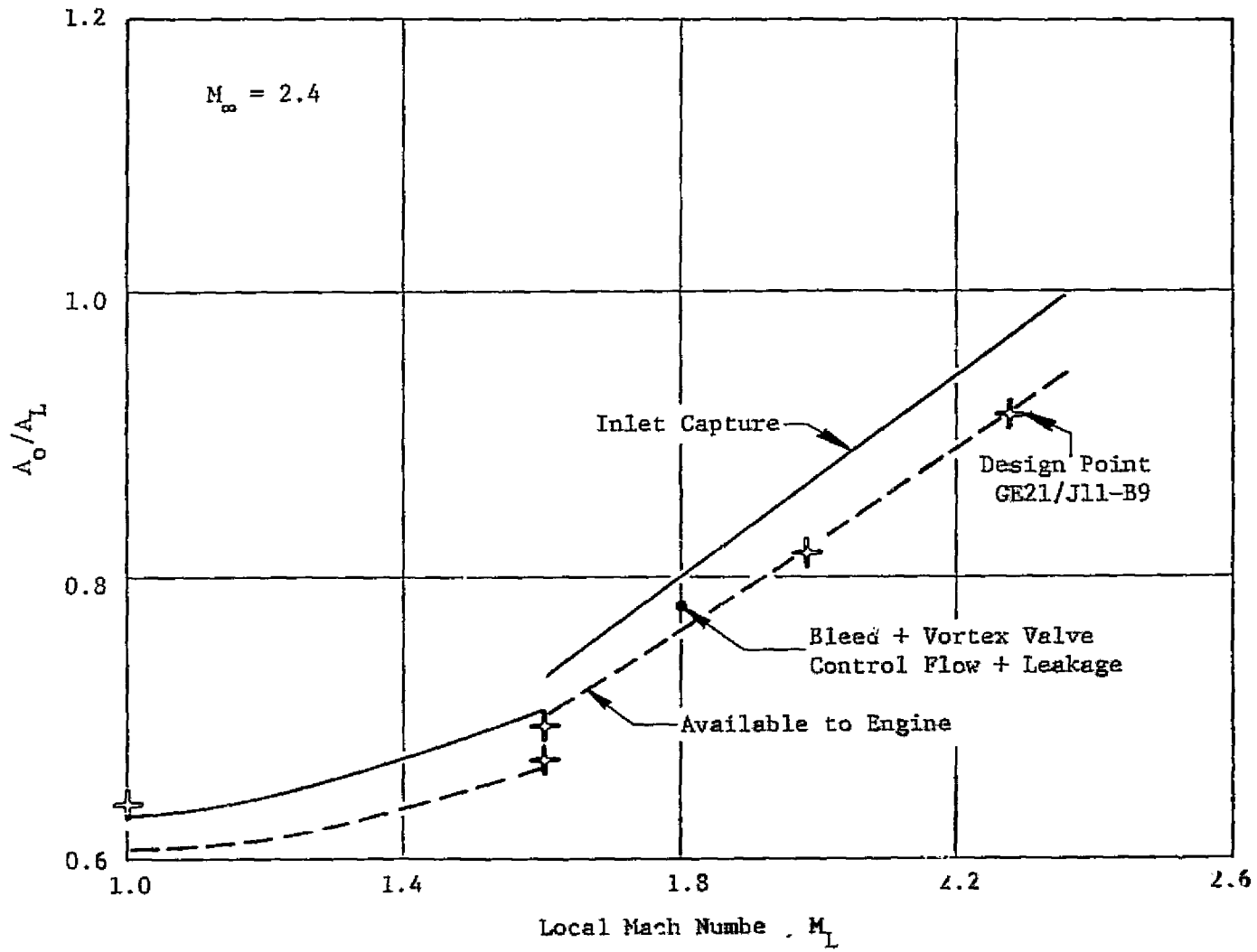
Figure 128. Inlet Mass Flow Characteristics.

A significant factor in the range improvement and engine size reduction was the increase in supersonic cruise thrust. In part, this was accomplished by an 8% increase in cruise airflow. The flow increase, in turn, resulted in improved inlet/engine matching, thereby, avoiding further inlet complexity and weight penalties.

The subsonic cruise efficiency of the B9-powered airplane is poorer than the supersonic cruise efficiency. It is desirable that means of improving the relative subsonic efficiency, without sacrificing total design mission range, should be pursued.

The B9 has a maximum range of capability of 7880 km (4225 nmi) at 283 kg/sec (625 lb/sec), which is an increase of 852 km (460 nmi) plus a reduction in engine size of 57 kg/sec (125 lb/sec) relative to the B5-powered airplane. The reduced B9 engine size is a result of the improved supersonic cruise thrust. Climb thrust at $M = 1.1$ is lower than for B5 and, therefore, the transonic thrust margin is lower. However, the thrust margin still exceeds the 0.3 objective at the size for maximum range.

The B9 engine improves both the subsonic and supersonic range factors, relative to the B5 engine, due to the lower subsonic sfc and larger supersonic cruise thrust. (See Figure 129).

Table 34 compares the detailed mission breakdowns of B9 and B5-powered airplanes at 294 kg/sec (650 lb/sec) size. This engine size was chosen because it is the closest available data point.

Nacelle Design

The installation design study identifies a structural arrangement for supporting the engine-plus-nozzle assembly and the inlet, from the upper cowl segment, and the related means of supporting the entire pod assembly from the airplane (wing structure. An arrangement for the aircraft and engine accessories is also defined. The nacelle design discussed herein is shown in Figure 130, and a reduced copy of the complete design layout is shown in Figure 131.

The layout shown in Figure 131 is based on the initially defined B5 engine forward mount attach points, which were specified as being at the 1.57 rad (90°) and 4.71 rad (270°) radial locations (i.e., on the horizontal centerline when viewed from the front).

In the course of the study, radial location requirements were varied allowing the mounts to be raised as much as 0.523 rad (30°) above the horizontal, without an engine weight penalty.

It was concluded that the 0.523 rad (30°) relocation would provide satisfactory engine and inlet support, improve engine access, and provide a significant weight saving. The relocation would require that the lower cowl
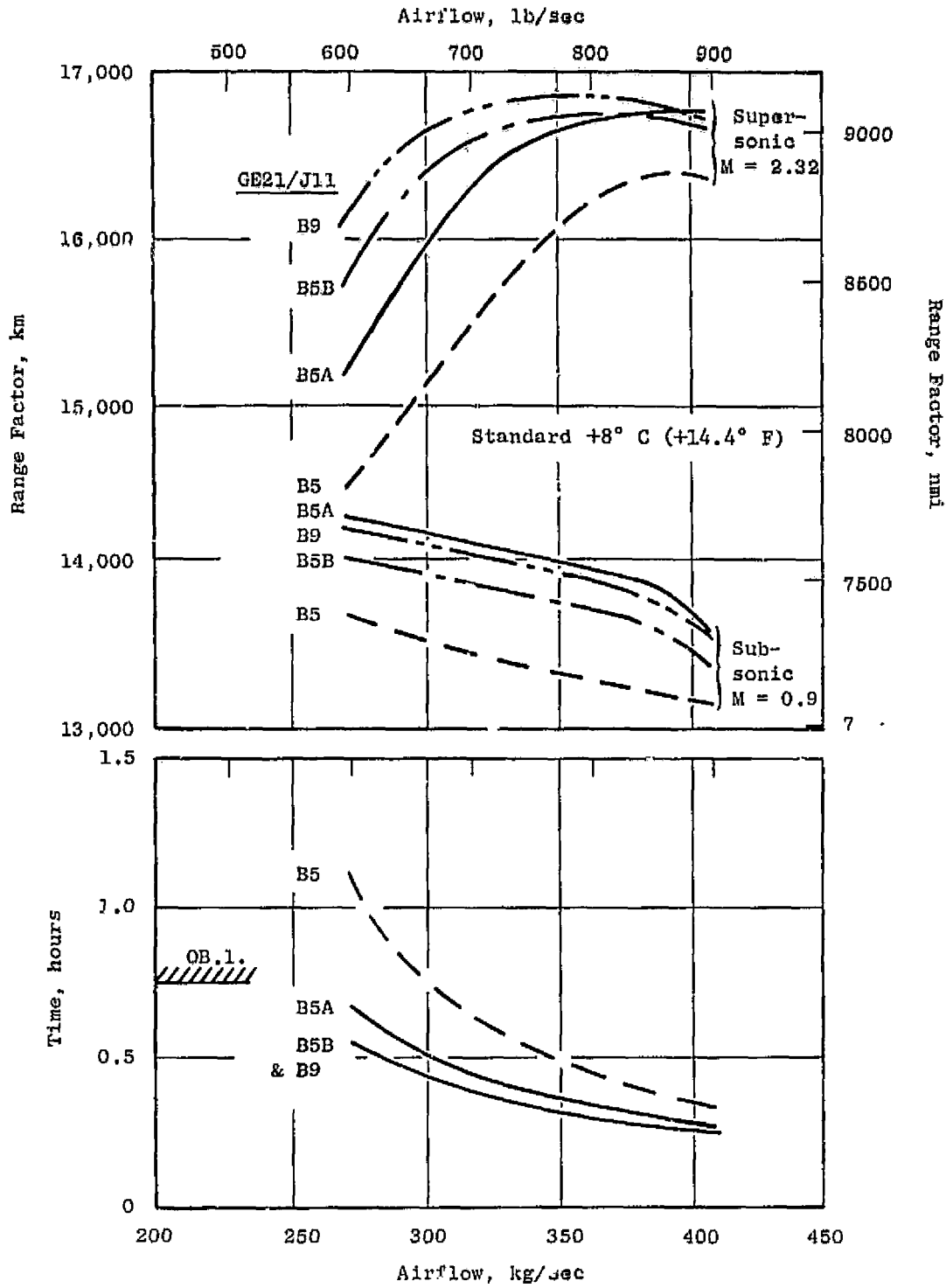
Figure 129. Range Factor Performance of GE21/J11 Variants.

Table 34. Mission Breakdown B9 Versus B5.

Temp = Std +8° C (+14.4° F)
No. Pass = 273
Airflow = 295 kg/sec (650 lb/sec)

	GE21/J11B9		GE21/J11B5	
Max. TOGW kg (lb)	340,200	(750,000)	340,200	(750,000)
OEW kg (lb)	151,942	(334,970)	152,192	(335,520)
Engine Pod Wt. kg (lb)	28,599	(63,050)	28,849	(63,600)
OEW-Eng Pod Wt kg (lb)	123,343	(271,920)		(271,920)
Range km (nmi)	7871	(4250)	6886	(3718)
Taxi and TO Fuel kg (lb)	2374	(5234)	---	(5234)
Climb (Subsonic to M = 0.85)				
Time, hr	0.126		0.127	
Fuel, kg (lb)	9617	(21,201)	9488	(20,917)
Dist, km (nmi)	96	(52)	94	(51)
Climb (Super/Transonic to Cruise Alt)				
Time, hr	0.324		0.657	
Fuel, kg (lb)	23,765	(52,393)	40,129	(88,467)
Dist, km (nmi)	559	(302)	1091	(589)
Cruise at M = 2.32				
Dist, km (nmi)	6856	(3702)	5350	(2889)
RF, km (nmi)	16,557	(8940)	14,883	(8036)
L/D	8.80		8.45	
sfc, kg/hr/N (lb/hr/lbf)	0.1364	(1.335)	0.1456	(1.425)
SF_2, km/kg (nmi/lb)	0.0816	(0.020)	0.07308	0.0179
Descent + Approach				
Time, hr	0.358		0.361	
Fuel, kg (lb)	1966	(3893)	1737	(3830)
Dist, km (nmi)	390	(200)	361	(195)
Reserves Total, kg (lb)	21,945	(48,380)	22,142	(48,814)
Fuel for 6%, kg (lb)	8426	(18,576)	8399	(18,517)
Fuel for 260 nmi, kg (lb)	6464	(14,251)	6742	(14,866)
Fuel for 0.5 hr Hold, kg (lb)	7055	(15,553)	7000	(15,432)
Subsonic Cruise (Alt = 37,800 ft)				
M = 0.9				
RF, km (nmi)	14,118	(7623)	13,560	(7322)
L/D	14.52		14.52	
sfc, kg/hr/N (lb/hr/lbf)	0.1023	(1.001)	0.1065	(1.042)
$RF_M = 0.9 / RF_M = 2.32$	0.85		0.91	

258

Figure 130. Installation of AST Nacelle on GE21/J11B5 Engine.

ORIGINAL PAGE IS
OF POOR QUALITY

Figure 131.   GE21/J11B5 Engine Nacelle

E21/J11B5 Engine Nacelle.
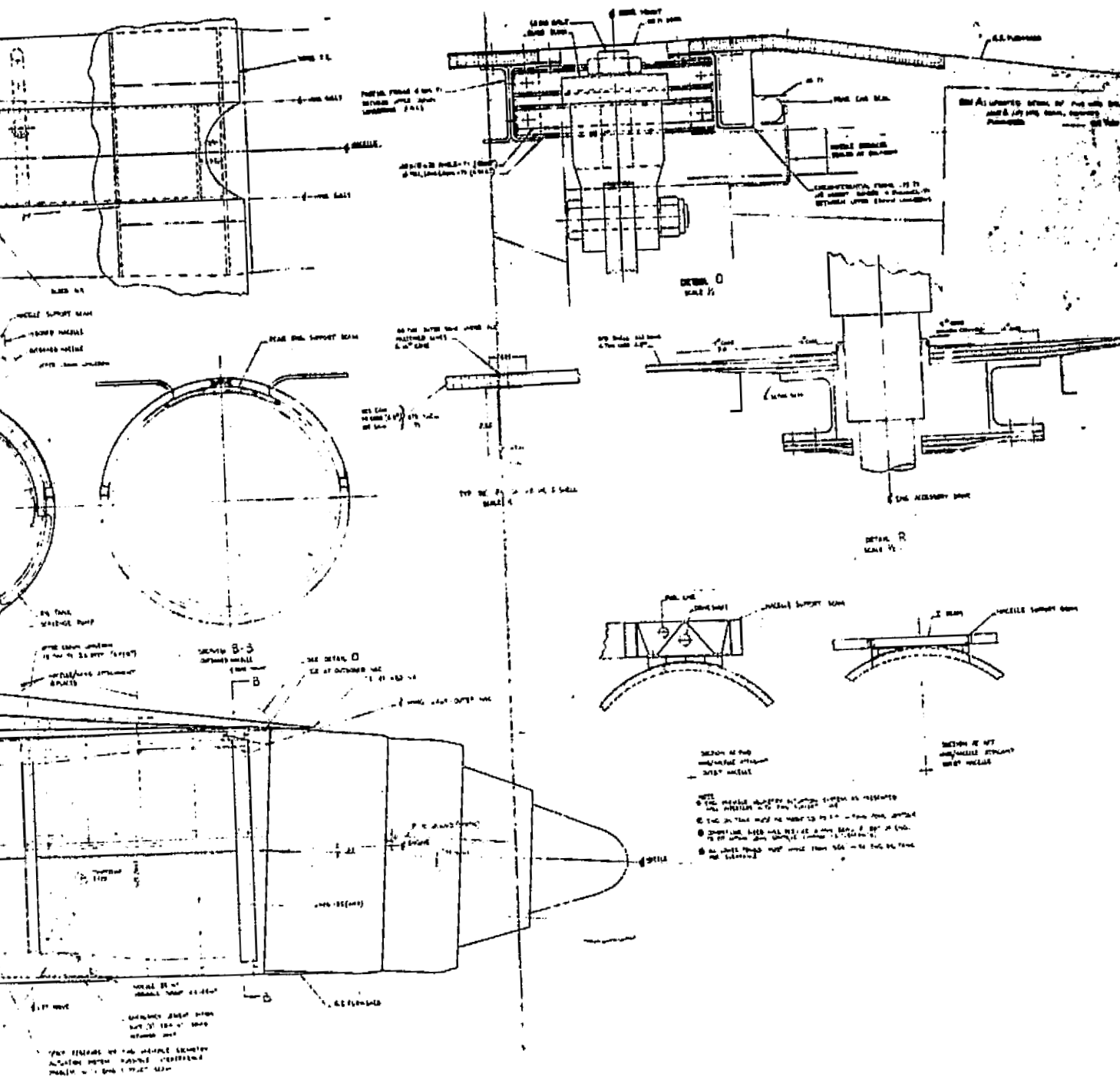
segment be split into two parts thus adding one longitudinal seal (see Figure 132). Figure 133 shows an improved hinge and latch system which subsequently was considered also.

To initiate the nacelle design study, certain design criteria and ground rules were established (listed in Table 35). Structural design, environmental control system, and engine-driven accessory location are the main items considered for the design criteria and ground rules.

The nacelle design structural loading factors are the same as the 1971 SST design. The support structure is designed for strength only, since stiffness requirements have not yet been established.

Since a specific environmental control system (ECS) design has not been established for the engine/airplane definition, a minimum system has been assumed consisting of a single air-to-air heat exchanger and an air-to-liquid exchanger to precool the engine bleed air. It is assumed that secondary heat exchangers will be located outside the nacelle and that a boost compressor will not be required. An ejector is not required for gr' ' operation of the heat exchanger in the nacelle. Engine-driven fuel and h: lic system components can be located outisde of the nacelle. The engir. .rication system will remain intact on the engine.

The pod geometry already established on the basis of prior aerodynamic and performance analysis studies would be retained to the maximum extent, consistent with the structural requirements and assumed freedom of location of engine accessories.

Nacelle Description

The nacelle installation shown in Figures 130 and 131 consists of an upper cowl segment, which provides the principal support for the engine-plus-nozzle assembly and for the inlet and a lower cowl segment, which completes the enclosure. Titanium is used throughout the structure. The upper cowl segment is attached to a pair of fore and aft support beams, which carry the pod load into the wing structure. The cowl-to-beam attachment is through four pedestal fittings.

The engine front mount consists of a pair of uniball fittings located on the fan case rear frame. For the layout shown in Figure 131, these fittings are located on the engine horizontal centerline. A deep section yoke, integral with the upper cowl structure, carries the front mount loads to the second and third pedestal fittings. The front mount system reacts the engine thrust, side, torque, and a major portion of the vertical loads. The side load is taken on one side only.

The engine rear mount is designed to react vertical loads only. The engine-plus-nozzle center of gravity (c.g.) is located only a short distance aft of the front mount plane, therefore, the rear-mount vertical loads are
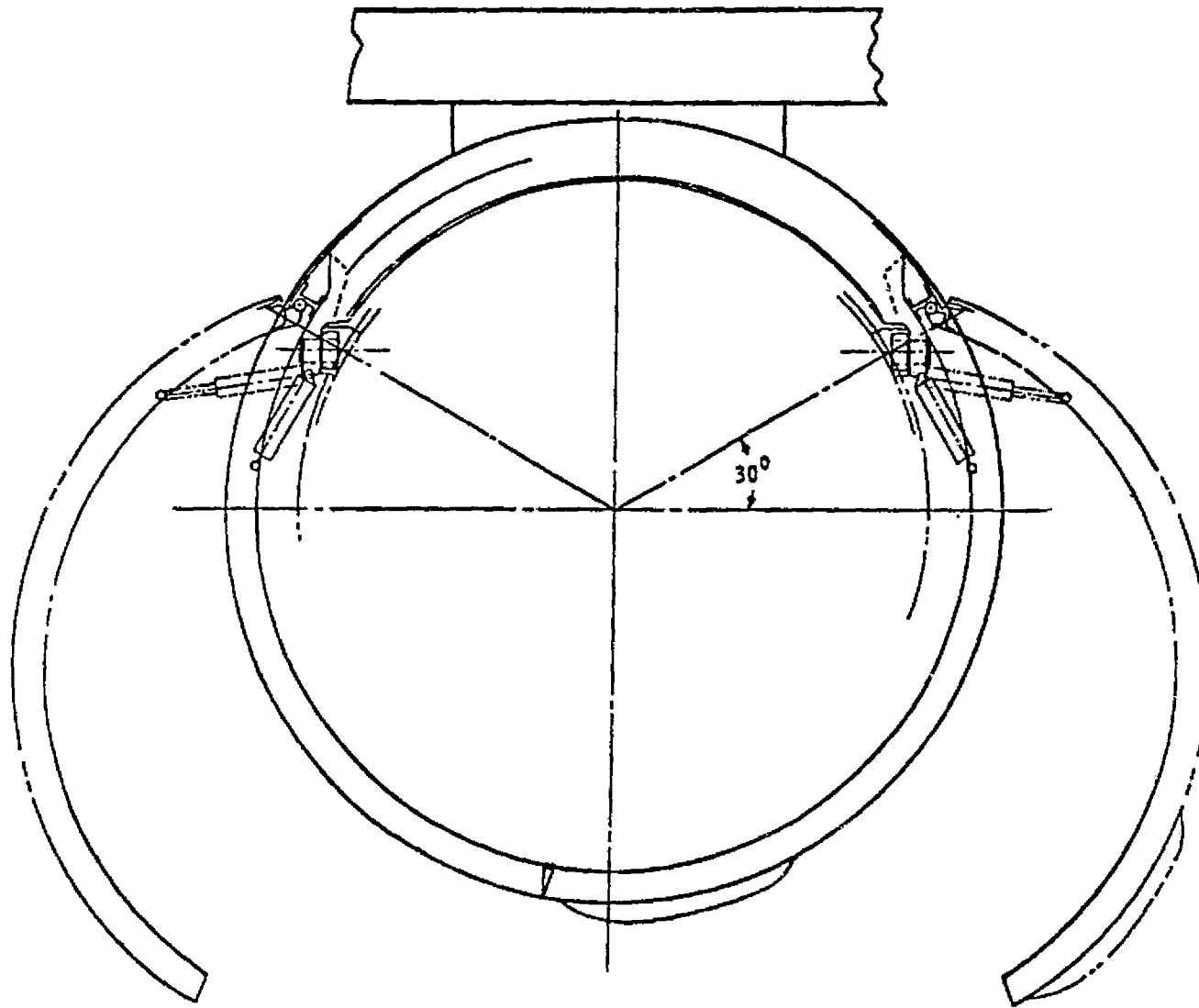
Figure 132. GE21/J11B5 Nacelle Installation Forward Mounts at 30°.
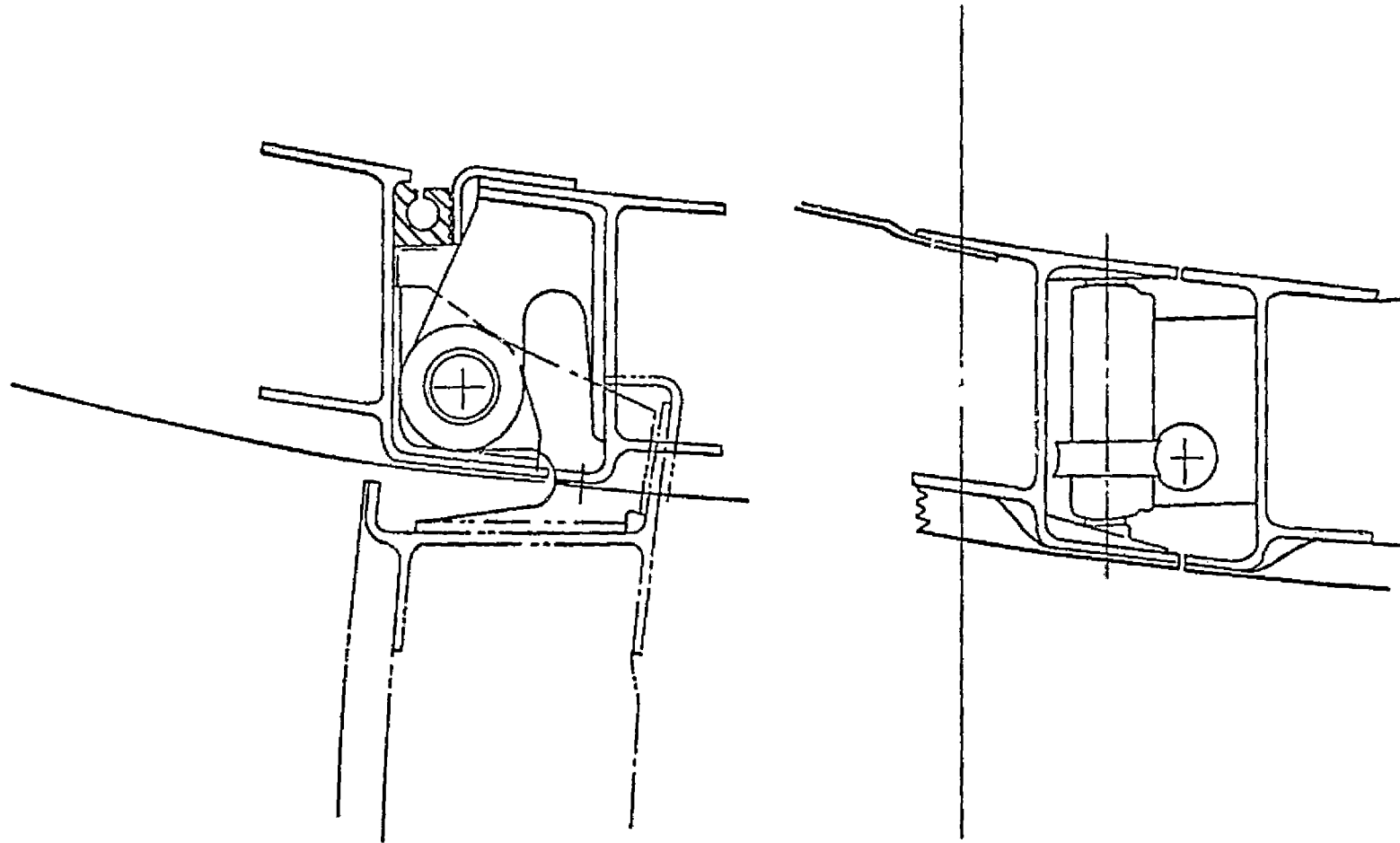
Figure 133. GE21/J11B5 Nacelle Installation Cowl Hinge and Latch.

Table 35. Nacelle Study Ground Rules and Assumptions.

1. Strength Designed Pod Support Structure

2. No ECS Boost Compressor Required

3. ECS Ram Air-to-Transport Fluid Heat Exhchanger Located
   in Body

4. No Ejector Required for Ground Operation of Heat Exchanger
   in Nacelle

5. Engine Lube System Remains Intact on ...gine

6. Engine Fue¹ and Hydraulic Systems Components Can Be
   Located Outside Nacelle

7. Structural Loading Factors Same as 1971 SST

relatively low. A pair of integral fore and aft cowl beams, extending from the front mount yoke to the rear mount plane, carry the rear mount loads forward into the pedestal fittings.

The upper cowl structure consists of a honeycomb sandwich outer cover, with circumferential frames. Full-length longitudinal members are provided at the hinge and latch lines for mating with the lower cowl segment. Short longitudinal members are also provided between the front two circumferentials to distribute the inlet loads into the structure.

The lower cowl structure is similar to the upper except for the yoke and beam mount support elements. Latch and hinge fittings are provided at each circumferential member location to join the upper and lower cowl segments. Since the nacelle is pressurized, seal elements are incorporated along the longidudinal mating members. Circumferential seals are also provided fore and aft.

A top centerline power takeoff (PTO) shaft penetrates the front mount yoke and provides the drive for the engine fuel pump, hydraulic pump, tach generator, and other engine accessories which are located in the wing cavity forward of the engine front frame. The aircraft accessories, located adjacent to the engine accessories, are driven from the same PTO. Provisions are made for disconnecting the PTO shaft and the engine fuel, hydraulic, and electric lines at the top of the nacelle to facilitate engine removal.

The engine lube pump and related system components are engine mounted. The environmental control system (ECS) heat exchanger (which precools the engine bleed air) is mounted aft of the lube pump. Cooling air is taken from the inlet, through the nacelle and heat exchanger, and ducted from the heat exchanger to a discharge nozzle. The nozzle, with a variable throat for flow control, constitutes the base of the fairing over the lube pump.

Structural and Weight Analysis

The preliminary sizing of the structural cowl was based on the load cases presented in Table 36. The design weight used for the engine plus inlet plus cowl was 7507 kg (16,550 lb) with center of gravity 465 cm (183.3 in.) aft of the inlet lip, 50.8 cm (20 in.) aft of the forward engine mounts. The inlet weight used was 1256 kg (2770 lb) with c.g. 162 cm (64 in.) back from the inlet lip. Nacelle pressure differentials considered in the sizing are presented in Table 37.

The material selected for the honeycomb shell, frames and longerons was titanium. The estimated design temperature for the cowl is 204° C (400° F).

A honeycorb shell with hoop tension frames and a closed box horseshoe section picking-up the forward engine mounts is the concept selected for sizing. The core depth was selected to provide adequate stability allowables

Table 36. Design Load Cases.

Condition	Limit Design Factor	Ultimate Design Factor
1. Landing	4 W	6 W
2. Landing Maneuver	4 W + 1 T	6 W + 1.5 T
3. Forward Thrust	1 W + 1 T	3 W + 3 T
4. Yaw	1.66 W Sideways	2.5 W Sideways
5. Crash	6 W Forward	9 W Forward
6. Engine Seizure	1 M_r	1 M_r

W = Installed Weight
T = Thrust
M_r = Engine Rolling Moment

1. Reacted by One Side of Cowl Only.

Table 27. Cowl Pressure Differentials.

Condition	$P_{Max.}$ N/m^2(psi)	$[P_{Max.}-P_A]$ N/m^2(psi)
Mach = 2.4 Climb Placard 16,764 m (55,000 ft) Altitude	124,794 (18.1)	103,421 (15.0)
Mach = 2.4 Upset Dive 14,936 m (49,000 ft) Altitude	166,162 (24.1)	153,752 (22.3)
Mach = 2.4 Climb Placard with Full Engine Stall (Hammer Shock)	161,336 (23.4)	151,683 (22.0)

P_A = Ambient Pressure

The Latter Two Conditions Are Infrequent (Limit) Transients.

for the curved panels of the horseshoe. The core depth was maintained along the entire length of the cowl. The field core densities were picked to:

1. Provide sufficient transverse shear strength for the loads being carried around the curved box sections and

2. Provide sufficient transverse shear strength to carry pressure loads to the hoop tension frames. The minimum density core allowed was 78.5 kg/m^3 (4.9 lb/ft^3). Dense core was used under all fastener lines along with local outside skin pad-ups to assure no knife edges bear against the fasteners.

The aft engine mount was treated as a link which can transmit only vertical load into the cowl. With the c.g. of the system relative, close to the forward engine mounts, the load transmitted by the aft mount is small; less than 8896 N (2000 lbs) at one g. As the trailing edge wing depth in the vicinity of the aft engine mount is too small to permit a direct transfer of load into the wing at the mount, a frame-longeron system was used in the cowl to carry these aft mount loads forward to a deeper section of the wing.

Although detailed external inlet-nacelle-nozzle airload information was not available, an attempt was made, based on available data, to estimate these loads. The indications are that any impact to the total cowl weight would be small.

The weight evaluation process made full use of the part definitions provided by the drawings (Figures 131 and 132) and reflect sized structual elements.

Weight calculations were made of all defined parts with allowances for nonoptimum elements, fasteners, clips, doublers, etc. Representative weight allowances were selected for undefined elements including latch/lift drive system, burst protection, insulation, etc.

A weight statement for the nacelle structure is given in Table 38. In addition, the total propulsion pod weight would include the engine, nozzle, and inlet.

For the preferred forward mount location shown in Figure 131 [0.5235 rad (30°) above the horizontal], a weight reduction of 145 kg (320 lb) per pod was estimated.

The design was based on certain ground rules and assumptions which were favorable to low drag and simple internal nacelle systems. The remote location of the engine accessories creates certain problems with respect to ready accessibility, wing panel structural load paths, and engine certification and warranties. The impact of such changes in these initial ground rules and assumptions must be evaluated before a final concept can be adopted.

Table 38   Nacelle Weight Statement.
(per Pod)

	Subtotal		Totals	
	kg	(lb)	kg	(lb)
Total Nacelle Structure			1105	(2440)
Upper Segment Structure			185	(409)
Outer Panel	129	(285)		
Internal Structure	56	(124)		
Lower Segment Structure			197	(434)
Outer Panel	145	(320)		
Internal Structure	52	(114)		
Forward Mount (Yoke)			264	(583)
Outer Panel	80	(177)		
Inner Panel	66	(146)		
Internal Structure	36	(80)		
Fittings	18	(40)		
Caps	64	(140)		
Lift/Latch System			25	(56)
Drive	7	(16)		
Lift System	4	(9)		
Latch System	14	(31)		
Pod Support Structure			253	(559)
Rear Mount Beams and Fittings	17	(38)		
Wing to Pod Fittings	14	(31)		
Beam (Wing) Strength	222	(490)		
Seals			9	(20)
Insulation and Firewall Allowance			41	(90)
Burst Protection Provisions			68	(150)
Landing Gear Up Landing Provisions			0	0
Emergency Descent Bypass Provisions			3	(6)
Heat Exchanger Nozzle Provisions			6	(14)
Diverter			36	(80)
Miscellaneous and Round-Off			18	(39)

The engine installation definition is lacking in the smaller but important details. Borescope access, fuel, hydraulic and wiring runs, actuation systems definitions, etc., must all be defined.

Technology Sensitivity Study

A sensitivity study was conducted on the B9 cycle, based on technology sensitivity factors provided by GE for various components. Adverse changes in component efficiencies, weight, and cooling flows were examined. For each change, GE provided an engine thrust, sfc and/or weight increment. These increments were evaluated in terms of loss in design range from the baseline level.

Figure 134 shows the airplane range sensitivities to increases in subsonic and supersonic sfc, and to increases in weight (balance not considered). Table 39 lists the component changes provided by GE and the resultant range loss increment. The study emphasizes the relatively strong influence of turbine cooling flow requirements and nozzle gross thrust coefficients when compared with other component efficiencies and engine weight factors.

It should be noted that the subsonic range losses are based only on the impact of increasing the cruise-to-alternate portion of the reserve fuel on the design mission and is not indicative of the relative importance of the subsonic efficiency in real-world airline operations. Therefore, Figure 134 should not be used as a final basis for defining optimum trades between subsonic and supersonic engine performance.

The AST studies have indicated that the major advantage of advanced engine technology stems from the projected high-cycle temperatures with low cooling flow penalties.

Summary

From the work described in this section a summary has been prepared below.

- An engine cycle was defined which matched the Boeing AST configuration and performance characteristics.

- The GE21/J11B9 has improvements relative to the B5, including higher cruise airflows.

- These B9 characteristics result in an increased supersonic cruise thrust and a lower subsonic cruise sfc.

- The B9 powered aircraft has a maximum range capability of 7880 km (4255 nmi) at 283 kg/sec (625 lb/sec), which is an increase of 852 km (460 nmi) relative to the B5 airplane. In addition, the

272
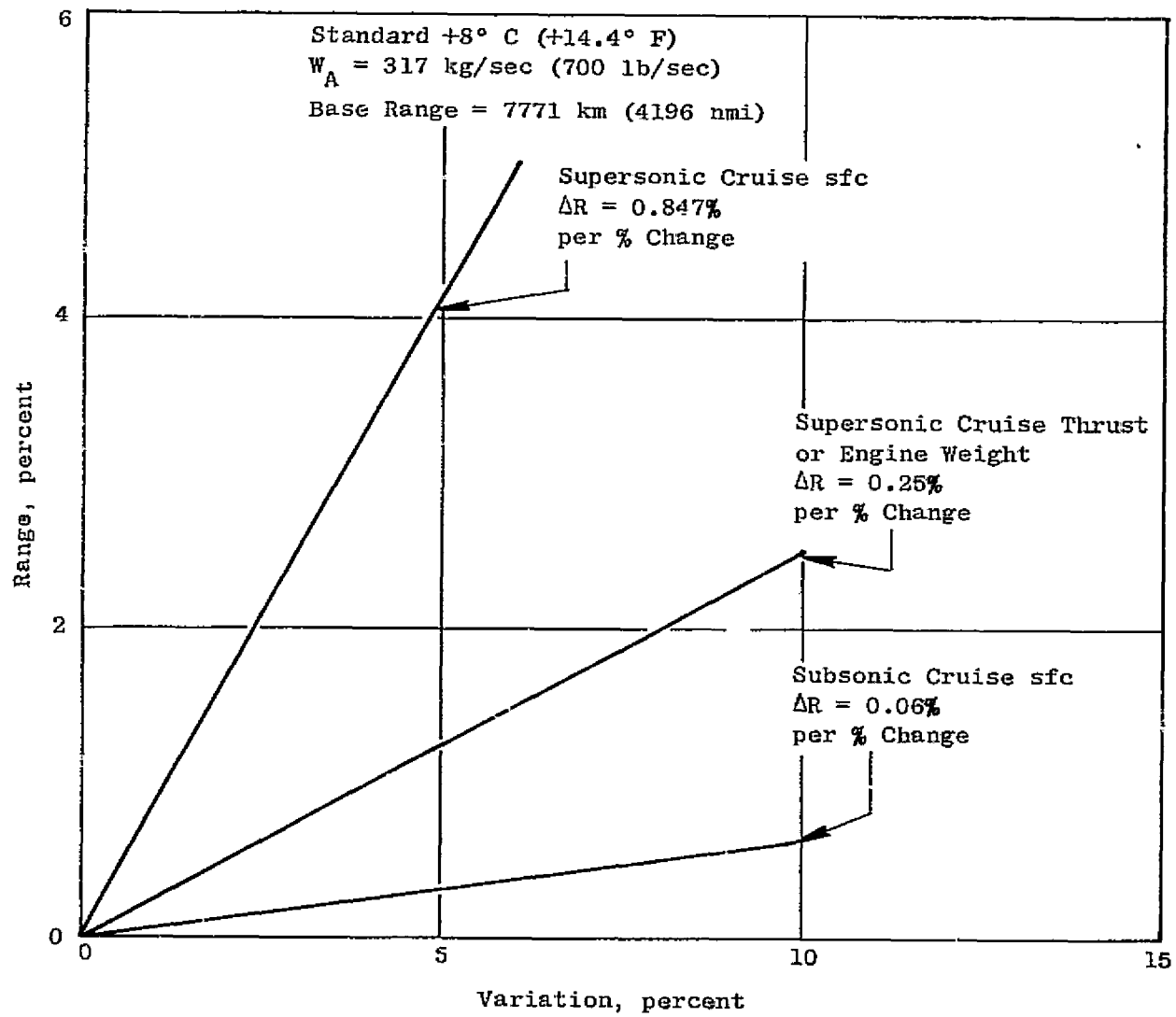
Figure 134. Range Sensitivities for the GE21/J11B9.

Table 39. Range Sensitivities, GE21/J11B9 Technology.

Base Range = 7771 km (4196 nmi)

Component or Item	ΔTech	Range Loss, km (nmi)			Range Loss (%)
		M = 2.32	M = 0.9	Total	Total
No. 1 Fan Block η	−0.01	27.6 (14.9)	1.8 (1.0)	22.4 (15.9)	(0.38)
No. 2 Fan Block η	−0.01	14.6 (7.9)	0.2 (0.1)	14.8 (8.0)	(0.19)
HP Comp η	−0.01	30.7 (16.6)	1.1 (0.6)	31.8 (17.2)	(0.41)
HPT η	−0.01	34.6 (18.7)	1.5 (0.8)	36.1 (19.5)	(0.46)
LPT η	−0.01	14.4 (7.8)	1.3 (0.7)	15.7 (8.5)	(0.20)
Turbine W_{Cool}	+2%	119.1 (64.3)	3.3 (1.8)	122.4 (66.1)	(1.58)
Cfg	−0.01	219.5 (118.5)	8.9 (4.8)	224.4 (123.3)	(2.94)
Fan Block Material (Composite Vs. Titanium)	−0.005η_f	15.2 (8.2)	0.9 (0.5)	16.1 (8.7)	(0.21)
Composite Structure	+1% Eng. Wt.	---- ----	---- ----	19.3 (10.4)	(0.25)

required B9 engine size is reduced as a result of the improved supersonic cruise thrust. Although the transonic thrust margin is lower, it still exceeds the 0.3 objective at the size for maximum range.

- Through the process of iterative cycle change and evaluation of airplane range effects, the B5 engine evolved into the B9. Improvements in engine specific weight and the reduced engine size requirements resulted in a total propulsion reduction in total propulsion system weight. This weight reduction has significant implication in terms of the ability to balance the airplane and minimize flutter stiffness penalties.

- A significant factor in the range improvement and engine size reduction was the increase in supersonic cruise thrust. This was accomplished, in part, by an 8% increase in cruise airflow. In turn, the flow increase resulted in improved inlet/engine matching thus avoiding further inlet complexity and weight penalties.

- An improved airflow schedule for the B9 engine was identified which was well-matched to the Boeing axisymmetric inlet supply airflow.

- The nacelle design defined in this study is considered a representative, efficient, low-drag concept. It can well serve as a baseline definition for further development, trade, and evaluation studies.

- The installation design study resulted in a satisfactory definition of a structural arrangement for supporting the engine-plus-nozzle assembly and the inlet from the upper cowl segment and the related means of supporting the entire pod assembly from the airplane (wing) structure.

- A satisfactory arrangement for the aircraft and engine accessories was defined also.

- It is concluded that the relocation of the forward mount to a position 0.523 rad(30°) above the horizontal would provide satisfactory engine and inlet support, improve engine access, an; provide a significant weight saving. The relocation would require that the lower cowl segment be split into two parts.

- The use of two lower cowl segments, with the raised hinge lines, provides better engine access.

- For the preferred forward mount location shown in Figure 132 (0.5235 rad or 30° above the horizontal), a weight reduction of 145 kg/pod (320 lb/pod) was estimated.

- The AST studies have indicated that the major advantage of advanced engine technology stems from the projected high-cycle temperatures with low cooling flow penalties.

- A sensitivity study emphasizes the relatively strong influence of turbine cooling flow requirements and nozzle gross thrust coefficients.

Recommendations

The recommendations for continued development of engine installation and integration technology are listed in Table 40. A general recommendation pertaining to engine cycle technology is also noted. The AST studies indicate that the major advantage of advanced eng.ie technology stems from the projected high cycle temperatures with low cooling flow penalties. Developments related to this capability should be emphasized.

Means of improving the relative subsonic efficiency, without sacrificing total design mission range, should be pursued.

The remote location of the engine accessories creates certain problems with respect to ready accessibility, wing panel structural load paths, and engine certification and warranties. The impact of such changes in these initial ground rules and assumptions must be evaluated before a final concept can be adopted.

The engine installation definition is lacking in the smaller, but important details. Borescope access, fuel, hydraulic and wiring runs, actuation systems definitions, etc., must all be defined further to ensure a realistic and compatible definition.

276

Table 40. Technology Requirements, Installation
and Integration.

● Control Concepts
     Engine ⎫
              ⎬ Integrated System
     Inlet ⎭
     Flight Controls Integration

● Inlet/Engine Compatability

● Nozzle Installation
     Boattail Drag and Int.rference Effects
     Internal Performance
     Inlet Bypass Air Capacity and Performance Effects
     Thrust Reversing

● ECS Integration

● High Cycle Temperatures with Low Cooling Penalties

● Fuel Qualitites – Trends in Specifications

4.6 TECHNOLOGY RECOMMENDATIONS

Throughout the Phase III and IV studies, the GE21 double-bypass variable cycle engine (VCE) has remained the favored General Electric AST/SCAR engine cycle concept. The concept has evolved through a series of improvements resulting from both internal and airframe company related integration studies and is considered to be in a sufficient state of maturity to permit the identification of needed technology development effort.

Concurrent with the NASA-Lewis sponsored AST Phase III systems studies, GE has been involved in extensive planning activitiy associated with the NASA VCE Test-Bed Program. Key technology requirement areas already have been identified and programs have been recommended to NASA, some of which are currently under contract. The General Electric VCE Test-Bed Program, as recommended to NASA, will provide for (1) scale model testing (statically and under simulated flight effects) of the annular acoustic plug nozzle, (2) a fan component program, the fan from which could be utilized in a later variable cycle experimental engine, (3) an early acoustic demonstration of the annular acoustic nozzle on an existing high technology engine, and (4) a VCE test-bed engine that, to a high degree, would demonstrate the combination of all unique VCE features incorporated in the GE21 double-bypass variable cycle engine.

There are additional areas of needed technology not covered already by the VCE Test-Bed Program. These areas are identified in Table 41. In the following sections some are discussed in detail.

4.6.1 Annular Acoustic Nozzle

Scale model nozzle programs are being conducted as part of the VCE Test-Bed Program. Under Contract NAS3-19777, parametric studies involving static testing were conducted to analyze the effects of changing various parameters associated with the inherent suppression characteristics of the annular plug nozzle. Acoustic data on various nozzle configurations taken under static testing conditions were recorded and aero performance was detained at approximately takeoff Mach numbers.

Under Contract NAS3-20619, the more promising configuration from NAS3-19777, and a configuration to explore shock noise, will be utilized to determine the impact of flight effects on the inherent suppression characteristics of the annular nozzle.

Under Contract NAS3-20582, in approximately mid-1978, an annular acoustic plug nozzle will be designed, fabricated, and tested on a YJ101 engine modified to a variable cycle configuration. The capability will exist to test suppressor configurations which can be incorporated into the annular plug nozzle. Prior to this early acoustic demonstration, a test will be conducted utilizing the modified YJ101 engine to demonstrate the bypass flow mixing devices similar to those incorporated in the GE21 double-bypass VCE

278

design. These flow mixing devices are considered to be an integral part of the GE-AST acoustic nozzle system.

At the present time, there are no programs identified to analyze the aerodynamic performance characteristics of the annular plug nozzle under supersonic flight conditions. While there is a high degree of confidence in the performance aspects of this nozzle, based on extensive prior testing of similar nozzle configurations, it is felt that effort is required in this area on specific AST nozzle configurations, and a wind tunnel program is therefore recommended.

4.6.2 Operational Demonstration of the GE21 VCE Concept

As previously mentioned, as part of the recommended VCE Test-Bed Program, a VCE test-bed engine, based on the YJ101, will be configured with a combination of all key technology features of the GE21 VCE. Included will be the annular acoustic plug nozzle, the bypass flow mixing devices, and the split fan concept with a new rear block fan stage. A series of tests will be conducted in late 1979/early 1980 to demonstrate the performance, operational modes, and acoustic characteristics of this variable cycle engine. At that time, it is felt the proof of the GE21 VCE concept will have been demonstrated. Programs beyond, or in addition to, the test-bed engine will address advanced technology component and engine systems work, and obtain validation of the weights and component performance projected for the 1985 technology level of the GE21 VCE.

4.6.3 Front Block Fan Program

As part of the VCE Test-Bed Program, a program has been recommended to develop a new front block fan (Stages 1 and 2). The objective of the program would be to develop the technology required to obtain the projected GE21 VCE fan efficiency levels under the various mission-related operating modes. The fan that resulted from this program could be made available for use on an advanced technology test-bed program.

Table 41. Key Technology Requirements of the GE21 Variable Cycle Engine.

● Annular Acoustic Nozzle

● Operational Demonstration of the GE21 VCE Concept

● Bypass Flow Mixing Devices

● Front Block Fan

● Rear Block Fan

● Full Authority Digital Electronic Control System

● High Temperature, Low Emissions Main Burner

● Low Temperature Rise, Low Emissions Augmentor
  (for Transonic Acceleration)

● Propulsion System Integration

5.0 CONCLUSIONS

1. An improved double-bypass variable cycle engine has been identified. It incorporates certain advanced technology features, including:

   - Mechanical design improvements

   - Reduced levels of turbine cooling air

   - Improved fan and compressor aerodynamics

   - Advanced materials and coatings

   - High-flowed fans

   - Low emissions combustor

   - Advanced electronic controls

2. Progress has been achieved in evolving a simpler and lighter variable cycle engine design through the incorporation of:

   - Annular exhaust nozzle with a fixed primary

   - Improved aerodynamic flowpaths

   - Lightweight components

3. The selected annular nozzle system design has the following features:

   - Simple design, three actuation systems eliminated

   - Major weight saving

   - Practical, similar systems in commercial service

   - Minimum leakage, no variable flaps and seals

   - A simple suppressor can be added if needed

   - A better nacelle installation is possible

4. Early in-house General Electric mission studies have identified an attractive double-bypass variable cycle with a 30% high-flowed fan having the following cycle parameters:

PR_{Fan}	4.0
PR_{OA}	20
BPR	0.35
$T41_{Max.}$	1538° C (2800° F)
$T41_{Supercruise}$	1480° C (2700° F)

5. Further in-house GE studies have been completed in which the double-bypass VCE design has been refined and improved. Fan high-flow percentages have been varied, using 10%, 20%, and 30%. The most attractive cycles for a double-bypass VCE were found to be:

- Fan high-flow, 20% or 10%

PR_{Fan}	4.0
PR_{OA}	17.5
BPR	0.35
$T41_{Max.}$	1538° C (2800° F)
$T41_{Supercruise}$	1482° C (2700° F)

6. Further cooperative studies with the aircraft systems contractors have identified cycles best matched to their aircraft with the following parameters:

- Fan high-flow, 10%

PR_{Fan}	3.7
PR_{OA}	15-17
BPR	0.25-0.35
$T41_{Max.}$	1538° C (2800° F)
$T41_{Supercruise}$	1482° C (2700° F)

Range improvements of from 555 to 926 km (300 to 500 nmi) resulted.

7. Double-annular combustor provides significant emission reductions.

- Meets 1984 EPA proposed airport standard

- Does not meet CIAP supersonic cruise proposed standard

8. Very low cruise NO_x levels may be obtainable with 1985 technology pre-
    mixing combustor. However, the development of the premixing combustor
    will require major design effort if CIAP goals are to be met.

9. Final emission standards chosen may have a major impact on the AST air-
    craft and its propulsion system.

10. Advanced engine accessories provide large improvement in weight and
    volume. Further effort is required to integrate advanced technology
    controls and accessories to AST VCE and airplane.

11. A VCE test-bed configuration has been established, closely repre-
    senting AST VCE cycle and features.

12. Satisfactory inlets can be designed to match flow and other performance
    characteristics of General Electric variable cycle engines.

13. Acceptable nacelle designs can be achieved for General Electric GE21/J11
    double-bypass variable cycle engines with only minor engine configura-
    tion changes and minimal impact aircraft drag.

14. Engine size selection is greatly affected by jet nozzle acoustic
    characteristics, takeoff requirements, and aircraft size.

15. General Electric GE21/J11 engines with annular nozzles are estimated to
    meet FAR 36 noise requirements without need for a mechanical suppressor.
    A simple mechanical suppressor can be incorporated in the nozzle for a
    small weight penalty, if required.

16. Close relationships between airframe and engine manufacturers through
    continued integration studies should be maintained if potential advan-
    tages of new and improved engine cycles are to be exploited by matching
    the propulsion systems to the specific aircraft requirements. All
    advanced technology benefits can be lost if the engine is not properly
    matched to the aircraft.

6.0 REFERENCES

1. Allan, R.D., and Szeliga, R., "Advanced Supersonic Technology Propulsion System Study - Final Report," NASA CR-143634, July 1974.

2. Allan, R.D., "Advanced Supersonic Technology Propulsion System Study - Phase II Final Report," NASA CR-134913, December 1975.

3. LTV Report, "Advanced Supersonic Technology Concept Study - Reference Characteristics," NASA CR-132374, December 21, 1973.

4. Anderson, D., "Effects of Equivalence Ratio and Dwell Time on Exhaust Emissions from an Experimental Premixing, Prevaporizing Burner," NASA TMX-71592, March 6, 1975.

5. Dept. of Transportation, "Noise Standards: Aircraft Type Certification," Federal Aviation Regulations, Part 36, December 1, 1969.

6. Trucco, Horacio, "Study of Variable Cycle Engines Equipped with Supersonic Fans," Adv. Technology Labs., Inc. TR-201, NASA CR-134777, September 1975.

End
Date

Feb. 3, 1978